Kaoru Yamanouchi

Quantum Mechanics of Molecular Structures

Springer

Quantum Mechanics of Molecular Structures

Kaoru Yamanouchi

Quantum Mechanics of Molecular Structures

Springer

Kaoru Yamanouchi
Department of Chemistry
The University of Tokyo
Tokyo, Japan

Original Japanese edition *Koza, Gendai Kagaku he no Nyumon (4) Bunshi Kozo no Kettei* published by Iwanami Shoten, Publishers, Tokyo, 2001

ISBN 978-3-642-32380-5 ISBN 978-3-642-32381-2 (eBook)
DOI 10.1007/978-3-642-32381-2
Springer Heidelberg New York Dordrecht London

Library of Congress Control Number: 2012952030

Printed on acid-free paper

Springer is part of Springer Science+Business Media (www.springer.com)

Preface

The world we live in is filled with molecules. Starting with oxygen and nitrogen in the atmosphere, water, carbon dioxide, and ammonia are all molecules. Furthermore, plants and animals are all composed of molecules. In the field of chemistry, which is regarded as science for molecules, it has been one of the most important and long-lasting fundamental issues to know the geometrical structure of a variety of molecular species around us.

Roughly speaking, there are two major methods to investigate the geometrical structure of molecules in the gas phase. One is molecular spectroscopy and the other is gas electron diffraction. In molecular spectroscopy, molecules are irradiated with light or electric waves, and a diagram called a spectrum is measured. In the diagram, rich information regarding the dynamics of electrons within a molecule, the vibrational motion of nuclei within a molecule, and the overall rotational motion of a molecule are encoded. Specifically, from the spectrum related with the rotational motion of molecules, we can derive information which is directly connected to the geometrical structure of molecules.

Therefore, it can be described that the most central issue in the field of molecular spectroscopy is to know how we can extract information concerning molecular motion from an observed spectrum. If we regard a spectrum as a secret code, the issue is nothing but decoding the code and developing the methodology on the decoding procedure. In order to decode the spectrum and to derive information of molecules properly, we need to realize that molecules are described by quantum mechanics.

In the present textbook, we learn that the motion of electrons in a molecule, molecular vibration, and molecular rotation are all "quantized" and that the consequence of the quantization appears vividly in the spectrum. Furthermore, we understand how we can determine the geometrical structure of molecules, and simultaneously we appreciate the fundamentals of quantum mechanics of molecules.

On the other hand, in the gas electron diffraction experiment, we irradiate molecules with an electron beam which is accelerated to a very high speed. Though the electron beam is a beam of electrons, each of which is a particle, it has the character of waves. Consequently, the beam is scattered by more than one nuclei within a molecule, and the scattering waves interfere with each other. This means that the

information about the distances among the nuclei is recorded in an observed interference pattern. In the present textbook, we understand the fundamental mechanism of the scattering of electrons by a molecule on the basis of quantum mechanics, and in addition, we learn how the geometrical structure of molecules is determined from such an electron diffraction image.

By reading this textbook, readers can understand that the two most direct procedures to determine the geometrical structure of molecules are an analysis of a rotational spectrum and that of a gas electron diffraction image, and that the information obtained from a vibrational spectrum is a prerequisite for their analyses. And the readers can find an answer to the fundamental question, "What does the determination of the geometrical structure of molecules really mean?" through the understanding of the difference in the physical meaning of the molecular structure determined by molecular spectroscopy and that of the molecular structure determined by gas electron diffraction. When the readers study quantum mechanics, a variety of examples related with molecules introduced in the present textbook should be certainly helpful to appreciate the value of quantum mechanics.

I would like to note here that the kind cooperation I received from many people enabled me to write this textbook. First of all, I would like to thank Prof. Tadamasa Shida (Kanagawa Institute of Technology) and Prof. Koji Kaya (Institute for Molecular Science, Emeritus Professor of Keio University) for giving me the opportunity to write this textbook and for the helpful advice they offered regarding its contents.

Prof. Toshihiro Ogawa (Japan Aerospace Exploration Agency, Emeritus Professor of the University of Tokyo) and Prof. Yutaka Kondo (The University of Tokyo) kindly pointed me to some important references and documents on an infrared emission spectrum of the Earth that had been recorded by a satellite, which is referred to in Chap. 1. Prof. Ogawa's guidance was invaluable as I wrote on the absorption of infrared light by molecules in the atmosphere, and he gave me his kind permission to print the unpublished spectra, shown as Figs. 1.5 and 1.7 in Chap. 1.

Valuable comments and kind guidance were also given to me by Prof. Yasuki Endo (The University of Tokyo) and Prof. Satoshi Yamamoto (The University of Tokyo) on the references on the spectra of interstellar molecules, by Prof. Kazuo Tachibana (The University of Tokyo) on the photoabsorption of organic molecules, by Prof. Haruki Niwa (University of Electro-Communications) on bioluminescence, and by Dr. Tadaaki Tani (Fujifilm Co.) on photosencitizing dyes used in color photograph films. My thanks also go to Prof. Noriaki Kaifu (National Astronomical Observatory of Japan), who gave me kind permission to include his spectra of interstellar molecules. Prof. Kozo Kuchitsu (Josai University, Emeritus Professor of the University of Tokyo) also gave me his kind permission to use his electron diffraction photographs, and offered some valuable comments on the contents of Chap. 1. I would like to mention here that some of the materials dealt with in this textbook are based on my research results obtained when I was a graduate student in Prof. Kuchitsu's research group, and those obtained when I was a staff member of the research group of Prof. Soji Tsuchiya (now Waseda University, Emeritus Professor of the University of Tokyo).

I am indebted to the members of my research group, Ms. Kyoko Doi, Mr. Motoyuki Watanabe, Mr. Taiki Asano, Mr. Tomoya Okino, Ms. Aya Kaijiri, and Ms.

Misato Yarumura, who have kindly read through my drafts a number of times to help ensure the readability of the text while keeping its scientific rigorousness. Dr. Akiyoshi Hishikawa, Dr. Kennosuke Hoshina, and Dr. Ryuji Itakura have given me their valuable comments on the scientific content throughout the book. Mr. Takashi Amano also gave me some valuable comments on the discussions in Chaps. 2 and 3, and Ms. Keiko Kato on the topic of Chap. 4. I am also indebted to Dr. Kennosuke Hoshina for carefully checking over the numerical calculations in the text and for helping me with the illustrations of gas electron diffraction, and to Mr. Tokuei Sako and Mr. Takashi Amano for their help on the figures explaining vibrational wave functions in Chap. 2.

As my thanks go out to all of these people whose cooperation and support have been invaluable to me as I wrote this book, I would like to also express my sincere gratitude to the members of the editorial department of Iwanami Publishing Co. for their heartfelt efforts and valuable support in editing this book.

Last but not least, I would like to thank my mother, Kiyoko Yamanouchi, who passed away at the end of last year, for her presence and the comments she gave me after reading through a part of the text.

I am dedicating this volume to my wife Yuko, whose constant moral support and understanding have been indispensable as I kept on writing on weekends and holidays, and to my two daughters, Aki and Nao, who I hope may grow up to read this textbook in the future and give me their impressions and comments.

Tokyo, Japan Kaoru Yamanouchi
August 2001

Preface to the English Edition

It surprises me to note that it has now been ten years since I first published this textbook. To my gratitude, it was welcomed by university professors and researchers in Japan not only in the field of physical chemistry but also in physics, as a concise textbook that teaches students fundamental ideas of quantum mechanics through discussions of how geometrical structures of molecules are determined. I have since been using this textbook in my lecture course entitled Quantum Chemistry I at the University of Tokyo, for undergraduate science course students in the second semester of their second year.

Readers can learn about "a particle in a box" in Chap. 1, "harmonic oscillators" in Chap. 2, "angular momenta" in Chap. 3, and "the scattering theory and Schrödinger's equation for radial motion" in Chap. 4. Topics such as electronic transitions in dye molecules, molecular vibration, molecular rotation, and electron scattering by molecule will make it easy to grasp how useful it is to learn quantum mechanics. Reading this textbook, students may realize that quantum mechanics is indispensable in explaining a variety of phenomena occurring around us in our daily life.

Because of this feature, I have decided to call the English edition of this textbook "Quantum Mechanics of Molecular Structures," instead of "Determination of Molecular Structure," which would be a direct translation of the original title in Japanese.

I started my career as a scientist by studying microwave molecular spectroscopy and gas electron diffraction. Even now, I can very clearly remember how much it excited me to know how precisely I could determine the internuclear distances and bond angles of molecules by applying these two methods. Later, I started exploring more dynamical aspects of molecules, such as chemical bond breaking and rearrangement processes induced by light. In recent years, my major concerns have been responses of atoms and molecules to intense laser fields,[1] and my discussions

[1] See, for example, "K. Yamanouchi et al. eds., Progress in Ultrafast Intense Laser Science I–VIII, (2006)–(2011)" and "K. Yamanouchi ed., Lectures in Ultrafast Intense Laser Science I (2011)," in Springer's Series in Chemical Physics.

with colleagues involve how to investigate ultrafast atomic and molecular processes in the femtosecond and attosecond[2] time domains.

These topics may be seen as more advanced than those previously investigated in the field of structural chemistry, where microwave molecular spectroscopy and gas electron diffraction were used. Nevertheless, I am reminded of how important it is to have concrete knowledge and understanding of how molecules rotate and vibrate in the frontier research field.

Through the interactions between matter and ultrashort intense laser light, we can generate light in the wide wavelength range spanning from terahertz (THz) radiation to soft-X ray. Interestingly, we have learned that the THz radiation can be used as an ideal light source for high-resolution rotational spectroscopy through which transitions between high-J rotational levels of molecules in the gas phase can be measured with a high-resolution, as an extension of microwave molecular spectroscopy to a higher frequency domain. We have also recently investigated electron scattering processes in the presence of an ultrashort light field, which is called laser-assisted electron scattering, and found that it can be used as an ultrashort camera shutter for probing dynamical motions of molecules by gas electron diffraction. Thus, we can see that the classical and established research fields of molecular spectroscopy and gas electron diffraction are now being revisited and are pushing forward the frontiers of research.

I hope that this English edition of my textbook will be used worldwide in teaching undergraduate courses in universities, so that science course students can comprehend the quantum mechanical images of molecules around us. I also hope it will prove helpful in research scenes as a concise guidebook for molecular spectroscopy and gas electron diffraction.

I would like to thank Dr. Norio Takemoto, a former graduate student in my research group, for his help in revising some parts of the text in Chap. 2 in the Japanese edition, and Ms. Chie Sakuta for helping me edit this English edition. My thanks also go to Dr. Claus Ascheron, Physics Editor of Springer-Verlag at Heidelberg, for his kind support.

Tokyo, Japan Kaoru Yamanouchi
March 2012

[2] 1 femtosecond is 10^{-15} s and 1 attosecond is 10^{-18} second.

Contents

1 The Energy and Geometrical Structure of Molecules 1
1.1 Absorption and Emission of Light by Dye Molecules 2
1.2 Infrared Radiation from the Earth 7
1.3 Microwaves Arriving from Outer Space 12
1.4 The Hierarchical Structure of Molecular Energy Levels 13
1.5 The Diffraction of Electron Beams and Molecular Structures . . . 15
1.6 Methods of Molecular Structure Determination 18

2 Vibrating Molecules 21
2.1 How to Describe Vibrating Molecules 22
2.2 Molecular Vibration in Quantum Theory 26
2.2.1 Quantizing the Harmonic Oscillator 27
2.2.2 The Energy Level of the Harmonic Oscillator 27
2.2.3 Determination of Potentials by Infrared Absorption 32
2.2.4 Eigenfunctions of Harmonic Oscillators 34
2.2.5 The Hermite Recurrence Formula 36
2.2.6 The Eigenfunction System of a Harmonic Oscillator 38
2.3 The Harmonic Oscillator and Its Applications 40
2.3.1 Hermitian Operators and the Bracket Notation 41
2.3.2 Calculations of Expectation Values Using Eigenfunctions . 45
2.3.3 Matrix Elements of x and Selection Rules for Infrared Absorptions 47
2.3.4 Overtone Absorption 49
2.3.5 Matrix Elements of x^2 and the Expectation Value of the Potential Energy 52
2.3.6 Creation and Annihilation Operators 57
2.3.7 Evaluation of Perturbation Energy 61
2.3.8 Morse Potential 63
2.4 The Inversion Motion of Ammonia Molecules 68
2.4.1 The Infrared Absorption Spectrum 69
2.4.2 Parity of Wave Functions 71

2.4.3 Energy Level Splitting and Potential Barriers 72
2.4.4 The Geometrical Structure of Ammonia and the Period of the Inversion Motion 74
2.5 How to Treat the Vibration of Polyatomic Molecules 77
2.5.1 Degrees of Freedom of Molecular Motions 78
2.5.2 What Are Normal Modes? 80
2.5.3 Normal Modes and Matrix Diagonalization 87
2.5.4 The Vibrational Hamiltonian Represented by Normal Coordinates 89
2.5.5 The Quantum Theory of Normal Mode Vibrations 93
2.5.6 Normal Modes of a Polyatomic Molecule Composed of n Atoms 96
2.5.7 Representation of Normal Modes in Terms of Internal Coordinates 101
2.5.8 Analysis of Normal Modes by the GF Matrix Method . . . 105
2.5.9 Anharmonic Expansion of Potentials by Dimensionless Coordinates 112

3 Rotating Molecules 119
3.1 Molecular Rotation and Molecular Structure 120
3.1.1 Microwave Spectroscopy 120
3.1.2 The Quantum Theory of Molecular Rotation (Diatomic Molecules) 121
3.1.3 Rotational Energy Levels of Linear Molecules and Structure Determination by Means of Isotope Substitution . 125
3.2 The Angular Momentum of Molecular Rotation 128
3.2.1 Angular Momentum Operators 129
3.2.2 Commutation Relations of Angular Momentum Operators . 130
3.2.3 Raising and Lowering Operators 132
3.2.4 Eigenvalues of Angular Momentum Operators 134
3.2.5 Eigenfunctions of Angular Momentum Operators 136
3.3 Molecular Rotation from the Point of View of Classical Mechanics 141
3.3.1 Molecular Rotation and Euler Angles 141
3.3.2 Matrix Representation of the Coordinate Rotation 144
3.3.3 The Kinetic Energy and Angular Momentum of the Rotation of a Molecule 146
3.3.4 Classification of Molecules by Values of the Moments of Inertia 149
3.4 Molecular Rotation from the Point of View of Quantum Mechanics 152
3.4.1 Quantum Mechanical Hamiltonians of Molecular Rotations 152
3.4.2 Angular Momenta of Overall Rotations in Molecule-Fixed Coordinate Systems 157
3.4.3 Energy Level Diagrams of Prolate and Oblate Top Molecules 161

3.4.4 Energy Levels of Diatomic and Linear Molecules 163
3.4.5 Energy Levels of Spherical Top Molecules 164
3.4.6 Energy Levels of Asymmetric Top Molecules 164
3.4.7 Calculating the Rotational Energy Levels of an Asymmetric Top Molecule for $J = 0$ and $J = 1$ 166
3.4.8 Wang's Transformation 170
3.4.9 Symmetry in the Rotational Levels of an Asymmetric Top Molecule 173
3.5 Determination of Molecular Structures Based on Rotational Spectra 176
3.5.1 Molecular Structures of Symmetric Top Molecules 176
3.5.2 Determining the Rotational Constants of Asymmetric Top Molecules 179
3.5.3 Molecular Structures of Asymmetric Top Molecules 183
3.6 Rotating and Vibrating Molecules 188
3.6.1 Rotational Structures of Vibrational Transitions 188
3.6.2 Rotational Structures of Electronic Transitions 193

4 Scattering Electrons 197
4.1 Scattering Electron Waves 198
4.2 Electron Scattering by Atoms 204
4.2.1 The Schrödinger Equation for Scattering 204
4.2.2 Representation of the Scattering Amplitude by Use of the Born Approximation 208
4.2.3 Electron Scattering by Atoms 210
4.3 Electron Scattering by Molecules 212
4.3.1 The Scattering Amplitude of Electron Scattering by a Molecule 212
4.3.2 The Scattering and Interference of an Electron Beam by a Diatomic Molecule 214
4.4 Phase Shift of the Scattering Electron Wave 218
4.4.1 Partial-Wave Expansions of Scattered Waves 218
4.4.2 The Behavior of Partial Waves in the Asymptotic Region . 222
4.4.3 The Partial Wave Expansion of Plane Waves 224
4.4.4 The Partial Wave Expansion of Scattering Amplitudes . . . 226
4.4.5 Phase Shift in Electron Diffraction 230
4.5 The Effect of Molecular Vibration 232
4.5.1 Mean Square Amplitudes 232
4.5.2 The r_a Structure and the r_g Structure 238
4.6 Electron Beam Scattering by Polyatomic Molecules 241
4.6.1 Molecular Scattering Curves and Radial Distribution Curves 241
4.6.2 From a Molecular Scattering Curve to the Molecular Structure 244
4.6.3 The Shrinkage Effect 246

4.6.4 The r_α^0 Structure 250
4.6.5 An Example of Structure Determination 255

For Further Reading 259
Figure Sources 260

Subject Index 261

Formula Index 267

Chapter 1
The Energy and Geometrical Structure of Molecules

When a molecule absorbs light, it gains energy and reaches a state called an excited state. With visible or ultraviolet (UV) light, the electrons in the molecule are excited, and with infrared (IR) light, the molecular vibration is excited. When a molecule absorbs microwave, its molecular rotation is excited. This chapter seeks to explain that a molecule has discrete energy levels, by looking at three familiar examples; the color of dye molecules, the IR emission from the Earth detected by observation satellites, and microwaves arriving from space. We will also learn that we can calculate the distances among atoms within a molecule based on the scattering patterns of high energy electron beams, and that the precise geometrical structures of molecules can be determined by molecular spectroscopy and gas electron diffraction.

Summaries

1.1 Absorption and Emission of Light by Dye Molecules
Here we learn that various organic compounds absorb and emit light with specific wavelengths, and that all molecules have discrete energy levels. We will reach the understanding that we can use quantum theory to estimate the size of a molecule by looking at the wavelengths of the light that it absorbs.

1.2 Infrared Radiation from the Earth
We will see that a spectrum of the IR emitted from the Earth, as recorded by an observation satellite, gives us information on the vibrational motion of the molecules in the air. We will thus learn that a molecule has discrete energy levels associated with its vibrational motion.

1.3 Microwaves Arriving from Outer Space
We learn that the spectrum of electric waves arriving from space contains signals reflecting the variety of molecules in outer space, and that a molecule has discrete energy levels associated with its rotational motion.

1.4 The Hierarchical Structure of Molecular Energy Levels
We learn that exciting the vibrational motion of a molecule requires a photon with 100 to 1000 times the energy as that required for exciting its rotational motion, and that exciting the motion of the electrons within a molecule requires a photon with 10 to 100 times the energy as that required for exciting the vibrational motion of this molecule.

K. Yamanouchi, *Quantum Mechanics of Molecular Structures*,
DOI 10.1007/978-3-642-32381-2_1,

1.5 The Diffraction of Electron Beams and Molecular Structures
When molecules are irradiated with an electron beam accelerated to a high speed, interference fringes appear in the scattering pattern of the electron beam. By examining this phenomenon, we will reach an understanding of the wave nature of electrons. Then, we will learn that the geometrical structure of a molecule can be determined from its interference fringes.

1.6 Methods of Molecular Structure Determination
We will learn how we can obtain information about molecular structures from the electronic spectra, vibrational spectra, rotational spectra, and gas-phase electron diffraction, in this final section.

1.1 Absorption and Emission of Light by Dye Molecules

Objects surrounding us in our everyday lives have various colors. The reason we can see these different colors is because, of the light shining on each object, be it sunlight or the light from a lamp, certain wavelengths are efficiently absorbed by it while the others are reflected.

For example, there are a multitude of colors characterizing flowers of different plants. These are all due to a kind of organic compound called dyes. Examples of dyes include such groups of chemical compounds as the carotenoid dye and the flavonoid dye. An example of a carotenoid is the β-carotene, which is responsible for the red color found in carrots. The β-carotene is shown in the structural formula (1.1) in the form of a bond-line formula, where the vertices represent the locations of carbon atoms and all hydrogen atoms are omitted. An example of a flavonoid dye, the flavonol, is given by the structural formula (1.2). This dye gives a yellow color.

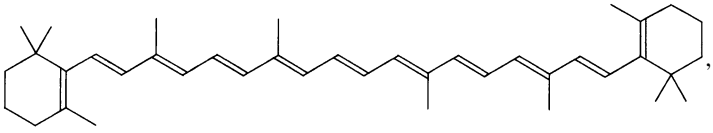

(1.1)

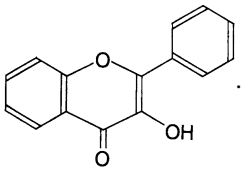

(1.2)

Another group of dye is the one called the cyanine dye, which is used as a sensitizing dye for color photographs. For example, this is one type of cyanine dye called the

thiacarbocyanine:

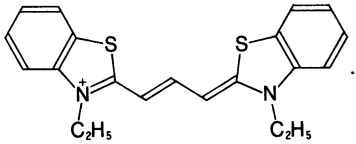

. (1.3)

This compound absorbs yellow-green light in methanol solutions. By adding another adjacent pair of a double bond and a single bond to the middle section of the molecule, lengthening the chain-like structure by one unit, we can make the compound absorb red light instead. When we shorten the chain by one unit, on the other hand, the compound starts to absorb blue light. Thus, this material allows us to design dyes with different absorption wavelengths.

These compounds absorb light of each their own specific wavelengths, from which they take the energy to be excited to a state where the electrons in each molecule are excited, that is, an electronically excited state. Most molecules then lose their energy by a radiationless process, in which no light emission occurs.

Aside from these cases where objects reflect light, we can also sense colors when objects themselves emit light, whose respective wavelengths, when they are within the visible region, are perceived by our eyes as different colors. A familiar example of this is the light emission of fireflies. In the body of a firefly is a kind of compound called the luciferin, which is described as

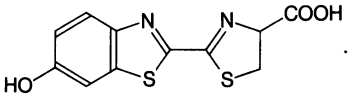

. (1.4)

When this compound is oxidized inside the body, the oxyluciferin, described as

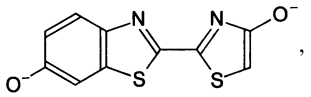

, (1.5)

is produced in its electronically excited state. This type of electronically excited state is what is known as a "singlet state," and emits light, thereby reverting to a singlet electronic ground state. The wavelength of this light lies in the region of yellowish green, which causes our perception of this color in the light of a firefly.

As shown in the above examples, molecules can be excited from a low energy level to a high energy level by photoabsorption, or brought down from a high energy level to a low energy level through the process of photoemission.

In the retina of our eyes, there is a visual substance called rhodopsin. When light is perceived, one of its constituents called the 11-cis-retinal, represented as

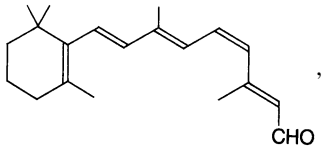

, (1.6)

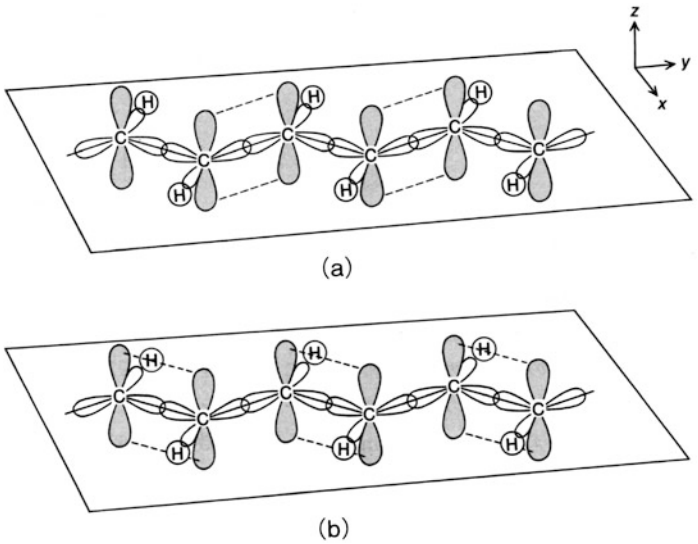

Fig. 1.1 Schematic illustration of a π-conjugated chain

absorbs the light. This 11-cis-retinal is known to be photoisomerized into the all-trans-retinal,

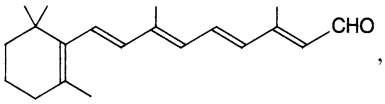

, (1.7)

through this photoabsorption process. Incidentally, vitamin A, shown as

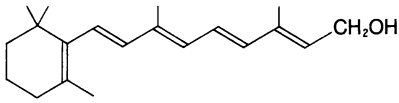

, (1.8)

is an alcohol form of the retinal, and the β-carotene, as previously depicted, can be regarded as a compound consisting of two vitamin A molecules or of two retinals. In fact, inside our bodies, β-carotene is broken down by our metabolisms to produce vitamin A.

The dye molecules and biological molecules discussed here all have a common structure, namely a chain of double bonds alternating with single bonds, which usually consist of carbon atoms. In the moiety of a carbon chain or a benzene ring, the carbon atoms form a type of electron orbital called the sp^2 hybridized orbital, which aligns the σ bonds onto the x-y plane. The p_z orbital, which does not participate in the hybridization, stands perpendicular to the plane, and forms alternating π bonds, as illustrated by the dashed lines in Fig. 1.1a. It seems also likely, however, that these π bonds between carbon atoms may be shifted onto their neighbors, so that the representation can be regarded as Fig. 1.1b. These dual possibilities are schematically expressed as line-bond figures in Fig. 1.2.

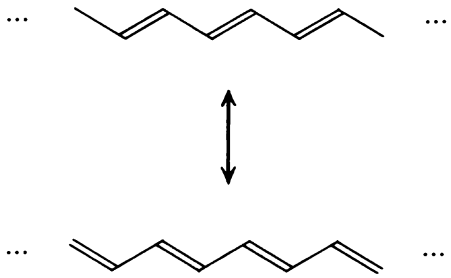

Fig. 1.2 A π-conjugated chain in a bond-line formula

It is a known fact that a π bond accommodates two electrons, which must be localized in the region between those specific carbon atoms. However, when the π bond shifts to the adjacent pair of carbon atoms, as shown in Fig. 1.2, the electrons initially localized in the first π bond transfer to the region of the second pair of atoms and are localized as their π electrons. From the point of view of each π electron, then, what this means is that the chain of π bonds allows it to be delocalized over the whole region of this chain. Such a molecular chain made up of π bonds is called a conjugated system of π bonds, or a π-conjugated chain. The word "conjugate" comes from the two Latin words, "con" (two or together) and "jugate" (join).

We have just looked at an example of a π-conjugated system that comes in the form of a chain, to understand its structure. However, benzene, of course, also forms a π-conjugated system. In this case, we can visualize the π-electrons as delocalizing throughout the benzene ring, as they shift between two Kekulé structural formulae,

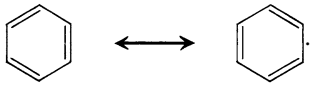

(1.9)

The example of the cyanine dye tells us that, by extending the region through which the electrons can move around, we can lengthen the photoabsorption wavelength of the molecule. This also means that, conversely, by measuring the photoabsorption wavelength of a molecule, we can gain information about its length and size, or more generally about its molecular structure.

Let us now overview the relationship between the optical wavelength and energy of light. Using the Planck constant h ($= 6.62606876 \times 10^{-34}$ J s) and the optical frequency ν, the energy of the light, ε, is given by

$$\varepsilon = h\nu. \tag{1.10}$$

This can be interpreted as the energy of a photon whose frequency is ν. Using the velocity of the light, c ($= 2.99792458 \times 10^8$ m s^{-1}), the optical wavelength λ is related to ν by

$$c = \lambda\nu, \tag{1.11}$$

so that we can write

$$\varepsilon = h\nu = hc \cdot \frac{1}{\lambda}. \tag{1.12}$$

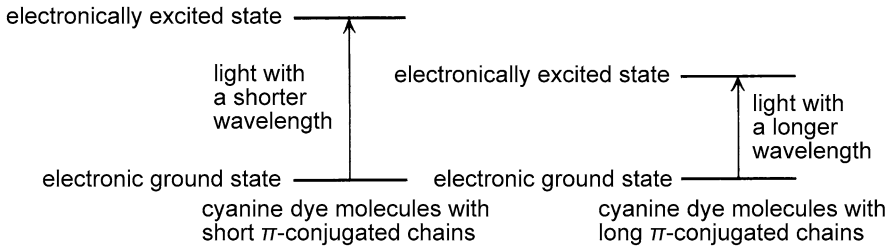

Fig. 1.3 The relationship between the length of a π-conjugated chain and its absorption wavelength

This signifies that the energy of light is proportional to the ν, or to $\frac{1}{\lambda}$ the reciprocal of the wavelength.

Therefore, we can understand from the fact that a cyanine dye with a short π-conjugated chain absorbs light with short wavelengths that the energy $\frac{hc}{\lambda}$ of the photon that it absorbs is larger than that absorbed by a cyanine dye with a longer π-conjugated chain, and that this causes the shorter-chain molecule to be excited to an electronically excited state of higher energy, as illustrated in Fig. 1.3.

For an accurate understanding of the relationship between the eigenenergy and size of a molecule, we need to describe the electron motion within the π-conjugated chain in terms of quantum theory. Let us for example determine the length of the π-conjugated chain of β-carotene, using the wavelength of the light that it absorbs.

According to quantum theory, the energy levels for a particle of mass m which moves within a box-type potential of length L are given by

$$E_n = \frac{h^2}{8mL^2}n^2, \tag{1.13}$$

where n is an integer whose magnitude is not less than 1. With β-carotene, we can regard the π-conjugated chain as a one-dimensional box into which all electrons are confined. In such a case, as the particle in question is an electron, we can substitute the mass of an electron, $m_e = 9.10938188 \times 10^{-31}$ kg, for m in Eq. (1.13). As the π-conjugated chain is composed of 11 π bonds, each of which is composed of two electrons, a total of 22 π electrons exist in the π-conjugated chain. Designating the levels by $n = 1, 2, \ldots$ and their respective energies by $E_1, E_2, \ldots$, and mapping them in sequence from the bottom as shown in Fig. 1.4, we can use the knowledge that each level holds two electrons, one with an upward electron spin and the other with a downward spin, to infer that eleven levels, denoted as $n = 1, 2, \ldots, 11$, are required to contain all of the π electrons. The level denoted by $n = 11$ here is called the Highest Occupied Molecular Orbital, or HOMO. The numbers designating such discrete energy levels are called quantum numbers.

When light is absorbed, one of the electrons occupying the $n = 11$ level of β-carotene is excited to the $n = 12$ level, which is called the Lowest Unoccupied Molecular Orbital, or LUMO. Thus the energy $h\nu$ of the absorbed photon is equal to the difference between E_{11} and E_{12}. The wavelength at which light absorption by

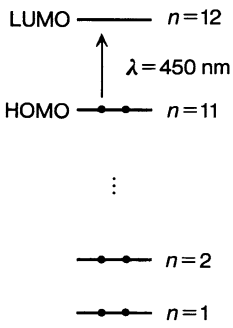

Fig. 1.4 Excitation from HOMO to LUMO induced by the photoabsorption of β-carotene

β-carotene reaches its maximum is known to be $\lambda = 450$ nm. Using this wavelength, we can obtain L, the length of the π-conjugated chain for β-carotene.

First, the energy of the absorbed photon can be described as

$$h\nu = \frac{hc}{\lambda}. \tag{1.14}$$

The energy difference between the two levels is derived from Eq. (1.13) as

$$E_{12} - E_{11} = \frac{h^2}{8m_e L^2}\left(12^2 - 11^2\right) = \frac{23h^2}{8m_e L^2}. \tag{1.15}$$

As these two energies become equal at $\lambda = 450$ nm, we can write

$$\frac{23h^2}{8m_e L^2} = \frac{hc}{\lambda}, \tag{1.16}$$

which allows us to derive the length of the π-conjugated chain, L, as

$$L = \sqrt{\frac{23h\lambda}{8m_e c}}. \tag{1.17}$$

By substituting the values for h, m_e, and c, as well as $\lambda = 450 \times 10^{-9}$ m, into this equation, we obtain $L = 1.77 \times 10^{-9}$ m $= 17.7$ Å. When we use the standard bond lengths for a C–C bond and a C=C bond instead, the length of the π-conjugated chain of β-carotene is estimated to be approximately 25 Å. Comparing these two values, we can see that the estimation of 17.7 Å, obtained from the box-type potential model, is reasonably good.

1.2 Infrared Radiation from the Earth

Infrared light is electromagnetic radiation whose wavelength ranges from 1 to 100 μm. Of the range of electromagnetic waves that is categorized as light, what

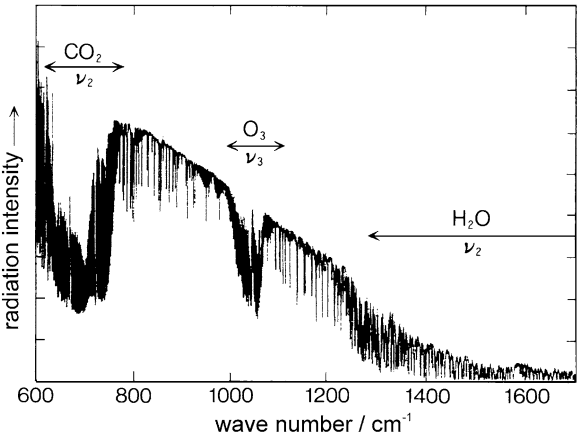

Fig. 1.5 Infrared radiation spectrum of the Earth observed by the IMG (Interferometric Monitor for Greenhouse gases) mounted on ADEOS (the Advanced Earth Observing Satellite)

we call infrared light, or the infrared beam, belongs to the region of the longest wavelengths. Electromagnetic waves with longer wavelengths than infrared light are categorized as microwave (whose wavelength range is from 1 mm to 1 m), and are commonly classified as electric waves rather than light. Electromagnetic waves in the wavelength rage of 100 μm to 1 mm are called far-infrared light, or terahertz (THz) waves.

When an electric heater glows red, it emits electromagnetic radiation covering a wide range of wavelengths from visible light centering around the red color to infrared light. Our very perception of its warmth is caused by the skin tissue on the surface of our bodies absorbing such electromagnetic radiation and thus being excited, their energy then to be converted into heat and cause a rise in temperature on our body surface.

Emission and absorption of infrared light are ubiquitous events. It is also something that happens on the global scale, as the Earth's surface constantly emits infrared light and the air both absorbs it and emits it. In this sense, we can say that the emission and absorption of infrared light is an important factor governing the global environment.

Today, satellites equipped with infrared detectors have been sent into orbit around the Earth to investigate the global atmospheric environment, and they monitor light in the infrared wavelength region emitted from the surface of the Earth. The spectrum shown in Fig. 1.5 gives an example of measurements performed by a satellite sent into orbit at the altitude of 800 km. The term "spectrum" is applied to a diagram which plots the transmittance or emission intensity of light, along the ordinate, as a function of its wavelength or wave number, a reciprocal of the wavelength, along the abscissa. In the case of this figure, the ordinate represents the radiation intensity of the infrared light.

Before we discuss this figure in depth, let us explain the idea of wave numbers, which here are plotted on the abscissa. A wave number is defined as the reciprocal

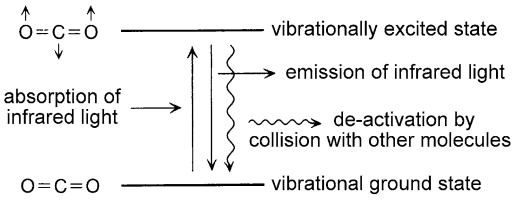

Fig. 1.6 Absorption and emission of infrared light by a CO_2 molecule

of a wavelength of light, as

$$\tilde{\nu} = \frac{1}{\lambda}, \tag{1.18}$$

and is usually expressed in the unit of cm^{-1}. In other words, a wave number describes how many periods of waves there are in 1 cm of light waves. Thus from Eqs. (1.12) and (1.18), we can write the energy of light as

$$\varepsilon = hc\tilde{\nu}. \tag{1.19}$$

The unit cm^{-1} used for wave numbers is called the reciprocal centimeter, or simply the centimeter-minus-one. In the past, the symbol K has been used, pronounced as "kayser," but this unit is no longer in use today.

When the wavelength of light is 5 μm, for example, the corresponding wave number is derived as

$$\tilde{\nu} = \frac{1}{5 \times 10^{-6}\ \mathrm{m}} = \frac{1}{5 \times 10^{-4}\ \mathrm{cm}} = 2000\ \mathrm{cm}^{-1}.$$

This value can be easily converted into the energy of the light, by multiplying it by hc. For green light with the wavelength of 500 nm, the wave number is calculated as

$$\tilde{\nu} = \frac{1}{500 \times 10^{-9}\ \mathrm{m}} = \frac{1}{5 \times 10^{-5}\ \mathrm{cm}} = 20000\ \mathrm{cm}^{-1}.$$

Thus we see that a photon of visible light whose wavelength is 500 nm = 0.5 μm has ten times the energy of a photon of infrared light with the wavelength of 5 μm.

One thing that we notice in Fig. 1.5 is that the radiation intensity of the observed light gradually decreases as the wave number increases, or the infrared light emitted from the Earth becomes weaker the shorter its wavelength. This pattern of the radiation intensity corresponds to the intensity distribution of black body radiation at 295 K, indicating that the surface temperature of the Earth is 295 K. Now, what merits our attention is that there are three dips in this spectrum, appearing at around 700, 1040, and 1600 cm^{-1}. These dips in intensity are known to be caused by the carbon dioxide (CO_2), ozone (O_3), and water (H_2O) molecules in the atmosphere, as they each absorb infrared light of specific wavelengths.

In the case of CO_2, for example, we know that a molecule absorbs infrared light of around 667 cm^{-1} and vibrates in what is called a bending vibration mode (the ν_2

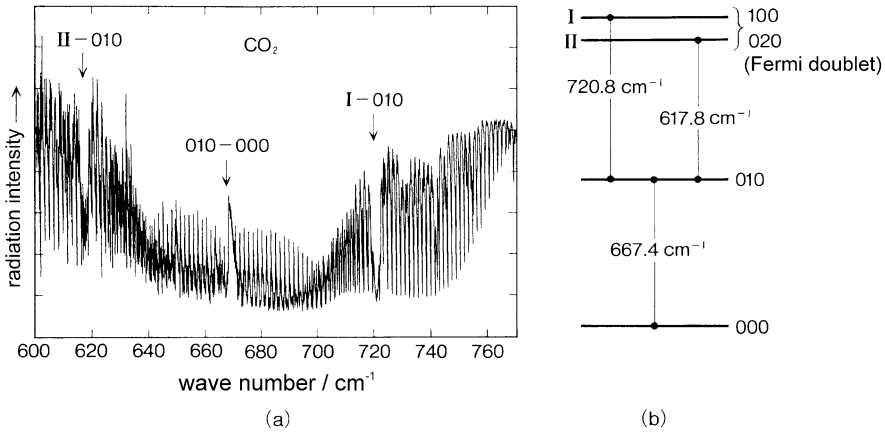

Fig. 1.7 (**a**) Magnified view of Fig. 1.5 around the area of the ν_2-mode absorption band for CO_2; (**b**) Relationship between the observed transitions and energy levels; The three digit numbers such as 010 given in the figure signify the vibrational quantum numbers for the symmetric stretching vibration, the bending vibration, and the anti-symmetric stretching vibration, respectively, from left to right

mode), where its skeletal structure bends back and forth. This means that, by absorbing this infrared light, CO_2 is excited to its vibrationally excited state, as schematically shown in Fig. 1.6. The energy gained by the infrared photoabsorption may be lost from the vibrationally exited molecule through a photo emission process, or it may be converted into kinetic energy when the CO_2 molecule collides with another molecule in the atmosphere. It is also possible for a vibrationally excited molecule to receive energy through a collision with another molecule and be excited to a state with even higher vibrational energy. Of the infrared light emitted by vibrationally excited CO_2 molecules, most is absorbed again by other CO_2 molecules in the atmosphere.

As has been described, molecules in the atmosphere such as CO_2 continuously repeat the cycle of absorption and emission of infrared light, as well as collide with each other randomly, which induce excitation and de-excitation. As a consequence, radiation equilibrium and thermal equilibrium are both achieved at any given time. Another significance of the atmosphere containing infrared-absorbing molecules is that the infrared light emitted from the surface of the Earth becomes trapped by these molecules and thus less likely to escape into outer space. It follows, therefore, that if the concentration of molecules in the atmosphere that absorb infrared light at a higher efficiency increases, then more infrared light is trapped in the atmosphere, causing the atmospheric temperature to rise. This is what we commonly call the greenhouse effect.

Taking into consideration the above discussion, we cannot regard the observed emission spectrum of infrared light shown in Fig. 1.5 as a simple result of the molecules in the atmosphere absorbing the infrared light emitted by the Earth. This point becomes clearer when we look at Fig. 1.7(a), which gives us a magnified view

of the spectral region surrounding 667 cm^{-1} in Fig. 1.5. In the center of Fig. 1.7(a) around 667 cm^{-1}, we see a thick, intense peak protruding upward. This peak indicates that we have observed infrared light being emitted from CO_2 molecules as they change their state from the state in which bending vibration is excited to the state in which it is not. The two thick downward peaks seen on both sides of this upward peak, on the other hand, at around 618 cm^{-1} and 721 cm^{-1}, correspond to the infrared absorption that occurs when molecules in the bending excited state are further excited to the two levels with higher vibrational energies. As illustrated in Fig. 1.7(b), these two states are formed as a mixture of the state in which the bending vibration is doubly excited and the state in which the two C=O bonds stretch and shrink in phase, through a mechanism called Fermi resonance. These two adjacent levels produced by Fermi resonance are referred to as the Fermi doublet.

Let us see why, then, the peak at 667 cm^{-1} is observed as an emission peak, and the two peaks on the sides of it as absorption peaks. With CO_2, its photoabsorption efficiency for infrared light around 667 cm^{-1} is extremely large, so that this range of infrared light emitted from the surface of the Earth is almost entirely trapped by the atmosphere as it propagates through the troposphere (0 to 20 km) and the stratosphere (15 to 50 km). This results in the infrared light emitted from CO_2 molecules around the top of the stratosphere (at altitudes exceeding 30 km) emerging in the observation as an emission peak. On both sides of this, on the other hand, there are areas where the absorption efficiencies of CO_2 are not so large, which is where the two peaks originating from the Fermi doublet are observed. Thus the spectral profile of the infrared light absorbed by the atmosphere near the surface of the Earth is maintained until it reaches the satellite, and this causes the two peaks to appear as absorption peaks.

In Fig. 1.7(a), we can also observe sharp, spike-like peaks on both sides of the peak at 667 cm^{-1}, as well as on both sides of the two Fermi-doublet peaks. These peaks can be attributed to the rotational structure of CO_2 molecules, which appears in the spectrum thanks to the wavelength resolution of this spectral measurement being as high as 0.05 cm^{-1}.

As we will learn in Sect. 3.6, such a type of spectrum is called a vibration-rotation spectrum. The thick central peak is referred to as the Q-branch ($\Delta J = 0$), the succession of sharp peaks on the side of it with higher wave numbers as the R-branch ($\Delta J = 1$), and the succession of sharp peaks on the other side, where the wave numbers are low, as the P-branch ($\Delta J = -1$). The J used in the parentheses ( ) here is called a rotational quantum number, which will be further discussed in Chap. 3, Rotating Molecules.

An important lesson that we can draw from the spectrum in Fig. 1.5 is that each molecular species, such as CO_2, O_3, or H_2O, has a specific set of vibrationally excited levels with its own designated energies. The dip appearing in this spectrum around 1040 cm^{-1} is ascribed to a vibrational motion of O_3 called the antisymmetric vibrational motion (the ν_3 mode), and the broad dip around 1600 cm^{-1} to the bending vibration (the ν_2 mode) of H_2O. These facts show that the energy of molecular vibration takes only discrete values, and that these values are intrinsic to the respective molecular species. In Chap. 2, Vibrating Molecules, we will discover

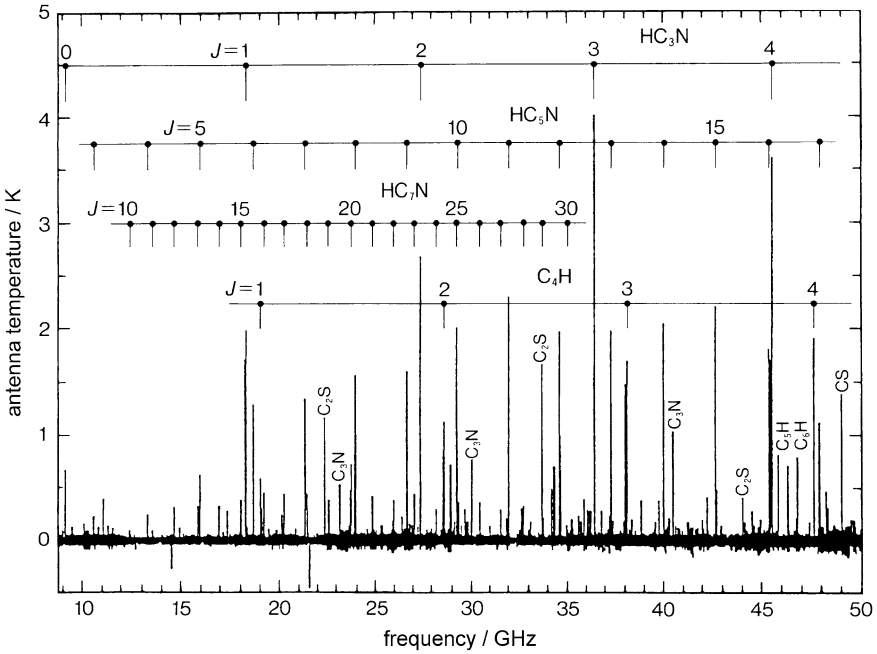

Fig. 1.8 The spectrum of the Taurus Dark Cloud observed at the Nobeyama Astronomical Observatory. The vertical axis represents the emission intensity, as converted into temperature. J stands for the rotational quantum number. For instance, $J = 3$ signifies the microwave radiation that accompanies a transition from the level of $J = 4$ to the level of $J = 3$

why the energy of molecular vibration takes discrete values by looking at the issue from the perspective of quantum theory.

1.3 Microwaves Arriving from Outer Space

In the field of radio astronomy, scientists study celestial bodies and interstellar substances by detecting electric waves in the region spanning microwaves and radio waves, or those with wavelengths from 1 mm to 30 m, which reach the Earth from outer space. Figure 1.8 shows the overall spectrum obtained by pointing a radio telescope toward the dark nebula in the constellation Taurus called TMC-1 (the Taurus Molecular Cloud 1). As annotated in the figure, the sharp peaks record microwaves radiated from mainly linear molecules, such as HC_3N (H–C≡C–C≡N), HC_5N (H–C≡C–C≡C–C≡N), and HC_7N (H–C≡C–C≡C–C≡C–C≡N). Observations of such spectra have made it clear that many kinds of molecular species exist in interstellar spaces.

An important thing to note here is that each molecular species radiates microwaves of specific frequencies. We should also pay attention to the fact that peaks

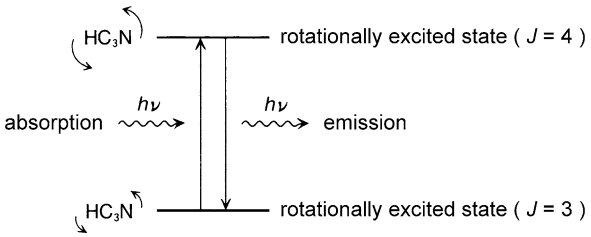

Fig. 1.9 Absorption and emission of microwave by HC_3N

belonging to the same molecular species are spaced at regular intervals in terms of frequency. For instance, the strongest peak observed in Fig. 1.8 is the transition of HC_3N, assigned as $J = 3$, and its frequency is roughly

$$\nu = 36.4 \text{ GHz} = 36.4 \times 10^9 \text{ s}^{-1},$$

its wavelength

$$\lambda = \frac{c}{\nu} = 0.824 \text{ cm}.$$

Expressed in terms of wave numbers, this becomes

$$\tilde{\nu} = \frac{1}{\lambda} = 1.21 \text{ cm}^{-1}.$$

The energy of this microwave is about 1000 times smaller than the vibrational level energies discussed in Sect. 1.2.

In fact, what causes this microwave radiation is the change of the state of the molecules from their rotationally excited state ($J = 4$) to a rotationally less excited state ($J = 3$), as illustrated in Fig. 1.9 (where J is the rotational quantum number). This shows us that the energy produced by the rotational motion of a molecule always takes a discrete value, as was the case with the vibrational motion.

We can also see from Fig. 1.8 that the intervals between adjacent peaks are narrower the longer the molecules, which hints to us that observing the energy gaps between rotational levels can lead to the determination of molecular structures. These intervals between adjacent peaks are in fact nearly equal to twice the values of what is called the rotational constants of the molecules. A rotational constant, in turn, is known to be inversely proportional to the moment of inertia of each molecule.

Therefore, by observing a rotational spectrum, we can calculate the moment of inertia of the molecule, and determine the structure of the molecule. In Chap. 3, Rotating Molecules, we examine this rotational motion of molecules from the standpoint of quantum theory, and discuss discrete energy levels and molecular structures.

1.4 The Hierarchical Structure of Molecular Energy Levels

As we have seen, we can irradiate molecules with light of specific wavelengths to excite them to a higher energy level. Such levels are classified into three types:

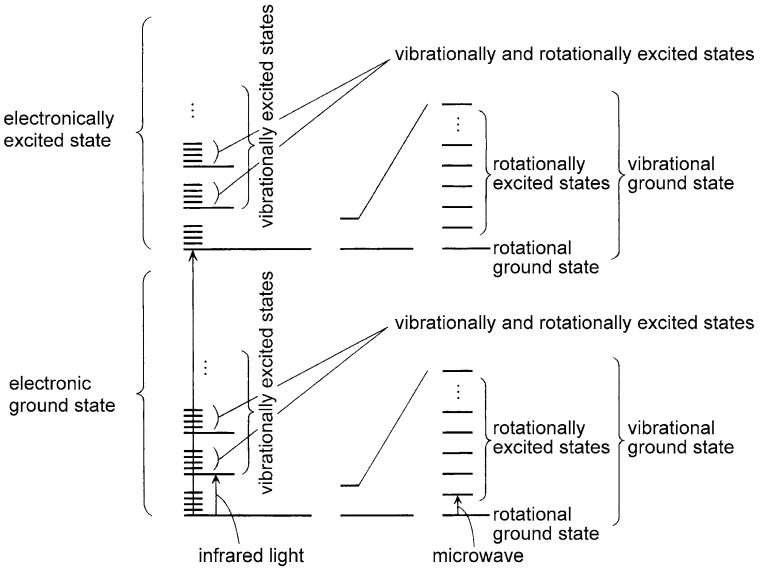

Fig. 1.10 The hierarchical structure of the energy levels of molecules

the level of the electronically excited state, that of the vibrationally excited state, and that of the rotationally excited state.

To excite a molecule to its electronically excited state, what is used is light in the visible or ultraviolet region, and the energy of its photons is 5×10^4 to 1×10^4 cm^{-1} in most cases. To excite a molecule to its vibrationally excited state, light in the infrared region is used, and the energy of its photons is usually 4×10^3 to 1×10^2 cm^{-1}. For the rotationally excited state, microwave is used, and the energy of its photon tends to be 2 to 0.5 cm^{-1}. This relationship found in the energy levels of molecules is illustrated in Fig. 1.10. What this shows is the hierarchical nature of energy levels, which is a characteristic feature of molecules, as they have three different types of excited states, electronic, vibrational, and rotational.

We will examine molecular vibration and molecular rotation in depth, from the point of quantum theory, in Chaps. 2 and 3, respectively. As will be discussed in Chap. 3, molecular vibration and rotation can occur simultaneously. This molecular state corresponds to the state in which both vibration and rotation are excited, as shown in Fig. 1.10. As we will learn in Chap. 3, we can determine the geometrical structure of a molecule from the energy of its rotational level. We can also determine molecular structures from rotational structures observed in vibrational spectra.

Another powerful method for determining the structures of molecules is the electron diffraction method. Chapter 4, Scattering Electrons, is concerned with grasping the principles of this method through a discussion based on the quantum theory of electron scattering. Let us briefly take a look at this electron diffraction method in the next section.

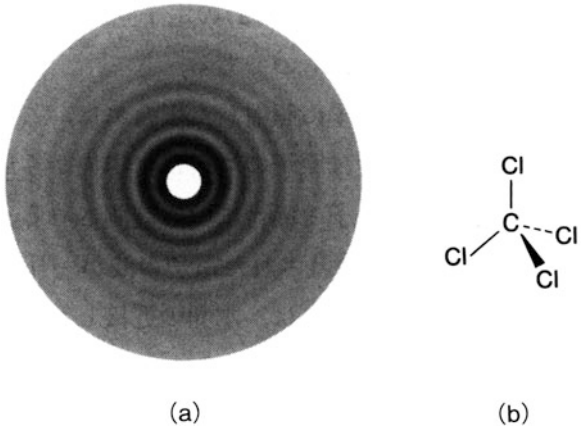

Fig. 1.11 An electron diffraction photograph (**a**) and the molecular structure of carbon tetrachloride (CCl_4) (**b**)

1.5 The Diffraction of Electron Beams and Molecular Structures

An experiment performed by Davidsson, Germer, Kikuchi, and Thompson in the late 1920s revealed that a diffraction image can be observed when we irradiate an accelerated electron beam onto a solid target such as metallic foil. This is a well-known case of the electron being shown to have the property of a wave. The wavelength of this electron is expressed as

$$\lambda = \frac{h}{m_e v}, \tag{1.20}$$

where m_e stands for the mass of the electron and v for the speed of the electron. When we view particles as waves, such as in this case, these waves are called matter waves or de Broglie waves. With electron beams, increasing the accelerating voltage causes the speed v to increase and the wavelength λ to decrease.

Due to such wave-like properties of electrons, we can observe highly interesting phenomena when we irradiate molecules in the gas phase with an electron beam. In an electron diffraction experiment, we accelerate electrons to around 10 to 60 keV and irradiate the gas target with them to record the scattered electrons on a photographic plate. Figure 1.11(a) shows one such electron diffraction photograph of carbon tetrachloride (CCl_4).

A point worth noting in this photograph is that we can observe in it a clear repetition of concentric rings formed by the dark and light shades of gray, which spread from the central area to the circumference. These characteristic patterns are called halos, taking its name from a term that originally refers to the ring of light often observed around the Sun or the Moon. When we observe such patterns of electron scattering, the density of electrons around the center becomes very high, with the number of scattered electrons rapidly decreasing as the distance from the center increases. Therefore, in order to obtain clearer halos we use a method called the rotating sector method, which reduces the number of electrons to reach the photo-

graphic plate the closer they are to the center. The electron diffraction photograph shown in Fig. 1.11(a) is taken using such a rotating sector.

When we irradiate an electron beam onto a group of atoms, on the other hand, we do not observe any halos. What we see in the case of atoms is a monotonic decline in the intensity of the scattered electron beam from the center outward. Halos are observed only with molecules because they are the result of the two scattered electron waves caused by each pair of atoms within each molecule interfering with each other. This situation can be compared to the way in which two sets of ripples interfere with one another on a water surface when we simultaneously throw in two stones at adjacent spots. Obviously, molecules in the gas phase point in various directions in space, with no spatially fixed alignment. However, as we will discuss in detail in Chap. 4, Scattering Electrons, when all of the interference patterns of the electrons scattered by the randomly oriented molecules add up together, what emerges is a pattern of halos such as the one shown in Fig. 1.11(a).

Let us then first consider a case where electrons are scattered by a triatomic molecule ABC, which can be, for example, a SO_2 or OCS molecule. The electrons form an interference pattern as they are scattered by atoms A and B, while at the same time they form another interference pattern as they are scattered by atoms B and C, and yet another as they are scattered by atoms A and C, even though this last pair of atoms are not directly linked by a chemical bond. Halos created by triatomic molecules are thus observed as a sum of these three types of interference patterns. In the case of carbon tetrachloride, too, we can look at the creation of the halos in a similar vein. A carbon tetrachloride molecule is known to have a regular tetrahedral structure as schematized in Fig. 1.11(b). There are four sets of atom pairs between the C atom and the Cl atoms to be found in this molecule, and these are all equivalent. Thus when electrons reach a carbon tetrachloride molecule as a wave, they are scattered by these four atom pairs to produce the same interference pattern. At the same time, there are six combinations of two Cl atoms to be found, none of them chemically bound, and all of these can be considered to give the same interference pattern, too. Therefore, the halos to be observed are created as a sum of these two types of interference patterns.

To explain this in more detail, we will now turn to some simulations of the molecular scattering curve which take the scattering degree of the electron as the vertical axis, and a variable s, called the scattering parameter, as the horizontal axis. We can assume that the scattering parameter is proportional to the distance of the point on the photographic plate where electrons hit as measured from the center of the circle shown in Fig. 1.11(a) in the direction of the radius. Now, the effect of the interference caused by the four sets of combinations between a C atom and a Cl atom can be represented by the molecular scattering curve shown in Fig. 1.12(b). This expresses a sine function with a specific period, whose amplitude decreases as s increases. When we Fourier transform this function, we can see that it consists of one component, as shown in Fig. 1.12(e).

This type of figure is called a radial distribution curve, and its horizontal axis represents the internuclear distance between the two atoms within the molecule. Thus, we can calculate the internuclear distance between the C atom and each of

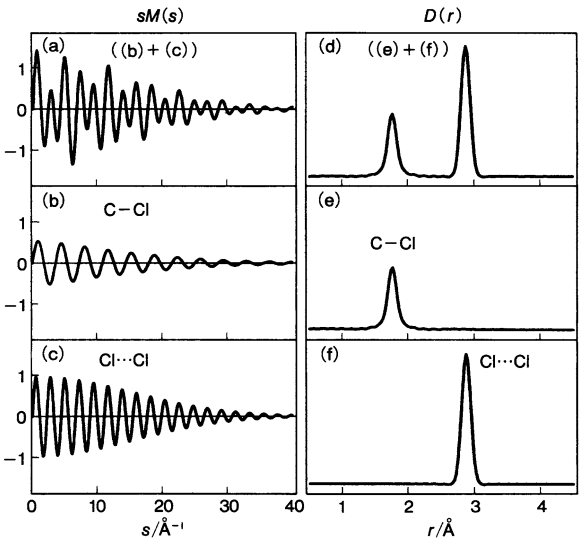

Fig. 1.12 A simulated molecular scattering curve ($sM(s)$) (**a**) and radial distribution curve ($D(r)$) (**d**) for CCl_4. The contribution of each type of atom pair in $sM(s)$ is given in (**b**) and (**c**) and that in $D(r)$ is given in (**e**) and (**f**)

the Cl atoms from the molecular scattering curve. Turning next to the interference effect caused by the six non-bonded atom pairs between two Cl atoms, we obtain a molecular scattering curve as shown in Fig. 1.12(c). When we Fourier transform this function, we can obtain the radial distribution curve shown in Fig. 1.12(f). When we compare Figs. 1.12(b) and 1.12(c), we see that the interval between adjacent dark shades in halos is smaller for the atom pair with the longer internuclear distance.

What we have discussed so far are the results of simulation. In reality, the interference pattern created by the four pairs of the C and Cl atoms and the one created by the six pairs between Cl atoms are observed at once, superimposed upon each other. Therefore the overall interference pattern observed as a molecular scattering curve will be as shown in Fig. 1.12(a), which is the sum of Figs. 1.12(b) and 1.12(c). We can in fact explain the dark and light shades constituting the halos in Fig. 1.11(a) by the interference pattern of Fig. 1.12(a). When we Fourier transform this molecular scattering curve, we obtain a radial distribution curve that has two peaks, as shown in Fig. 1.12(d). Needless to say, the positions of these two peaks reflect the internuclear distances of the C–Cl bond and of the non-bonded atom pair Cl···Cl. By synthesizing the interference patterns using these internuclear distances as variables so that they reproduce the observed interference patterns in the actual photograph, we obtain $r(\text{Cl–Cl}) = 1.767$ Å and $r(\text{Cl}\cdots\text{Cl}) = 2.888$ Å.

So far we have used the word "internuclear distance" to express the distance between two atoms, but sometimes this distance is called the "interatomic distance." In many cases these two terms are used interchangeably, but when we discuss molecular geometry in this textbook, we are not taking into account the positions of the electron in each atom, so it would be more appropriate to use the term "internuclear distance." It is for this reason that we adopt this terminology throughout this book, whether we are talking about molecular structures determined by molecular spectroscopy or those calculated by the electron diffraction method.

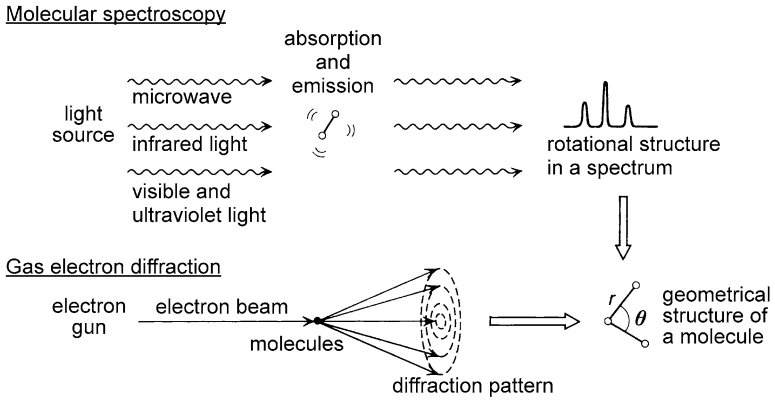

Fig. 1.13 Methods of determination of the geometrical structure of molecules using molecular spectroscopy and gas electron diffraction

As we have briefly shown in this section, it is possible to determine the geometrical structure of molecules by using the phenomenon where electron beams are scattered by molecules. In Chap. 4, Scattering Electrons, we will examine the scattering process from the point of view of quantum mechanics, to better understand the meaning of the molecular structures determined from electron diffraction images that are obtained through scattering. One issue that will be discussed, for instance, is the fact that the peaks shown in Fig. 1.12(d) have a width, which points to a certain distribution range that must be present in internuclear distances. Does this then mean that the structure of molecules is fluctuating? Such questions will be answered when we learn the quantum mechanics of the vibrational motion of molecules in Chap. 2, Vibrating Molecules.

Finally, when we fully recognize the different meanings of the molecular structures determined by the electron diffraction method and those determined by the method discussed in Chap. 3, Rotating Molecules, we will have reached a fundamental understanding concerning the nature of the motion and geometrical structure of molecules as they exist in the microscopic universe governed by the law of quantum mechanics.

1.6 Methods of Molecular Structure Determination

The way in which the methods discussed so far contribute to the determination of molecular structures is shown schematically in Fig. 1.13, and as a flow chart in Fig. 1.14. In molecular spectroscopy, we obtain the energies of discrete levels of a molecule by taking advantage of the absorption and emission of light observed in molecules. To determine the geometrical structure of a molecule, we mainly look for the energy level associated with its rotational motion, so that we can calculate the moment of inertia for the molecule. Once we have the moment of inertia, we

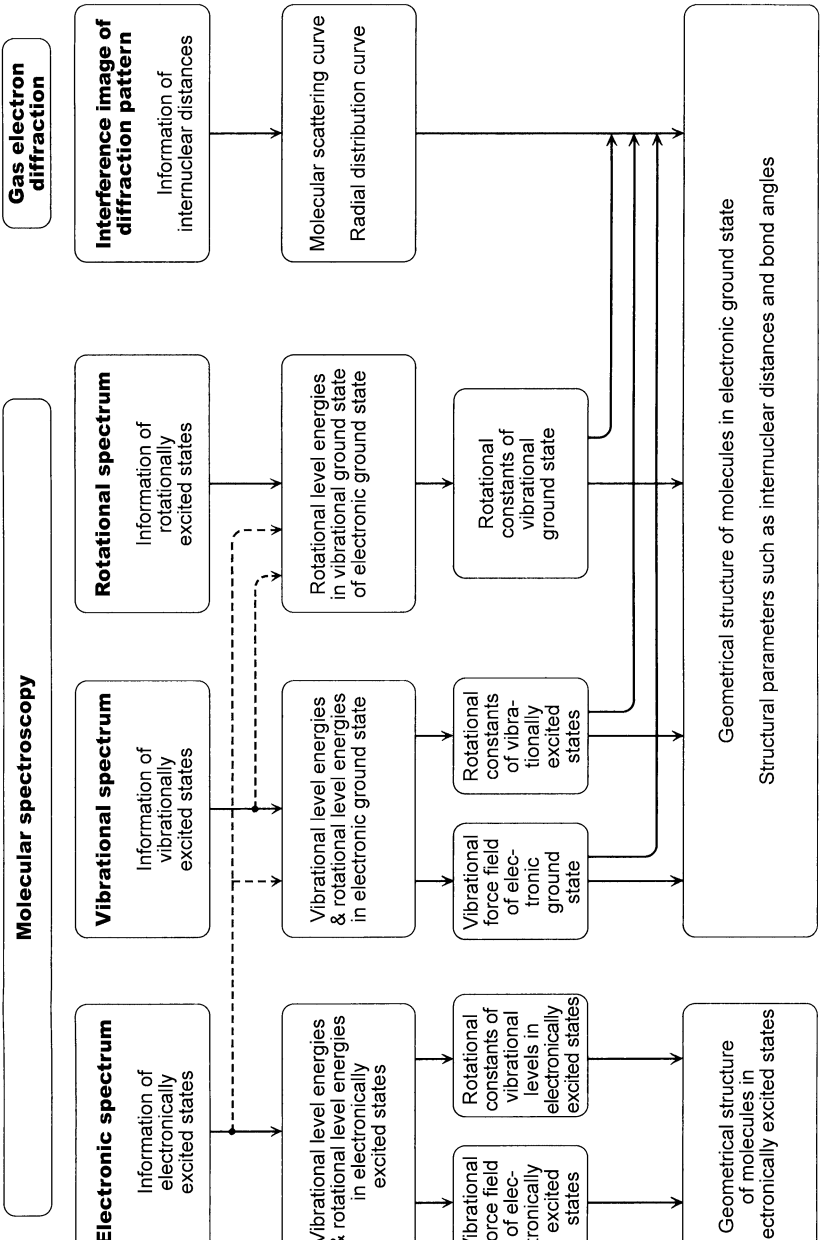

Fig. 1.14 Flow chart for the determination of geometrical structures of molecules

can determine the distances between the atoms that compose the molecule, or the internuclear distances. We can also determine the molecular structure of a molecule at its electronic ground state or its electronically excited state by observing the rotational structure of its absorption and emission spectra of the electronic transition in the visible and ultraviolet regions. An alternative to these spectroscopic methods is the electron diffraction method discussed in Sect. 1.5. When molecules are in the gas phase, their geometrical structures have been determined though rotational structures observed in the molecular spectroscopic method as well as through electron diffraction images obtained by the electron diffraction method.

Chapter 2
Vibrating Molecules

When we visualize the geometrical structure of molecules, we think of it as a static image consisting of bond lengths and angles. In reality, however, chemically bound atoms are constantly changing their positions with each other. This dynamical motion is called molecular vibration. A point of note is that this vibration is qualitatively different from what has been described as vibration in classical mechanics. As introduced in Chap. 1, the energy of molecular vibration can only take discrete values. Explaining this experimental observation requires the introduction of quantum mechanics. In this chapter, we will learn how to treat molecular vibration using quantum mechanics. We also seek to understand the meaning of eigenenergy and eigenfunction in quantum mechanics by looking at the case of molecules. Finally, we will discover that the number of normal modes based on which the vibrational form of polyatomic molecules can be described is equal to the number of vibrational degrees of freedom, by taking triatomic molecules as a concrete example.

Summaries

2.1 How to Describe Vibrating Molecules
The vibration of diatomic molecules are treated within the theory of classical mechanics. We will learn that in classical mechanics, energy is transferred between kinetic energy and potential energy.

2.2 Molecular Vibration in Quantum Theory
The harmonic oscillator, a model for diatomic molecules, will be discussed within quantum theory. We will learn that, by solving the Schrödinger equation, we can obtain the discrete energy level as the eigenvalue and the vibrational wave function as the eigenfunction. We will demonstrate that the form of the potential can be determined by observing the infrared absorption, and investigate the characteristics of the eigenfunction of the harmonic oscillator.

2.3 The Harmonic Oscillator and Its Applications
Using the eigenfunction of the harmonic oscillator, we will learn how to calculate the expectation value and evaluate the matrix elements. We will also learn how to use creation and annihilation operators in the evaluation of perturbation

K. Yamanouchi, *Quantum Mechanics of Molecular Structures*,
DOI 10.1007/978-3-642-32381-2_2,

energy. We will then introduce the Morse potential, which is a model for the potential of real molecules, and will develop a better understanding of molecular vibration by reference to experimental data.

2.4 The Inversion Motion of Ammonia Molecules

We seek to further our understanding of the inversion motion of ammonia molecules from the standpoint of quantum mechanics. We will note that the existence of a double-minimum potential can be identified in the observed spectrum of infrared absorption. Then we will learn that the wave packet, which is a superposition of wave functions, evolves with time and causes inversion motion.

2.5 How to Treat the Vibration of Polyatomic Molecules

After reviewing the degrees of freedom of vibration, we discuss the vibration of polyatomic molecules, which consist of three or more atoms. In particular, we learn that, in classical mechanics, there are modes of vibration in which a molecule vibrates as a whole along the normal coordinates. These modes are called normal modes. Then we discuss quantum theory, in which a harmonic oscillator is assigned to each normal mode, and the wave function of the whole molecule is described as the product of the wave functions of these harmonic oscillators. To derive a normal mode vibration, we introduce the internal coordinates, and learn the GF matrix method with concrete examples. Furthermore, we will discuss real molecules with anharmonicity, and learn that their multidimensional potential energy surfaces and wave functions are obtained from the experimental spectral data.

2.1 How to Describe Vibrating Molecules

Let us take a diatomic molecule AB, and identify the masses of the constituent atoms A and B as m_A and m_B. In classical mechanics, the kinetic energy T is given by

$$\begin{aligned} T &= \frac{1}{2}m_\mathrm{A}\boldsymbol{v}_\mathrm{A}^2 + \frac{1}{2}m_\mathrm{B}\boldsymbol{v}_\mathrm{B}^2 \\ &= \frac{1}{2}(m_\mathrm{A}+m_\mathrm{B})\left|\frac{m_\mathrm{A}\boldsymbol{v}_\mathrm{A}+m_\mathrm{B}\boldsymbol{v}_\mathrm{B}}{m_\mathrm{A}+m_\mathrm{B}}\right|^2 + \frac{1}{2}\left(\frac{m_\mathrm{A}m_\mathrm{B}}{m_\mathrm{A}+m_\mathrm{B}}\right)|\boldsymbol{v}_\mathrm{A}-\boldsymbol{v}_\mathrm{B}|^2 \end{aligned} \tag{2.1}$$

where $\boldsymbol{v}_\mathrm{A}$ and $\boldsymbol{v}_\mathrm{B}$ are the time derivatives of the three-dimensional position vectors of the corresponding atoms: $\boldsymbol{v}_\mathrm{A} = \frac{\mathrm{d}\boldsymbol{r}_\mathrm{A}}{\mathrm{d}t}$, $\boldsymbol{v}_\mathrm{B} = \frac{\mathrm{d}\boldsymbol{r}_\mathrm{B}}{\mathrm{d}t}$. When the molecule is thought of as two atoms bound with a spring, the potential energy V can be approximated by

$$V = \frac{1}{2}k(\boldsymbol{r}_\mathrm{AB}-\boldsymbol{r}_\mathrm{e})^2 \tag{2.2}$$

using the distance between A and B, $r_\mathrm{AB} = |\boldsymbol{r}_\mathrm{B}-\boldsymbol{r}_\mathrm{A}|$. Here, r_e represents the atomic distance where the potential energy is 0. This distance is called the *equilibrium internuclear distance*, and the subscript "e" stands for "equilibrium." As for $k(>0)$, this is the spring constant. From here on, the spring constant will be called the force constant. When the form of the potential represented as a function of a displacement

is given by a second-order function as in Eq. (2.2), it is called a harmonic potential. Therefore, in this approximation, the diatomic molecule is treated as a harmonic oscillator.

The first term of Eq. (2.1), a representation of kinetic energy, describes the kinetic energy of the center of mass of the entire molecule. What we are interested in is the relative motion of atoms in the molecule, so we set aside the overall center-of-mass motion, and focus solely on the second term, which represents the vibrational energy. Thus, the reduced mass μ is defined as

$$\mu = \frac{m_{\mathrm{A}} m_{\mathrm{B}}}{m_{\mathrm{A}} + m_{\mathrm{B}}}, \tag{2.3}$$

and therefore, the total energy H of the molecular vibration is given by

$$\begin{aligned} H &= [\text{the second term in Eq. (2.1)}] + V \\ &= \frac{1}{2}\mu |\boldsymbol{v}_{\mathrm{A}} - \boldsymbol{v}_{\mathrm{B}}|^2 + \frac{1}{2}k(r_{\mathrm{AB}} - r_{\mathrm{e}})^2. \end{aligned} \tag{2.4}$$

The H here is called the Hamiltonian of the molecular vibration.

Molecular vibration is described as a motion on the straight line that connects the atoms A and B, so it is convenient if we align this line with the x axis. When we consider a system where the value of B's x coordinate x_{B} is larger than the value of A's x coordinate x_{A} ($x_{\mathrm{B}} > x_{\mathrm{A}}$), the internuclear distance x_{AB} is $x_{\mathrm{AB}} = x_{\mathrm{B}} - x_{\mathrm{A}}$, and the x coordinate is represented as the deviation from the equilibrium internuclear distance, which is given by $x = x_{\mathrm{AB}} - r_{\mathrm{e}}$. That is, the origin on the x axis is the point where x_{AB} is equal to the equilibrium internuclear distance r_{e}. So the Hamiltonian of the molecular vibration can be reduced to one dimension and simply given by

$$\begin{aligned} H &= \frac{1}{2}\mu v_x^2 + \frac{1}{2}kx^2 \\ &= \frac{1}{2\mu}p_x^2 + \frac{1}{2}kx^2 \end{aligned} \tag{2.5}$$

where $v_x = \frac{\mathrm{d}x}{\mathrm{d}t} = \frac{\mathrm{d}x_{\mathrm{AB}}}{\mathrm{d}t}$ is the time derivative of x and $p_x = \mu v_x$ is the momentum. Equation (2.5) shows that molecular vibration can be described as the motion of a particle whose mass is μ.

The equation of the motion of a particle in classical mechanics is known to be

$$\frac{\mathrm{d}}{\mathrm{d}t}\left(\frac{\partial L}{\partial \dot{x}}\right) - \frac{\partial L}{\partial x} = 0 \tag{2.6}$$

where L is

$$L = T - V \tag{2.7}$$

and the time derivative of x is $\dot{x} = \frac{\mathrm{d}x}{\mathrm{d}t}$. This equation is called Lagrange's equation, and L is called the Lagrangian. In this system, T and V are

$$T = \frac{1}{2}\mu\dot{x}^2, \quad V = \frac{1}{2}kx^2,$$

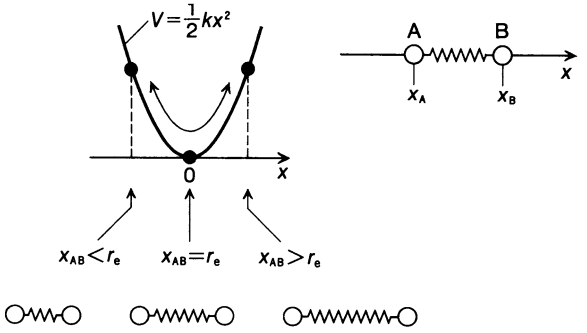

Fig. 2.1 Potential energy curve of diatomic molecule AB and the definition of the internuclear distance

so Lagrange's equation becomes

$$\mu\ddot{x} = -kx, \tag{2.8}$$

where $\ddot{x}$ represents the second-order time derivative $\ddot{x} = \frac{\mathrm{d}}{\mathrm{d}t}\dot{x} = \frac{\mathrm{d}^2x}{\mathrm{d}t^2}$, that is, acceleration. Equation (2.8) is Newton's equation of motion where the restoring force f is $f = -kx$.

This equation can be solved easily. For example, defining A as a positive constant, x is written as

$$x = A\sin\omega t \quad (\omega > 0). \tag{2.9}$$

The time dependence of this value is illustrated in Fig. 2.2(i). Since the left-hand side of this equation becomes $-\mu\omega^2 A\sin\omega t$, and the right-hand side becomes $-kA\sin\omega t$, we obtain the following equation by comparing these two coefficients:

$$k = \mu\omega^2. \tag{2.10}$$

Therefore, $x = A\sin\omega t$ is the solution of the differential equation (2.8) when

$$\omega = \sqrt{\frac{k}{\mu}}. \tag{2.11}$$

Naturally, either the formula illustrated in Fig. 2.2(ii)

$$x = A\sin(\omega t + \delta) \quad (\delta \text{ is a constant which satisfies } 0 \leqq \delta < 2\pi) \tag{2.12}$$

or the formula illustrated in (iii)

$$x = A\cos\omega t \tag{2.13}$$

can be the solution of Eq. (2.8) when $\omega = \sqrt{\frac{k}{\mu}}$. This type of motion is called *simple harmonic oscillation*. In classical mechanics, harmonic oscillators can be said to perform simple harmonic oscillations.

Of the three solutions (2.9), (2.12), and (2.13), Eq. (2.12) can be thought of as the general solution, since it matches Eq. (2.9) when $\delta = 0$, and it matches Eq. (2.13) when $\delta = \frac{\pi}{2}$. The value of δ is determined by the initial conditions.

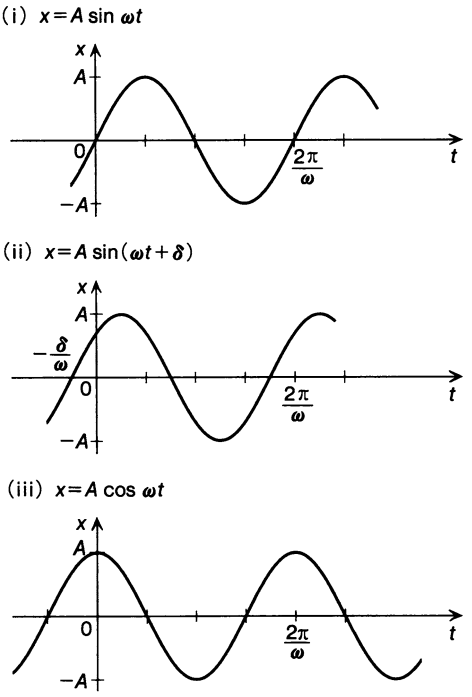

Fig. 2.2 Motion of a mass point in a harmonic potential

If Eq. (2.12) is given the initial condition of displacement $x = 0$ when $t = 0$, then from $0 = A \sin \delta$ we obtain $\delta = 0, \pi$, that is $x = A \sin \omega t$ or $x = -A \sin \omega t$. In both cases, the kinetic energy T and the potential energy V of this vibrational motion are calculated as:

$$T = \frac{1}{2}\mu \dot{x}^2 = \frac{1}{2}\mu(\omega A \cos \omega t)^2$$
$$= \frac{1}{2}\mu\omega^2 A^2 \cos^2 \omega t, \tag{2.14}$$
$$V = \frac{1}{2}kx^2 = \frac{1}{2}kA^2 \sin^2 \omega t$$
$$= \frac{1}{2}\mu\omega^2 A^2 \sin^2 \omega t. \tag{2.15}$$

These equations are plotted in Fig. 2.3. T and V alternately repeat an increase and a decrease as time lapses. At time $t = 0, \frac{\pi}{\omega}, \frac{2\pi}{\omega}, \ldots$, $V = 0$ and all of the energy exists as kinetic energy $T = \frac{1}{2}\mu\omega^2 A^2$. As $V = 0$, the displacement x is $x = 0$, and as shown in Fig. 2.1, the internuclear distance is $x_{AB} = r_e$. That is, the velocity is the maximum when passing through this point $x = 0$. On the other hand, at time $t = \frac{\pi}{2\omega}, \frac{3\pi}{2\omega}, \frac{5\pi}{2\omega}, \ldots$, $T = 0$ and $V = \frac{1}{2}\mu\omega^2 A^2 \sin^2(\omega \cdot \frac{\pi}{2\omega}) = \frac{1}{2}\mu\omega^2 A^2$, showing that all of the energy that existed as kinetic energy at $t = 0$ becomes potential energy.

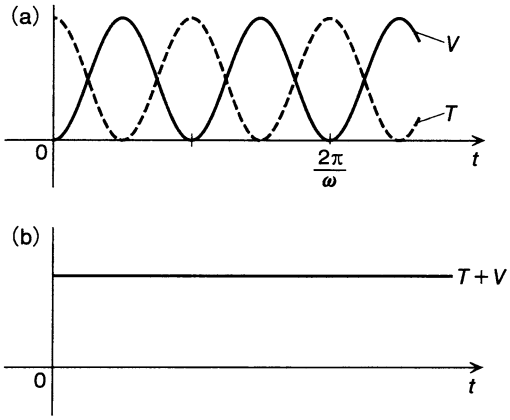

Fig. 2.3 Time evolution of the kinetic energy T and the potential energy V of a harmonic oscillator (**a**) and that of the sum of T and V (**b**)

Next, the total energy H is calculated by

$$H = T + V = \frac{1}{2}\mu\omega^2 A^2. \tag{2.16}$$

This shows that H has no time dependence and is a constant which is proportional to the squared amplitude A^2. Therefore, by changing the amplitude A, we can change the energy of the vibrational motion continuously.

In Chap. 1, the energy of the vibration of a molecule is introduced as a discrete value which is unique to each molecular species. However, as we have discussed in this subsection, the energy cannot be discrete as long as the vibration of diatomic molecules is treated in classical mechanics. This does not allow us to explain the experimental observation that molecules absorb light with specific wavelengths, inducing the excitation of vibrational motions. In order to introduce the notion of discreteness of energy, molecular vibration needs to be treated in quantum mechanics.

2.2 Molecular Vibration in Quantum Theory

In the previous section, we have treated the vibration of diatomic molecules in classical mechanics. When a diatomic molecule is thought of as a harmonic oscillator, its vibration is described as a simple harmonic oscillator and the kinetic energy and the potential energy have time dependence as illustrated in Fig. 2.3. However, in classical mechanics, there is the problem of the energy not being discrete. Therefore, we now turn to quantum mechanics, the mechanics for describing the motion of microscopic particles, to treat the motion of harmonic oscillators. Here, we use the word "quantum theory" to refer to discussions and treatments based on quantum mechanics.

2.2.1 Quantizing the Harmonic Oscillator

Following the procedure of quantum theory,

$$x \to \hat{x}, \tag{2.17}$$

$$p_x \to -\mathrm{i}\hbar\frac{\partial}{\partial x}, \tag{2.18}$$

where the Hamiltonian in classical mechanics is changed into the operator, and we obtain the one-dimensional Schrödinger equation

$$\hat{H}\psi = E\psi. \tag{2.19}$$

The operator $\hat{x}$ in Eq. (2.17) means multiplication of x. As it is cumbersome to add a caret($\hat{}$) to each operator, however, from here on operators are written without the carets.

In quantum theory, solving the Schrödinger equation (2.19) under the boundary condition which satisfies the wave function $\psi(x)$, E is obtained as an eigenvalue and $\psi(x)$ is calculated as its corresponding eigenfunction. Usually, the wave function $\psi(x)$ is required to be finite, continuous, and single-valued.

In the case of one-dimensional harmonic oscillators, the concrete form of the Schrödinger equation is given by

$$-\frac{\hbar^2}{2\mu}\frac{\mathrm{d}^2}{\mathrm{d}x^2}\psi(x) + \frac{1}{2}kx^2\psi(x) = E\psi(x). \tag{2.20}$$

The potential term of this equation consists solely of terms proportional to x^2. As previously discussed, potentials such as this are called harmonic potentials. At $x \to \pm\infty$, the potential term $\frac{1}{2}kx^2$ reaches infinity. For E to remain a finite value, $\psi(x)$ must become $\psi(x) \to 0$ at $x \to \pm\infty$. This is the boundary condition which $\psi(x)$ has to satisfy.

2.2.2 The Energy Level of the Harmonic Oscillator

Before solving the Schrödinger equation (2.20), let us go over some basic considerations. Firstly, in Eq. (2.20), when the potential energy is equal to the eigenvalue, that is, when

$$\frac{1}{2}ka^2 = E \tag{2.21}$$

holds at $x = a$, the eigenfunction $\psi(x)$ satisfies

$$\left[\frac{\mathrm{d}^2}{\mathrm{d}x^2}\psi(x)\right]_{x=a} = 0. \tag{2.22}$$

Equation (2.22) signifies that there is an inflection point on the wave function $\psi(x)$ at $x = a$.

In the range $x \gg a$, the term $\frac{1}{2}kx^2\psi(x)$ is much larger than the term $E\psi(x)$. Thus, in such an asymptotic region where the absolute value of x is large, $\psi(x)$ satisfies the following relation:

$$\frac{\hbar^2}{2\mu}\frac{\mathrm{d}^2}{\mathrm{d}x^2}\psi(x) = \frac{1}{2}kx^2\psi(x). \tag{2.23}$$

The solution of this equation is easily obtained, as shown below.

To simplify matters, we describe the force constant k as

$$k = \mu\omega^2 \tag{2.24}$$

where ω is the angular frequency of the harmonic oscillator in the corresponding system of classical mechanics. Equation (2.23) can then be expressed as

$$\frac{\mathrm{d}}{\mathrm{d}\xi^2}\psi(\xi) = \xi^2\psi(\xi), \tag{2.25}$$

where ξ is

$$\xi = \sqrt{\frac{\mu\omega}{\hbar}}x \tag{2.26}$$

and, using β, which is

$$\frac{\mu\omega}{\hbar} = \beta, \tag{2.27}$$

ξ is

$$\xi = \sqrt{\beta}x. \tag{2.28}$$

Here, the function of ξ which is obtained by exchanging the x in $\psi(x)$ for $x = \sqrt{\frac{\hbar}{\mu\omega}}\xi$ should strictly be represented by a symbol other than ψ. However, as there is little possibility of confusion, in Eq. (2.25) and in the following discussion, $\psi(\xi)$ is treated as the function where the x in $\psi(x)$ is substituted by $x = \sqrt{\frac{\hbar}{\mu\omega}}\xi$.

Problem 2.1

Using the ξ given by Eq. (2.26), show that Eq. (2.23) can be described as Eq. (2.25).

Solution

From Eq. (2.26), $x = \sqrt{\frac{\hbar}{\mu\omega}}\xi$, so that

$$\frac{\mathrm{d}^2}{\mathrm{d}x^2} = \frac{\mu\omega}{\hbar}\frac{\mathrm{d}^2}{\mathrm{d}\xi^2}, \qquad \frac{1}{2}kx^2 = \frac{1}{2}\mu\omega^2\frac{\hbar}{\mu\omega}\xi^2 = \frac{1}{2}\hbar\omega\xi^2.$$

Thus, Eq. (2.23) becomes

$$\frac{\hbar^2}{2\mu}\frac{\mu\omega}{\hbar}\frac{\mathrm{d}^2}{\mathrm{d}\xi^2}\psi(\xi) = \frac{1}{2}\hbar\omega\xi^2\psi(\xi),$$

then

$$\frac{\mathrm{d}^2}{\mathrm{d}\xi^2}\psi(\xi) = \xi^2\psi(\xi). \qquad \square$$

The asymptotic solution of Eq. (2.25) when $\xi \to \pm\infty$ is

$$\psi(\xi) = C\mathrm{e}^{\pm\frac{1}{2}\xi^2} \tag{2.29}$$

where C is a coefficient. If we take the $+$ sign in the exponent, $\psi(x) \to \infty$ at $\xi \to \pm\infty$ (i.e., at $x \to \pm\infty$). This cannot be the case because it fails to satisfy the boundary condition, $\psi(x) \to 0$. Therefore, in the asymptotic region of $\xi \to \pm\infty$, the solution of Eq. (2.25) is

$$\psi(\xi) = C\mathrm{e}^{-\frac{1}{2}\xi^2}, \tag{2.30}$$

which satisfies the boundary condition.

Thus, we can write the solution of the Schrödinger equation (2.20) as

$$\psi(\xi) = u(\xi)\mathrm{e}^{-\frac{1}{2}\xi^2} \tag{2.31}$$

using the series expansion of ξ,

$$u(\xi) = a_0 + a_1\xi + a_2\xi^2 + \cdots. \tag{2.32}$$

The reason why we use this expansion is that, as long as $u(\xi)$ only has finite order terms, the asymptotic behavior at $\xi \to \pm\infty$ is dominated by the exponential part and satisfies $\psi(\xi) \to 0$. Using ξ, the Schrödinger equation (2.20) is written as

$$\frac{\mathrm{d}^2\psi}{\mathrm{d}\xi^2} + \left(\frac{\alpha}{\beta} - \xi^2\right)\psi = 0 \tag{2.33}$$

where α is

$$\frac{2\mu E}{\hbar^2} = \alpha. \tag{2.34}$$

With Eq. (2.31), the first term on the left-hand side of Eq. (2.33) is given as

$$\frac{\mathrm{d}^2\psi}{\mathrm{d}\xi^2} = \frac{\mathrm{d}^2}{\mathrm{d}\xi^2}\left(u(\xi)\mathrm{e}^{-\frac{1}{2}\xi^2}\right) = \left\{\frac{\mathrm{d}^2u}{\mathrm{d}\xi^2} - 2\xi\frac{\mathrm{d}u}{\mathrm{d}\xi} + \left(\xi^2 - 1\right)u\right\}\mathrm{e}^{-\frac{1}{2}\xi^2},$$

so that Eq. (2.33) becomes

$$\frac{\mathrm{d}^2u}{\mathrm{d}\xi^2} - 2\xi\frac{\mathrm{d}u}{\mathrm{d}\xi} + \left(\frac{\alpha}{\beta} - 1\right)u = 0. \tag{2.35}$$

Problem 2.2

Prove that the Schrödinger equation (2.20) can be written with $\xi = \sqrt{\beta}x$ as Eq. (2.33).

Solution

From $x = \frac{1}{\sqrt{\beta}}\xi$, we can derive $\frac{\mathrm{d}^2}{\mathrm{d}x^2} = \beta\frac{\mathrm{d}^2}{\mathrm{d}\xi^2}$. Using this, Eq. (2.20) is written as

$$-\frac{\hbar^2}{2\mu}\beta\frac{\mathrm{d}^2\psi}{\mathrm{d}\xi^2} + \frac{1}{2}\mu\omega^2\frac{\xi^2}{\beta}\psi = E\psi,$$

that is,

$$\frac{\mathrm{d}^2\psi}{\mathrm{d}\xi^2} + \frac{2\mu E}{\hbar^2\beta}\psi - \left(\frac{\mu^2\omega^2}{\hbar^2\beta^2}\xi^2\right)\psi = 0.$$

Then, with $\beta = \frac{\mu\omega}{\hbar}$, $\alpha = \frac{2\mu E}{\hbar^2}$, we obtain

$$\frac{\mathrm{d}^2\psi}{\mathrm{d}\xi^2} + \left(\frac{\alpha}{\beta} - \xi^2\right)\psi = 0. \qquad \square$$

Next, the series expansion of $u(\xi)$, Eq. (2.32), is substituted into Eq. (2.35). Then, comparing the same-order terms, Eq. (2.35) is written as

$$\sum_{n=0}\left\{(n+2)(n+1)a_{n+2} - 2na_n + \left(\frac{\alpha}{\beta} - 1\right)a_n\right\}\xi^n = 0. \tag{2.36}$$

For this equation to hold regardless of the value of ξ, the inside of { } has to be 0. In other words, a_{n+2} is given by a_n as

$$a_{n+2} = \frac{2n + 1 - \frac{\alpha}{\beta}}{(n+2)(n+1)}a_n. \tag{2.37}$$

This is a recurrence formula, which signifies that if a_0 is determined, its coefficients $a_2, a_4, a_6, \ldots$ can be calculated, and if a_1 is determined, $a_3, a_5, a_7, \ldots$ can be calculated.

Then the question is how far the polynomial $u(\xi)$ extends. If we suppose that the number of its terms is infinite, the value of $u(\xi)$ around $\xi \to \infty$ will be the same as e^{ξ^2}. We can see this by comparing the coefficients of the series expansion corresponding to ξ. The expanded form of e^{ξ^2} will be

$$\mathrm{e}^{\xi^2} = 1 + \xi^2 + \frac{\xi^4}{2!} + \cdots + \frac{\xi^{2n}}{n!} + \frac{\xi^{2n+2}}{(n+1)!} + \cdots, \tag{2.38}$$

which can be written as

$$\mathrm{e}^{\xi^2} = b_0 + b_2\xi^2 + b_4\xi^4 + \cdots + b_{2n}\xi^{2n} + b_{2n+2}\xi^{2n+2}. \tag{2.39}$$

By taking the ratio of the coefficient of the ξ^{2n} term and that of the ξ^{2n+2} term,

$$\frac{b_{2n+2}}{b_{2n}} = \frac{n!}{(n+1)!} = \frac{1}{n+1}. \tag{2.40}$$

Then, the substitution $2n = m$ yields

$$\frac{b_{m+2}}{b_m} = \frac{1}{\frac{m}{2} + 1}, \tag{2.41}$$

which shows that, when m is sufficiently large, the ratio of the coefficients can be written as

$$\frac{b_{m+2}}{b_m} \sim \frac{2}{m}. \tag{2.42}$$

Meanwhile, Eq. (2.37) shows that, when n is sufficiently large, the ratio of the coefficients of the series expansion of $u(\xi)$ is

$$\frac{a_{n+2}}{a_n} \sim \frac{2n}{n \cdot n} = \frac{2}{n}. \tag{2.43}$$

This ratio is the same as the ratio of the expansion coefficients of e^{ξ^2}, as can be shown from Eq. (2.42) with m replaced by n. Thus we can see that, if the series expansion shown in Eq. (2.32) continues infinitely, then the value of $u(\xi)$ will be dominated by the high-order terms when ξ is sufficiently large, causing it to coincide with e^{ξ^2}. The wave function $\psi(\xi)$ is given by Eq. (2.31), so at $\xi \to \pm\infty$ we obtain $\psi(\xi) \to e^{\xi^2} \cdot e^{-\frac{\xi^2}{2}} = e^{\frac{\xi^2}{2}}$, which diverges infinitely. As wave functions have to be finite, we see that there must be a problem with $u(\xi)$ being treated as an infinite polynominal series. Thus $u(\xi)$ is required to end at a finite number of terms, which in turn demands that the numerator of the ratio obtained from Eq. (2.37), that is,

$$\frac{a_{n+2}}{a_n} = \frac{2n + 1 - \frac{\alpha}{\beta}}{(n+2)(n+1)}, \tag{2.44}$$

be 0 at some n. This gives us

$$(2n + 1) - \frac{\alpha}{\beta} = 0. \tag{2.45}$$

By recovering the original variables in α and β using Eqs. (2.34) and (2.27), this can be written as

$$E_n = \hbar\omega\left(n + \frac{1}{2}\right) = h\nu\left(n + \frac{1}{2}\right) \quad (n = 0, 1, 2, \ldots) \tag{2.46}$$

where the eigenenergy of an assigned n is represented by E_n, because each n gives a different eigenenergy.

Equation (2.46) is what shows that the vibrational motion of a diatomic molecule can only have specific discrete energies. When a system is in a state where its energy is discrete, it is described as being quantized. Each of the states which have their specific energies is called a quantum level, or simply a level, and the number which assigns that level is called the quantum number. Using these terms, we can summarize what we have studied so far as follows.

When the potential energy of the vibrational motion of a diatomic molecule is given by $V(x) = \frac{1}{2}\mu\omega^2 x^2$, that is, when the diatomic molecule is treated as a one-dimensional harmonic oscillator, its vibrational energy is quantized and the energy of each of its vibrational levels is described by its quantum number n as

$$E_n = \hbar\omega\left(n + \frac{1}{2}\right).$$

This signifies that the vibrational energy obtains $\hbar\omega$ each time the vibrational number n increases by 1, and cannot have any intermediate value. This is illustrated in Fig. 2.4.

As Fig. 2.4 clearly shows,

$$E_0 = \frac{1}{2}\hbar\omega, \quad E_1 = \frac{3}{2}\hbar\omega, \quad E_2 = \frac{5}{2}\hbar\omega, \quad \ldots,$$

and the difference of energy between each pair of neighboring levels is equally $\hbar\omega$. The equality of the energy separations between quantum levels is a characteristic feature of quantized harmonic oscillators. This also means that the lowest energy

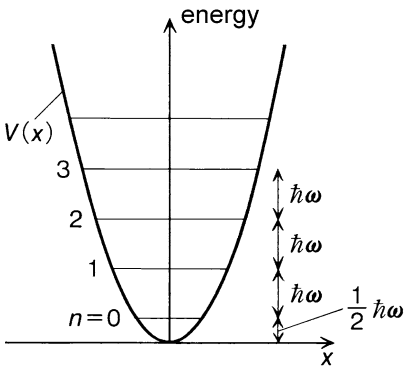

Fig. 2.4 A harmonic potential and the energy levels of a quantized harmonic oscillator

level has a finite energy value $E_0 = \frac{1}{2}\hbar\omega > 0$. In other words, the energy never becomes 0. This energy of the lowest energy level is called the zero-point energy. The level where $n = 0$ is called the vibrational ground level, and its state is called the vibrational ground state. By contrast, a level (state) where $n \geqq 1$ is called a vibrationally excited level (state).

2.2.3 Determination of Potentials by Infrared Absorption

Using what we have learned about the quantization of harmonic oscillators, we will now see that the shape of the potential for molecular vibration can be determined by the infrared absorption of molecules. As introduced in Sect. 1.2, a molecule is excited into a higher energy level by absorbing infrared light of a specific wavelength. In the case of heteronuclear diatomic molecules such as HCl or CO, a molecule in the vibrational ground state ($n = 0$) is excited into the first vibrationally excited state ($n = 1$) by absorbing infrared light.

When we view a diatomic molecule as a harmonic oscillator, the energy difference between the $n = 1$ state and the $n = 0$ state is written as

$$\Delta E = E_1 - E_0 = \hbar\omega,$$

as can be seen from Eq. (2.46) or from Fig. 2.4. When the frequency of the infrared light is denoted as ν_{IR}, the energy of this light is written as $h\nu_{\mathrm{IR}}$. It is only when this energy is equivalent to the energy difference between the vibrational states, that is, when $h\nu_{\mathrm{IR}} = \hbar\omega$, that this infrared light is absorbed by the molecules and the molecules are excited.

In the case of $H^{35}Cl$, the infrared absorption from $n = 0$ to $n = 1$ is observed at $\tilde{\nu}_{\mathrm{IR}} = 2886.0\ \mathrm{cm}^{-1}$. Converting the wave number into energy by Eq. (1.19), this observation shows that

$$hc\tilde{\nu}_{\mathrm{IR}} = \hbar\omega \tag{2.47}$$

holds. Therefore, the force constant k, which has been given in Eq. (2.24), can be written with $\tilde{\nu}_{\mathrm{IR}}$ as

$$k = \mu\omega^2 = \mu(2\pi c\tilde{\nu}_{\mathrm{IR}})^2. \tag{2.48}$$

This becomes $k = 4.808 \times 10^2$ N/m when we substitute the numerical values.

The force constant k determines the shape of the harmonic potential $V(x) = \frac{1}{2}kx^2$. Similarly, in the case of polyatomic molecules such as CO_2, O_3 and H_2O, which are introduced in Sect. 1.2, the shape of the potential for the molecular vibration can be determined through the measurement of the wave number of the infrared absorption.

Problem 2.3
Confirm that the force constant k of $H^{35}Cl$ is $k = 4.808 \times 10^2$ N/m, using $m(\mathrm{H}) = 1.0079$ amu and $m(^{35}\mathrm{Cl}) = 34.9689$ amu as the masses of H and Cl.

Solution
The reduced mass is $\mu = \frac{m(\mathrm{H})m(^{35}\mathrm{Cl})}{m(\mathrm{H})+m(^{35}\mathrm{Cl})} = 0.97966$ amu.

We can obtain k by substituting this μ value and the observed $\tilde{\nu}_{\mathrm{IR}}$ value into Eq. (2.48). □

Problem 2.4
Find the equation that gives the wave number $\tilde{\nu}_{\mathrm{IR}}$ [cm^{-1}] for the infrared absorption from $n = 0$ to $n = 1$, using the force constant k [N/m] and the reduced mass μ [amu].

Solution
Equation (2.48) can be written as

$$\tilde{\nu}_{\mathrm{IR}} = \frac{1}{2\pi c}\sqrt{\frac{k}{\mu}}. \tag{2.49}$$

Therefore,

$$\tilde{\nu}_{\mathrm{IR}}\ [\mathrm{cm}^{-1}] = 1.3028 \times 10^2 \sqrt{\frac{k\ [\mathrm{N/m}]}{\mu\ [\mathrm{amu}]}}. \tag{2.50}$$

□

Problem 2.5
Determine the wave number of the infrared absorption of $D^{35}Cl$ from $n = 0$ to $n = 1$. Use $m(\mathrm{D}) = 2.0141$ amu as the mass of D (deuteron).

Solution
The vibrational potential remains the same when H is replaced by D. Thus, substituting $k = 4.808 \times 10^2$ N/m and $\mu = \frac{m(\mathrm{D})m(^{35}\mathrm{Cl})}{m(\mathrm{D})+m(^{35}\mathrm{Cl})} = 1.904$ amu into Eq. (2.50), we obtain $\tilde{\nu}_{\mathrm{IR}}(\mathrm{DCl}) = 2070\ \mathrm{cm}^{-1}$. This is a good estimation, as the observed absorption frequency is $\tilde{\nu}_{\mathrm{IR}}^{\mathrm{obs}} = 2083.9\ \mathrm{cm}^{-1}$. The difference between the estimated and observed values indicates that the potential is not perfectly harmonic. □

2.2.4 Eigenfunctions of Harmonic Oscillators

We have learned that the quantization of a harmonic oscillator results in the expression of eigenenergy E_n as Eq. (2.46). Then, our next goal is to find the wave function $\psi_n(\xi)$ which has the eigenenergy E_n. To this end, we must obtain the concrete form of the finite polynomial series $u(\xi)$ which has been introduced as Eq. (2.31).

Substituting the quantization condition (2.45) into the differential equation (2.35) of $u(\xi)$, we can write

$$\frac{\mathrm{d}^2u}{\mathrm{d}\xi^2} - 2\xi\frac{\mathrm{d}u}{\mathrm{d}\xi} + 2nu = 0. \tag{2.51}$$

This equation is known as the Hermite differential equation.

The $u(\xi)$ which satisfies this differential equation is known as the Hermite polynomial $H_n(\xi)$, and can be defined as

$$H_n(\xi) \equiv (-1)^n \mathrm{e}^{\xi^2}\frac{\mathrm{d}^n}{\mathrm{d}\xi^n}\mathrm{e}^{-\xi^2}. \tag{2.52}$$

Equation (2.51) can be written with $H_n(\xi)$ as

$$\frac{\mathrm{d}^2H_n(\xi)}{\mathrm{d}\xi^2} - 2\xi\frac{\mathrm{d}H_n(\xi)}{\mathrm{d}\xi} + 2nH_n(\xi) = 0. \tag{2.53}$$

When we calculate Eq. (2.52), we obtain the polynomials as follows:

$$\begin{aligned} H_0(\xi) &= \mathrm{e}^{\xi^2}\mathrm{e}^{-\xi^2} = 1, \\ H_1(\xi) &= (-1)\mathrm{e}^{\xi^2}\frac{\mathrm{d}}{\mathrm{d}\xi}\mathrm{e}^{-\xi^2} \\ &= (-1)\mathrm{e}^{\xi^2}(-2\xi)\mathrm{e}^{-\xi^2} \\ &= 2\xi, \\ H_2(\xi) &= 4\xi^2 - 2. \end{aligned}$$

Problem 2.6
Obtain $H_3(\xi)$ by calculating Eq. (2.52) for $n = 3$.

Solution

$$\begin{aligned} \frac{\mathrm{d}^3}{\mathrm{d}\xi^3}\left(\mathrm{e}^{-\xi^2}\right) &= \frac{\mathrm{d}^2}{\mathrm{d}\xi^2}\left\{(-2\xi)\mathrm{e}^{-\xi^2}\right\} = \frac{\mathrm{d}}{\mathrm{d}\xi}\left\{(-2)\mathrm{e}^{-\xi^2} + (-2\xi)^2\mathrm{e}^{-\xi^2}\right\} \\ &= 12\xi\mathrm{e}^{-\xi^2} - 8\xi^3\mathrm{e}^{-\xi^2}. \end{aligned}$$

Therefore,

$$H_3(\xi) = (-1)^3\mathrm{e}^{\xi^2}\left(12\xi\mathrm{e}^{-\xi^2} - 8\xi^3\mathrm{e}^{-\xi^2}\right) = 8\xi^3 - 12\xi. \qquad \square$$

Table 2.1 shows $H_n(\xi)$ $(n = 0, \ldots, 4)$. Plotting these Hermite polynomials as functions of ξ, we can see that the number of points where the value of the polynomial becomes 0 (these points are called zeros) increases by one each time n increases by one.

Table 2.1 Hermite polynomials

$H_0(\xi) = 1$
$H_1(\xi) = 2\xi$
$H_2(\xi) = 4\xi^2 - 2$
$H_3(\xi) = 8\xi^3 - 12\xi$
$H_4(\xi) = 16\xi^4 - 48\xi^2 + 12$

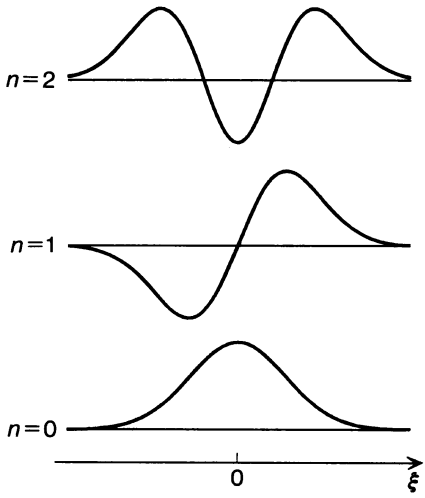

Fig. 2.5 Eigenfunctions $\psi_n(\xi)$ $(n = 0, 1, 2)$ of a harmonic oscillator

The number of zeros in $H_n(\xi)$ is n. For example, in the case of $H_3(\xi) = 8\xi^3 - 12\xi$, which is a third-order function of ξ, the curve intersects the ξ axis (i.e., the horizontal axis) at three points, $\xi = -\sqrt{\frac{3}{2}}, 0, \sqrt{\frac{3}{2}}$, which become the zeros.

Substituting the Hermite polynomial given above into Eq. (2.31), we can write the wave function of a harmonic oscillator as

$$\psi_n(\xi) = N_n H_n(\xi) \mathrm{e}^{-\frac{1}{2}\xi^2}, \tag{2.54}$$

where N_n is the normalizing constant, and will be obtained in Sect. 2.2.6. For $n = 0, 1, 2,$

$$\begin{cases} \psi_0(\xi) = N_0 \mathrm{e}^{-\frac{1}{2}\xi^2}, \\ \psi_1(\xi) = N_1(2\xi)\mathrm{e}^{-\frac{1}{2}\xi^2}, \\ \psi_2(\xi) = N_2(4\xi^2 - 2)\mathrm{e}^{-\frac{1}{2}\xi^2}. \end{cases} \tag{2.55}$$

These eigenfunctions are plotted as shown in Fig. 2.5. In the case of $n = 0$, the wave function is a Gauss-type function, which can also be called a Gaussian. In the case of $n = 1$, the wave function as a whole is an odd function, and consists of the product of an odd function 2ξ and an even function, the Gaussian. This wave function has its only node at $\xi = 0$ and approaches asymptotically to 0 at $\xi \to \pm\infty$ due to the factor of $\mathrm{e}^{-\frac{1}{2}\xi^2}$. In the case of $n = 2$, the wave function is the product of the Gaussian and

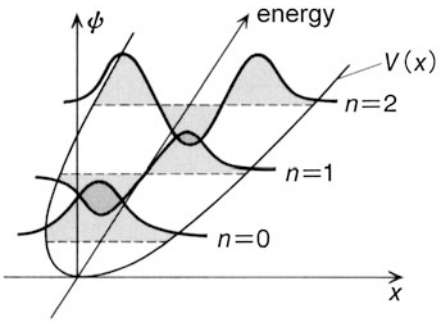

Fig. 2.6 Eigenenergies and eigenfunctions of a harmonic oscillator

a quadratic function which is convex downward and crosses the ξ axis at two points. Therefore this wave function has two nodes and approaches 0 when $\xi \to \pm\infty$. We note here that the parity of a wave function alternates even $\to$ odd $\to$ even ... as n increases from $n = 0$.

Furthermore, the number of zeros in a wave function increases from 0, 1, 2, ... as the quantum number n increases from $n = 0, 1, 2, \ldots$, in correspondence with the number of zeros in the Hermite polynomial. These zeros, that is, the points at which $\psi(x)$ crosses the x axis, are called the nodes of a wave function.

The eigenenergies (eigenvalues) and the corresponding eigenfunctions of a harmonic oscillator are shown in Fig. 2.6 as a three-dimensional image. It illustrates that an increase of n by one leads to the increase of energy by $\hbar\omega$ and the addition of another node to the wave function.

2.2.5 The Hermite Recurrence Formula

The Hermite polynomial $H_n(\xi)$ found in the wave function of a harmonic oscillator is known to satisfy the Hermite recurrence formula as follows:

$$H_{n+1}(\xi) = 2\xi H_n(\xi) - 2n H_{n-1}(\xi). \tag{2.56}$$

This equation is useful because it allows us to obtain $H_{n+1}(\xi)$ from $H_n(\xi)$ and $H_{n-1}(\xi)$. Using $H_0(\xi) = 1$ and $H_1(\xi) = 2\xi$, as have previously been obtained from Eq. (2.52), we can easily calculate $H_2(\xi)$ with the recurrence formula above:

$$H_2(\xi) = 2\xi(2\xi) - 2 \cdot 1 \cdot 1 = 4\xi^2 - 2.$$

Problem 2.7
Obtain the Hermite polynomial $H_3(\xi)$ using the recurrence formula (2.56).

Solution
Substituting $H_1(\xi) = 2\xi$ and $H_2(\xi) = 4\xi^2 - 2$ into Eq. (2.56) gives us

$$\begin{aligned} H_3(\xi) &= 2\xi H_2(\xi) - 2 \cdot 2 \cdot H_1(\xi) = 2\xi(4\xi^2 - 2) - 2 \cdot 2 \cdot 2\xi \\ &= 8\xi^3 - 12\xi. \end{aligned}$$

□

The recurrence formula (2.56) is proved as follows. Firstly, we take the fact that

$$\frac{\mathrm{d}^{n+1}}{\mathrm{d}\xi^{n+1}}\mathrm{e}^{-\xi^2} = -2\xi\frac{\mathrm{d}^n}{\mathrm{d}\xi^n}\mathrm{e}^{-\xi^2} - 2n\frac{\mathrm{d}^{n-1}}{\mathrm{d}\xi^{n-1}}\mathrm{e}^{-\xi^2} \tag{2.57}$$

and multiply both sides of this equation from the left by $(-1)^{n+1}\mathrm{e}^{\xi^2}$. Using (2.52), we can immediately obtain the Hermite recurrence formula:

$$H_{n+1}(\xi) = 2\xi H_n(\xi) - 2nH_{n-1}(\xi).$$

Problem 2.8
Prove Eq. (2.57).

Solution
Performing the differentiation on the left-hand side of Eq. (2.57),

$$\frac{\mathrm{d}^{n+1}}{\mathrm{d}\xi^{n+1}}\mathrm{e}^{-\xi^2} = \frac{\mathrm{d}^n}{\mathrm{d}\xi^n}\left(-2\xi\mathrm{e}^{-\xi^2}\right)$$

$$\frac{\mathrm{d}^n}{\mathrm{d}\xi^n}\left(-2\xi\mathrm{e}^{-\xi^2}\right) = \frac{\mathrm{d}^{n-1}}{\mathrm{d}\xi^{n-1}}\left\{(-2)\mathrm{e}^{-\xi^2} + (-2\xi)\frac{\mathrm{d}}{\mathrm{d}\xi}\mathrm{e}^{-\xi^2}\right\}$$

$$= (-2)\frac{\mathrm{d}^{n-1}}{\mathrm{d}\xi^{n-1}}\mathrm{e}^{-\xi^2} + \frac{\mathrm{d}^{n-1}}{\mathrm{d}\xi^{n-1}}\left\{(-2\xi)\frac{\mathrm{d}}{\mathrm{d}\xi}\mathrm{e}^{-\xi^2}\right\}.$$

Similarly,

$$\frac{\mathrm{d}^{n-1}}{\mathrm{d}\xi^{n-1}}\left\{(-2\xi)\frac{\mathrm{d}}{\mathrm{d}\xi}\mathrm{e}^{-\xi^2}\right\} = (-2)\frac{\mathrm{d}^{n-1}}{\mathrm{d}\xi^{n-1}}\mathrm{e}^{-\xi^2} + \frac{\mathrm{d}^{n-2}}{\mathrm{d}\xi^{n-2}}\left\{(-2\xi)\frac{\mathrm{d}^2}{\mathrm{d}\xi^2}\mathrm{e}^{-\xi^2}\right\}$$

$$\frac{\mathrm{d}^{n-2}}{\mathrm{d}\xi^{n-2}}\left\{(-2\xi)\frac{\mathrm{d}^2}{\mathrm{d}\xi^2}\mathrm{e}^{-\xi^2}\right\} = (-2)\frac{\mathrm{d}^{n-1}}{\mathrm{d}\xi^{n-1}}\mathrm{e}^{-\xi^2} + \frac{\mathrm{d}^{n-3}}{\mathrm{d}\xi^{n-3}}\left\{(-2\xi)\frac{\mathrm{d}^3}{\mathrm{d}\xi^3}\mathrm{e}^{-\xi^2}\right\}$$

$$\vdots$$

$$\frac{\mathrm{d}^{n-(n-1)}}{\mathrm{d}\xi^{n-(n-1)}}\left\{(-2\xi)\frac{\mathrm{d}^{n-1}}{\mathrm{d}\xi^{n-1}}\mathrm{e}^{-\xi^2}\right\} = (-2)\frac{\mathrm{d}^{n-1}}{\mathrm{d}\xi^{n-1}}\mathrm{e}^{-\xi^2} + \frac{\mathrm{d}^{n-n}}{\mathrm{d}\xi^{n-n}}\left\{(-2\xi)\frac{\mathrm{d}^n}{\mathrm{d}\xi^n}\mathrm{e}^{-\xi^2}\right\}.$$

Summing up both sides of these equations leads to

$$\frac{\mathrm{d}^{n+1}}{\mathrm{d}\xi^{n+1}}\mathrm{e}^{-\xi^2} = -2\xi\frac{\mathrm{d}^n}{\mathrm{d}\xi^n}\mathrm{e}^{-\xi^2} - 2n\frac{\mathrm{d}^{n-1}}{\mathrm{d}\xi^{n-1}}\mathrm{e}^{-\xi^2}.$$

□

It can also be proved that $H_n(\xi)$ satisfies the Hermite differential equation (2.53) by making use of the recurrence formula (2.56). From Eq. (2.52) we immediately derive

$$\frac{\mathrm{d}H_n(\xi)}{\mathrm{d}\xi} = -H_{n+1}(\xi) + 2\xi H_n(\xi). \tag{2.58}$$

Problem 2.9
Confirm Eq. (2.58).

Solution
By definition, $H_n(\xi) = (-1)^n \mathrm{e}^{\xi^2} \frac{\mathrm{d}^n \mathrm{e}^{-\xi^2}}{\mathrm{d}\xi^n}$. Therefore,

$$\begin{aligned}\frac{\mathrm{d}H_n(\xi)}{\mathrm{d}\xi} &= (-1)^n \mathrm{e}^{\xi^2} \frac{\mathrm{d}^{n+1}\mathrm{e}^{-\xi^2}}{\mathrm{d}\xi^{n+1}} + (-1)^n (2\xi)\mathrm{e}^{\xi^2} \frac{\mathrm{d}^n \mathrm{e}^{-\xi^2}}{\mathrm{d}\xi^n} \\ &= -H_{n+1}(\xi) + 2\xi H_n(\xi).\end{aligned}$$

□

Comparing Eqs. (2.56) and (2.58) gives

$$\frac{\mathrm{d}H_n(\xi)}{\mathrm{d}\xi} = 2n H_{n-1}(\xi). \tag{2.59}$$

Thus, calculating the second-order differential part of $H_n(\xi)$ using Eqs. (2.58) and (2.59) leads to the following:

$$\begin{aligned}\frac{\mathrm{d}^2 H_n(\xi)}{\mathrm{d}\xi^2} &= \frac{\mathrm{d}}{\mathrm{d}\xi}\big(-H_{n+1}(\xi) + 2\xi H_n(\xi)\big) \\ &= -\frac{\mathrm{d}H_{n+1}(\xi)}{\mathrm{d}\xi} + 2\xi \frac{\mathrm{d}H_n(\xi)}{\mathrm{d}\xi} + 2H_n(\xi) \\ &= -2(n+1)H_n(\xi) + 2\xi \frac{\mathrm{d}H_n(\xi)}{\mathrm{d}\xi} + 2H_n(\xi) \\ &= -2n H_n(\xi) + 2\xi \frac{\mathrm{d}H_n(\xi)}{\mathrm{d}\xi}.\end{aligned}$$

This is no other than the Hermite differential equation

$$\frac{\mathrm{d}^2 H_n(\xi)}{\mathrm{d}\xi^2} - 2\xi \frac{\mathrm{d}H_n(\xi)}{\mathrm{d}\xi} + 2n H_n(\xi) = 0.$$

2.2.6 The Eigenfunction System of a Harmonic Oscillator

The eigenfunction of a harmonic oscillator (2.54)

$$\psi_n(\xi) = N_n H_n(\xi)\mathrm{e}^{-\frac{1}{2}\xi^2}$$

is called a Hermite-Gaussian function because it is expressed as the product of the n-th order Hermite polynomial $H_n(\xi)$ and the Gaussian $\mathrm{e}^{-\frac{1}{2}\xi^2}$. Now we are going to calculate the integral

$$I = \int_{-\infty}^{\infty} \psi_n^*(\xi)\psi_n(\xi)\mathrm{d}x \tag{2.60}$$

to obtain the normalization constant N_n. Here, $\psi_n^*(\xi)$ stands for the complex conjugate of $\psi_n(\xi)$. The integral I is called the scalar product (inner product) of the wave function (cf. Sect. 2.3). The asterisk on the upper right of a wave function stands for its complex conjugate. Here, $\psi_n(\xi)$ is a real function and $\xi = \sqrt{\beta}x$. Therefore, Eq. (2.60) is calculated as follows by converting the integral variable x to ξ:

$$I = (N_n)^2 \int_{-\infty}^{\infty} H_n^2(\xi) \mathrm{e}^{-\xi^2} \mathrm{d}\xi / \sqrt{\beta}$$
$$= (N_n)^2 \int_{-\infty}^{\infty} \frac{\mathrm{d}^n H_n(\xi)}{\mathrm{d}\xi^n} \mathrm{e}^{-\xi^2} \mathrm{d}\xi / \sqrt{\beta}. \tag{2.61}$$

Problem 2.10
Derive Eq. (2.61).

Solution

$$J = \int_{-\infty}^{\infty} H_n^2(\xi) \mathrm{e}^{-\xi^2} \mathrm{d}\xi = \int_{-\infty}^{\infty} (-1)^n H_n(\xi) \mathrm{e}^{-\xi^2} \frac{\mathrm{d}^n \mathrm{e}^{-\xi^2}}{\mathrm{d}\xi^n} \mathrm{e}^{-\xi^2} \mathrm{d}\xi$$
$$= \int_{-\infty}^{\infty} (-1)^n H_n(\xi) \frac{\mathrm{d}^n \mathrm{e}^{-\xi^2}}{\mathrm{d}\xi^n} \mathrm{d}\xi$$
$$= (-1)^n \left[H_n(\xi) \frac{\mathrm{d}^{n-1} \mathrm{e}^{-\xi^2}}{\mathrm{d}\xi^{n-1}} \right]_{-\infty}^{\infty}$$
$$- (-1)^n \int_{-\infty}^{\infty} \frac{\mathrm{d}H_n(\xi)}{\mathrm{d}\xi} \cdot \frac{\mathrm{d}^{n-1} \mathrm{e}^{-\xi^2}}{\mathrm{d}\xi^{n-1}} \mathrm{d}\xi.$$

The value of the inside of [ ] in the first term becomes 0 at $\xi \to \pm\infty$, and thus only the second term remains. Repeating this partial integration n times gives

$$J = \int_{-\infty}^{\infty} \frac{\mathrm{d}^n H_n(\xi)}{\mathrm{d}\xi^n} \mathrm{e}^{-\xi^2} \mathrm{d}\xi.$$

This verifies that Eq. (2.61) holds. □

As $H_n(\xi)$ is an n-th order polynomial of ξ, $\frac{\mathrm{d}^n H_n(\xi)}{\mathrm{d}\xi^n}$ is a constant. To be more specific, from Eq. (2.59) it is calculated to be

$$\frac{\mathrm{d}^n H_n(\xi)}{\mathrm{d}\xi^n} = 2^n n!.$$

Therefore,

$$I = (N_n)^2 2^n n! \int_{-\infty}^{\infty} \mathrm{e}^{-\xi^2} \mathrm{d}\xi / \sqrt{\beta}$$
$$= (N_n)^2 2^n n! \sqrt{\frac{\pi}{\beta}}, \tag{2.62}$$

using

$$\int_{-\infty}^{\infty} \mathrm{e}^{-\xi^2} \mathrm{d}\xi = \sqrt{\pi}.$$

The normalization condition demands $I = 1$ (cf. Sect. 2.3), so

$$(N_n)^2 = \frac{1}{2^n n!} \sqrt{\frac{\beta}{\pi}}.$$

Therefore, the normalization constant is obtained as

$$N_n = \left(\frac{1}{2^n n!}\sqrt{\frac{\beta}{\pi}}\right)^{\frac{1}{2}} = \left(\frac{1}{2^n n!}\sqrt{\frac{\mu\omega}{\pi\hbar}}\right)^{\frac{1}{2}}. \tag{2.63}$$

Any two eigenfunctions in the eigenfunction system $\{\psi_n(x)\} = \{\psi_0(x), \psi_1(x), \psi_2(x), \ldots\}$ are orthogonal to each other. That the two wave functions $\psi_m(x)$ and $\psi_n(x)$ $(m \neq n)$ are orthogonal to each other means that their scalar product, defined as $\int_{-\infty}^{\infty} \psi_m^*(x)\psi_n(x)\mathrm{d}x$, is 0. This can be confirmed by calculation. First, the scalar product becomes

$$\begin{aligned}\int_{-\infty}^{\infty} \psi_m^*(x)\psi_n(x)\mathrm{d}x &= \int_{-\infty}^{\infty} N_m N_n H_m(\xi)H_n(\xi)\mathrm{e}^{-\xi^2}\mathrm{d}\xi/\sqrt{\beta} \\ &= (-1)^n \int_{-\infty}^{\infty} N_m N_n H_m(\xi)\frac{\mathrm{d}^n \mathrm{e}^{-\xi^2}}{\mathrm{d}\xi^n}\mathrm{d}\xi/\sqrt{\beta}. \end{aligned} \tag{2.64}$$

Then, the differential of $\mathrm{e}^{-\xi^2}$ can be converted to that of $H_m(\xi)$ by partial integration, as has been done in deriving Eq. (2.61). If m is chosen so that $m < n$, the right hand side of integral (2.64) will be

$$(-1)^{n+m+1}\int_{-\infty}^{\infty} N_m N_n \frac{\mathrm{d}^{m+1}H_m(\xi)}{\mathrm{d}\xi^{m+1}}\frac{\mathrm{d}^{n-m-1}}{\mathrm{d}\xi^{n-m-1}}\mathrm{e}^{-\xi^2}\mathrm{d}\xi/\sqrt{\beta}.$$

Since $H_m(\xi)$ is an m-th order polynomial of ξ, $\frac{\mathrm{d}^{m+1}H_m(\xi)}{\mathrm{d}\xi^{m+1}} = 0$. Thus,

$$\int_{-\infty}^{\infty} \psi_m^*(x)\psi_n(x)\mathrm{d}x = 0. \tag{2.65}$$

In the case of $m > n$, too, the same calculation with m exchanged for n proves that $\psi_m(x)$ and $\psi_n(x)$ are orthogonal to each other. Therefore, Eq. (2.65) is valid whenever $m \neq n$.

This orthogonality of eigenfunctions in the case of $m \neq n$ stems from the fact that the Hamiltonian H of a harmonic oscillator is an operator called the Hermitian operator (explained in Sect. 2.3). Eigenfunctions belonging to different eigenvalues of a Hermitian operator are orthogonal to each other. We call $\{\psi_n(x)\}$ an orthogonal function system, because it is an ensemble of functions orthogonal to each other. When its members are normalized, it is called an orthonormal function system. Thus, the eigenfunctions of a harmonic oscillator form an orthonormal function system.

2.3 The Harmonic Oscillator and Its Applications

In the preceding section, we have taken harmonic oscillators as the model of diatomic molecules, and learned that quantum theory only allows their energies to take discrete values. Our next question is what kind of values kinetic and potential energies can take. As has been illustrated with HCl, in the case of heteronuclear

diatomic molecules, molecules in the $n = 0$ state are excited into the $n = 1$ state by absorbing an amount of energy equal to the energy difference between the two states. Then, is it possible for molecules in the $n = 0$ state to be excited into the $n = 2$ state? To answer these questions, in this section we will learn about the expectation values of operators and the matrix elements of operators.

Taking diatomic molecules as an example, to calculate the expectation values of coordinate operators is to determine the average internuclear distance of the molecules. In addition, when an operator $\hat{h}$ represents a transition dipole moment, the probability of the atomic or molecular system being excited from the eigenstate ψ_n into ψ_m is proportional to the quantity $|\int \psi_m^* \hat{h} \psi_n \, \mathrm{d}\tau|^2 = |\langle m|\hat{h}|n\rangle|^2$. As this shows, describing atoms and molecules governed by the law of quantum theory generally involves the calculation of $h_{mn} = \langle m|h|n\rangle = \int \psi_m^* h \psi_n \, \mathrm{d}\tau$, where the operator $\hat{h}$ stands for a physical quantity. In these equations, m and n are numbers specifying states, and correspond to the vibrational quantum numbers in the case of harmonic oscillators. When the system is in the n-th state, the diagonal element h_{nn} of the matrix is the expectation value of the operator $\hat{h}$.

In this section, we will calculate matrix elements using eigenfunctions of harmonic oscillators, and apply it to determining expectation values of energy and selection rules in vibrational spectra.

2.3.1 Hermitian Operators and the Bracket Notation

All operators representing physical quantities such as positions, momenta, and energies are classified as Hermitian operators. A Hermitian operator is defined as an operator $\hat{H}$ for which the equation

$$\int \psi_m^* \hat{H} \psi_n \, \mathrm{d}\tau = \left(\int \psi_n^* \hat{H} \psi_m \, \mathrm{d}\tau \right)^* \tag{2.66}$$

holds with arbitrary wave functions ψ_m and ψ_n. In this equation, $\mathrm{d}\tau$, representing an infinitesimal volume, is given by

$$\mathrm{d}\tau = \mathrm{d}x \, \mathrm{d}y \, \mathrm{d}z$$

when integrations are performed in the three-dimensional space. It follows that

$$\int \psi_m^* \hat{H} \psi_n \, \mathrm{d}\tau = \int_{-\infty}^{\infty} \int_{-\infty}^{\infty} \int_{-\infty}^{\infty} \psi_m^* \hat{H} \psi_n \, \mathrm{d}x \, \mathrm{d}y \, \mathrm{d}z. \tag{2.67}$$

Furthermore, in the case of one-dimensional integrations on the x axis for the one-dimensional harmonic oscillators, which we have dealt with in the previous section, $\mathrm{d}\tau$ is equal to $\mathrm{d}x$. Then it follows that

$$\int \psi_m^* \hat{H} \psi_n \, \mathrm{d}\tau = \int_{-\infty}^{\infty} \psi_m^* \hat{H} \psi_n \, \mathrm{d}x. \tag{2.68}$$

Equation (2.66) reflects the fact that a diagonal element of the matrix, $\int \psi_n^* \hat{H} \psi_n \, \mathrm{d}\tau$, is always a real number. This is a requirement because diagonal elements of matrices

are expectation values of physical quantities. From here on, the caret symbol in $\hat{H}$ will be omitted.

By using the definition in Eq. (2.66), it can readily be illustrated that the eigenvalues of Hermitian operators are real numbers. Here, we express a wave function of Hermitian operator H as ψ_n and its eigenvalue as ε_n. Then,

$$H\psi_n = \varepsilon_n \psi_n. \tag{2.69}$$

By multiplying this from the left by ψ_n^* and integrating it, we find

$$\int \psi_n^* H \psi_n \, \mathrm{d}\tau = \varepsilon_n \int \psi_n^* \psi_n \, \mathrm{d}\tau. \tag{2.70}$$

On the other hand, it follows from Eq. (2.69) and the definition in Eq. (2.66) that

$$\begin{aligned} \int \psi_n^* H \psi_n \, \mathrm{d}\tau &= \left(\int \psi_n^* H \psi_n \, \mathrm{d}\tau \right)^* \\ &= \varepsilon_n^* \int \psi_n^* \psi_n \, \mathrm{d}\tau. \end{aligned} \tag{2.71}$$

Equations (2.70) and (2.71) lead to

$$\varepsilon_n \int \psi_n^* \psi_n \, \mathrm{d}\tau = \varepsilon_n^* \int \psi_n^* \psi_n \, \mathrm{d}\tau,$$

or

$$\left(\varepsilon_n - \varepsilon_n^* \right) \int \psi_n^* \psi_n \, \mathrm{d}\tau = 0. \tag{2.72}$$

Moreover, $\psi_n^* \psi_n \, \mathrm{d}\tau$, which is equal to $|\psi_n|^2 \, \mathrm{d}\tau$, is proportional to the probability with which the system in the state ψ_n is detected in $\mathrm{d}\tau = \mathrm{d}x \, \mathrm{d}y \, \mathrm{d}z$ if it is three-dimensional (or in the infinitestimal region $\mathrm{d}x$ if it is one-dimensional). This is called Born's probability interpretation of wave functions. Hence,

$$\int \psi_n^* \psi_n \, \mathrm{d}\tau = c \quad \text{(where } c \text{ is a positive constant)}. \tag{2.73}$$

From Eqs. (2.72) and (2.73),

$$\varepsilon_n = \varepsilon_n^*.$$

This indicates that ε_n is a real number. By the way, the probability with which the system is detected at some point in the whole space should be 1. When ψ_n is given so that

$$\int \psi_n^* \psi_n \, \mathrm{d}\tau = 1 \tag{2.74}$$

is valid, ψ_n is referred to as being "normalized."

Scalar products of two eigenfunctions ψ_m and ψ_n are given by

$$\int \psi_m^* \psi_n \, \mathrm{d}\tau,$$

which corresponds to taking the complex conjugate of ψ_m, multiplying it with ψ_n, and performing the integration. Putting this in a short form, we describe them as

$$\langle \psi_m | \psi_n \rangle,$$

or

$$\langle m | n \rangle$$

when it is sufficient to specify only the m and n. Namely,

$$\langle m | n \rangle = \langle \psi_m | \psi_n \rangle = \int \psi_m^* \psi_n \, \mathrm{d}\tau. \tag{2.75}$$

Additionally, when the operation of an operator H on ψ_n results in ψ_n', that is, when $\psi_n' = H\psi_n$, the scalar product of ψ_m and ψ_n' is given by

$$\langle \psi_m | \psi_n' \rangle = \langle \psi_m | H \psi_n \rangle,$$

which is rewritten as

$$\langle \psi_m | H | \psi_n \rangle.$$

This can be regarded as H bracketed by $\langle \psi_m |$ and $| \psi_n \rangle$, which is why we call $\langle \psi_m |$ the bra state and $| \psi_n \rangle$ the ket state from the word "bracket." In summary, we can write

$$\langle m | H | n \rangle = \langle \psi_m | H | \psi_n \rangle = \int \psi_m^* H \psi_n \, \mathrm{d}\tau. \tag{2.76}$$

The representation of wave functions with bra and ket as in Eqs. (2.75) and (2.76) is called the bracket notation.

With the bracket notation, Eq. (2.66), the definition of Hermitian operators, is written as

$$\langle m | H | n \rangle = \langle n | H | m \rangle^*. \tag{2.77}$$

This is to say that, in calculating matrix elements $\langle m | H | n \rangle$, the result obtained when we first operate H on $| n \rangle$ and then take its scalar product with $\langle m |$ is equivalent to that obtained when we operate H on $| m \rangle$, take its scalar product with $\langle n |$, and then take the complex conjugate of the entire matrix element. The normalization condition (2.74) is given by

$$\langle n | n \rangle = \langle \psi_n | \psi_n \rangle = 1. \tag{2.78}$$

Problem 2.11
Show that the eigenvalues of Hermitian operators are real numbers using the bracket notation.

Solution
When the eigenvalue of a Hermitian operator is ε_n and the corresponding eigenfunction is $| n \rangle$,

$$H | n \rangle = \varepsilon_n | n \rangle.$$

Therefore,

$$\langle n|H|n\rangle = \varepsilon_n \langle n|n\rangle.$$

Taking the complex conjugate of both sides of this equation, we have

$$\langle n|H|n\rangle^* = \varepsilon_n^* \langle n|n\rangle.$$

From the definition of Hermitian operators,

$$\langle n|H|n\rangle^* = \langle n|H|n\rangle.$$

Thus,

$$(\varepsilon_n - \varepsilon_n^*)\langle n|n\rangle = 0.$$

Since $\langle n|n\rangle > 0$, $\varepsilon_n = \varepsilon_n^*$, which shows that ε_n is a real number. □

Problem 2.12
Show that eigenfunctions of Hermitian operators which give different eigenvalues are orthogonal to each other.

Solution
Let

$$H|n\rangle = \varepsilon_n|n\rangle, \qquad H|m\rangle = \varepsilon_m|m\rangle, \quad \varepsilon_m \neq \varepsilon_n,$$

where both ε_n and ε_m are real numbers. Then,

$$\langle m|H|n\rangle = \langle m|\varepsilon_n|n\rangle = \varepsilon_n\langle m|n\rangle,$$
$$\langle n|H|m\rangle^* = \langle n|\varepsilon_m|m\rangle^* = \varepsilon_m\langle n|m\rangle^*.$$

From $\langle n|m\rangle^* = \langle m|n\rangle$ and the definition of Hermitian operators in Eq. (2.77),

$$\varepsilon_n\langle m|n\rangle = \varepsilon_m\langle m|n\rangle.$$

Therefore,

$$(\varepsilon_n - \varepsilon_m)\langle m|n\rangle = 0.$$

Since $\varepsilon_n \neq \varepsilon_m$, $\langle m|n\rangle = 0$.

In the previous section, this has been illustrated concretely in Eq. (2.65) by the example of the eigenfunctions of harmonic oscillators. It is because the Hamiltonian operator of harmonic oscillators

$$H = -\frac{\hbar^2}{2\mu}\frac{\mathrm{d}^2}{\mathrm{d}x^2} + \frac{1}{2}\mu\omega^2 x^2$$

is a Hermitian operator that Eq. (2.65) holds for the eigenfunctions of harmonic oscillators. □

When $\langle m|H|n\rangle$ is written as H_{mn} and arranged as

$$\begin{pmatrix} H_{11} & H_{12} & H_{13} & \cdots \\ H_{21} & H_{22} & H_{23} & \cdots \\ & \vdots & & \ddots \end{pmatrix},$$

it forms a matrix. Thus, H_{mn} is called a matrix element. Representing Eq. (2.77) in the matrix form results in

$$\begin{pmatrix} H_{11} & H_{12} & \cdots \\ H_{21} & H_{22} & \cdots \\ & \vdots & \ddots \end{pmatrix} = \begin{pmatrix} H_{11}^* & H_{21}^* & \cdots \\ H_{12}^* & H_{22}^* & \cdots \\ & \vdots & \ddots \end{pmatrix}. \tag{2.79}$$

Hence, the matrices of Hermitian operators, if we take their transposes and then their complex conjugates, become equal to the original matrices.

2.3.2 Calculations of Expectation Values Using Eigenfunctions

Generally speaking, when a Hermitian operator $\hat{h}$ representing a physical quantity is given, the matrix element described by eigenstates ψ_n of the Hamiltonian,

$$\langle \hat{h} \rangle_n \equiv \langle n|\hat{h}|n\rangle = \int \psi_n^* \hat{h} \psi_n \, \mathrm{d}\tau, \tag{2.80}$$

is called the expectation value of the operator $\hat{h}$ for ψ_n.

Let us then calculate the expectation value by using the normalized eigenfunctions of harmonic oscillators. When the vibrational quantum number of a harmonic oscillator equals n, the expectation value of coordinate operator x is given by

$$\langle x \rangle_n \equiv \langle n|x|n\rangle = \int_{-\infty}^{\infty} \psi_n^* x \psi_n \, \mathrm{d}x. \tag{2.81}$$

As derived in the previous section,

$$\psi(\xi) = \left(\frac{1}{2^n n!} \sqrt{\frac{\beta}{\pi}} \right)^{\frac{1}{2}} H_n(\xi) \mathrm{e}^{-\frac{1}{2}\xi^2}.$$

Hence,

$$\begin{aligned} \langle x \rangle_n &= \frac{1}{2^n n!} \sqrt{\frac{\beta}{\pi}} \int_{-\infty}^{\infty} H_n(\xi) x H_n(\xi) \mathrm{e}^{-\xi^2} \, \mathrm{d}x \\ &= \frac{1}{2^n n!} \frac{1}{\sqrt{\pi}} \int_{-\infty}^{\infty} H_n(\xi) \xi H_n(\xi) \mathrm{e}^{-\xi^2} \, \mathrm{d}\xi / \sqrt{\beta}. \end{aligned} \tag{2.82}$$

Since the recurrence formula for Hermite polynomials (2.56) can be expressed as

$$\xi H_n(\xi) = n H_{n-1}(\xi) + \frac{1}{2} H_{n+1}(\xi), \tag{2.83}$$

$$\begin{aligned} \langle x \rangle_n &= \frac{1}{2^n n!} \frac{1}{\sqrt{\beta\pi}} \left(n \int_{-\infty}^{\infty} H_n(\xi) H_{n-1}(\xi) \mathrm{e}^{-\xi^2} \, \mathrm{d}\xi \right. \\ &\quad \left. + \frac{1}{2} \int_{-\infty}^{\infty} H_n(\xi) H_{n+1}(\xi) \mathrm{e}^{-\xi^2} \, \mathrm{d}\xi \right) \\ &= 0. \end{aligned} \tag{2.84}$$

This is because both of the two integrals in the bracket in Eq. (2.84) become zero as a result of the orthogonality of the Hermite-Gaussian functions shown in Eqs. (2.64) and (2.65). Equation (2.84) shows that the average position of x is 0, no matter which eigenstate the system is in.

This means that, if the distance between two atoms A and B in a diatomic molecule AB, whose potential is harmonic in the exact sense, is denoted as x_{AB} and the value of x_{AB} at the equilibrium position is r_{e}, the expectation value of x defined as $x = x_{\mathrm{AB}} - r_{\mathrm{e}}$ becomes 0, that is, the expectation value of x_{AB} is equal to r_{e} at all of its vibrational levels.

Problem 2.13
Treating a diatomic molecule as a harmonic oscillator, determine $\langle x_{\mathrm{AB}}\rangle_n$, the expectation value of x_{AB}, in the eigenstate ψ_n.

Solution

$$\begin{aligned}\langle x\rangle_n &= \langle n|x|n\rangle \\ &= \langle n|x_{\mathrm{AB}} - r_{\mathrm{e}}|n\rangle \\ &= \langle n|x_{\mathrm{AB}}|n\rangle - \langle n|r_{\mathrm{e}}|n\rangle.\end{aligned}$$

Since r_{e} is a constant,

$$\langle n|r_{\mathrm{e}}|n\rangle = r_{\mathrm{e}}\langle n|n\rangle = r_{\mathrm{e}}.$$

Therefore,

$$\langle x\rangle_n = \langle x_{\mathrm{AB}}\rangle_n - r_{\mathrm{e}}.$$

As Eq. (2.84) indicates that $\langle x\rangle_n = 0$, $\langle x_{\mathrm{AB}}\rangle_n = r_{\mathrm{e}}$. □

Next, we will determine the expectation value of the Hamiltonian of a harmonic oscillator for the eigenstate ψ_n, namely $|n\rangle$. When H stands for the Hamiltonian, the Schrödinger equation is given by

$$H|n\rangle = \varepsilon_n|n\rangle. \tag{2.85}$$

Therefore,

$$\begin{aligned}\langle H\rangle_n &= \langle n|H|n\rangle \\ &= \langle n|\varepsilon_n|n\rangle \\ &= \varepsilon_n\langle n|n\rangle \\ &= \varepsilon_n.\end{aligned} \tag{2.86}$$

As the Hamiltonian under consideration is that of a harmonic oscillator,

$$\langle H\rangle_n = \hbar\omega\left(n + \frac{1}{2}\right).$$

If a Hamiltonian fulfills Eq. (2.85), Eq. (2.86) always holds. Thus, Eq. (2.86) shows that the expectation value of the Hamiltonian for the eigenstate $|n\rangle$ is generally equivalent to its energy eigenvalue.

2.3.3 Matrix Elements of x and Selection Rules for Infrared Absorptions

When heteronuclear diatomic molecules absorb infrared radiations, their vibrational quantum number shifts from $n = 0$ to $n = 1$, or from $n = 1$ to $n = 2$. That is, the molecules change their state to a state in which the vibrational quantum number is larger by one than that of the original state.

When molecules absorb light and change their state like this from a low-energy eigenstate, $|n\rangle$, to a high-energy eigenstate, $|m\rangle$, this is referred to as the molecules being excited from $|n\rangle$ to $|m\rangle$. Contrarily, when they lose their energy by emitting light with a corresponding amount of energy, this is also described as the molecules being excited from $|m\rangle$ to $|n\rangle$. These phenomena are referred to as *optical transition*.

It is known that the probability P of an optical transition is proportional to the square modulus of the matrix element $\mu_{mn} = \langle m|\boldsymbol{\mu}|n\rangle$ of the transition dipole moment $\boldsymbol{\mu}$. Namely,

$$P \propto \left|\langle m|\boldsymbol{\mu}|n\rangle\right|^2, \tag{2.87}$$

where $\boldsymbol{\mu}$ is a three-dimensional vector operator representing the magnitude and direction of the polarization of a molecule. In the case of diatomic molecules, the polarization is induced along the molecular axis, which makes it a one-dimensional direction (here, the direction of the x axis), so that we can treat it as a scalar operator and treat it as $\boldsymbol{\mu} = \mu_x$.

When $|m\rangle$ and $|n\rangle$ are the eigenstates of vibrations of heteronuclear diatomic molecules and if μ_x is a constant,

$$\langle m|\mu_x|n\rangle = \mu_x\langle m|n\rangle = 0,$$

because $|m\rangle$ and $|n\rangle$ are mutually orthogonal. This means that no absorption of infrared radiation occurs. However, when their internuclear distance stretches or shrinks, this causes μ_x to change its value along with x. When we expand μ_x with respect to x around $x = 0$, we write it as

$$\mu_x = \mu_x^0 + \left(\frac{\mathrm{d}\mu_x}{\mathrm{d}x}\right)_{\mathrm{e}} x, \tag{2.88}$$

representing the extent of the change as proportional to the magnitude of $\left(\frac{\mathrm{d}\mu_x}{\mathrm{d}x}\right)_{\mathrm{e}}$. In this equation, μ_x^0 is a constant, and the subscript e in $\left(\frac{\mathrm{d}\mu_x}{\mathrm{d}x}\right)_{\mathrm{e}}$ indicates that it is the value of $\left(\frac{\mathrm{d}\mu_x}{\mathrm{d}x}\right)$ at the equilibrium internuclear distance. From Eq. (2.88),

$$\langle m|\mu_x|n\rangle = \langle m|\mu_x^0|n\rangle + \langle m|\left(\frac{\mathrm{d}\mu_x}{\mathrm{d}x}\right)_{\mathrm{e}} x|n\rangle = \left(\frac{\mathrm{d}\mu_x}{\mathrm{d}x}\right)_{\mathrm{e}} \langle m|x|n\rangle \tag{2.89}$$

is obtained. Consequently, the probability of a transition accompanying the absorption of infrared radiation is proportional to

$$\left(\frac{\mathrm{d}\mu_x}{\mathrm{d}x}\right)_{\mathrm{e}}^2 \left|\langle m|x|n\rangle\right|^2. \tag{2.90}$$

In the case of homonuclear diatomic molecules such as O_2 and N_2, no absorption of infrared radiation can occur, for $\frac{\mathrm{d}\mu_x}{\mathrm{d}x} = 0$ because of the symmetry of the molecules. On the other hand, for heteronuclear diatomic molecules, since $\frac{\mathrm{d}\mu_x}{\mathrm{d}x} \neq 0$, transition may or may not occur depending on whether $|\langle m|x|n\rangle|^2$ takes a value other than zero.

In infrared absorption, the transitions that are most commonly observed are those from $|n\rangle$ to $|n+1\rangle$. In this case, the rule of the transitions can be described as $\Delta n = m - n = 1$. Such rules of transitions in the case of absorptions and emissions of light are generally referred to as "selection rules for transitions."

Then, we can deduce the selection rule for the transition by calculating the matrix element

$$\begin{aligned}\langle x\rangle_{m,n} &\equiv \langle \psi_m|x|\psi_n\rangle \\ &= \int_{-\infty}^{\infty} \psi_m^* x \psi_n \,\mathrm{d}x,\end{aligned} \tag{2.91}$$

where $|\psi_n\rangle$ and $|\psi_m\rangle$ are eigenfunctions of a harmonic oscillator. Since

$$x\psi_n = \frac{1}{\sqrt{\beta}} \xi N_n H_n(\xi) \mathrm{e}^{-\frac{1}{2}\xi^2},$$

using the recurrence formula of Hermite polynomials,

$$\begin{aligned}x\psi_n &= \frac{N_n}{\sqrt{\beta}}\left(n H_{n-1} + \frac{1}{2} H_{n+1}\right)\mathrm{e}^{-\frac{1}{2}\xi^2} \\ &= \left(\frac{n}{\sqrt{\beta}}\frac{N_n}{N_{n-1}}\right)\psi_{n-1} + \left(\frac{1}{2\sqrt{\beta}}\frac{N_n}{N_{n+1}}\right)\psi_{n+1}\end{aligned} \tag{2.92}$$

is obtained. When we multiply this equation from the left by ψ_m^* and integrate it, then apply the orthonormal relation

$$\langle \psi_m|\psi_n\rangle = \delta_{mn}, \tag{2.93}$$

we realize that only the following two instances of $\langle x\rangle_{m,n}$ have non-zero values:

$$\langle x\rangle_{n-1,n} = \frac{n}{\sqrt{\beta}}\frac{N_n}{N_{n-1}} = \sqrt{\frac{n}{2\beta}}, \tag{2.94}$$

$$\langle x\rangle_{n+1,n} = \frac{1}{2\sqrt{\beta}}\frac{N_n}{N_{n+1}} = \sqrt{\frac{n+1}{2\beta}}. \tag{2.95}$$

Incidentally, δ_{mn} in Eq. (2.93) is called Kronecker's delta, and satisfies the following relation:

$$\delta_{mn} = \begin{cases} 1 & (m = n), \\ 0 & (m \neq n). \end{cases}$$

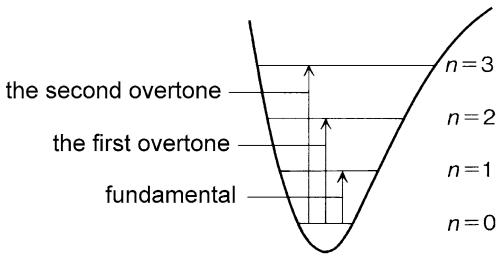

Fig. 2.7 Fundamental and overtones of molecular vibration

Thus, all $\langle x\rangle_{m,n}$ except Eqs. (2.94) and (2.95) are equal to zero. That is,

$$\langle x\rangle_{m,n} = 0 \quad (m \neq n+1, m \neq n-1). \tag{2.96}$$

These results summarized in matrix form, within the range of $0 \leqq n \leqq 3$, $0 \leqq m \leqq 3$ is as follows:

$$\boldsymbol{X} = \begin{pmatrix} 0 & \sqrt{\frac{1}{2\beta}} & 0 & 0 \\ \sqrt{\frac{1}{2\beta}} & 0 & \sqrt{\frac{2}{2\beta}} & 0 \\ 0 & \sqrt{\frac{2}{2\beta}} & 0 & \sqrt{\frac{3}{2\beta}} \\ 0 & 0 & \sqrt{\frac{3}{2\beta}} & 0 \end{pmatrix}. \tag{2.97}$$

This matrix signifies that molecules are excited from $|n\rangle$ to $|n+1\rangle$ when they absorb infrared radiation. This is the selection rule for infrared absorption, which is written as $\Delta n = 1$.

2.3.4 Overtone Absorption

As explained above, in the infrared absorption, the selection rule in the vibrational spectrum is $\Delta n = 1$. However, as represented in Fig. 2.7, sometimes in an absorption spectrum, a transition from $n = 0$ to $n = 2$, or to a level with a larger n value, is observed albeit at a low intensity. This type of absorption is called an overtone absorption. The transition from $n = 0$ to $n = 2$ is called the first overtone, and that from $n = 0$ to $n = 3$ is called the second overtone. In the case of HCl molecules, overtone absorptions were observed, as listed in Table 2.2. In contrast with the overtones, the transition from $n = 0$ to $n = 1$ is called the fundamental tone, or simply fundamental.

Let us consider why these overtone transitions with $\Delta n = m - n \geqq 2$ are observed. This is because real molecules are not, strictly-speaking, harmonic oscillators. It is true that the bottom part of the potential $V(x)$ of a real molecule AB is very close to the harmonic potential

$$V^{\mathrm{HO}}(x) = \frac{1}{2}\mu\omega^2 x^2, \tag{2.98}$$

Table 2.2 Fundamental and overtones of $H^{35}Cl$

Transition	$m \leftarrow n$	Wave number/cm^{-1}
Fundamental	$1 \leftarrow 0$	2885.90
First overtone	$2 \leftarrow 0$	5668.05
Second overtone	$3 \leftarrow 0$	8346.98
Third overtone	$4 \leftarrow 0$	10923.11
Fourth overtone	$5 \leftarrow 0$	13396.55

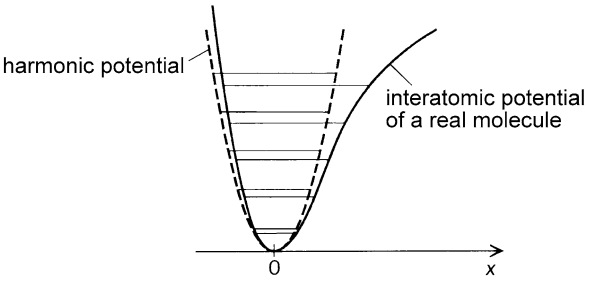

Fig. 2.8 A harmonic potential and an anharmonic potential

where the superscript HO on V stands for "harmonic oscillator," and signifies that the potential is that of a harmonic oscillator.

However, as schematically shown in Fig. 2.8, $V(x)$ tends to become lower than the harmonic oscillator as $x = x_{AB} - r_e$ increases, that is, as the internuclear distance is elongated. When x becomes much larger, the potential starts to stop increasing and its slope approaches zero. This corresponds to the fact that, when the distance between A and B increases to a certain extent, the diatomic molecule is decomposed into atoms A and B, and this causes the induction force, $-\frac{dV(x)}{dx}$, acting between A and B to become sufficiently small. If the diatomic molecule AB were to have a harmonic potential, this would mean that the potential energy would not stop increasing no matter how large x became, and that, consequently, the molecule would never be broken into two atoms. Such a model could not describe the potentials of real molecules.

We will then account for the deviation from the harmonic oscillator in the following manner. In the low vibrational energy range, that is, in the region for relatively small vibrational quantum numbers, $V(x)$ is close to a harmonic potential. Therefore, near $x = 0$, $V(x)$ can be expanded in terms of x in the form of a polynomial using constants f and g as

$$V(x) = \frac{1}{2}\mu\omega^2 x^2 + fx^3 + gx^4 + \cdots. \tag{2.99}$$

Along with this expansion, eigenenergies and eigenfunctions for the Hamiltonian

$$H = -\frac{\hbar^2}{2\mu}\frac{d^2}{dx^2} + V(x) \tag{2.100}$$

also deviate from those of a harmonic oscillator. The third- and higher-order terms for x such as the fx^3 and gx^4 in Eq. (2.99) are called anharmonic terms. Poten-

tials such as the one given by Eq. (2.99), in which anharmonic terms are added to the harmonic potential, and potentials in general that are different from harmonic potentials, are called anharmonic potentials.

The n-th eigenenergy of the harmonic oscillator is denoted as $\varepsilon_n^{\mathrm{HO}}$, and the corresponding eigenfunction is denoted as $\psi_n^{\mathrm{HO}}(x)$. As we learned in Sect. 2.2, a set of eigenfunctions, $\{\psi_n^{\mathrm{HO}}\} = \{\psi_0^{\mathrm{HO}}, \psi_1^{\mathrm{HO}}, \psi_2^{\mathrm{HO}}, \ldots\}$, forms a system of orthonormal functions. Each of the eigenfunctions in an orthonormal set behaves like a unit vector spanning an n-dimensional space. For example, let us assume that $\boldsymbol{e}_x$, $\boldsymbol{e}_y$ and $\boldsymbol{e}_z$ are unit vectors in a three-dimensional space whose directions are the x, y, and z axes of the orthogonal x-y-z axis system, respectively. Then, their scalar products are

$$\boldsymbol{e}_x \cdot \boldsymbol{e}_y = \boldsymbol{e}_y \cdot \boldsymbol{e}_z = \boldsymbol{e}_z \cdot \boldsymbol{e}_x = 0.$$

At the same time, since they are unit vectors, the scalar products of themselves are

$$\boldsymbol{e}_x \cdot \boldsymbol{e}_x = \boldsymbol{e}_y \cdot \boldsymbol{e}_y = \boldsymbol{e}_z \cdot \boldsymbol{e}_z = 1.$$

These relations correspond respectively to the orthogonal relation

$$\int_{-\infty}^{\infty} \psi_m^{\mathrm{HO}}(x)\psi_n^{\mathrm{HO}}(x)\,\mathrm{d}x = 0 \quad (m \neq n)$$

and the normalization relation

$$\int_{-\infty}^{\infty} \psi_n^{\mathrm{HO}}(x)\psi_n^{\mathrm{HO}}(x)\,\mathrm{d}x = 1$$

of $\{\psi_n^{\mathrm{HO}}\}$. Here, because ψ_n^{HO} is a real function, the asterisk to mark the complex conjugate in the definition of the scalar product has been omitted.

An arbitrary point $\boldsymbol{a} = (a_x, a_y, a_z)$ in the three-dimensional space can be expressed using $\boldsymbol{e}_x$, $\boldsymbol{e}_y$ and $\boldsymbol{e}_z$ as

$$\boldsymbol{a} = a_x\boldsymbol{e}_x + a_y\boldsymbol{e}_y + a_z\boldsymbol{e}_z.$$

In correspondence with this equation, an arbitrary wave function ψ_n can be expressed using $\{\psi_i^{\mathrm{HO}}\}$ as

$$\psi_n = \sum_i c_{ni}\psi_i^{\mathrm{HO}}. \tag{2.101}$$

Therefore, if the eigenfunction of the Hamiltonian (2.100) with an anharmonic potential of Eq. (2.99) is denoted as $\psi_n(x)$, $\psi_n(x)$ should be expressed as in Eq. (2.101). Of course, if the magnitude of the anharmonic term is small, ε_n is shifted only slightly from $\varepsilon_n^{\mathrm{HO}}$, and the ψ_n is defined as only slightly deformed from ψ_n^{HO}. Therefore, the largest coefficient in $\{c_{ni}\}$ should be c_{nn}. However, generally, as long as there is an anharmonic term as there is in Eq. (2.99), c_{ni} $(i \neq n)$ does not equal zero. If we can approximate that

$$\psi_0 = \psi_0^{\mathrm{HO}} \tag{2.102}$$

when $n = 0$, and the wave function of $n = 2$, which is orthogonal with ψ_0^{HO}, can be approximated as

$$\psi_2 = c_{21}\psi_1^{\mathrm{HO}} + c_{22}\psi_2^{\mathrm{HO}} + c_{23}\psi_3^{\mathrm{HO}}, \tag{2.103}$$

then according to Eq. (2.90) we can say that the transition probability from $n = 0$ to $n = 2$ is proportional to

$$I = \left(\frac{\mathrm{d}\mu}{\mathrm{d}x}\right)_{\mathrm{e}}^2 \left|\langle\psi_2|x|\psi_0\rangle\right|^2. \tag{2.104}$$

Then, by substituting Eqs. (2.102) and (2.103) into Eq. (2.104), and using the fact that, from Eq. (2.96), $\langle\psi_m^{\mathrm{HO}}|x|\psi_n^{\mathrm{HO}}\rangle = 0$ (when $|m - n| \neq 1$) holds for wave functions of harmonic oscillators, as well as the fact that, from Eq. (2.97), $\langle\psi_1^{\mathrm{HO}}|x|\psi_0^{\mathrm{HO}}\rangle = \sqrt{\frac{1}{2\beta}}$ holds, we can obtain

$$\begin{aligned} I &= \left(\frac{\mathrm{d}\mu_x}{\mathrm{d}x}\right)_{\mathrm{e}}^2 \left|\langle\sum_{i=1}^{3} c_{2i}\psi_i^{\mathrm{HO}}\middle|x\middle|\psi_0^{\mathrm{HO}}\rangle\right|^2 \\ &= \left(\frac{\mathrm{d}\mu_x}{\mathrm{d}x}\right)_{\mathrm{e}}^2 \left|\sum_{i=1}^{3} c_{2i}\langle\psi_i^{\mathrm{HO}}\middle|x\middle|\psi_0^{\mathrm{HO}}\rangle\right|^2 \\ &= c_{21}^2\left(\frac{\mathrm{d}\mu_x}{\mathrm{d}x}\right)_{\mathrm{e}}^2 \frac{1}{2\beta} \neq 0. \end{aligned} \tag{2.105}$$

Even though the c_{21}^2 is not a large value, we can see that it is possible for overtone transitions to be observed as long as $c_{21}^2 \neq 0$. Simply put, the first overtone transition occurs because the wave function of the $n = 2$ state includes a component of the wave function of the $n = 1$ state of the harmonic oscillator.

2.3.5 Matrix Elements of x^2 and the Expectation Value of the Potential Energy

The expectation value $\langle H\rangle_n$ of the Hamiltonian H of a harmonic oscillator at the eigenstate represented as ψ_n is equal to the energy eigenvalue, as explained in Sect. 2.3.2, and is expressed as

$$\langle H\rangle_n = \hbar\omega\left(n + \frac{1}{2}\right). \tag{2.106}$$

Then, let us examine what values the expectation value $\langle T\rangle_n = \langle n|T|n\rangle$ of the kinetic energy operator,

$$T = -\frac{\hbar^2}{2\mu}\frac{\mathrm{d}^2}{\mathrm{d}x^2}, \tag{2.107}$$

and the expectation value $\langle V\rangle_n = \langle n|V|n\rangle$ of the potential energy,

$$V = \frac{1}{2}\mu\omega^2 x^2, \tag{2.108}$$

take at this eigenstate. Here, we will first derive the expectation value $\langle V\rangle_n$ of the potential energy V. Since

$$\langle V\rangle_n = \langle n|V|n\rangle = \frac{1}{2}\mu\omega^2\langle n|x^2|n\rangle, \tag{2.109}$$

the matrix elements of x^2, $\langle x^2\rangle_n = \langle n|x^2|n\rangle$, need to be evaluated. We can do so by evaluating $\langle n|\xi^2|n\rangle$, because $x^2 = \frac{1}{\beta}\xi^2$.

By applying the recurrence formula (2.83) twice, we obtain

$$\begin{aligned}\xi^2 H_n &= \xi\left(nH_{n-1} + \frac{1}{2}H_{n+1}\right)\\ &= n(\xi H_{n-1}) + \frac{1}{2}(\xi H_{n+1})\\ &= n(n-1)H_{n-2} + \frac{2n+1}{2}H_n + \frac{1}{4}H_{n+2}.\end{aligned} \tag{2.110}$$

This equation can be written with the normalization constant N_n in Eq. (2.63) as

$$\xi^2|n\rangle = n(n-1)\left(\frac{N_n}{N_{n-2}}\right)|n-2\rangle + \left(\frac{2n+1}{2}\right)|n\rangle + \frac{1}{4}\left(\frac{N}{N_{n+2}}\right)|n+2\rangle. \tag{2.111}$$

Therefore, multiplying Eq. (2.111) from the left by $\langle n|$ and using the equations for orthonormality, Eqs. (2.65) and (2.74), that is, $\langle n|n-2\rangle = \langle n|n+2\rangle = 0$ and $\langle n|n\rangle = 1$, we obtain

$$\langle n|\xi^2|n\rangle = \left(n + \frac{1}{2}\right). \tag{2.112}$$

That is,

$$\langle n|x^2|n\rangle = \frac{1}{\beta}\left(n + \frac{1}{2}\right). \tag{2.113}$$

Therefore, from Eqs. (2.109),

$$\langle V\rangle_n = \frac{1}{2}\mu\omega^2\langle n|x^2|n\rangle = \frac{\mu\omega^2}{2\beta}\left(n + \frac{1}{2}\right) \tag{2.114}$$

is obtained. By substituting $\beta = \frac{\mu\omega}{\hbar}$ into this equation, we obtain

$$\langle V\rangle_n = \frac{1}{2}\mu\omega^2 \cdot \frac{\hbar}{\mu\omega}\left(n + \frac{1}{2}\right) = \frac{1}{2}\hbar\omega\left(n + \frac{1}{2}\right), \tag{2.115}$$

which is half the expectation value of the eigenenergy

$$\langle H\rangle_n = \hbar\omega\left(n + \frac{1}{2}\right).$$

Since

$$\langle H\rangle_n = \langle T\rangle_n + \langle V\rangle_n \tag{2.116}$$

holds,

$$\langle V\rangle_n = \langle T\rangle_n = \frac{1}{2}\hbar\omega\left(n + \frac{1}{2}\right) \tag{2.117}$$

is derived for a harmonic oscillator. This relationship, $\langle V\rangle_n = \langle T\rangle_n$, is called the virial theorem for harmonic oscillators.

Problem 2.14
Calculate the expectation value $\langle T\rangle_n$ of the kinetic energy of a harmonic oscillator, $T = -\frac{\hbar^2}{2\mu}\frac{\mathrm{d}^2}{\mathrm{d}x^2}$.

Solution
In the derivation above in the text, $\langle T\rangle_n$ was obtained indirectly using the relation $\langle T\rangle_n = \langle H\rangle_n - \langle V\rangle_n$. Here, we will directly evaluate $\langle n|\frac{\mathrm{d}^2}{\mathrm{d}x^2}|n\rangle$.

From Eq. (2.59),

$$\begin{aligned}\frac{\mathrm{d}^2}{\mathrm{d}x^2}|n\rangle &= \beta\frac{\mathrm{d}^2}{\mathrm{d}\xi^2}\left(N_n H_n \mathrm{e}^{-\frac{1}{2}\xi^2}\right)\\ &= \beta N_n\left\{4n(n-1)H_{n-2}\mathrm{e}^{-\frac{1}{2}\xi^2} - 4n\xi H_{n-1}\mathrm{e}^{-\frac{1}{2}\xi^2} - H_n\mathrm{e}^{-\frac{1}{2}\xi^2}\right.\\ &\quad\left. + \xi^2 H_n\mathrm{e}^{-\frac{1}{2}\xi^2}\right\}. \end{aligned} \tag{2.118}$$

By multiplying this equation from the left by $\langle n|$, we obtain

$$\begin{aligned}&\langle n|\frac{\mathrm{d}^2}{\mathrm{d}x^2}|n\rangle\\ &= \langle n|\beta\left\{4n(n-1)\left(\frac{N_n}{N_{n-2}}\right)|n-2\rangle - 4n\xi\left(\frac{N_n}{N_{n-1}}\right)|n-1\rangle - |n\rangle + \xi^2|n\rangle\right\}\\ &= \beta\left\{(-4n)\left(\frac{N_n}{N_{n-1}}\right)\langle n|\xi|n-1\rangle - 1 + \langle n|\xi^2|n\rangle\right\}\\ &= \beta\left\{(-4n)\sqrt{\frac{1}{2n}}\sqrt{\beta}\sqrt{\frac{n}{2\beta}} - 1 + \left(n+\frac{1}{2}\right)\right\}\\ &= -\beta\left(n+\frac{1}{2}\right). \end{aligned} \tag{2.119}$$

Therefore,

$$\langle T\rangle_n = -\frac{\hbar^2}{2\mu}\langle n|\frac{\mathrm{d}^2}{\mathrm{d}x^2}|n\rangle = -\frac{\hbar^2}{2\mu}(-\beta)\left(n+\frac{1}{2}\right),$$

and using $\beta = \frac{\mu\omega}{\hbar}$,

$$\langle T\rangle_n = \frac{1}{2}\hbar\omega\left(n+\frac{1}{2}\right)$$

is derived. □

In the derivation of $\langle V\rangle_n$ above, $\langle n|x^2|n\rangle$, diagonal matrix elements of x^2, was evaluated. As is clear from Eq. (2.111), the matrix element of $\langle m|x^2|n\rangle$ takes a non-zero value for off-diagonal matrix elements when $m = n-2$, $n+2$ in addition to the diagonal ($m = n$) elements. Thus, the non-zero elements are summarized as

$$\langle n-2|x^2|n\rangle = \frac{\sqrt{(n-1)n}}{2\beta}, \tag{2.120a}$$

$$\langle n|x^2|n\rangle = \frac{2n+1}{2\beta}, \tag{2.120b}$$

$$\langle n+2|x^2|n\rangle = \frac{\sqrt{(n+1)(n+2)}}{2\beta}. \tag{2.120c}$$

For all other m values

$$\langle m|x^2|n\rangle = 0 \quad (m \neq n-2, n, n+2). \tag{2.120d}$$

Problem 2.15
Express the matrix elements of x^2 in a matrix form as in Eq. (2.97).

Solution
Equations (2.120a) through (2.120d) can be expressed in a matrix form for the range $0 \leqq n \leqq 4$ and $0 \leqq m \leqq 4$ as

$$\boldsymbol{Y} = \begin{pmatrix} \frac{1}{2\beta} & 0 & \frac{\sqrt{2}}{2\beta} & 0 & 0 \\ 0 & \frac{3}{2\beta} & 0 & \frac{\sqrt{6}}{2\beta} & 0 \\ \frac{\sqrt{2}}{2\beta} & 0 & \frac{5}{2\beta} & 0 & \frac{\sqrt{12}}{2\beta} \\ 0 & \frac{\sqrt{6}}{2\beta} & 0 & \frac{7}{2\beta} & 0 \\ 0 & 0 & \frac{\sqrt{12}}{2\beta} & 0 & \frac{9}{2\beta} \end{pmatrix}. \tag{2.121}$$

□

Problem 2.16
Show that the matrix $\boldsymbol{Y}$ in Eq. (2.121), consisting of the matrix elements of x^2, can be obtained by multiplying the matrix $\boldsymbol{X}$ in Eq. (2.97) by itself.

Solution

$$\boldsymbol{X}\cdot\boldsymbol{X} = \begin{pmatrix} 0 & \sqrt{\frac{1}{2\beta}} & 0 & \\ \sqrt{\frac{1}{2\beta}} & 0 & \sqrt{\frac{2}{2\beta}} & \cdots \\ 0 & \sqrt{\frac{2}{2\beta}} & 0 & \\ & \vdots & & \ddots \end{pmatrix} \begin{pmatrix} 0 & \sqrt{\frac{1}{2\beta}} & 0 & \\ \sqrt{\frac{1}{2\beta}} & 0 & \sqrt{\frac{2}{2\beta}} & \cdots \\ 0 & \sqrt{\frac{2}{2\beta}} & 0 & \\ & \vdots & & \ddots \end{pmatrix}$$

$$= \begin{pmatrix} \frac{1}{2\beta} & 0 & \frac{\sqrt{2}}{2\beta} & \\ 0 & \frac{3}{2\beta} & 0 & \cdots \\ \frac{\sqrt{2}}{2\beta} & 0 & \frac{5}{2\beta} & \\ & \vdots & & \ddots \end{pmatrix} = \boldsymbol{Y}.$$

□

Generally, $\langle m|AB|n\rangle$, a matrix element of AB (the product of two Hermitian operators A and B) evaluated using a set of eigenfunctions $\{\psi_i\}$, can be expressed as a sum of the products of the matrix elements of A, $\langle m|A|k\rangle$, and those of B, $\langle k|B|n\rangle$, as

$$\langle m|AB|n\rangle = \sum_k \langle m|A|k\rangle\langle k|B|n\rangle. \tag{2.122}$$

This equation can be derived in the following manner.

First, operating A on $|m\rangle$ gives us

$$A|m\rangle = \sum_k a_{mk}|k\rangle. \tag{2.123}$$

Then, by multiplying this from the left side by $\langle k|$, we obtain

$$\langle k|A|m\rangle = a_{mk}.$$

Since A is a Hermitian operator,

$$\langle m|A|k\rangle^* = a_{mk}.$$

This means that

$$\langle m|A|k\rangle = a^*_{mk}, \tag{2.124}$$

which corresponds to the expression of $\langle m|$ as

$$\langle m|A = \sum_k a^*_{mk}\langle k|. \tag{2.125}$$

Similarly, by operating B on $|n\rangle$,

$$B|n\rangle = \sum_j b_{nj}|j\rangle \tag{2.126}$$

is obtained. When we multiply this equation from the left by $\langle j|$, we obtain

$$\langle j|B|n\rangle = b_{nj}. \tag{2.127}$$

From Eqs. (2.125) and (2.126),

$$\begin{aligned}\langle m|AB|n\rangle &= \sum_j \sum_k a^*_{mk} b_{nj}\langle k|j\rangle \\ &= \sum_j a^*_{mj} b_{nj} \\ &= \sum_j \langle m|A|j\rangle\langle j|B|n\rangle\end{aligned}$$

is proved. In deriving this, the orthonormal condition $\langle k|j\rangle = \delta_{kj}$ and Eqs. (2.124) and (2.127) have been used.

Equation (2.122) can be used to evaluate the matrix elements of x^2. Since the operator x is a Hermitian operator,

$$\begin{aligned}\langle m|x^2|n\rangle &= \langle m|x\cdot x|n\rangle \\ &= \sum_j \langle m|x|j\rangle\langle j|x|n\rangle. \end{aligned} \tag{2.128}$$

This is the same result as is obtained when the matrix (x_{mn}) is squared, as we have confirmed in Problem 2.16 by multiplying $\boldsymbol{X}$ by itself.

Problem 2.17
Derive the matrix elements of x^2 using Eq. (2.128).

Solution
As we have already obtained the matrix elements of x, $\langle m|x|j\rangle$, as shown in Eqs. (2.94) through (2.96), we can use Eq. (2.128) to derive the matrix elements of x^2 as the sum of the non-zero matrix elements of x, as follows:

$$\begin{aligned}\langle n-2|x^2|n\rangle &= \langle n-2|x|n-1\rangle\langle n-1|x|n\rangle \\ &= \sqrt{\frac{n-1}{2\beta}}\sqrt{\frac{n}{2\beta}} = \sqrt{\frac{(n-1)n}{2\beta}}, \\ \langle n|x^2|n\rangle &= \langle n|x|n-1\rangle\langle n-1|x|n\rangle \\ &\quad + \langle n|x|n+1\rangle\langle n+1|x|n\rangle \\ &= \sqrt{\frac{n}{2\beta}}\sqrt{\frac{n}{2\beta}} + \sqrt{\frac{n+1}{2\beta}}\sqrt{\frac{n+1}{2\beta}} = \frac{2n+1}{2\beta}, \\ \langle n+2|x^2|n\rangle &= \langle n+2|x|n+1\rangle\langle n+1|x|n\rangle \\ &= \sqrt{\frac{n+2}{2\beta}}\sqrt{\frac{n+1}{2\beta}} = \frac{\sqrt{(n+1)(n+2)}}{2\beta}. \end{aligned}$$

These are the same results as those found in Eqs. (2.120a) through (2.120d). □

2.3.6 Creation and Annihilation Operators

Up to Sect. 2.3.5, we have been discussing the procedure of calculating matrix elements using eigenfunctions of harmonic oscillators. However, this procedure is not always easy, as it relies on operations such as using the Hermite recurrence formula. Let us now take a look at a more straightforward method that serves the same purpose.

As already shown in Eqs. (2.92), (2.94), and (2.95),

$$x|n\rangle = \sqrt{\frac{n}{2\beta}}|n-1\rangle + \sqrt{\frac{n+1}{2\beta}}|n+1\rangle. \tag{2.129}$$

This shows that the coordinate operator x has the function of increasing or decreasing the vibrational quantum number in $|n\rangle$ by one.

From Eq. (2.59), when we operate a differential operator $\frac{\mathrm{d}}{\mathrm{d}x}$ on $|n\rangle$, it becomes

$$\begin{aligned}\frac{\mathrm{d}}{\mathrm{d}x}|n\rangle &= \sqrt{\beta}\frac{\mathrm{d}}{\mathrm{d}\xi}\left(N_n H_n \mathrm{e}^{-\frac{1}{2}\xi^2}\right)\\ &= \sqrt{\beta}N_n\left(2n H_{n-1}\mathrm{e}^{-\frac{1}{2}\xi^2} - \xi H_n \mathrm{e}^{-\frac{1}{2}\xi^2}\right)\\ &= \sqrt{\beta}2n\left(\frac{N_n}{N_{n-1}}\right)|n-1\rangle - \sqrt{\beta}\xi\left(\frac{N_n}{N_n}\right)|n\rangle\\ &= \sqrt{\beta}2n\sqrt{\frac{1}{2n}}|n-1\rangle - \sqrt{\beta}\sqrt{\beta}x|n\rangle\\ &= \sqrt{2n\beta}|n-1\rangle - \beta x|n\rangle. \end{aligned} \tag{2.130}$$

Using Eq. (2.129), $\frac{\mathrm{d}}{\mathrm{d}x}|n\rangle$ can be expressed as

$$\frac{\mathrm{d}}{\mathrm{d}x}|n\rangle = \sqrt{\beta}\left(\sqrt{\frac{n}{2}}|n-1\rangle - \sqrt{\frac{n+1}{2}}|n+1\rangle\right), \tag{2.131}$$

which shows that the differential operator $\frac{\mathrm{d}}{\mathrm{d}x}$ also has the function of increasing or decreasing the vibrational quantum number in $|n\rangle$ by one.

Then, if we define two operators a and $a^\dagger$ (a dagger) as

$$a = \frac{1}{\sqrt{2}}\left(\xi + \frac{\mathrm{d}}{\mathrm{d}\xi}\right), \tag{2.132a}$$

$$a^\dagger = \frac{1}{\sqrt{2}}\left(\xi - \frac{\mathrm{d}}{\mathrm{d}\xi}\right), \tag{2.132b}$$

we find that a useful and neat relationship,

$$\begin{cases} a\psi_n = \sqrt{n}\psi_{n-1}, \\ a^\dagger\psi_n = \sqrt{n+1}\psi_{n+1}, \end{cases} \tag{2.133}$$

that is,

$$\begin{cases} a|n\rangle = \sqrt{n}|n-1\rangle, \\ a^\dagger|n\rangle = \sqrt{n+1}|n+1\rangle, \end{cases} \tag{2.134}$$

exists. Because the operator a functions to annihilate (decrease) the quantum number n by one, it is called an annihilation operator or a lowering operator. Similarity, as the operator $a^\dagger$ functions to create (increase) the quantum number n by one, it is called a creation operator or a raising operator.

Problem 2.18

Prove Eq. (2.134) by rewriting Eqs. (2.129) and (2.131) with the coordinate variable ξ.

Solution

Since $\xi = \sqrt{\beta}x$, Eq. (2.129) becomes

$$\xi|n\rangle = \sqrt{\frac{n}{2}}|n-1\rangle + \sqrt{\frac{n+1}{2}}|n+1\rangle. \tag{2.135}$$

Also, as $\frac{\mathrm{d}}{\mathrm{d}\xi} = \frac{1}{\sqrt{\beta}}\frac{\mathrm{d}}{\mathrm{d}x}$, Eq. (2.131) becomes

$$\frac{\mathrm{d}}{\mathrm{d}\xi}|n\rangle = \sqrt{\frac{n}{2}}|n-1\rangle - \sqrt{\frac{n+1}{2}}|n+1\rangle. \tag{2.136}$$

Therefore, using the definitions in Eqs. (2.132a) and (2.132b), we can obtain

$$a|n\rangle = \frac{1}{\sqrt{2}}\left(\xi + \frac{\mathrm{d}}{\mathrm{d}\xi}\right)|n\rangle = \frac{1}{\sqrt{2}}2\sqrt{\frac{n}{2}}|n-1\rangle = \sqrt{n}|n-1\rangle, \tag{2.137}$$

$$\begin{aligned} a^\dagger|n\rangle &= \frac{1}{\sqrt{2}}\left(\xi - \frac{\mathrm{d}}{\mathrm{d}\xi}\right)|n\rangle = \frac{1}{\sqrt{2}}2\sqrt{\frac{n+1}{2}}|n+1\rangle \\ &= \sqrt{n+1}|n+1\rangle, \end{aligned} \tag{2.138}$$

which are identical to Eq. (2.134). □

These creation and annihilation operators are useful tools allowing us to easily evaluate matrix elements. For example, from the definitions of a and $a^\dagger$ in Eqs. (2.132a) and (2.132b),

$$\xi = \frac{a + a^\dagger}{\sqrt{2}} \tag{2.139}$$

is obtained. Therefore,

$$\begin{aligned} \langle n|x|n-1\rangle &= \frac{1}{\sqrt{\beta}}\langle n|\frac{a+a^\dagger}{\sqrt{2}}|n-1\rangle \\ &= \sqrt{\frac{1}{2\beta}}\left\{\langle n|a|n-1\rangle + \langle n|a^\dagger|n-1\rangle\right\} \\ &= \sqrt{\frac{1}{2\beta}}(0+\sqrt{n}) = \sqrt{\frac{n}{2\beta}} \end{aligned} \tag{2.140}$$

is readily derived. In a similar manner, $\langle n|x^2|n\rangle$ is expressed as

$$\langle n|x^2|n\rangle = \frac{1}{\beta}\langle n|\left(\frac{a+a^\dagger}{\sqrt{2}}\right)^2|n\rangle,$$

and therefore

$$\begin{aligned} \langle n|x^2|n\rangle &= \frac{1}{2\beta}\langle n|aa + aa^\dagger + a^\dagger a + a^\dagger a^\dagger|n\rangle \\ &= \frac{1}{2\beta}\langle n|aa^\dagger + a^\dagger a|n\rangle \\ &= \frac{2n+1}{2\beta} \end{aligned} \tag{2.141}$$

is readily obtained.

Since the Hamiltonian of a harmonic oscillator is expressed using ξ and $\frac{\mathrm{d}}{\mathrm{d}\xi}$ as

$$\begin{aligned} H &= -\frac{\hbar^2}{2\mu}\frac{\mathrm{d}^2}{\mathrm{d}x^2} + \frac{1}{2}\mu\omega^2 x^2 \\ &= \frac{1}{2}\hbar\omega\left(-\frac{\mathrm{d}^2}{\mathrm{d}\xi^2} + \xi^2\right), \end{aligned} \tag{2.142}$$

it can be expressed with a and $a^\dagger$ as

$$H = \hbar\omega\left(a^\dagger a + \frac{1}{2}\right). \tag{2.143}$$

Thus, the expectation value of energy becomes

$$\begin{aligned} \langle n|H|n\rangle &= \hbar\omega\left(\langle n|a^\dagger a|n\rangle + \frac{1}{2}\right) \\ &= \hbar\omega\left(n + \frac{1}{2}\right). \end{aligned} \tag{2.144}$$

Problem 2.19
Prove that H, the Hamiltonian of a harmonic oscillator, can be expressed in the form of Eq. (2.143).

Solution

$$a^\dagger a = \frac{1}{\sqrt{2}}\left(\xi - \frac{\mathrm{d}}{\mathrm{d}\xi}\right)\cdot\frac{1}{\sqrt{2}}\left(\xi + \frac{\mathrm{d}}{\mathrm{d}\xi}\right) = \frac{1}{2}\left(\xi^2 + \xi\frac{\mathrm{d}}{\mathrm{d}\xi} - \frac{\mathrm{d}}{\mathrm{d}\xi}\xi - \frac{\mathrm{d}^2}{\mathrm{d}\xi^2}\right).$$

On the other hand, for a general function $\varphi(\xi)$,

$$\left(\xi\frac{\mathrm{d}}{\mathrm{d}\xi} - \frac{\mathrm{d}}{\mathrm{d}\xi}\xi\right)\varphi = \xi\frac{\mathrm{d}\varphi}{\mathrm{d}\xi} - \frac{\mathrm{d}\xi}{\mathrm{d}\xi}\varphi - \xi\frac{\mathrm{d}\varphi}{\mathrm{d}\xi} = -\varphi,$$

indicating that

$$\xi\frac{\mathrm{d}}{\mathrm{d}\xi} - \frac{\mathrm{d}}{\mathrm{d}\xi}\xi = -1. \tag{2.145}$$

Therefore,

$$a^\dagger a = \frac{1}{2}\left(\xi^2 - \frac{\mathrm{d}^2}{\mathrm{d}\xi^2}\right) - \frac{1}{2}$$

is obtained. From this equation and Eq. (2.142), Eq. (2.143) is derived. □

Problem 2.20
Express $\langle V\rangle_n$ and $\langle T\rangle_n$ of a harmonic oscillator using creation and annihilation operators.

Solution
From Eq. (2.141),

$$\langle V\rangle_n = \frac{1}{2}\mu\omega^2\langle n|x^2|n\rangle$$
$$= \frac{\mu\omega^2}{4\beta}(2n+1) = \frac{1}{2}\hbar\omega\left(n+\frac{1}{2}\right)$$

is obtained. From Eqs. (2.132a) and (2.132b),

$$\frac{\mathrm{d}}{\mathrm{d}\xi} = \frac{a-a^\dagger}{\sqrt{2}}. \tag{2.146}$$

Therefore,

$$\langle T\rangle_n = -\frac{\hbar^2}{2\mu}\langle n|\frac{\mathrm{d}^2}{\mathrm{d}x^2}|n\rangle$$
$$= -\frac{\hbar^2}{2\mu}\left(-\frac{\beta}{2}\right)\langle n|aa^\dagger + a^\dagger a|n\rangle$$
$$= \frac{1}{2}\hbar\omega\left(n+\frac{1}{2}\right)$$

is obtained. □

2.3.7 *Evaluation of Perturbation Energy*

As already described in Sect. 2.3.4, the interatomic potential, $V(x)$, of real diatomic molecules in general, deviates from that of a harmonic oscillator, and has an anharmonicity represented using an additional contribution from anharmonic terms, that is,

$$V(x) = \frac{1}{2}\mu\omega^2x^2 + fx^3 + gx^4. \tag{2.147}$$

In the present subsection, we will learn how the eigenenergy of a vibrational level with the vibrational quantum number n deviates from the energy of the harmonic oscillator,

$$\varepsilon_n^{\mathrm{HO}} = \hbar\omega\left(n+\frac{1}{2}\right),$$

by the presence of the anharmonic terms fx^3 and gx^4.

The first-order perturbation energy $\varepsilon_n^{(1)}$ is equal to the expectation value of the perturbing term H', that is

$$\varepsilon_n^{(1)} = \langle n|H'|n\rangle. \tag{2.148}$$

In the present case, $H' = fx^3 + gx^4$, and therefore,

$$\varepsilon_n^{(1)} = \langle n|fx^3|n\rangle + \langle n|gx^4|n\rangle. \tag{2.149}$$

This shows that once we evaluate $\langle n|x^3|n\rangle$ and $\langle n|x^4|n\rangle$, the first-order perturbation energy can be readily derived. Using a and $a^\dagger$, we can write

$$\langle n|x^3|n\rangle = 0, \tag{2.150}$$

$$\begin{aligned}\langle n|x^4|n\rangle &= \frac{1}{4\beta^2}\left\{\langle n|\left(a+a^\dagger\right)^4|n\rangle\right\} \\ &= \frac{1}{4\beta^2}\left\{\langle n|aaa^\dagger a^\dagger + aa^\dagger aa^\dagger + a^\dagger aaa^\dagger \right. \\ &\quad \left. + a^\dagger a^\dagger aa + a^\dagger aa^\dagger a + aa^\dagger a^\dagger a|n\rangle\right\} \\ &= \frac{3}{4\beta^2}\left(2n^2+2n+1\right),\end{aligned} \tag{2.151}$$

and thus

$$\varepsilon_n^{(1)} = \frac{3g}{4\beta^2}\left(2n^2+2n+1\right) \tag{2.152}$$

is obtained. This means that the level energy increases (when $g > 0$) or decreases (when $g < 0$) by $|\varepsilon_n^{(1)}|$, and that its third-order anharmonic term, fx^3, does not generate an energy shift within the range of first-order perturbation. However, if we consider second-order perturbation, it can be shown that the third-order anharmonic term can generate an energy shift.

Perturbation theory shows that the second-order perturbation energy $\varepsilon_n^{(2)}$ can be expressed as

$$\varepsilon_n^{(2)} = \sum_{m\neq n} \frac{\langle n|H'|m\rangle\langle m|H'|n\rangle}{\varepsilon_n^{\mathrm{HO}} - \varepsilon_m^{\mathrm{HO}}}. \tag{2.153}$$

Supposing that the contribution from the fourth-order anharmonic term is negligible, H' can be written with just the third-order anharmonic term fx^3, as

$$H' = fx^3 = f\left(\frac{a+a^\dagger}{\sqrt{2\beta}}\right)^3. \tag{2.154}$$

Since $(a+a^\dagger)^3|n\rangle$ is calculated as

$$\begin{aligned}(a+a^\dagger)^3|n\rangle &= \sqrt{n}\sqrt{n-1}\sqrt{n-2}|n-3\rangle + 3n\sqrt{n}|n-1\rangle \\ &\quad + 3(n+1)\sqrt{n+1}|n+1\rangle \\ &\quad + \sqrt{n+1}\sqrt{n+2}\sqrt{n+3}|n+3\rangle,\end{aligned} \tag{2.155}$$

the summation over m in Eq. (2.153) need only be taken for $m = n-3, n-1, n+1, n+3$. Therefore, we can evaluate that

$$\varepsilon_n^{(2)} = -f^2\left(\frac{1}{2\beta}\right)^3 \frac{1}{\hbar\omega}\left(30n^2+30n+11\right). \tag{2.156}$$

This shows that $\varepsilon_n^{(2)} < 0$, indicating that the third-order anharmonicity always lowers the eigenenergy. From these arguments, we can evaluate the n-th vibrational level energy of the anharmonic oscillator whose potential energy is given by Eq. (2.147) as

$$\begin{aligned}\varepsilon_n &= \varepsilon_n^{\mathrm{HO}} + \varepsilon_n^{(1)} + \varepsilon_n^{(2)} \\ &= \hbar\omega\left(n+\frac{1}{2}\right) + \frac{3g}{4\beta^2}\left(2n^2+2n+1\right) \\ &\quad - \frac{f^2}{8\beta^3\hbar\omega}\left(30n^2+30n+11\right). \end{aligned} \tag{2.157}$$

When we measure the vibrational level energies of diatomic molecules and examine their dependence on the vibrational quantum number, we see that in most cases, the energy can be expresses as a form expanded in terms of $(n+\frac{1}{2})$ as

$$\varepsilon_n = \hbar\omega\left(n+\frac{1}{2}\right) - \hbar\omega\chi\left(n+\frac{1}{2}\right)^2 + \cdots, \tag{2.158}$$

where χ is called an anharmonic constant. As will be explained in Sect. 2.3.8, the eigenenergy of the Morse oscillator, whose interatomic potential (called the Morse potential) is known to be a good approximation of the potential function of diatomic molecules, can be expressed by the expansion up to the second term. That is, the eigenenergy of the Morse potential can be written with only the $(n+\frac{1}{2})$ and $(n+\frac{1}{2})^2$ terms.

As our next step, let us compare Eqs. (2.157) and (2.158), and express the anharmonic constant χ using the coefficients for the anharmonic terms, f and g. Firstly, if we rewrite the second and third terms in Eq. (2.157) using $(n+\frac{1}{2})^2 = (n^2+n+\frac{1}{4})$,

$$\varepsilon_n^{(1)} + \varepsilon_n^{(2)} = \frac{3}{2\beta}\left(\frac{g}{\beta} - \frac{5f^2}{2\beta^2\hbar\omega}\right)\left(n+\frac{1}{2}\right)^2 + \Delta. \tag{2.159}$$

As Δ does not have an n-dependence and its contribution is considered to be small, we will hereafter assume that $\Delta \sim 0$ and treat it as negligible. If we equate the second term in Eq. (2.158) and the first term in Eq. (2.159),

$$\chi = \frac{3\hbar\omega}{2k}\left\{-\frac{g}{k} + \frac{5}{2}\left(\frac{f}{k}\right)^2\right\} \tag{2.160}$$

is obtained, where $k = \mu\omega^2$ represents a quadratic force constant.

2.3.8 *Morse Potential*

A Morse potential is a model potential known to well describe the shape of an interatomic potential of a diatomic molecule in the wide internuclear distance region. The Morse potential $V_{\mathrm{M}}(x)$ is expressed in the form of a function of the displacement x as

$$V_{\mathrm{M}}(x) = D_{\mathrm{e}}\left(\mathrm{e}^{-\alpha x} - 1\right)^2. \tag{2.161}$$

As illustrated in Fig. 2.9, the slope of the potential becomes gradually smaller as x increases. When $x \to \infty$, the slope,

$$\frac{\mathrm{d}V_{\mathrm{M}}(x)}{\mathrm{d}x} = -2\alpha D_{\mathrm{e}}\left(\mathrm{e}^{-\alpha x} - 1\right)\mathrm{e}^{-\alpha x}, \tag{2.162}$$

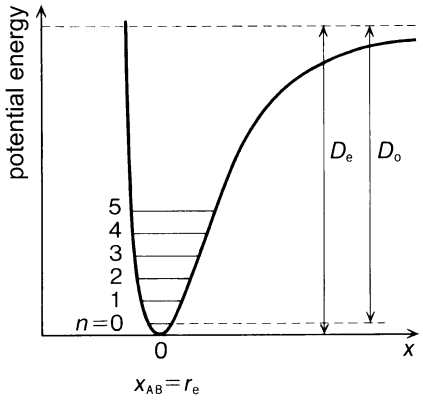

Fig. 2.9 A Morse potential and its dissociation energy

becomes $\frac{dV_M(x)}{dx} \to 0$, and the diatomic molecule dissociates into two atoms.

From Eq. (2.162), it can be seen that $\left(\frac{dV_M(x)}{dx}\right) = 0$ when $x = 0$. This means that $x = 0$ represents an equilibrium position where the slope of the potential becomes zero. Furthermore, it can be understood from Eq. (2.161) that $V_M(x) = 0$ at $x = 0$ and $V_M(x) \to D_e$ at $x \to \infty$. This D_e is called the dissociation energy, "D" standing for "dissociation," and it can be regarded as the energy required to separate the two atoms in a diatomic molecule to an infinite distance, starting from their equilibrium internuclear distance of the molecule. As was explained in Sect. 2.1, x is defined as the difference between the internuclear distance x_{AB} and the equilibrium internuclear distance r_e,

$$x = x_{AB} - r_e.$$

Therefore, $x_{AB} = r_e$ holds at the equilibrium position of $x = 0$.

In Fig. 2.9, D_0 represents the energy required for dissociation as measured from the $n = 0$ level, which is called the spectroscopic dissociation energy in contrast with D_e, the dissociation energy measured from the equilibrium position.

The Morse potential has another characteristic feature besides describing the potential energies of diatomic molecules. Namely, the Schrödinger equation

$$-\frac{\hbar^2}{2\mu}\frac{d^2}{dx^2}\psi + V_M(x)\psi = E\psi \tag{2.163}$$

of an oscillator which oscillates under the Morse potential has an exact solution, and its eigenenergies are expressed as

$$E_n = \hbar\omega\left(n + \frac{1}{2}\right) - \hbar\omega\chi\left(n + \frac{1}{2}\right)^2 \tag{2.164}$$

using the first-order and the second-order expression terms of $(n + \frac{1}{2})$. It is also known that the parameters ω and χ appearing in the expansion coefficients in Eq. (2.164) can be written with the Morse potential parameter α and D_e as

$$\omega = \alpha\sqrt{\frac{2D_\mathrm{e}}{\mu}} \tag{2.165}$$

$$\chi = \frac{\hbar\omega}{4D_\mathrm{e}}. \tag{2.166}$$

Sometimes, the Morse function is expressed as

$$V_\mathrm{M}(x) = D_\mathrm{e}\left\{\left(\mathrm{e}^{-\alpha x} - 1\right)^2 - 1\right\} = D_\mathrm{e}\mathrm{e}^{-2\alpha x} - 2D_\mathrm{e}\mathrm{e}^{-\alpha x} \tag{2.167}$$

so that the potential energy becomes zero when the two atoms are separated at an infinite distance.

Problem 2.21
Prove Eqs. (2.165) and (2.166) by expanding a Morse potential around $x = 0$ by a polynomial of x. To derive Eq. (2.166), use Eq. (2.160).

Solution
In a similar manner as in Sect. 2.3.7, we can expand $V_\mathrm{M}(x)$ in terms of x as

$$V_\mathrm{M}(x) = \frac{1}{2}\mu\omega^2 x^2 + fx^3 + gx^4 + \cdots. \tag{2.168}$$

From the definition of the Morse potential given by Eq. (2.161),

$$\left(\frac{\mathrm{d}^2 V_\mathrm{M}(x)}{\mathrm{d}x^2}\right)_{x=0} = 2\alpha^2 D_\mathrm{e}, \quad \left(\frac{\mathrm{d}^3 V_\mathrm{M}(x)}{\mathrm{d}x^3}\right)_{x=0} = -6\alpha^3 D_\mathrm{e}, \quad \left(\frac{\mathrm{d}^4 V_\mathrm{M}(x)}{\mathrm{d}x^4}\right)_{x=0} = 14\alpha^4 D_\mathrm{e} \tag{2.169}$$

are obtained. From Eq. (2.168), we can show that

$$\left(\frac{\mathrm{d}^2 V_\mathrm{M}(x)}{\mathrm{d}x^2}\right)_{x=0} = \mu\omega^2, \quad \left(\frac{\mathrm{d}^3 V_\mathrm{M}(x)}{\mathrm{d}x^3}\right)_{x=0} = 6f, \quad \left(\frac{\mathrm{d}^4 V_\mathrm{M}(x)}{\mathrm{d}x^4}\right)_{x=0} = 24g. \tag{2.170}$$

Therefore, from Eqs. (2.169) and (2.170),

$$\mu\omega^2 = 2\alpha^2 D_\mathrm{e}, \tag{2.171a}$$

$$f = -\alpha^3 D_\mathrm{e}, \tag{2.171b}$$

$$g = \frac{7}{12}\alpha^4 D_\mathrm{e} \tag{2.171c}$$

are obtained. From Eq. (2.171a), we can immediately derive

$$\omega = \alpha\sqrt{\frac{2D_\mathrm{e}}{\mu}}.$$

On the other hand, by substituting Eqs. (2.171b) and (2.171c) into Eq. (2.160),

$$\chi = \frac{3\hbar\omega}{2k}\left\{-\frac{7}{24}\alpha^2 + \frac{5}{2}\left(-\frac{\alpha}{2}\right)^2\right\} = \frac{\hbar\omega\alpha^2}{2\mu\omega^2}$$

is obtained using $k = \mu\omega^2$. Then, by using Eq. (2.171a),

$$\chi = \frac{\hbar\omega}{4D_e}$$

is obtained. □

From Eqs. (2.165) and (2.166), we learn that, if we derive vibrational level energies from experiments and they are expanded as shown in Eq. (2.164), then both the shape of the Morse potential and the dissociation energy of the diatomic molecule can be determined by assuming that the shape of the interatomic potential is represented by a Morse function.

Indeed, from Eq. (2.166),

$$D_e = \frac{(\hbar\omega)^2}{4\hbar\omega\chi} \tag{2.172}$$

is obtained, and α can be determined from Eq. (2.165).

Problem 2.22

Prove that, when the vibrational level energies of a diatomic molecule is expressed as Eq. (2.164), the relation

$$D_e = D_0 + \frac{\hbar\omega}{2} - \frac{\hbar\omega\chi}{4} \tag{2.173}$$

holds between the two dissociation energies D_e and D_0.

Solution

As is clear from Fig. 2.9, $D_e - D_0$ is the energy of the $n = 0$ level (vibrational ground level) as measured from the bottom of the interatomic potential. Thus it is equal to the zero-point energy $E_0 = D_e - D_0$. From Eq. (2.164),

$$E_0 = \frac{\hbar\omega}{2} - \frac{\hbar\omega\chi}{4}.$$

Therefore, Eq. (2.173) can be derived. □

Let us examine how the vibrational level energies are affected by the anharmonicity of the potential, for the level energy data of $H^{35}Cl$ from $n = 1$ to $n = 5$ listed in Table 2.2.

As summarized in Table 2.3, we can see that the energy difference $\Delta G_{n+\frac{1}{2}} = E_{n+1} - E_n$ gradually decreases as the vibrational quantum number n increases. The extent of the decrease is approximately the same for each increase of n by one, and the average of the four values is $-103.12\ \mathrm{cm}^{-1}$.

This situation is graphically represented in Fig. 2.10. Such a plot is called the Birge-Sponer plot. This type of linear decrease in $\Delta G_{n+\frac{1}{2}}$ is known to be observed for many diatomic molecules, and it can be explained with equations as follows.

Table 2.3 Anharmonicity appearing in vibrational level energies of $H^{35}Cl$

n	$E_n - E_0/\text{cm}^{-1}$	$\Delta G_{n+\frac{1}{2}}/\text{cm}^{-1}$	$\Delta^2 G_{n+\frac{1}{2}}/\text{cm}^{-1}$
0	0		
		2885.90	
1	2885.90		−103.75
		2782.15	
2	5668.05		−103.22
		2678.93	
3	8346.98		−102.80
		2576.13	
4	10923.11		−102.69
		2473.44	
5	13396.55		

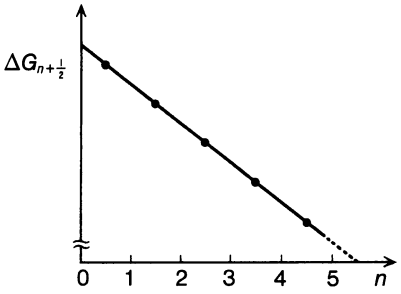

Fig. 2.10 Binge-Sponer's plot of the vibrational levels of $H^{35}Cl$

Assuming that the vibrational energy of a diatomic molecule is expressed by Eq. (2.164), and following the convention in vibrational spectroscopy of expressing the equation in terms of wave numbers (cm^{-1}), Eq. (2.164) becomes

$$E_n = \omega_e\left(n+\frac{1}{2}\right) - \omega_e x_e\left(n+\frac{1}{2}\right)^2, \tag{2.174}$$

where both ω_e and $\omega_e x_e$ have the unit of cm^{-1}, and are related with the parameters in Eq. (2.164) as

$$hc\omega_e = \hbar\omega, \tag{2.175a}$$

$$hc\omega_e x_e = \hbar\omega\chi. \tag{2.175b}$$

In molecular spectroscopy, $\omega_e x_e$ is often treated as a parameter representing the anharmonicity of the potential without separating ω_e and x_e. From Eq. (2.174),

$$E_{n+1} = \omega_e\left(n+\frac{3}{2}\right) - \omega_e x_e\left(n+\frac{3}{2}\right)^2,$$

and therefore

$$\Delta G_{n+\frac{1}{2}} = E_{n+1} - E_n = \omega_e - 2\omega_e x_e (n+1) \tag{2.176}$$

is readily derived. The value $-2\omega_e x_e$ is the slope of the linear decrease. Since $-2\omega_e x_e = -103.12\ \mathrm{cm}^{-1}$,

$$\omega_e x_e = 51.56\ \mathrm{cm}^{-1}$$

can be obtained, and when $n = 0$,

$$2885.9 = \omega_e - 2\omega_e x_e$$

holds. Therefore,

$$\omega_e = 2989.0\ \mathrm{cm}^{-1}.$$

Consequently, assuming that the potential is expressed by a Morse potential, the dissociation energy D_e can be obtained from Eqs. (2.172), (2.175a), and (2.175b) as

$$D_e = \frac{(hc\omega_e)^2}{4hc\omega_e x_e} = \frac{hc\omega_e^2}{4\omega_e x_e}.$$

When D_e is expressed in terms of wave numbers,

$$D_e = \frac{\omega_e^2}{4\omega_e x_e}. \tag{2.177}$$

By substituting the numerical values,

$$D_e = 43327.5\ \mathrm{cm}^{-1} = 5.37192\ \mathrm{eV}$$

is derived. This value is overestimated by 16 % with respect to the value calculated from Eq. (2.173) using the literature value of D_0, which is $D_e = 4.618$ eV. This indicates that the interatomic potential of HCl begins to deviate from the Morse function as its energy becomes closer to the dissociation limit, that is, the gradient of the potential energy curve in the large internuclear distance region becomes lower than that of the Morse potential curve.

2.4 The Inversion Motion of Ammonia Molecules

So far, we have viewed molecular vibration as the stretching and shrinking of the internuclear distance of a diatomic molecule, taking harmonic potentials with additional anharmonic terms, or Morse functions, as examples of the potential function for molecular vibration. The potential of the vibrational motion for polyatomic molecules can also generally be approximated, in the vicinity of the equilibrium geometrical structure, by the sum of the potentials of harmonic oscillators. However, when we expand our view to include molecular vibration in regions that are distant from the equilibrium position, we see that the potential can have varying forms, some of which are largely different from that of a harmonic oscillator. The potential of the inversion motion of an ammonia molecule is one such example.

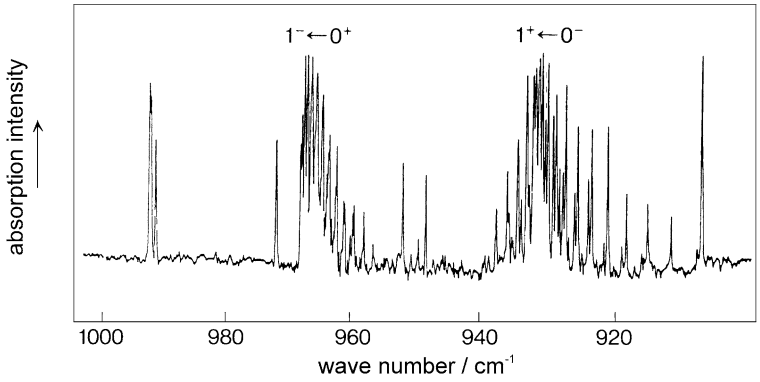

Fig. 2.11 A part of the infrared absorption spectrum of ammonia

As an aside, in Sects. 2.2 and 2.3 we represented the vibrational quantum number as n, but in molecular spectroscopy it is conventionally represented with v for 'vibration'. We will henceforth follow this convention and use v to represent the vibrational quantum number.

2.4.1 The Infrared Absorption Spectrum

A part of the infrared absorption spectrum of ammonia molecules is shown in Fig. 2.11. In the spectrum, we can see two strong absorption bands, closely spaced, at 968.32 cm^{-1} and 931.71 cm^{-1}. The individual sharp peaks in each absorption band correspond to transitions from the rotational level of the vibrational ground state to the rotational levels of the vibrationally excited state. As we discuss in Sect. 3.6, these line structures in the vibrational band are called rotational structures. For the moment, we will focus our attention on the two parts where sharp peaks are concentrated to form strong absorption peaks. Both of these two absorption peaks originate from the vibrational motion in which the three H–N–H angles of the ammonia molecule increase and decrease in unison, or, in other words, the three H atoms move up and down as shown in Fig. 2.12. This collective motion corresponds to the type of normal mode vibration that will be explained in Sect. 2.5, and as long as we consider only the small amplitude vibration in the vicinity of a pyramidal equilibrium structure such as the one in Fig. 2.12, we can approximate the vibration by a harmonic oscillator. Then the infrared absorption process in which the vibrational quantum number v changes from $v = 0$ to $v = 1$ would have to be observed as one peak. The fact that we observe two adjacent absorption peaks in the spectrum is a direct consequence of the inversion motion of ammonia molecules (Fig. 2.13(a)), which cannot be treated as a simple harmonic oscillator.

Intuitively speaking, the ammonia molecule on the right side (r) as shown in Fig. 2.13(a) can be thought of as going over the central potential barrier with the

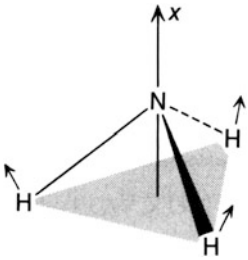

Fig. 2.12 Equilibrium structure of ammonia. The length of the perpendicular line drawn from the N atom to the plane formed by the three H atoms is 0.374 Å

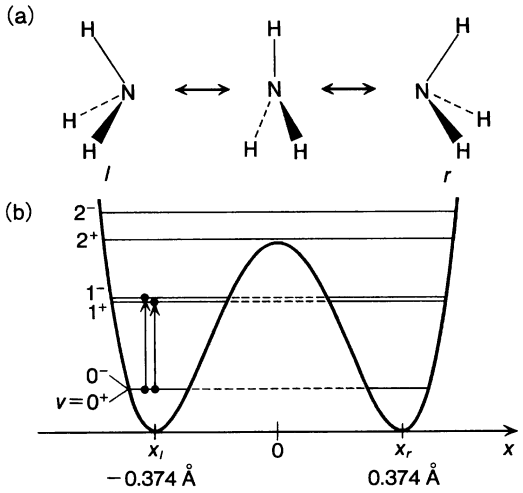

Fig. 2.13 Inversion motion of ammonia (**a**) and its double minimum potential (**b**)

increase of the vibrational energy, and turning inside out to form the ammonia molecule shown on the left side (l). The geometrical structures of ammonia at the two equilibrium positions on the r side and the l side are identical, constituting mirror images of each other. In order to describe this inversion motion, we define the straight line drawn perpendicular to the plane formed by the three H atoms and passing through the N atom, as well as the center of mass of the three H atoms, as the x axis. The origin of the x axis ($x = 0$) is set on the N atom. The potential function along the x axis can be drawn as Fig. 2.13(b). As shown in this figure, the potential takes the minimum value at the two equilibrium positions $x_r = 0.374$ Å and $x_l = -0.374$ Å. When the molecule becomes planar at $x = 0$, it comes to the top of the central barrier, which means that the potential takes a local maximum value. When the value of x increases beyond x_r, the potential energy increases monotonously, and likewise the potential energy increases monotonously when the value of x decreases beyond x_l.

A potential with two local minima such as the one shown in Fig. 2.13(b) is called a double minimum potential. The potential of ammonia along the x axis is a well-known example of a double minimum potential. To treat the vibrational motion of ammonia under the double minimum potential in quantum mechanics, and to calculate the vibrational level energy (the eigenenergy) and the vibrational wave

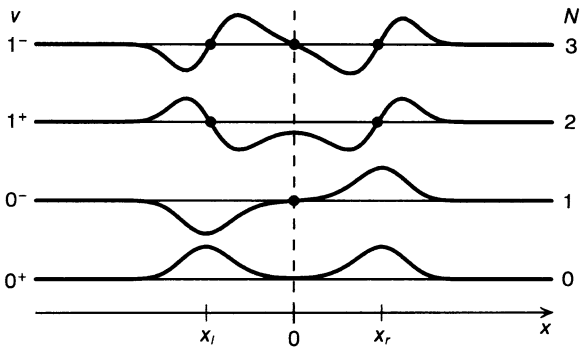

Fig. 2.14 Vibrational wave functions of the inversion motion of ammonia. The zeros (nodes) are marked by "●"

function (the eigenfunction), we need to represent the potential $V(x)$ as the sum of the harmonic potential and the Gaussian function, that is,

$$V(x) = \frac{1}{2}\mu\omega^2 x^2 + A\mathrm{e}^{-Bx^2} \quad \text{(where } A \text{ and } B \text{ are positive constants)}, \tag{2.178}$$

and numerically solve the one-dimensional Schrödinger's equation

$$-\frac{\hbar^2}{2\mu}\frac{\mathrm{d}^2}{\mathrm{d}x^2}\psi + V(x)\psi = \varepsilon\psi. \tag{2.179}$$

Sometimes, instead of using Eq. (2.178), the double minimum potential is represented as the sum of a quadratic function with negative curvature and a quartic function with positive curvature, as

$$V(x) = -Ax^2 + Bx^4 \quad \text{(where } A \text{ and } B \text{ are positive constants)}. \tag{2.180}$$

As schematically shown in Fig. 2.13(b), we can regard each individual vibrational state as being split into two levels due to the existence of the central barrier with a finite height. Accordingly, we assign the vibrational quantum number v of 0^+, 0^-, 1^+, 1^-, ..., to each vibrational level, in increasing order of energy from the ground vibrational state, $v = 0^+$. In fact, the two main peaks observed in the infrared absorption spectrum (Fig. 2.11) correspond to the transitions from $v = 0^+$ to $v = 1^-$ and from $v = 0^-$ to $v = 1^+$.

2.4.2 Parity of Wave Functions

The classification with $+$ and $-$ signs can be understood from the shape of the vibrational wave functions. The wave functions of the four low-lying levels $v = 0^+$, 0^-, 1^+, 1^- are described in Fig. 2.14.

We will examine the parity of the vibrational wave function $\psi_v(x)$ with the vibrational quantum number v by changing the sign of the coordinate from x

to $-x$. When $\psi_v(-x) = +\psi_v(x)$ holds, $\psi_v(x)$ is an even function, and we attach a plus sign on the right shoulder of the vibrational quantum number v. When $\psi_v(-x) = -\psi_v(x)$ holds, $\psi_v(x)$ is an odd function, and we attach a minus sign on the right shoulder of v.

From Fig. 2.14, we can see that

$$\psi_{0^+}(-x) = \psi_{0^+}(x), \qquad \psi_{1^+}(-x) = \psi_{1^+}(x)$$

holds for $v = 0^+, 1^+$, which tells us that these are even functions. On the other hand,

$$\psi_{0^-}(-x) = -\psi_{0^-}(x), \qquad \psi_{1^-}(-x) = -\psi_{1^-}(x)$$

holds for $v = 0^-, 1^-$, characterizing them as odd functions.

As has been discussed in Sect. 2.3.3, in order for infrared light absorption to occur from the level with quantum number v'' to that with v', it is required that

$$\int_{-\infty}^{\infty} \psi_{v'}^* x \psi_{v''} \, \mathrm{d}x$$

has a non-zero value. Since x is an odd function, the parity of integrand $\psi_{v'}^* \times x \times \psi_{v''}$ in the integral above becomes odd when $\psi_{v'}$ and $\psi_{v''}$ have the same parity, that is,

$$\text{even} \times \text{odd} \times \text{even} = \text{odd},$$
$$\text{odd} \times \text{odd} \times \text{odd} = \text{odd}.$$

If we integrate an odd function from $-\infty$ to ∞ we end up with 0, so that infrared absorption does not occur. On the other hand, when either $\psi_{v'}$ or $\psi_{v''}$ is an even function and the other is an odd function, the parity of the integrand becomes even, i.e.,

$$\text{even} \times \text{odd} \times \text{odd} = \text{even},$$
$$\text{odd} \times \text{odd} \times \text{even} = \text{even}.$$

In this case, the integral can take a non-zero value, and infrared light absorption can occur. Thus, we can see that infrared absorption occurs with transitions from 0^+ (even) to 1^- (odd) and from 0^- (odd) to 1^+ (even), and that the different energy separations in these two transitions are what causes there to be two peeks in the absorption spectrum.

2.4.3 Energy Level Splitting and Potential Barriers

The number of nodes N in the wave functions, marked by black dots in Fig. 2.14, increases as $N = 0, 1, 2, 3$ when v changes as $v = 0^+, 0^-, 1^+, 1^-$. Drawing upon the case of harmonic oscillators discussed in Sect. 2.2, we can assign quantum numbers $v = 0$, 1, 2, 3 to these wave functions. Meanwhile, if we focus our attention on either of the two neighboring potential wells (for instance, just the left potential

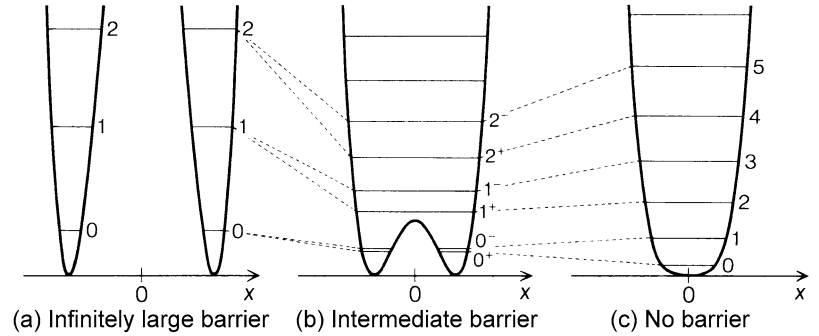

Fig. 2.15 Energy levels splitting with changes in the height of the barrier: (**a**) Infinitely large barrier; (**b**) Intermediate barrier; (**c**) No barrier

well) and ignore the other, we find that the wave function has zero nodes in the case of $v = 0^+$ and $v = 0^-$, and one in the case of $v = 1^+$ and $v = 1^-$.

Such characteristics of the number of nodes in the wave function can be understood systematically by looking at how the energies of the vibrational levels change when the height of the barrier of the double minimum potential shown in Eq. (2.178) is varied, as schematized in Fig. 2.15. As shown in Fig. 2.15(a), if we increase the barrier separating the two wells, the energies of the 0^+ and 0^- levels become closer, and the shapes of the two wave functions become hardly distinguishable as long as we only look at either the left or the right well. The same can be said of 1^+ and 1^-, or 2^+ and 2^-. When the height of the barrier is infinitely large, the energies of such pairs of levels coincide with each other, which we describe as the two levels being degenerated. As the barrier becomes lower, on the other hand, the two-fold degeneracy is removed, and 0^+ and 0^- become recognizable as individual levels with different parities. Lowering the barrier further results in a further widening of the energy spacing between the pair of levels, as shown in Fig. 2.15(c), and the potential ultimately approaches that of a harmonic oscillator. Then the levels $v = 0^+$, 0^-, 1^+, 1^- start to better suit being labeled as $v = 0, 1, 2, 3$.

The wave functions in Fig. 2.14 extend over the two wells separated by the central barrier. According to Born's probability interpretation, when a system is in an eigenstate represented by an eigenfunction $\psi(x)$, the probability of finding the system in the region between x and $x + \mathrm{d}x$ is given by

$$\psi^*(x)\psi(x)\,\mathrm{d}x = \left|\psi(x)\right|^2 \mathrm{d}x.$$

This shows that ammonia can be found with some probability in both the right- and left-side bound wells. This is the phenomenon called quantum mechanical tunneling.

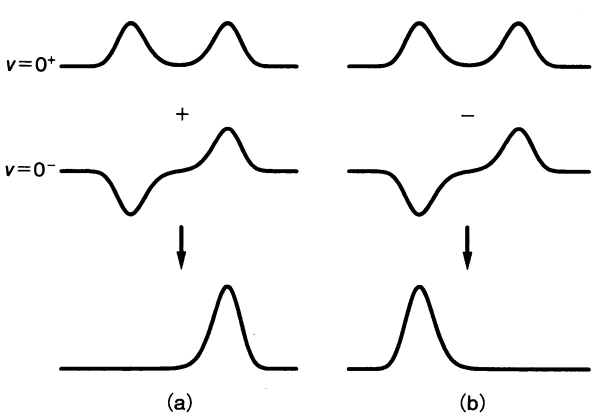

Fig. 2.16 Superpositions of the wave functions of ammonia, $v = 0^+$ and $v = 0^-$

2.4.4 *The Geometrical Structure of Ammonia and the Period of the Inversion Motion*

Ammonia molecules are known to have a trigonal pyramidal structure. Here, the word structure is used to refer to the geometrical structure of the molecule at the equilibrium position of the potential, or in other words, the position at which $\frac{dV}{dx}$ becomes 0 and the potential takes a local minimum value. Therefore, as shown in Fig. 2.13, ammonia takes the equilibrium structure at $x = x_r$ and $x = x_l$.

On the other hand, as shown in Fig. 2.14, the wave functions for $v = 0^+$ and $v = 0^-$ both correspond to stationary states, and neither can describe the time-dependent image of an ammonia molecule repeating the inversion motion between right and left.

As shown in Sect. 2.4.2, the wave functions for $v = 0^+$ and $v = 0^-$ in Fig. 2.14 have different parities, but they are very similar in terms of the probability distributions of $|\psi_{0^+}(x)|^2$ and $|\psi_{0^-}(x)|^2$. We will now consider the sum of $\psi_{0^+}(x)$ and $\psi_{0^-}(x)$. As shown in Fig. 2.16(a), the sum

$$\psi_r(x) = \psi_{0^+}(x) + \psi_{0^-}(x) \tag{2.181a}$$

gives us a wave function localized in the right well. Similarly, as shown in Fig. 2.16(b), the difference

$$\psi_l(x) = \psi_{0^+}(x) - \psi_{0^-}(x), \tag{2.181b}$$

becomes a wave function localized in the left well. Thus, if the manner of superposition of the two wave functions varies with time, this can describe the inversion motion that occurs between the left and the right.

Generally speaking, the stationary-state wave function $\psi(x)$ can be related with $\Psi(x, t)$, the solution of the time-dependent Schrödinger equation

$$H(x)\Psi(x, t) = \mathrm{i}\hbar\frac{\partial\Psi(x, t)}{\partial t}, \tag{2.182a}$$

by

$$\Psi(x,t) = \psi(x)\exp\left(-\mathrm{i}\frac{E}{\hbar}t\right) = \psi(x)\exp(-\mathrm{i}\omega t), \tag{2.182b}$$

where the angular frequency ω is defined as $\omega = \frac{E}{\hbar}$. Consequently, the two stationary-state wave functions $\psi_{0^+}(x)$ and $\psi_{0^-}(x)$ can be rewritten with a time-dependent factor as the following time-dependent expressions:

$$\Psi_{0^+}(x,t) = \psi_{0^+}(x)\exp(-\mathrm{i}\omega_1 t), \tag{2.183a}$$

$$\Psi_{0^-}(x,t) = \psi_{0^-}(x)\exp(-\mathrm{i}\omega_2 t), \tag{2.183b}$$

where $\omega_1 = \frac{E_1}{\hbar}$, $\omega_2 = \frac{E_2}{\hbar}$, and E_1 and E_2 represent the eigenenergies of the two eigenstates $v = 0^+$ and $v = 0^-$, respectively. From Eq. (2.183a),

$$\begin{aligned}\left|\Psi_{0^+}(x,t)\right|^2 &= \Psi^*_{0^+}(x,t)\Psi_{0^+}(x,t)\\ &= \psi^*_{0^+}(x)\mathrm{e}^{\mathrm{i}\omega_1 t}\cdot\psi_{0^+}(x)\mathrm{e}^{-\mathrm{i}\omega_1 t}\\ &= \left|\psi_{0^+}(x)\right|^2\end{aligned} \tag{2.184a}$$

where $|\Psi_{0^+}(x,t)|^2\,\mathrm{d}x$ represents the probability with which the system is found in the domain between x and $x + \mathrm{d}x$ at time t. Similarly, from Eq. (2.183b),

$$\left|\Psi_{0^-}(x,t)\right|^2 = \left|\psi_{0^-}(x)\right|^2. \tag{2.184b}$$

In both cases, the time-dependent factor cancels itself out.

As the next step, we will write the sum of Eqs. (2.183a) and (2.183b) as

$$\begin{aligned}\Psi_0(x,t) &\equiv \Psi_{0^+}(x,t) + \Psi_{0^-}(x,t)\\ &= \psi_{0^+}(x)\mathrm{e}^{-\mathrm{i}\omega_1 t} + \psi_{0^-}(x)\mathrm{e}^{-\mathrm{i}\omega_2 t}.\end{aligned} \tag{2.185}$$

The probability of finding this system in the domain between x and $\mathrm{d}x$ is

$$\left|\Psi_0(x,t)\right|^2\mathrm{d}x = \left|\psi_{0^+}(x)\mathrm{e}^{-\mathrm{i}\omega_1 t} + \psi_{0^-}(x)\mathrm{e}^{-\mathrm{i}\omega_2 t}\right|^2\mathrm{d}x. \tag{2.186}$$

The squared modulus can be calculated as

$$\begin{aligned}&\left(\psi^*_{0^+}\mathrm{e}^{\mathrm{i}\omega_1 t} + \psi^*_{0^-}\mathrm{e}^{\mathrm{i}\omega_2 t}\right)\left(\psi_{0^+}\mathrm{e}^{-\mathrm{i}\omega_1 t} + \psi_{0^-}\mathrm{e}^{-\mathrm{i}\omega_2 t}\right)\\ &= |\psi_{0^+}|^2 + |\psi_{0^-}|^2 + \psi^*_{0^+}\psi_{0^-}\mathrm{e}^{\mathrm{i}(\omega_1-\omega_2)t} + \psi^*_{0^-}\psi_{0^+}\mathrm{e}^{\mathrm{i}(\omega_2-\omega_1)t}\\ &= |\psi_{0^+}|^2 + |\psi_{0^-}|^2 + 2(\psi_{0^+}\psi_{0^-})\cos\omega t,\end{aligned} \tag{2.187}$$

where

$$\omega = \omega_2 - \omega_1 = \frac{E_2 - E_1}{\hbar}. \tag{2.188}$$

Since ψ_{0^+} and ψ_{0^-} are real functions with no imaginary parts, $|\Psi_0(x,t)|^2$ in Eq. (2.186) can be rewritten using the identity equation

$$(x+y)^2\cos^2\theta + (x-y)^2\sin^2\theta = x^2 + y^2 + 2xy\cos 2\theta$$

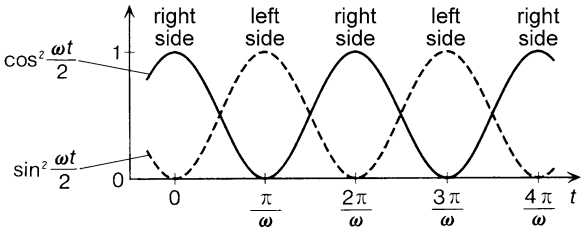

Fig. 2.17 Variation of coefficients representing the inversion motion of ammonia

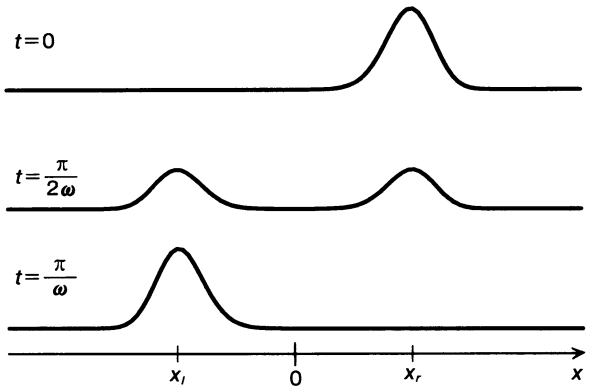

Fig. 2.18 Plots for $|\Psi_0(x,t)|^2$ at $t=0$, $\frac{\pi}{2\omega}$, $\frac{\pi}{\omega}$

and Eq. (2.187) as

$$\left|\Psi_0(x,t)\right|^2 = (\psi_{0+}+\psi_{0-})^2\cos^2\frac{\omega t}{2} + (\psi_{0+}-\psi_{0-})^2\sin^2\frac{\omega t}{2}. \tag{2.189}$$

This can also be written with the $\psi_r(x)$ and $\psi_l(x)$ in Eqs. (2.181a) and (2.181b) as

$$\left|\Psi_0(x,t)\right|^2 = \psi_r^2(x)\cos^2\frac{\omega t}{2} + \psi_l^2(x)\sin^2\frac{\omega t}{2}. \tag{2.190}$$

Let us then examine the temporal variation of $|\Psi_0(x,t)|^2$ as a function of time t. The time-dependent coefficients $\cos^2\frac{\omega t}{2}$ and $\sin^2\frac{\omega t}{2}$, for $\psi_r^2(x)$ and $\psi_l^2(x)$ in Eq. (2.190), respectively, alternate between an increase and a decrease as the time increases, as shown in Fig. 2.17. At $t=0$, the probability distribution becomes

$$\left|\Psi_0(x,0)\right|^2 = \psi_r^2(x),$$

which describes the system being localized in the right well. When t increases, the contribution of $\psi_r^2(x)$ decreases, and in turn, that of $\psi_l^2(x)$ increases. At $t=\frac{\pi}{\omega}$, it becomes

$$\left|\Psi_0\left(x,\frac{\pi}{\omega}\right)\right|^2 = \psi_l^2(x),$$

which describes a localization in the left well. Similarly, at $t=\frac{2\pi}{\omega}$, ammonia returns to the right well. This characteristic time evolution of $|\Psi_0(x,t)|^2$ is shown in Fig. 2.18.

The important lesson here is that, when two eigenfunctions representing stationary states are superposed, the probability of a system being found in the coordinate space varies with time. The superposition of eigenstates $\psi_i(\boldsymbol{r}, t)$,

$$\psi_{wp}(\boldsymbol{r}, t) = \sum_i a_i \psi_i(\boldsymbol{r}, t), \tag{2.191}$$

is generally referred to as a wave packet, and we can say that wave packets evolve with time. The inversion motion of ammonia can be described as the wave packet constructed by the superposition of ψ_{0^+} and ψ_{0^-} evolving with time to alternate between the two wells, the left and the right.

The period of the inversion motion, $T = \frac{2\pi}{\omega}$, can be represented as

$$T = \frac{2\pi}{\omega} = \frac{2\pi\hbar}{E_2 - E_1} = \frac{h}{\Delta E}, \tag{2.192}$$

where ΔE is the energy gap between the $v = 0^+$ and $v = 0^-$ levels, and its value is known to be 0.79 cm^{-1} from experiments. Therefore, we can derive

$$T \cong 42 \text{ ps}.$$

The time required for tunneling from the left well to the right, then, is 21 ps, a half of the period T.

Problem 2.23
Confirm that the period of the inversion motion of ammonia is $T = 42$ ps when $\Delta E = 0.79\ \text{cm}^{-1}$. Also consider what value T would take if ΔE were $0.079\ \text{cm}^{-1}$.

Solution
From Eq. (2.192), we obtain

$$T = \frac{h}{\Delta E} = \frac{h}{ch\tilde{\nu}} = \frac{1}{c\tilde{\nu}} = \frac{1}{3 \times 10^{10}\ \text{cm s}^{-1} \cdot 0.79\ \text{cm}^{-1}} \cong 42 \text{ ps}.$$

Consequently, when $\Delta E = 0.079\ \text{cm}^{-1}$, $T = 420$ ps. □

The energy gap ΔE between $v = 0^+$ and $v = 0^-$ decreases when the height of the barrier increases, as shown in Fig. 2.15. With the decrease of ΔE, as we have just seen in the question above, the inversion period T stretches in inverse proportion to ΔE. That is to say, the higher the central barrier of the double minimum potential becomes, the longer the period of the "left → right → left" oscillation of the wave packet becomes. This signifies that a higher barrier causes the system to take longer in tunneling through to the other side of the well.

2.5 How to Treat the Vibration of Polyatomic Molecules

So far, we have examined vibrations that occur in the form of one-dimensional motions, such as the vibration of diatomic molecules and the inversion motion of ammonia molecules. For polyatomic molecules in general, that is, molecules consisting

of three or more atoms, the vibrational motion can no longer be described as a simple one-dimensional vibration. It is easy to understand that, for example, in the case of triatomic molecules such as CO_2, there must be two types of vibration: one in which the internuclear distances of the two C=O bonds become longer and shorter in phase, and one in which the internuclear distance of one C=O bond becomes longer as the other becomes shorter.

There are thus generally a variety of vibrational motions occurring in a polyatomic molecule, and these different types of vibration are called vibrational modes. The number of vibrational modes for a molecule is determined by the number of atoms it has and its symmetry. We will first seek to understand how many vibrational modes are found in different types of molecules by examining the degrees of freedom for vibration, and learn the definition of normal modes, which are the modes by which whole molecules vibrate. We will then further discuss the procedure for obtaining the different normal modes and their associated vibrational frequencies.

2.5.1 Degrees of Freedom of Molecular Motions

When we regard an atom as a mass point in a three-dimensional space, there are three possibilities for its degree of freedom: one, if it can only move along a straight line (e.g., the x-Cartesian coordinate), two if the motion is restricted on a flat plane (e.g., the x-y plane), and three if the mass point can move around three-dimensionally (described by the x-y-z Cartesian coordinate system).

Atoms constituting a molecule are connected to each other with a chemical bond, and cannot make any independent movements. In addition to the translational and rotational motion of the molecule in the 3D space, there are vibrational motions taking place within the molecule, by which the atoms are displaced around the equilibrium position.

Let us first consider the case of a heteronuclear diatomic molecule, such as HCl or CO. Since each of the two atoms (we will call them atom A and atom B) has three degrees of freedom, the total degrees of freedom for molecule AB becomes 6 ($= 3 + 3$). If we regard the molecule as one body, it has three degrees of translational freedom as a matter of course, so the remaining three degrees are the sum of the degrees of freedom for the rotation of the molecule as a whole and for the vibration within the molecule. Placing nuclei A and B on the z axis of a molecule-fixed x-y-z Cartesian coordinate system so that their center of mass coincides with the origin of the coordinate system, as shown in Fig. 2.19(a), the molecular vibration of AB can be conceptualized as a motion that changes $R = |z_A - z_B|$. Since no other vibration exists, there is just one degree of freedom in the vibrational motion of a diatomic molecule. Consequently, the remaining degrees of freedom (two) can be attributed to the rotation. This is consistent with the fact that there are two types of rotation, one around the x axis and the other around the y axis. In summary, the degrees of freedom for diatomic molecules can be broken down as: 6 (total) = 3 (translation) + 2 (rotation) + 1 (vibration). There is no rotation around the z axis since the atoms are regarded here as mass points.

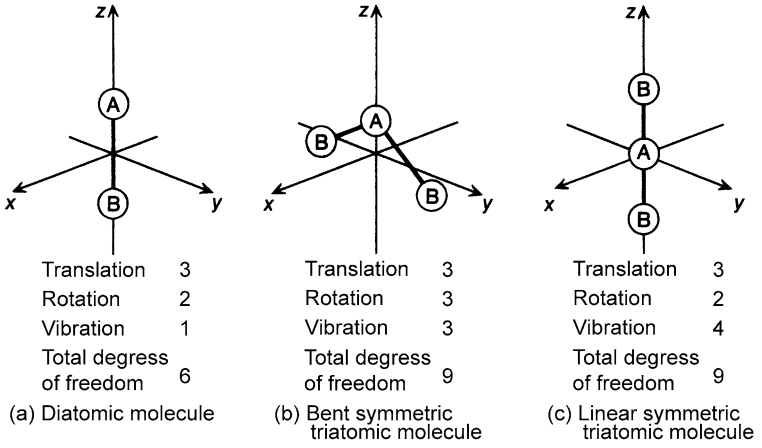

Fig. 2.19 The degrees of freedom of motion for diatomic and triatomic molecules: (**a**) a diatomic molecule, (**b**) a bent symmetric triatomic molecule (**c**) a linear symmetric triatomic molecule

We will turn our attention next to the symmetric triatomic molecule, or AB_2. First, let us consider a bent triatomic molecule such as H_2O or SO_2 (Fig. 2.19(b)). The total degrees of freedom can be derived as $3 \times 3 = 9$. Supposing the three atoms are located on the y-z plane, there can be a rotation around each of the three axes, x, y, and z, so that there are three degrees of rotational freedom. Since there are three degrees of translational freedom, the rest of the degrees of freedom, $9 - 3 - 3 = 3$, are those for vibration. The specific patterns of vibration represented by these degrees of freedom will later be dealt with in Sects. 2.5.8–2.5.9.

In the case of a linear triatomic molecule such as CO_2 or CS_2, we can locate the molecular axis on the z axis in the same manner as we did with the diatomic molecule, as shown in Fig. 2.19(c). Since there can be no rotation around the z axis, there are two degrees of freedom for the overall rotation, namely the rotation around the x axis and that around the y axis. Then, by subtracting the two degrees of rotational freedom and the three degrees of translational freedom from the nine degrees of freedom, we obtain four as the degrees of vibrational freedom. The reason that a linear molecule has one more degree of vibrational freedom than a bent molecule is that a bent molecule has only one form of bending vibration while a linear molecule has two, one on the x-y plane and the other on the y-z plane. Although the triatomic molecule we have discussed here is of the symmetric type (ABA), the numbers of the degrees of freedom for the translation, rotation and vibration of an asymmetric triatomic molecule, ABC, will be the same as the corresponding numbers for a symmetric triatomic molecule.

Similar rules hold for a polyatomic molecule consisting of n atoms. If it is a linear polyatomic molecule, it has three degrees of translational freedom and two degrees of rotational freedom, so by subtracting these numbers from the total degrees of freedom, $3n$, we can derive $3n - 5$ as its degrees of vibrational freedom. If the polyatomic molecule is bent (non-linear), it has three degrees of vibrational freedom

Table 2.4 The degrees of freedom for the translation, rotation and vibration of molecules

		Degrees of freedom of translation	Degrees of freedom of rotation	Degrees of freedom of vibration	Total degrees of freedom
Diatomic molecule		3	2	1	6
Triatomic molecule	Linear type	3	2	4	9
	Bent type (Non-linear type)	3	3	3	9
n-atomic molecule ($n \geqq 3$)	Linear type	3	2	$3n-5$	$3n$
	Bent type (Non-linear type)	3	3	$3n-6$	$3n$

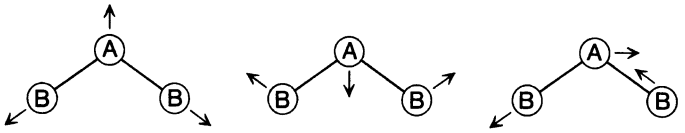

Fig. 2.20 The three patterns of typical normal mode vibration for a bent symmetric triatomic molecule AB_2

and three degrees of rotational freedom, making the degree of vibrational freedom $3n-6$. A summary of the degrees of freedom for the molecular motion of different types of molecules is given in Table 2.4.

2.5.2 What Are Normal Modes?

Like diatomic molecules, a polyatomic molecule vibrates around its equilibrium geometrical structure while it translates and rotates. In the case of a bent polyatomic molecule consisting of n atoms ($n \geqq 3$), the degrees of freedom for vibration is $3n-6$. As we have already examined, a bent triatomic molecule such as H_2O or SO_2 has $3 \times 3 - 6 = 3$ degrees of freedom of vibration. This means that there are three different types in the molecular vibration. How does a molecule vibrate in three different ways? These three vibrational patterns are called normal modes, and their typical patterns are shown in Fig. 2.20. The main goal of this subsection is to learn how to find the normal modes intrinsic to each molecular species.

In order to familiarize ourselves with the concept of normal modes, let us first look at the normal modes of a linear triatomic molecule, whose motion is restricted on the one-dimensional axis, as this is the simplest model of coupled molecular

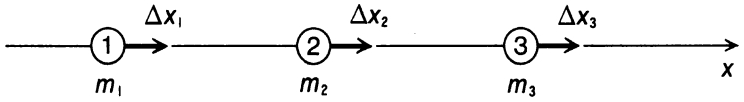

Fig. 2.21 The movements along the x axis for the three atoms in a linear triatomic molecule

vibration. We will consider the three atoms to be moving along the x axis, as shown in Fig. 2.21. The kinetic energy T is then written as

$$T = \frac{1}{2}m_1\Delta\dot{x}_1^2 + \frac{1}{2}m_2\Delta\dot{x}_2^2 + \frac{1}{2}m_3\Delta\dot{x}_3^2, \tag{2.193}$$

where Δx_1, Δx_2, and Δx_3 represent the displacement of the respective atoms from their equilibrium positions. When we neglect the third- and higher-order terms of the displacement, the potential energy V is expressed as,

$$V = \frac{1}{2}k_{12}(\Delta x_1 - \Delta x_2)^2 + \frac{1}{2}k_{23}(\Delta x_2 - \Delta x_3)^2, \tag{2.194}$$

where k_{12} is the force constant between atom 1 and atom 2, and k_{23} that between atom 2 and atom 3. This is a well-known problem of a coupled oscillator. In order to derive a formula of the classical equation of motion, we need to construct the Lagrangian $L = T - V$ for each i-th ($i = 1, 2, 3$) atom, and construct the following equation:

$$\frac{\mathrm{d}}{\mathrm{d}t}\left(\frac{\partial L}{\partial(\Delta\dot{x}_i)}\right) - \frac{\partial L}{\partial(\Delta x_i)} = 0 \quad (i = 1, 2, 3). \tag{2.195}$$

By introducing a set of mass-weighted Cartesian displacement coordinates,

$$\eta_i = \sqrt{m_i}\Delta x_i, \tag{2.196}$$

we can write Eq. (2.193) more simply as

$$T = \frac{1}{2}\dot{\eta}_1^2 + \frac{1}{2}\dot{\eta}_2^2 + \frac{1}{2}\dot{\eta}_3^2, \tag{2.197}$$

and Eq. (2.194) as

$$V = \frac{1}{2}k_{12}\left(\frac{\eta_1}{\sqrt{m_1}} - \frac{\eta_2}{\sqrt{m_2}}\right)^2 + \frac{1}{2}k_{23}\left(\frac{\eta_2}{\sqrt{m_2}} - \frac{\eta_3}{\sqrt{m_3}}\right)^2. \tag{2.198}$$

Since T in Eq. (2.197) explicitly depends only on the derivate of the coordinate, $\{\frac{\mathrm{d}\eta_i}{\mathrm{d}t}\} = \{\dot{\eta}_i\}$, and V in Eq. (2.198) explicitly depends only on the coordinate $\{\eta_i\}$, the equation of motion, Eq. (2.195), is rewritten using η_1, η_2, and η_3 as

$$\frac{\mathrm{d}}{\mathrm{d}t}\left(\frac{\partial T}{\partial\dot{\eta}_i}\right) + \frac{\partial V}{\partial\eta_i} = 0 \quad (i = 1, 2, 3). \tag{2.199}$$

Next, we substitute Eqs. (2.197) and (2.198) into Eq. (2.199) and obtain the simultaneous differential equations,

$$\begin{cases} \ddot{\eta}_1 + \dfrac{k_{12}}{m_1}\eta_1 - \dfrac{k_{12}}{\sqrt{m_1 m_2}}\eta_2 = 0, \\ \ddot{\eta}_2 - \dfrac{k_{12}}{\sqrt{m_1 m_2}}\eta_1 + \dfrac{k_{12}+k_{23}}{m_2}\eta_2 - \dfrac{k_{23}}{\sqrt{m_2 m_3}}\eta_3 = 0, \\ \ddot{\eta}_3 - \dfrac{k_{23}}{\sqrt{m_2 m_3}}\eta_2 + \dfrac{k_{23}}{m_3}\eta_3 = 0, \end{cases} \tag{2.200}$$

where $\{\ddot{\eta}_i\} = \{\frac{\mathrm{d}^2\eta_i}{\mathrm{d}t^2}\}$.

What we are trying to derive here are the frequencies and corresponding forms of molecular vibration for a molecule that vibrates repeatedly at a specific frequency. In order to fulfill the requirement that the displacements of the three coordinates should oscillate in phase at a common frequency ν, or at a common angular frequency $\omega(=2\pi\nu)$, we will express the mass-weighted Cartesian displacement coordinates as

$$\begin{cases} \eta_1 = \eta_1^\circ \exp(\mathrm{i}\omega t), \\ \eta_2 = \eta_2^\circ \exp(\mathrm{i}\omega t), \\ \eta_3 = \eta_3^\circ \exp(\mathrm{i}\omega t), \end{cases} \tag{2.201}$$

where η_1°, η_2°, and η_3° ($\geqq 0$) are constants representing the maximum values of the respective displacements. By substituting Eq. (2.201) into Eq. (2.200), the simultaneous linear equations,

$$\begin{cases} \dfrac{k_{12}}{m_1}\eta_1^\circ - \dfrac{k_{12}}{\sqrt{m_1 m_2}}\eta_2^\circ = \omega^2\eta_1^\circ, \\ -\dfrac{k_{12}}{\sqrt{m_1 m_2}}\eta_1^\circ + \dfrac{k_{12}+k_{23}}{m_2}\eta_2^\circ - \dfrac{k_{23}}{\sqrt{m_2 m_3}}\eta_3^\circ = \omega^2\eta_2^\circ, \\ -\dfrac{k_{23}}{\sqrt{m_2 m_3}}\eta_2^\circ + \dfrac{k_{23}}{m_3}\eta_3^\circ = \omega^2\eta_3^\circ, \end{cases} \tag{2.202}$$

are obtained.

Problem 2.24

Confirm that Eq. (2.202) is derived from Eqs. (2.200) and (2.201). Also prove that the same set of equations, Eq. (2.202), is obtained whether we adopt $\eta_i = \eta_i^\circ \cos\omega t$ or $\eta_i = \eta_i^\circ \cos(\omega t + \delta)$, where δ is a constant phase.

Solution

In both cases, $\mathrm{d}^2\eta_i/\mathrm{d}t^2 = -\omega^2\eta_i$ is obtained, so that we can derive Eq. (2.202) by adopting the above η_i functions or from $\eta_i = \eta_i^\circ \exp(\mathrm{i}\omega t)$. The same result is given, of course, when we adopt $\eta_i = \eta_i^\circ \sin\omega t$ or $\eta_i = \eta_i^\circ \sin(\omega t + \delta)$. □

To give the present discussion a clearer correspondence with the general case of three-dimensional molecular vibration to be introduced later, we will represent

Eq. (2.202) in matrix form. When a 3×3 matrix $\boldsymbol{C} = \{c_{ij}\}$ $(1 \leqq i, j \leqq 3)$ is defined as

$$\boldsymbol{C} = \begin{pmatrix} \frac{k_{12}}{m_1} & -\frac{k_{12}}{\sqrt{m_1 m_2}} & 0 \\ -\frac{k_{12}}{\sqrt{m_1 m_2}} & \frac{k_{12}+k_{23}}{m_2} & -\frac{k_{23}}{\sqrt{m_2 m_3}} \\ 0 & -\frac{k_{23}}{\sqrt{m_2 m_3}} & \frac{k_{23}}{m_3} \end{pmatrix}, \tag{2.203}$$

and a three-dimensional row vector $\boldsymbol{\eta}^\circ$ is expressed as

$$\boldsymbol{\eta}^\circ = \begin{pmatrix} \eta_1^\circ \\ \eta_2^\circ \\ \eta_3^\circ \end{pmatrix}. \tag{2.204}$$

Equation (2.202) is represented as

$$\boldsymbol{C}\boldsymbol{\eta}^\circ = \omega^2 \boldsymbol{\eta}^\circ. \tag{2.205}$$

It is obvious from Eq. (2.205) that this problem is equivalent to an eigenvalue problem in which we derive the eigenvalue ω^2 and the corresponding eigenvector $\boldsymbol{\eta}^\circ$ for a given matrix $\boldsymbol{C}$. By using a 3×3 unit matrix

$$\boldsymbol{E} = \begin{pmatrix} 1 & 0 & 0 \\ 0 & 1 & 0 \\ 0 & 0 & 1 \end{pmatrix}, \tag{2.206}$$

Eq. (2.205) can be rewritten as

$$\left(\boldsymbol{C} - \omega^2 \boldsymbol{E}\right)\boldsymbol{\eta}^\circ = 0. \tag{2.207}$$

The condition for the simultaneous linear equations with respect to $\{\eta_i^\circ\}$ to have a non-trivial solution, that is, a solution other than the meaningless solution

$$\eta_1^\circ = \eta_2^\circ = \eta_3^\circ = 0, \tag{2.208}$$

is expressed as

$$\det\left|\boldsymbol{C} - \omega^2 \boldsymbol{E}\right| = 0, \tag{2.209}$$

where $\det|\boldsymbol{A}|$ represents the determinant of a matrix $\boldsymbol{A}$.

Equation (2.209) can be written explicitly using the matrix elements as

$$\begin{vmatrix} \frac{k_{12}}{m_1} - \omega^2 & -\frac{k_{12}}{\sqrt{m_1 m_2}} & 0 \\ -\frac{k_{12}}{\sqrt{m_1 m_2}} & \frac{k_{12}+k_{23}}{m_2} - \omega^2 & -\frac{k_{23}}{\sqrt{m_2 m_3}} \\ 0 & -\frac{k_{23}}{\sqrt{m_2 m_3}} & \frac{k_{23}}{m_3} - \omega^2 \end{vmatrix} = 0. \tag{2.210}$$

This is a cubic equation with respect to ω^2, and has three solutions. For each of the ω^2 values, there is a corresponding eigenvector representing the specific form of the molecular vibration.

Now we will consider a linear symmetric triatomic molecule such as CO_2 or CS_2, and solve Eq. (2.209), or, equivalently, Eq. (2.210), under the condition that

$$\begin{cases} k_{12} = k_{23} = k, & (2.211) \\ m_1 = m_3 = M. & (2.212) \end{cases}$$

Here, we will represent the mass of the central atom m_2 as

$$m_2 = m. \tag{2.213}$$

Substituting Eqs. (2.211) through (2.213) into Eq. (2.210), we obtain

$$\begin{vmatrix} \frac{k}{M} - \omega^2 & -\frac{k}{\sqrt{mM}} & 0 \\ -\frac{k}{\sqrt{mM}} & \frac{2k}{m} - \omega^2 & -\frac{k}{\sqrt{mM}} \\ 0 & -\frac{k}{\sqrt{mM}} & \frac{k}{M} - \omega^2 \end{vmatrix} = 0. \tag{2.214}$$

By calculating and factorizing this determinant, we derive

$$\left(\omega^2 - \frac{k}{M}\right)\left\{\omega^2 - \frac{k(2M+m)}{Mm}\right\}\omega^2 = 0, \tag{2.215}$$

which gives us three solutions, or three eigenvalues,

$$\omega^2 = \frac{k}{M}, \quad \frac{k(2M+m)}{Mm}, \quad 0. \tag{2.216}$$

Therefore, the vibrational angular frequencies ω are expressed as

$$\omega = \sqrt{\frac{k}{M}}, \quad \sqrt{\frac{k(2M+m)}{Mm}}, \quad 0 \tag{2.217}$$

and the vibrational frequencies can be derived as

$$\nu = \frac{1}{2\pi}\sqrt{\frac{k}{M}}, \quad \frac{1}{2\pi}\sqrt{\frac{k(2M+m)}{Mm}}, \quad 0. \tag{2.218}$$

What is worth noting here is that a motion with the frequency of $\nu = 0$ is found as one of the solutions. As is to be explained below, this corresponds to the translational motion of an entire molecule along the x axis. To understand the forms of such molecular motions, we simply need to derive the eigenvectors corresponding to the three eigenvalues in Eq. (2.216).

(i) Molecular motion for $\omega^2 = \frac{k}{M}$ $(\nu = \frac{1}{2\pi}\sqrt{\frac{k}{M}})$

By substituting $\omega^2 = \frac{k}{M}$ into Eq. (2.202) and using Eqs. (2.211) through (2.213), we obtain

$$\begin{cases} \eta_2^\circ = 0, \\ \eta_3^\circ = -\eta_1^\circ. \end{cases} \tag{2.219}$$

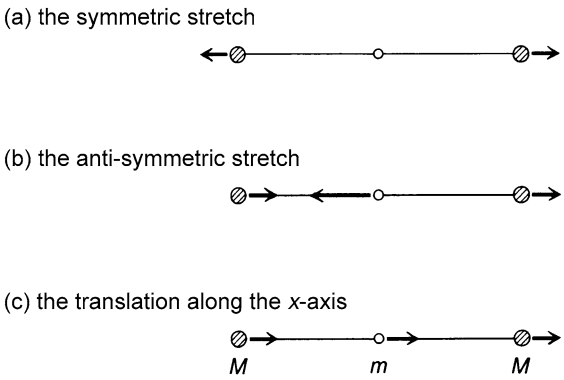

Fig. 2.22 The one-dimensional motions of an AB_2-type symmetric triatomic molecule: (**a**) the symmetric stretch, (**b**) the anti-symmetric stretch, (**c**) the translation along the x axis

That is, the eigenvector is represented as

$$\boldsymbol{\eta}^{\circ} = \begin{pmatrix} \eta_1^{\circ} \\ 0 \\ -\eta_1^{\circ} \end{pmatrix}. \tag{2.220}$$

If $\boldsymbol{\eta}^{\circ}$ fulfills the normalization condition,

$$\left|\boldsymbol{\eta}^{\circ}\right| = \sqrt{\left(\eta_1^{\circ}\right)^2 + \left(\eta_2^{\circ}\right)^2 + \left(\eta_3^{\circ}\right)^2} = 1, \tag{2.221}$$

the normalized eigenvector becomes

$$\boldsymbol{\eta}_{(1)}^{\circ} = \begin{pmatrix} \frac{1}{\sqrt{2}} \\ 0 \\ -\frac{1}{\sqrt{2}} \end{pmatrix}, \tag{2.222}$$

where the subscript "(1)" shows that this eigenvector is associated with the first eigenvalue, $\frac{k}{M}$, in Eq. (2.216). Using Eq. (2.196), the displacements of the atoms are obtained from the corresponding components in the normalized eigenvector as

$$\Delta x_1 = \frac{1}{\sqrt{2M}}, \quad \Delta x_2 = 0, \quad \Delta x_3 = -\frac{1}{\sqrt{2M}}. \tag{2.223}$$

Clearly, this corresponds to the symmetric stretch mode, in which the central atom remains stationary and the side atoms stretch in phase in two opposite directions. The vibration is illustrated in Fig. 2.22(a) using displacement vectors.

(ii) Molecular motion for $\omega^2 = \frac{k(2M+m)}{Mm}$ $\left(\nu = \frac{1}{2\pi}\sqrt{\frac{k(2M+m)}{Mm}}\right)$

By substituting $\omega^2 = \frac{k(2M+m)}{Mm}$ into Eq. (2.202) and using Eqs. (2.211) through (2.213), we obtain

$$\begin{cases} \eta_3^{\circ} = \eta_1^{\circ}, \\ \eta_2^{\circ} = -2\sqrt{\dfrac{M}{m}}\eta_1^{\circ}. \end{cases} \tag{2.224}$$

From the normalization condition in Eq. (2.221), we derive

$$\boldsymbol{\eta}^{\circ}_{(2)} = \begin{pmatrix} \sqrt{\frac{m}{2(2M+m)}} \\ -\sqrt{\frac{2M}{2M+m}} \\ \sqrt{\frac{m}{2(2M+m)}} \end{pmatrix}. \tag{2.225}$$

Therefore, the displacements of atoms are expressed as

$$\begin{cases} \Delta x_1 = \Delta x_3 = \sqrt{\dfrac{m}{2M(2M+m)}}, \\ \Delta x_2 = -\sqrt{\dfrac{2M}{m(2M+m)}}, \end{cases} \tag{2.226}$$

indicating that the side atoms move in the same direction to the same extent while the central atom moves in phase in the opposite direction. This motion is the antisymmetric stretch mode, and its form is depicted in Fig. 2.22(b).

(iii) Molecular motion for $\omega^2 = 0$ ($\nu = 0$)

As in (i) and (ii), a set of solutions,

$$\begin{cases} \eta^{\circ}_3 = \eta^{\circ}_1, \\ \eta^{\circ}_2 = \sqrt{\dfrac{m}{M}}\eta^{\circ}_1, \end{cases} \tag{2.227}$$

can be obtained, and it is normalized as

$$\boldsymbol{\eta}^{\circ}_{(3)} = \begin{pmatrix} \sqrt{\frac{M}{2M+m}} \\ \sqrt{\frac{m}{2M+m}} \\ \sqrt{\frac{M}{2M+m}} \end{pmatrix}. \tag{2.228}$$

This allows us to derive the displacements of the atoms as

$$\Delta x_1 = \Delta x_2 = \Delta x_3 = \frac{1}{\sqrt{2M+m}}, \tag{2.229}$$

which represents the motion of the three atoms moving in phase in the same direction to the same extent. This is exactly what we call the translational motion of the entire molecule. The motion is illustrated in Fig. 2.22(c).

From (i), (ii), and (iii), we understand that two of the three eigenvalues represent molecular vibrations, and the remaining one represents the translation of the entire molecule. The two kinds of molecular vibration obtained here as eigenvectors are what we call normal modes.

2.5.3 Normal Modes and Matrix Diagonalization

We will now summarize the discussion above as a diagonalization problem of the matrix $\boldsymbol{C}$ in Eq. (2.203). First, let us confirm the orthogonality of each pair among the normalized eigenvectors, Eqs. (2.222), (2.225), and (2.228). This is readily shown, as

$$\begin{cases} \boldsymbol{\eta}^{\circ}_{(1)} \cdot \boldsymbol{\eta}^{\circ}_{(2)} = 0, \\ \boldsymbol{\eta}^{\circ}_{(2)} \cdot \boldsymbol{\eta}^{\circ}_{(3)} = 0, \\ \boldsymbol{\eta}^{\circ}_{(3)} \cdot \boldsymbol{\eta}^{\circ}_{(1)} = 0. \end{cases} \tag{2.230}$$

Since these three vectors are all normalized, we can describe Eq. (2.230) as

$$\boldsymbol{\eta}^{\circ}_{(i)} \cdot \boldsymbol{\eta}^{\circ}_{(j)} = \delta_{ij}. \tag{2.231}$$

If we represent an orthogonal matrix $\boldsymbol{L}_{\eta}$ which has these orthonormal vectors as its column vectors as

$$\boldsymbol{L}_{\eta} = \begin{pmatrix} \frac{1}{\sqrt{2}} & \sqrt{\frac{m}{2(2M+m)}} & \sqrt{\frac{M}{2M+m}} \\ 0 & -\sqrt{\frac{2M}{2M+m}} & \sqrt{\frac{m}{2M+m}} \\ -\frac{1}{\sqrt{2}} & \sqrt{\frac{m}{2(2M+m)}} & \sqrt{\frac{M}{2M+m}} \end{pmatrix}, \tag{2.232}$$

and introduce a diagonal matrix whose diagonal matrix elements are the three eigenvalues ω_1^2, ω_2^2, and ω_3^2,

$$\boldsymbol{\Lambda} = \begin{pmatrix} \omega_1^2 & 0 & 0 \\ 0 & \omega_2^2 & 0 \\ 0 & 0 & \omega_3^2 \end{pmatrix}, \tag{2.233}$$

we can derive the set of equations in matrix form as

$$\boldsymbol{C}\boldsymbol{L}_{\eta} = \boldsymbol{L}_{\eta}\boldsymbol{\Lambda}. \tag{2.234}$$

Problem 2.25
Confirm the orthogonal relations in Eq. (2.230).

Solution
For example, we can derive

$$\begin{aligned} \boldsymbol{\eta}^{\circ}_{(2)} \cdot \boldsymbol{\eta}^{\circ}_{(3)} &= \sqrt{\frac{m}{2(2M+m)}}\sqrt{\frac{M}{2M+m}} - \sqrt{\frac{2M}{2M+m}}\sqrt{\frac{m}{2M+m}} \\ &\quad + \sqrt{\frac{m}{2(2M+m)}}\sqrt{\frac{M}{2M+m}} \\ &= \frac{\sqrt{Mm}}{2M+m}\left(\frac{1}{\sqrt{2}} - \sqrt{2} + \frac{1}{\sqrt{2}}\right) = 0. \end{aligned}$$

We can also derive $\boldsymbol{\eta}^{\circ}_{(1)} \cdot \boldsymbol{\eta}^{\circ}_{(2)} = 0$ and $\boldsymbol{\eta}^{\circ}_{(3)} \cdot \boldsymbol{\eta}^{\circ}_{(1)} = 0$ in a similar manner. □

Problem 2.26
Prove Eq. (2.234).

Solution
From Eq. (2.205), we obtain

$$\boldsymbol{C}\boldsymbol{\eta}^{\circ}_{(1)} = \omega_1^2 \boldsymbol{\eta}^{\circ}_{(1)}$$
$$\boldsymbol{C}\boldsymbol{\eta}^{\circ}_{(2)} = \omega_2^2 \boldsymbol{\eta}^{\circ}_{(2)}$$
$$\boldsymbol{C}\boldsymbol{\eta}^{\circ}_{(3)} = \omega_3^2 \boldsymbol{\eta}^{\circ}_{(3)}.$$

Therefore, by setting the three column vectors $\{\boldsymbol{\eta}^{\circ}_{(i)}\}$ in a row, we can derive

$$\boldsymbol{C}\left(\boxed{\boldsymbol{\eta}^{\circ}_{(1)}}\boxed{\boldsymbol{\eta}^{\circ}_{(2)}}\boxed{\boldsymbol{\eta}^{\circ}_{(3)}}\right) = \left(\boxed{\boldsymbol{\eta}^{\circ}_{(1)}}\boxed{\boldsymbol{\eta}^{\circ}_{(2)}}\boxed{\boldsymbol{\eta}^{\circ}_{(3)}}\right)\begin{pmatrix}\omega_1^2 & 0 & 0\\ 0 & \omega_2^2 & 0\\ 0 & 0 & \omega_3^2\end{pmatrix}.$$

This equation is identical to Eq. (2.234). □

As the next step, we will introduce ${}^t\boldsymbol{L}_\eta$, a transpose of the matrix $\boldsymbol{L}_\eta$, as

$${}^t\boldsymbol{L}_\eta = \begin{pmatrix} \frac{1}{\sqrt{2}} & 0 & -\frac{1}{\sqrt{2}} \\ \sqrt{\frac{m}{2(2M+m)}} & -\sqrt{\frac{2M}{2M+m}} & \sqrt{\frac{m}{2(2M+m)}} \\ \sqrt{\frac{M}{2M+m}} & \sqrt{\frac{m}{2M+m}} & \sqrt{\frac{M}{2M+m}} \end{pmatrix}, \tag{2.235}$$

and calculate ${}^t\boldsymbol{L}_\eta\boldsymbol{L}_\eta$. It can be readily shown that

$${}^t\boldsymbol{L}_\eta\boldsymbol{L}_\eta = \begin{pmatrix}1 & 0 & 0\\ 0 & 1 & 0\\ 0 & 0 & 1\end{pmatrix} = \boldsymbol{E}. \tag{2.236}$$

This signifies that ${}^t\boldsymbol{L}_\eta$ is $\boldsymbol{L}_\eta^{-1}$, the inverse matrix of $\boldsymbol{L}_\eta$. That is,

$${}^t\boldsymbol{L}_\eta = \boldsymbol{L}_\eta^{-1}. \tag{2.237}$$

Problem 2.27
Derive Eq. (2.236).

Solution
When $\boldsymbol{\eta}^{\circ}_{(i)} = \begin{pmatrix} a_i \\ b_i \\ c_i \end{pmatrix}$, the row vector ${}^t(\boldsymbol{\eta}^{\circ}_{(i)})$, which is the transpose of this column vector, can be written as

$${}^t\left(\boldsymbol{\eta}^{\circ}_{(i)}\right) = (\,a_i\ b_i\ c_i\,).$$

Using these row vectors, ${}^t\boldsymbol{L}_\eta$ is expressed as

$$ {}^t\boldsymbol{L}_\eta = \begin{pmatrix} \boxed{{}^t(\boldsymbol{\eta}^\circ_{(1)})} \\ \boxed{{}^t(\boldsymbol{\eta}^\circ_{(2)})} \\ \boxed{{}^t(\boldsymbol{\eta}^\circ_{(3)})} \end{pmatrix}. $$

Consequently, $\boldsymbol{L}_\eta$ is expressed as

$$ \boldsymbol{L}_\eta = \begin{pmatrix} \boxed{\boldsymbol{\eta}^\circ_{(1)}} & \boxed{\boldsymbol{\eta}^\circ_{(2)}} & \boxed{\boldsymbol{\eta}^\circ_{(3)}} \end{pmatrix}. $$

Therefore, the (i, j) element of ${}^t\boldsymbol{L}_\eta\boldsymbol{L}_\eta$, $({}^t\boldsymbol{L}_\eta\boldsymbol{L}_\eta)_{ij}$, can be calculated as

$$ \left({}^t\boldsymbol{L}_\eta\boldsymbol{L}_\eta\right)_{ij} = {}^t\left(\boldsymbol{\eta}^\circ_{(i)}\right)\left(\boldsymbol{\eta}^\circ_{(j)}\right) = \begin{pmatrix} a_i & b_i & c_i \end{pmatrix} \begin{pmatrix} a_j \\ b_j \\ c_j \end{pmatrix} = a_i a_j + b_i b_j + c_i c_j = \boldsymbol{\eta}^\circ_{(i)} \cdot \boldsymbol{\eta}^\circ_{(j)}. $$

From the orthonormal condition given in Eq. (2.231), we obtain

$$ \left({}^t\boldsymbol{L}_\eta\boldsymbol{L}_\eta\right)_{ij} = \delta_{ij}. $$

This is what Eq. (2.236) represents. □

By operating ${}^t\boldsymbol{L}_\eta = \boldsymbol{L}_\eta^{-1}$ from the left on both sides of Eq. (2.234) as

$$ \boldsymbol{L}_\eta^{-1}\boldsymbol{C}\boldsymbol{L}_\eta = \boldsymbol{L}_\eta^{-1}\boldsymbol{L}_\eta\boldsymbol{\Lambda} \tag{2.238} $$

and using Eq. (2.236), we derive

$$ \boldsymbol{L}_\eta^{-1}\boldsymbol{C}\boldsymbol{L}_\eta = \boldsymbol{\Lambda}. \tag{2.239} $$

This indicates that, once we find a $\boldsymbol{L}_\eta$ that diagonalizes matrix $\boldsymbol{C}$, eigenvalues line up as those diagonal elements. The procedure that we have followed so far to derive the frequencies and patterns of the normal modes can be summarized as the diagonalization of the matrix $\boldsymbol{C}$ represented in Eq. (2.203).

2.5.4 *The Vibrational Hamiltonian Represented by Normal Coordinates*

The potential was given at the beginning of this section in the form of Eq. (2.198). When the dependence of the third-order and higher-order terms of the coordinates are ignored, the dependence of the potential on the coordinates is represented as

$$ V = \sum_{i=1}^{3}\sum_{j=1}^{3}\frac{1}{2}c_{ij}\eta_i\eta_j. \tag{2.240} $$

Here, the coefficient c_{ij} is the (i, j) element of the matrix $\boldsymbol{C}$ given in Eq. (2.203). Indeed, from Eq. (2.199), the coefficient of the term η_j in the sum of the terms obtained by $\frac{\partial V}{\partial \eta_i}$ is c_{ij}, so that

$$c_{ij} = \frac{\partial^2 V}{\partial \eta_i \partial \eta_j} = \frac{1}{\sqrt{m_i m_j}} \left(\frac{\partial^2 V}{\partial (\Delta x_i) \partial (\Delta x_j)} \right). \tag{2.241}$$

This is what Eq. (2.240) means. When Eq. (2.240) is represented with matrix $\boldsymbol{C}$, it becomes

$$V = \frac{1}{2} {}^t\boldsymbol{\eta} \boldsymbol{C} \boldsymbol{\eta}, \tag{2.242}$$

and the kinetic energy is represented as

$$T = \frac{1}{2} {}^t\dot{\boldsymbol{\eta}} \dot{\boldsymbol{\eta}}, \tag{2.243}$$

where $\dot{\boldsymbol{\eta}}$ is defined as

$$\dot{\boldsymbol{\eta}} = \begin{pmatrix} \dot{\eta}_1 \\ \dot{\eta}_2 \\ \dot{\eta}_3 \end{pmatrix}. \tag{2.244}$$

By operating ${}^t\boldsymbol{L}_\eta$ on Eq. (2.234) from the right, we derive

$$\boldsymbol{C} \boldsymbol{L}_\eta {}^t\boldsymbol{L}_\eta = \boldsymbol{L}_\eta \boldsymbol{\Lambda} {}^t\boldsymbol{L}_\eta,$$

and, consequently, using ${}^t\boldsymbol{L}_\eta = \boldsymbol{L}_\eta^{-1}$, we can obtain

$$\boldsymbol{C} = \boldsymbol{L}_\eta \boldsymbol{\Lambda} {}^t\boldsymbol{L}_\eta. \tag{2.245}$$

Substituting Eq. (2.245) into Eq. (2.242), we derive

$$V = \frac{1}{2} {}^t\boldsymbol{\eta} \boldsymbol{L}_\eta \boldsymbol{\Lambda} {}^t\boldsymbol{L}_\eta \boldsymbol{\eta}. \tag{2.246}$$

As the next step, we introduce a column vector $\boldsymbol{Q} = \begin{pmatrix} Q_1 \\ Q_2 \\ Q_3 \end{pmatrix}$ that is defined as

$$\boldsymbol{Q} = {}^t\boldsymbol{L}_\eta \boldsymbol{\eta}. \tag{2.247}$$

Since the transpose of this vector is

$${}^t\boldsymbol{Q} = {}^t\left({}^t\boldsymbol{L}_\eta \boldsymbol{\eta}\right) = {}^t\boldsymbol{\eta} \boldsymbol{L}_\eta. \tag{2.248}$$

Equation (2.246) can be expressed with $\boldsymbol{Q}$ as

$$V = \frac{1}{2} {}^t\boldsymbol{Q} \boldsymbol{\Lambda} \boldsymbol{Q}. \tag{2.249}$$

From Eq. (2.247), we obtain

$$\boldsymbol{\eta} = \boldsymbol{L}_\eta \boldsymbol{Q}, \tag{2.250}$$

and therefore the kinetic energy is expressed as

$$T = \frac{1}{2}{}^t\dot{\boldsymbol{\eta}}\dot{\boldsymbol{\eta}} = \frac{1}{2}\left({}^t\dot{\boldsymbol{Q}}\,{}^t\boldsymbol{L}_\eta\right)\left(\boldsymbol{L}_\eta\,\dot{\boldsymbol{Q}}\right) = \frac{1}{2}{}^t\dot{\boldsymbol{Q}}\,\dot{\boldsymbol{Q}}. \tag{2.251}$$

We can represent Eq. (2.249) explicitly using the components of the matrix $\boldsymbol{\Lambda}$ and those of vector $\boldsymbol{Q}$ as

$$\begin{aligned} V &= \frac{1}{2}(Q_1\ Q_2\ Q_3)\begin{pmatrix} \omega_1^2 & 0 & 0 \\ 0 & \omega_2^2 & 0 \\ 0 & 0 & \omega_3^2 \end{pmatrix}\begin{pmatrix} Q_1 \\ Q_2 \\ Q_3 \end{pmatrix} \\ &= \frac{1}{2}\omega_1^2 Q_1^2 + \frac{1}{2}\omega_2^2 Q_2^2 + \frac{1}{2}\omega_3^2 Q_3^2. \end{aligned} \tag{2.252}$$

This shows that we can eliminate the cross terms between different coordinates, such as $\eta_i\eta_j (i \neq j)$, from the potential, by the coordinate transformation given by Eq. (2.247). Similarly, the kinetic energy can be given simply as

$$\begin{aligned} T &= \frac{1}{2}(\dot{Q}_1\ \dot{Q}_2\ \dot{Q}_3)\begin{pmatrix} \dot{Q}_1 \\ \dot{Q}_2 \\ \dot{Q}_3 \end{pmatrix} \\ &= \frac{1}{2}\dot{Q}_1^2 + \frac{1}{2}\dot{Q}_2^2 + \frac{1}{2}\dot{Q}_3^2. \end{aligned} \tag{2.253}$$

These three coordinates, Q_1, Q_2, and Q_3, are called normal coordinates. Using the normal coordinates, the Hamiltonian $H = T + V$ representing the total energy can be expressed as

$$H = \left(\frac{1}{2}\dot{Q}_1^2 + \frac{1}{2}\omega_1^2 Q_1^2\right) + \left(\frac{1}{2}\dot{Q}_2^2 + \frac{1}{2}\omega_2^2 Q_2^2\right) + \left(\frac{1}{2}\dot{Q}_3^2 + \frac{1}{2}\omega_3^2 Q_3^2\right). \tag{2.254}$$

The third parenthesis of this equation, in which $\omega_3^2 = 0$, simply represents the translational energy. Therefore, when deriving the Hamiltonian of the normal mode vibration, we ignore this part and express the Hamiltonian as

$$H = H_1 + H_2 \tag{2.255}$$

where H_1 and H_2 are each the Hamiltonian of a one-dimensional harmonic oscillator,

$$\begin{cases} H_1 = \dfrac{1}{2}\dot{Q}_1^2 + \dfrac{1}{2}\omega_1^2 Q_1^2, & \text{(2.256a)} \\ H_2 = \dfrac{1}{2}\dot{Q}_2^2 + \dfrac{1}{2}\omega_2^2 Q_2^2. & \text{(2.256b)} \end{cases}$$

These Hamiltonians have a form identical to

$$H = \frac{1}{2}\mu\dot{x}^2 + \frac{1}{2}kx^2. \tag{2.257}$$

Indeed, from Eqs. (2.247) and (2.196), we can derive,

$$Q_1 = \frac{1}{\sqrt{2}}(\eta_1 - \eta_3) = \sqrt{M}X_1, \tag{2.258}$$

where

$$X_1 = \frac{1}{\sqrt{2}}(\Delta x_1 - \Delta x_3). \tag{2.259}$$

Similarly, for Q_2, we can derive

$$\begin{aligned} Q_2 &= \sqrt{\frac{m}{2(2M+m)}}\eta_1 - \sqrt{\frac{2M}{2M+m}}\eta_2 + \sqrt{\frac{m}{2(2M+m)}}\eta_3 \\ &= \sqrt{\frac{2Mm}{2M+m}}X_2, \end{aligned} \tag{2.260}$$

where

$$X_2 = \frac{1}{\sqrt{2}}\left(\frac{\Delta x_1 - \Delta x_2}{\sqrt{2}}\right) + \frac{1}{\sqrt{2}}\left(\frac{\Delta x_3 - \Delta x_2}{\sqrt{2}}\right). \tag{2.261}$$

Therefore,

$$H_1 = \frac{1}{2}M\dot{X}_1^2 + \frac{1}{2}M\omega_1^2 X_1^2 \tag{2.262}$$

$$H_2 = \frac{1}{2}\left(\frac{2Mm}{2M+m}\right)\dot{X}_2^2 + \frac{1}{2}\left(\frac{2Mm}{2M+m}\right)\omega_2^2 X_2^2 \tag{2.263}$$

are obtained. As it becomes apparent when we substitute $k = M\omega_1^2$ into Eq. (2.262) and $k = (\frac{2Mm}{2M+m})\omega_2^2$ into Eq. (2.263), both of these equations have the same form as Eq. (2.257).

The general procedure for deriving all of the normal modes of a polyatomic molecule with n atoms and N degrees of freedom of vibration will be introduced in Sect. 2.5.6, but there, too, the framework of the discussion in the present section will be applicable. That is, using the normal coordinates $\{Q_i\}$, the Hamiltonian will be given as the sum of the Hamiltonians of N harmonic oscillators as

$$H = \sum_{i=1}^{N} H_i, \tag{2.264}$$

where

$$H_i = \frac{1}{2}\dot{Q}_i^2 + \frac{1}{2}\omega_i^2 Q_i^2 \quad (i = 1, \ldots, N). \tag{2.265}$$

Problem 2.28

Explain why neither a constant term nor a first-order term with respect to η_i exists in the potential V in Eq. (2.240).

Solution
Generally, when the potential V is expanded as a Taylor series around the equilibrium position, V is expressed as

$$V = V_0 + \sum_{i=1}^{3} \left(\frac{\partial V}{\partial \eta_i} \right)_{\mathrm{e}} \eta_i + \frac{1}{2} \sum_{i=1}^{3} \sum_{j=1}^{3} \left(\frac{\partial^2 V}{\partial \eta_i \partial \eta_j} \right)_{\mathrm{e}} \eta_i \eta_j + (\text{third- and higher-order terms}). \tag{2.266}$$

Among the expansion terms, the potential V_0 only shifts the energy by a constant value, so that we can regard it as $V_0 = 0$. At the same time, each of the first derivatives of the potential with respect to the displacement coordinates around the equilibrium position, that is, $\left(\frac{\partial V}{\partial \eta_i}\right)_{\mathrm{e}}$, is zero. Therefore, within the harmonic approximation, in which the third- and higher-order expansion terms are neglected, V can be given by Eq. (2.240). □

2.5.5 The Quantum Theory of Normal Mode Vibrations

The discussion in Sect. 2.5.4 allows us to readily quantize the vibrational motion of a polyatomic molecule consisting of n atoms. First of all, let us consider how the Hamiltonian of the i-th normal mode given by Eq. (2.265) can be quantized. The quantization of a coordinate x which has the dimension of the length and its conjugate momentum p is achieved by the transformation of the observables x and p into corresponding operators in quantum mechanics as

$$x \to x, \quad p \to -\mathrm{i}\hbar \frac{\partial}{\partial x}.$$

Then, by quantizing x and p, respectively, the Hamiltonian of a harmonic oscillator in classical mechanics

$$H = \frac{p^2}{2\mu} + \frac{1}{2}\mu\omega^2 x^2 \tag{2.267}$$

is transformed into a Hamiltonian in quantum mechanics as

$$\hat{H} = -\frac{\hbar^2}{2\mu} \frac{\partial^2}{\partial x^2} + \frac{1}{2}\mu\omega^2 x^2. \tag{2.268}$$

As shown in Eqs. (2.258) through (2.263), the normal coordinate Q_i is related to x by use of the reduced mass μ_i as

$$Q_i = \sqrt{\mu_i} x. \tag{2.269}$$

Therefore, the quantum mechanical Hamiltonian of Eq. (2.268) can be expressed with the normal coordinate Q_i in Eq. (2.269), as

$$\hat{H}_i = -\frac{\hbar^2}{2} \frac{\partial^2}{\partial Q_i^2} + \frac{1}{2}\omega_i^2 Q_i^2. \tag{2.270}$$

By comparing this result with Eq. (2.265), we learn that a Hamiltonian in classical mechanics composed of the normal coordinates Q_i and their derivatives $\dot{Q}_i$ can be quantized by replacing Q_i and the momenta conjugated with Q_i, given as

$$P_i = \frac{\partial T}{\partial \dot{Q}_i} = \frac{\partial}{\partial \dot{Q}_i}\left(\frac{1}{2}\dot{Q}_i^2\right) = \dot{Q}_i, \tag{2.271}$$

with corresponding operators, respectively, through the following transformations:

$$Q_i \to Q_i, \qquad P_i = \dot{Q}_i \to -\mathrm{i}\hbar\frac{\partial}{\partial Q_i}. \tag{2.272}$$

By use of this quantum mechanical Hamiltonian, Schrödinger's equation of the i-th harmonic oscillator can be represented with the eigenvalues $E_{v_i}^{(i)}$ and the eigenfunctions $\phi_{v_i}^{(i)}(Q_i)$ as,

$$H_i\phi_{v_i}^{(i)}(Q_i) = E_{v_i}^{(i)}\phi_{v_i}^{(i)}(Q_i), \tag{2.273}$$

where v_i represents the vibrational quantum number of the i-th harmonic oscillator, and the eigenfunction $\phi_n^{(i)}(Q_i)$ is given by

$$\phi_n^{(i)}(Q_i) = \left(\frac{1}{2^n n!}\sqrt{\frac{\omega}{\pi\hbar}}\right)^{\frac{1}{2}} H_n\left(\sqrt{\frac{\omega}{\hbar}}Q_i\right)\mathrm{e}^{-\frac{1}{2}(\sqrt{\frac{\omega}{\hbar}}Q_i)^2}. \tag{2.274}$$

This representation can be readily derived by expressing the wave functions of a harmonic oscillator, which we learned in Sect. 2.2, using the relation

$$\xi = \sqrt{\frac{\mu\omega}{\hbar}}x = \sqrt{\frac{\omega}{\hbar}}Q_i. \tag{2.275}$$

The eigenfunctions $\{\phi_n^{(i)}(Q_i)\}$ fulfill the orthonormal relation

$$\int_{-\infty}^{\infty}\phi_m^{(i)}(Q_i)\phi_n^{(i)}(Q_i)\,\mathrm{d}Q_i = \delta_{mn}, \tag{2.276}$$

and the eigenenergy $E_n^{(i)}$ is expressed as

$$E_n^{(i)} = \hbar\omega_i\left(n + \frac{1}{2}\right). \tag{2.277}$$

When we express the Schrödinger equation as

$$H\Psi = E\Psi, \tag{2.278}$$

using the eigenfunction Ψ, the eigenvalue E, and the quantum mechanical Hamiltonian H obtained by the quantization of the total Hamiltonian of Eq. (2.264) in classical mechanics, Ψ can be represented as the product of the eigenfunctions $\phi_{v_i}^{(i)}(Q_i)$ of each respective harmonic oscillator, as

$$\begin{aligned}\Psi_{\boldsymbol{v}}\left(\{Q_i\}\right) &= \phi_{v_1}^{(1)}(Q_1)\phi_{v_2}^{(2)}(Q_2)\cdots\phi_{v_N}^{(N)}(Q_N)\\ &= \prod_{i=1}^{N}\phi_{v_i}^{(i)}(Q_i),\end{aligned} \tag{2.279}$$

and the eigenvalue E is given by,

$$E(\boldsymbol{v}) = E_{v_1}^{(1)} + E_{v_2}^{(2)} + \cdots = \sum_{i=1}^{N} E_{v_i}^{(i)} \tag{2.280}$$

where $\boldsymbol{v}$ represents the set of quantum numbers $\boldsymbol{v} = (v_1, v_2, \ldots, v_N)$. Therefore, once we have derived the frequency $\nu_i = \frac{\omega_i}{2\pi}$ and the quantum number v_i for each of the harmonic oscillators, we can calculate the total vibrational energy according to Eq. (2.280), as the sum of the eigenvalues of these harmonic oscillators.

For example, in the case of a bent triatomic molecule SO_2, which has three degrees of freedom of vibration, there are three normal modes, the symmetric stretch (ν_1), the bending (ν_2), and the anti-symmetric stretch (ν_3). These normal modes are also called the ν_1 mode, the ν_2 mode, and the ν_3 mode. The frequencies of these normal modes are known to be

$$\tilde{\nu}_1 = 1151 \text{ cm}^{-1},$$
$$\tilde{\nu}_2 = 517 \text{ cm}^{-1},$$
$$\tilde{\nu}_3 = 1362 \text{ cm}^{-1}.$$

From Eqs. (2.277) and (2.280), the vibrational energy of the entire molecule is expressed as,

$$\begin{aligned} E(\boldsymbol{v}) &= \sum_{i=1}^{3} \hbar\omega_i \left(v_i + \frac{1}{2} \right) \\ &= \hbar\omega_1 \left(v_1 + \frac{1}{2} \right) + \hbar\omega_2 \left(v_2 + \frac{1}{2} \right) + \hbar\omega_3 \left(v_3 + \frac{1}{2} \right). \end{aligned} \tag{2.281}$$

This equation can be rewritten in terms of wave numbers as

$$\tilde{E}(\boldsymbol{v}) = \frac{E(\boldsymbol{v})}{hc} = \tilde{\nu}_1 \left(v_1 + \frac{1}{2} \right) + \tilde{\nu}_2 \left(v_2 + \frac{1}{2} \right) + \tilde{\nu}_3 \left(v_3 + \frac{1}{2} \right). \tag{2.282}$$

Once the set of quantum numbers $\boldsymbol{v} = (v_1, v_2, v_3)$ is given, we can calculate the vibrational energy from Eq. (2.282).

For example, $\tilde{E}\ (1, 2, 0)$, the vibrational energy of SO_2 for the vibrational levels $\boldsymbol{v} = (1, 2, 0)$, is calculated as

$$\begin{aligned} \tilde{E}(1, 2, 0) &= \tilde{\nu}_1 \left(1 + \frac{1}{2} \right) + \tilde{\nu}_2 \left(2 + \frac{1}{2} \right) + \tilde{\nu}_3 \left(0 + \frac{1}{2} \right) \\ &= \frac{3}{2}\tilde{\nu}_1 + \frac{5}{2}\tilde{\nu}_2 + \frac{1}{2}\tilde{\nu}_3 = 3700 \text{ cm}^{-1}. \end{aligned}$$

Problem 2.29

Derive the energy of the vibrational levels $\boldsymbol{v} = (1, 2, 0)$ of SO_2 in terms of wave numbers, as measured from the zero-point vibrational level.

Solution
The zero-point energy $\tilde{E}(0,0,0)$ is given by

$$\tilde{E}(0,0,0) = \frac{1}{2}\tilde{\nu}_1 + \frac{1}{2}\tilde{\nu}_2 + \frac{1}{2}\tilde{\nu}_3,$$

and therefore the vibrational energy becomes

$$\tilde{E}(1,2,0) - \tilde{E}(0,0,0) = \tilde{\nu}_1 + 2\tilde{\nu}_2 = 2185\ \mathrm{cm}^{-1}.$$

The vibrational energy measured from the zero-point vibrational level is called the term value of the vibration. □

As seen from solving Problem 2.29, the term value for $\boldsymbol{v} = (1,2,0)$ of SO_2 is calculated to be 2185 cm^{-1}. However, the corresponding value obtained from spectroscopic measurements is 2180 cm^{-1}, which is lower than the estimate by 5 cm^{-1}. This is because (i) each of the normal modes ν_1, ν_2, and ν_3 has some anharmonicity and cannot be represented as a pure harmonic oscillator and (ii) the normal modes are not independent of one another due to the anharmonic couplings through which the oscillators interact with one another. The effect of this type of anharmonicity becomes the more pronounced the larger the vibrational quantum numbers are.

In order to represent the effect of the anharmonicities in vibrational modes, we often expand the observed energy levels phenomenologically as

$$\tilde{E}(\boldsymbol{v}) = \sum_i \tilde{\nu}_i\left(v_i + \frac{1}{2}\right) + \sum_{i\leqq j}\sum x_{ij}\left(v_i + \frac{1}{2}\right)\left(v_j + \frac{1}{2}\right) + \sum_{i\leqq j\leqq k}\sum\sum y_{ijk}\left(v_i + \frac{1}{2}\right)\left(v_j + \frac{1}{2}\right)\left(v_k + \frac{1}{2}\right) + \cdots. \quad (2.283)$$

Such a description is called the Dunham-type expansion.

2.5.6 Normal Modes of a Polyatomic Molecule Composed of n Atoms

Let us now extend the procedure we learned with the model of a linear triatomic molecule in Sects. 2.5.2 through 2.5.4 to the general case of a polyatomic molecule composed of n atoms. We will first consider the bent triatomic molecule shown in Fig. 2.23, and represent the displacements of the three atoms 1, 2, and 3 from their equilibrium positions as $(\Delta x_1, \Delta y_1, \Delta z_1)$, $(\Delta x_2, \Delta y_2, \Delta z_2)$, and $(\Delta x_3, \Delta y_3, \Delta z_3)$, respectively. Then, the kinetic energy of the entire molecule becomes

$$T = \frac{1}{2}\sum_{i=1}^{3} M_i\left(\Delta\dot{x}_i^2 + \Delta\dot{y}_i^2 + \Delta\dot{z}_i^2\right), \quad (2.284)$$

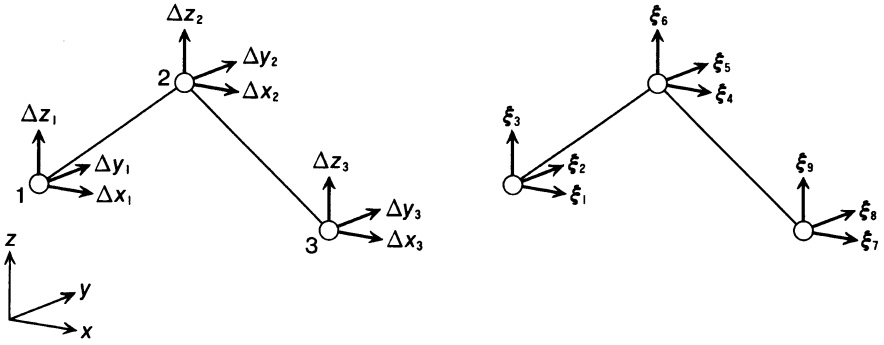

Fig. 2.23 The displacement of atoms from their equilibrium positions in a bent triatomic molecule

where M_i is the mass of the i-th atom. In order to make the representation of this formula simpler, we will henceforth write

$$\Delta x_1,\ \Delta y_1,\ \Delta z_1,\ \Delta x_2,\ \Delta y_2,\ \Delta z_2,\ \Delta x_3,\ \Delta y_3,\ \Delta z_3,$$

in this order, as

$$\xi_1,\ \xi_2,\ \xi_3,\ \xi_4,\ \xi_5,\ \xi_6,\ \xi_7,\ \xi_8,\ \xi_9.$$

The relative values of these displacements need to satisfy the requirement that the vibration does not cause the molecule as a whole to translate nor rotate. This requirement is called Eckart's condition.

If we assume that $m_1 = m_2 = m_3 = M_1$, $m_4 = m_5 = m_6 = M_2$, and $m_7 = m_8 = m_9 = M_3$, Eq. (2.284) becomes

$$T = \frac{1}{2}\sum_{i=1}^{9} m_i \dot{\xi}_i^2. \tag{2.285}$$

By using ξ_i, the potential V around the equilibrium geometry can be represented as

$$V = \frac{1}{2}\sum_{i=1}^{9}\sum_{j=1}^{9}\left(\frac{\partial^2 V}{\partial\xi_i \partial\xi_j}\right)_{\mathrm{e}} \xi_i \xi_j, \tag{2.286}$$

where third-order terms such as $\xi_i\xi_j\xi_k$ and higher-order terms are neglected. The kinetic energy and the potential energy represented respectively in Eqs. (2.285) and (2.286) are those for a triatomic molecule, but by replacing the sum as $9 \to 3n$, we can turn them into representations of the kinetic and potential energies for an n-atomic molecule.

As the next step, we will derive the normal modes of a polyatomic molecule consisting of n atoms. The procedure is exactly the same as the one described in Sects. 2.5.2 through 2.5.4. First, we express the Lagrangian $L = T - V$ using the T and V for an n-atomic molecule corresponding to Eqs. (2.285) and (2.286), and transform the classical equation of motion

$$\frac{\mathrm{d}}{\mathrm{d}t}\left(\frac{\partial L}{\partial \dot{\xi}_i}\right) - \frac{\partial L}{\partial \xi_i} = 0 \tag{2.287}$$

into

$$\frac{\mathrm{d}}{\mathrm{d}t}(m_i\dot{\xi}_i)+\sum_j^{3n}\left(\frac{\partial^2 V}{\partial\xi_i\partial\xi_j}\right)_{\mathrm{e}}\xi_j=0. \tag{2.288}$$

By introducing mass-weighted coordinates

$$\eta_i=\sqrt{m_i}\xi_i \quad (i=1,2\ldots,3n), \tag{2.289}$$

we can express Eq. (2.288) as

$$\frac{\mathrm{d}}{\mathrm{d}t}\dot{\eta}_i+\sum_j^{3n}c_{ij}\eta_j=0, \tag{2.290}$$

where the coefficients c_{ij} are given by

$$c_{ij}=\frac{1}{\sqrt{m_i m_j}}\left(\frac{\partial^2 V}{\partial\xi_i\partial\xi_j}\right)_{\mathrm{e}}. \tag{2.291}$$

Since the vibrations treated here are those where the atoms in a molecule vibrate collectively with a common frequency starting from their equilibrium positions, we will consider these atoms to be vibrating at a common angular frequency ω, given as

$$\eta_i=\eta_i^\circ\exp(\mathrm{i}\omega t). \tag{2.292}$$

By substituting this into Eq. (2.290), we can readily obtain

$$-\omega^2\eta_i^\circ+\sum_j^{3n}c_{ij}\eta_j^\circ=0. \tag{2.293}$$

This is a simultaneous linear equation with regards to the displacement amplitudes η_j°, and can be represented in matrix form as

$$\begin{pmatrix} c_{11} & c_{12} & c_{13} & \\ c_{21} & c_{22} & c_{23} & \cdots \\ c_{31} & c_{32} & c_{33} & \\ & \vdots & & \ddots \end{pmatrix}\begin{pmatrix}\eta_1^\circ\\ \eta_2^\circ\\ \eta_3^\circ\\ \vdots\end{pmatrix}=\omega^2\begin{pmatrix}\eta_1^\circ\\ \eta_2^\circ\\ \eta_3^\circ\\ \vdots\end{pmatrix}, \tag{2.294}$$

or, equivalently, as

$$\begin{pmatrix} c_{11}-\omega^2 & c_{12} & c_{13} & \\ c_{21} & c_{22}-\omega^2 & c_{23} & \cdots \\ c_{31} & c_{32} & c_{33}-\omega^2 & \\ & \vdots & & \ddots \end{pmatrix}\begin{pmatrix}\eta_1^\circ\\ \eta_2^\circ\\ \eta_3^\circ\\ \vdots\end{pmatrix}=0. \tag{2.295}$$

The condition for this simultaneous linear equation to have a non-trivial solution, that is, a solution aside from $\eta_1^\circ = \eta_2^\circ = \cdots = \eta_{3n}^\circ = 0$, is

$$\begin{vmatrix} c_{11} - \omega^2 & c_{12} & c_{13} & \\ c_{21} & c_{22} - \omega^2 & c_{23} & \cdots \\ c_{31} & c_{32} & c_{33} - \omega^2 & \\ & \vdots & & \ddots \end{vmatrix} = 0, \tag{2.296}$$

that is,

$$\left| \boldsymbol{C} - \omega^2 \boldsymbol{E} \right| = 0. \tag{2.297}$$

There can potentially be $3n$ solutions for the eigenvalues ω^2, but out of them, 6 (5 in the case of a linear molecule) are solutions that give $\omega^2 = 0$. These are the 3 solutions corresponding to the translation of the entire molecule, and the 3 (or 2 in the case of a linear molecule) corresponding to the rotation of the entire molecule. When we denote the k-th eigenvalue as ω_k^2 and the associated eigenvector as

$$\boldsymbol{\eta}_k^\circ = \begin{pmatrix} \eta_{1k}^\circ \\ \eta_{2k}^\circ \\ \vdots \end{pmatrix}, \tag{2.298}$$

Eq. (2.294) is written as

$$\boldsymbol{C}\boldsymbol{\eta}_k^\circ = \omega_k^2 \boldsymbol{\eta}_k^\circ, \tag{2.299}$$

where $\boldsymbol{\eta}_k^\circ$ is normalized so that

$$\sum_i \left(\eta_{ik}^\circ\right)^2 = 1. \tag{2.300}$$

Using an $\boldsymbol{L}_\eta$ matrix

$$\boldsymbol{L}_\eta = \begin{pmatrix} \eta_{11}^\circ & \eta_{12}^\circ & \eta_{13}^\circ & \\ \eta_{21}^\circ & \eta_{22}^\circ & \eta_{23}^\circ & \cdots \\ \eta_{31}^\circ & \eta_{32}^\circ & \eta_{33}^\circ & \\ & \vdots & & \ddots \end{pmatrix}, \tag{2.301}$$

we obtain

$$\boldsymbol{C}\boldsymbol{L}_\eta = \boldsymbol{L}_\eta \boldsymbol{\Lambda}, \tag{2.302}$$

where $\boldsymbol{\Lambda}$ is a diagonal matrix expressed as

$$\boldsymbol{\Lambda} = \begin{pmatrix} \omega_1^2 & & & \\ & \omega_2^2 & & \mathrm{O} \\ & & \ddots & \\ & \mathrm{O} & & \\ & & & \omega_{3n}^2 \end{pmatrix}. \tag{2.303}$$

By operating $\boldsymbol{L}_\eta^{-1}$ from the left on both sides of Eq. (2.302), we derive

$$\boldsymbol{L}_\eta^{-1}\boldsymbol{C}\boldsymbol{L}_\eta = \boldsymbol{\Lambda}. \tag{2.304}$$

What Eq. (2.304) signifies is that, by the diagonalization of the matrix

$$\boldsymbol{C} = \begin{pmatrix} c_{11} & c_{12} & c_{13} & \\ c_{21} & c_{22} & c_{23} & \cdots \\ c_{31} & c_{32} & c_{33} & \\ & \vdots & & \ddots \end{pmatrix}, \tag{2.305}$$

the $3n$ values of ω^2 are obtained as eigenvalues, and the displacement of each of the atoms is obtained as an eigenvector associated with the corresponding eigenvalue. In other words, the normal mode frequencies $\{\omega_k\}$ as well as the corresponding normal coordinates $\{\boldsymbol{\eta}_k^\circ\}$ have been derived, both of which are characteristic to each molecular species.

By use of a column vector of the original displacement coordinates,

$$\boldsymbol{\eta} = \begin{pmatrix} \eta_1 \\ \eta_2 \\ \vdots \\ \eta_{3n} \end{pmatrix}, \tag{2.306}$$

the potential energy V can be represented as

$$V = \frac{1}{2}{}^t\boldsymbol{\eta}\boldsymbol{C}\boldsymbol{\eta}. \tag{2.307}$$

We introduce here a vector $\boldsymbol{Q}$ that is defined with the orthogonal matrix $\boldsymbol{L}_\eta$ derived through the diagonalization process as

$$\boldsymbol{Q} = \boldsymbol{L}_\eta^{-1}\boldsymbol{\eta}. \tag{2.308}$$

Equation (2.308) can also be written as

$$\boldsymbol{\eta} = \boldsymbol{L}_\eta\,\boldsymbol{Q}, \tag{2.309}$$

which can be substituted into Eq. (2.307) to give us

$$V = \frac{1}{2}{}^t(\boldsymbol{L}_\eta\,\boldsymbol{Q})\boldsymbol{C}(\boldsymbol{L}_\eta\,\boldsymbol{Q}) = \frac{1}{2}{}^t\boldsymbol{Q}({}^t\boldsymbol{L}_\eta\boldsymbol{C}\boldsymbol{L}_\eta)\,\boldsymbol{Q}. \tag{2.310}$$

Using Eq. (2.304), we can express V as

$$V = \frac{1}{2}{}^t\boldsymbol{Q}\boldsymbol{\Lambda}\,\boldsymbol{Q} = \frac{1}{2}\left(\omega_1^2 Q_1^2 + \omega_2^2 Q_2^2 + \cdots\right). \tag{2.311}$$

Meanwhile, the kinetic energy T can be written as

$$T = \frac{1}{2}{}^t\dot{\boldsymbol{\eta}}\dot{\boldsymbol{\eta}}, \tag{2.312}$$

so that we can derive

$$
\begin{aligned}
T &= \frac{1}{2}{}^t(\boldsymbol{L}_\eta \dot{\boldsymbol{Q}})(\boldsymbol{L}_\eta \dot{\boldsymbol{Q}}) \\
&= \frac{1}{2}{}^t\dot{\boldsymbol{Q}}\left({}^t\boldsymbol{L}_\eta \boldsymbol{L}_\eta\right)\dot{\boldsymbol{Q}} \\
&= \frac{1}{2}{}^t\dot{\boldsymbol{Q}}\,\dot{\boldsymbol{Q}} \\
&= \frac{1}{2}\left(\dot{Q}_1^2 + \dot{Q}_2^2 + \cdots\right).
\end{aligned} \tag{2.313}
$$

As Eq. (2.311) illustrates, by use of the coordinates $\boldsymbol{Q}$ transformed as Eq. (2.308) by the eigenvectors derived after diagonalization, the second-order cross terms in the potential disappear, and the kinetic and potential energies are represented, respectively, as

$$T = \frac{1}{2}{}^t\dot{\boldsymbol{Q}}\,\dot{\boldsymbol{Q}}, \tag{2.314}$$

$$V = \frac{1}{2}{}^t\boldsymbol{Q}\boldsymbol{\Lambda}\,\boldsymbol{Q}. \tag{2.315}$$

Of the coordinates represented by $\boldsymbol{Q}$, $3n-6$ ($3n-5$ in the case of a linear molecule) represent the normal coordinates, and the vibrations along these coordinates are the normal modes.

2.5.7 *Representation of Normal Modes in Terms of Internal Coordinates*

We have already looked at the general procedure for deriving normal modes in Sect. 2.5.6, but it is difficult to get a clear picture of molecular vibration if we start with the η_i coordinate system. A more straightforward approach to normal modes in line with the physical picture of vibration would be to construct them by first examining vibrations along chemical bonds and along bond angles.

For example, let us consider the bent triatomic molecule shown in Fig. 2.24. The changes in the two internuclear distances from the equilibrium structure are denoted as Δr_A and Δr_B, and the change in the bond angle from the equilibrium structure is denoted as $\Delta\theta$, so that

$$
\begin{aligned}
\Delta r_\mathrm{A} &= r_\mathrm{A} - r_\mathrm{A,e}, \\
\Delta r_\mathrm{B} &= r_\mathrm{B} - r_\mathrm{B,e}, \\
\Delta\theta &= \theta - \theta_\mathrm{e},
\end{aligned}
$$

where $r_\mathrm{A,e}$, $r_\mathrm{B,e}$, and θ_e represent the corresponding values at the equilibrium structure. A coordinate system such as this is called an internal coordinate system. When the internal coordinates shown in Fig. 2.24 are described as vector $\boldsymbol{s} = (s_1, s_2, s_3)$, its components are $s_1 = \Delta r_\mathrm{A}$, $s_2 = \Delta r_\mathrm{B}$, and $s_3 = \Delta\theta$. Our goal now is to describe molecular vibration in terms of internal coordinates and derive the normal modes.

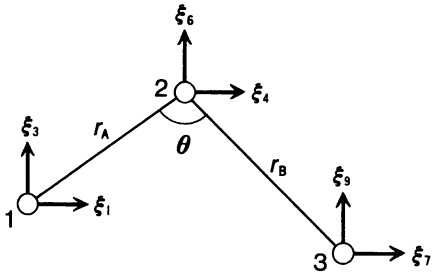

Fig. 2.24 The internal coordinates of a bent triatomic molecule

The number of internal coordinates that we have just chosen, three, corresponds to the number of the degrees of freedom for the vibration of a triatomic molecule.

In the case of a bent polyatomic molecule consisting of n atoms, the internal coordinate vector $\boldsymbol{s}$ has $3n-6$ components, so that

$$\boldsymbol{s} = \begin{pmatrix} s_1 \\ s_2 \\ \vdots \\ s_{3n-6} \end{pmatrix}, \tag{2.316}$$

and it is related to a displacement vector $\boldsymbol{\eta}$ represented in the orthogonal coordinate system by the relation,

$$\boldsymbol{s} = \boldsymbol{B}\boldsymbol{\eta}, \tag{2.317}$$

where matrix $\boldsymbol{B}$ is a rectangular matrix with $3n-6$ rows and $3n$ columns. In the case of the bent triatomic molecule mentioned above, Eq. (2.317) can be written explicitly as

$$\begin{pmatrix} \Delta r_{\mathrm{A}} \\ \Delta r_{\mathrm{B}} \\ \Delta\theta \end{pmatrix} = \begin{pmatrix} b_{11} & b_{12} & \dots & b_{19} \\ b_{21} & b_{22} & \dots & b_{29} \\ b_{31} & b_{32} & \dots & b_{39} \end{pmatrix} \begin{pmatrix} \eta_1 \\ \eta_2 \\ \eta_3 \\ \vdots \\ \eta_9 \end{pmatrix}, \tag{2.318}$$

where $\boldsymbol{B}$ is a rectangular 3×9 matrix. Now, the displacement vector $\boldsymbol{\eta}$ can express not only motions expressed by $\boldsymbol{s}$ but also motions corresponding to the three degrees of freedom for the rotation and the three for the translation of the molecule. Therefore, we can add the six coordinates associated with the translation and rotation of the whole molecule $(s_{3n-5}, \dots, s_{3n})$ to the internal coordinate system $\boldsymbol{s}$ to define the vector $\boldsymbol{s}'$, expressing the internal coordinate system extended to the $3n$-th dimension, as

$$\boldsymbol{s}' = \begin{pmatrix} \boldsymbol{s} \\ s_{3n-5} \\ \vdots \\ s_{3n} \end{pmatrix}. \tag{2.319}$$

When we use $\boldsymbol{\eta}$ to rewrite the transformation of $\boldsymbol{s}'$ using a $3n$ by $3n$ matrix $\boldsymbol{B}'$ as

$$\boldsymbol{s}' = \boldsymbol{B}'\boldsymbol{\eta}, \tag{2.320}$$

we can express $\boldsymbol{\eta}$ as $\boldsymbol{s}'$ inversely transformed by $\boldsymbol{B}'^{-1}$, as

$$\boldsymbol{\eta} = \boldsymbol{B}'^{-1}\boldsymbol{s}'. \tag{2.321}$$

Thus, the kinetic energy of the whole molecule can be written as

$$\begin{aligned} T &= \frac{1}{2}{}^t\dot{\boldsymbol{\eta}}\dot{\boldsymbol{\eta}} = \frac{1}{2}{}^t\left(\boldsymbol{B}'^{-1}\dot{\boldsymbol{s}}'\right)\left(\boldsymbol{B}'^{-1}\dot{\boldsymbol{s}}'\right) \\ &= \frac{1}{2}{}^t\dot{\boldsymbol{s}}'\left(\boldsymbol{B}'\,{}^t\boldsymbol{B}'\right)^{-1}\dot{\boldsymbol{s}}'. \end{aligned} \tag{2.322}$$

When we define a $3n \times 3n$ square matrix $\mathfrak{G}$ as

$$\mathfrak{G} = \boldsymbol{B}'\,{}^t\boldsymbol{B}', \tag{2.323}$$

Eq. (2.322) becomes $T = \frac{1}{2}{}^t\dot{\boldsymbol{s}}'\mathfrak{G}^{-1}\dot{\boldsymbol{s}}'$.

In the meantime, we will assume that the potential energy V can be represented with the internal coordinate $\boldsymbol{s}'$ as

$$V = \frac{1}{2}{}^t\boldsymbol{s}'\mathfrak{F}\boldsymbol{s}', \tag{2.324}$$

where $\mathfrak{F}$ is a matrix whose diagonal elements are the coefficients of the restoring force along the respective internal coordinates. The matrix $\mathfrak{F}$ is also a $3n \times 3n$ square matrix.

As we have already established, the equation to be solved in the coordinate system represented by $\boldsymbol{\eta}$ is Eq. (2.294). The potential energy expressed by $\boldsymbol{\eta}$, or

$$V = \frac{1}{2}{}^t\boldsymbol{\eta}\boldsymbol{C}\boldsymbol{\eta}, \tag{2.325}$$

can be rewritten using Eq. (2.321) as

$$V = \frac{1}{2}{}^t\left(\boldsymbol{B}'^{-1}\boldsymbol{s}'\right)\boldsymbol{C}\left(\boldsymbol{B}'^{-1}\boldsymbol{s}'\right) = \frac{1}{2}{}^t\boldsymbol{s}'{}^t\left(\boldsymbol{B}'^{-1}\right)\boldsymbol{C}\,\boldsymbol{B}'^{-1}\boldsymbol{s}'. \tag{2.326}$$

Comparing this with Eq. (2.324), we can see that the relationship

$${}^t\left(\boldsymbol{B}'^{-1}\right)\boldsymbol{C}\,\boldsymbol{B}'^{-1} = \mathfrak{F} \tag{2.327}$$

holds.

Using vector $\boldsymbol{s}'^{\circ}$, which is transformed from eigenvector $\boldsymbol{\eta}^{\circ}$ as

$$\boldsymbol{s}'^{\circ} = \boldsymbol{B}'\boldsymbol{\eta}^{\circ}, \tag{2.328}$$

we can rewrite Eq. (2.294) as

$$\boldsymbol{C}\,\boldsymbol{B}'^{-1}\boldsymbol{s}'^{\circ} = \omega^2\boldsymbol{B}'^{-1}\boldsymbol{s}'^{\circ}. \tag{2.329}$$

Multiplying both sides of this equation from the left by $\boldsymbol{B}'$ and using Eq. (2.327), we obtain

$$\boldsymbol{B}'{}^t\boldsymbol{B}'\mathfrak{F}\boldsymbol{s}'^{\circ} = \omega^2\boldsymbol{s}'^{\circ}. \tag{2.330}$$

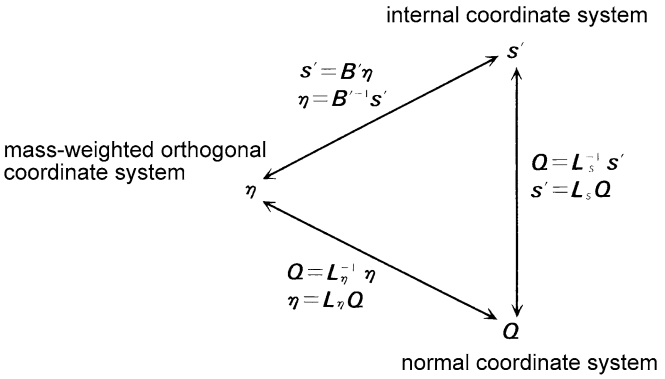

Fig. 2.25 Transformations among the three coordinate systems: $\boldsymbol{\eta}$, $\boldsymbol{s}'$, and $\boldsymbol{Q}$

When we substitute the definition of the $\mathfrak{G}$ matrix given in Eq. (2.323) into this equation, we can see that the equation to be solved is

$$\mathfrak{G}\mathfrak{F}\boldsymbol{s}'^{\circ} = \omega^2 \boldsymbol{s}'^{\circ}, \tag{2.331}$$

and thus that the eigen equation is

$$\left|\mathfrak{G}\mathfrak{F} - \omega^2 \boldsymbol{E}\right| = 0. \tag{2.332}$$

When we set internal coordinates $\boldsymbol{s}_1, \ldots, \boldsymbol{s}_{3n-6}$ to describe vibration, independent of the coordinates $\boldsymbol{s}_{3n-5}, \ldots, \boldsymbol{s}_{3n}$ relating to the translation and rotation of the entire molecule, $\boldsymbol{F}$ becomes the left-top $(3n-6) \times (3n-6)$ corner of matrix $\mathfrak{F}$ and all of the elements of $\mathfrak{F}$ except $\boldsymbol{F}$ becomes zero. Thus, we can separate from Eq. (2.332) what corresponds to $\omega \neq 0$ and write it as

$$\left|\boldsymbol{G}\boldsymbol{F} - \omega^2 \boldsymbol{E}\right| = 0, \tag{2.333}$$

where $\boldsymbol{G}$ is the left-top $(3n-6) \times (3n-6)$ corner of $\mathfrak{G}$ and

$$\boldsymbol{G} = \boldsymbol{B}^t \boldsymbol{B} \tag{2.334}$$

holds, from Eq. (2.323) and the relationship between $\boldsymbol{B}'$ and $\boldsymbol{B}$.

This signifies that, once the internal coordinate representations of matrices $\boldsymbol{G}$ and $\boldsymbol{F}$ are given, we can derive the normal mode vibrations as well as their frequencies by diagonalizing the product of these two matrices, $\boldsymbol{G}\boldsymbol{F}$. This procedure for treating molecular vibration is called the GF matrix method. Figure 2.25 gives a summary of how the three types of coordinate systems that we have looked at so far, the mass-weighted orthogonal coordinate system $\boldsymbol{\eta} = \{\eta_i\}$ $(i = 1, \ldots, 3n)$, the normal coordinate system $\boldsymbol{Q} = \{Q_i\}$ $(i = 1, \ldots, 3n)$, and the internal coordinate system $\boldsymbol{s}' = \{s_i\}$ $(i = 1, \ldots, 3n)$ can be transformed from one system to another.

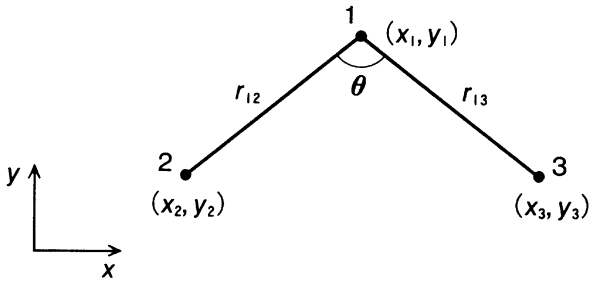

Fig. 2.26 The internal coordinates of a bent symmetric triatomic molecule

Problem 2.30
Transform the kinetic and potential energies represented by internal coordinate $\boldsymbol{s}'$ into a representation in terms of $\boldsymbol{Q}$, by using the coordinate transformation $\boldsymbol{s}' = \boldsymbol{B}'\boldsymbol{L}_\eta \boldsymbol{Q}$.

Solution
From Eqs. (2.322) and (2.324),

$$\begin{aligned} T &= \frac{1}{2}{}^t\dot{\boldsymbol{Q}}\,{}^t\boldsymbol{L}_\eta\,{}^t\boldsymbol{B}'\left({}^t\boldsymbol{B}'\right)^{-1}\boldsymbol{B}'^{-1}\boldsymbol{B}'\boldsymbol{L}_\eta\,\dot{\boldsymbol{Q}} \\ &= \frac{1}{2}{}^t\dot{\boldsymbol{Q}}\,{}^t\boldsymbol{L}_\eta\boldsymbol{L}_\eta\,\dot{\boldsymbol{Q}} = \frac{1}{2}{}^t\dot{\boldsymbol{Q}}\,\dot{\boldsymbol{Q}}, \\ V &= \frac{1}{2}{}^t\boldsymbol{Q}\,{}^t\boldsymbol{L}_\eta\,{}^t\boldsymbol{B}'^t\left(\boldsymbol{B}'^{-1}\right)\boldsymbol{C}\boldsymbol{B}'^{-1}\boldsymbol{B}'\boldsymbol{L}_\eta\,\boldsymbol{Q} \\ &= \frac{1}{2}{}^t\boldsymbol{Q}\,{}^t\boldsymbol{L}_\eta\boldsymbol{C}\boldsymbol{L}_\eta\,\boldsymbol{Q} = \frac{1}{2}{}^t\boldsymbol{Q}\boldsymbol{\Lambda}\,\boldsymbol{Q}. \end{aligned}$$

In Fig. 2.25, $\boldsymbol{B}'\boldsymbol{L}_\eta$ is represented as $\boldsymbol{B}'\boldsymbol{L}_\eta = \boldsymbol{L}_s$. □

2.5.8 Analysis of Normal Modes by the GF Matrix Method

Taking SO_2 as a typical example of a triatomic molecule, we will now derive the normal modes and the associated frequencies using the GF matrix method introduced in Sect. 2.5.7.

We will begin by assigning the number 1 to the S atom and the numbers 2 and 3 to the two O atoms, as shown in Fig. 2.26. Here we assume that these three atoms are all on the x-y plane, and that the line connecting the two O atoms is set parallel to the x axis of the space-fixed coordinate system. The internuclear distances between the S atom and the two O atoms are denoted as r_{12} and r_{13}, respectively, and the bond angle between them as θ. The internal coordinate $\boldsymbol{s}$ is represented as

$$\boldsymbol{s} = \begin{pmatrix} \Delta r_{12} \\ \Delta r_{13} \\ \Delta\theta \end{pmatrix} \tag{2.335}$$

by using the displacements Δr_{12}, Δr_{13}, and $\Delta\theta$ of the respective internal coordinates, r_{12}, r_{13}, and θ, from their equilibrium values. The distance r_{12} is written as

$$r_{12} = \left\{(x_1 - x_2)^2 + (y_1 - y_2)^2\right\}^{\frac{1}{2}}, \tag{2.336}$$

so that, by differentiating both sides of this equation at the equilibrium position, we can derive

$$\mathrm{d}r_{12} = \left(\frac{\partial r_{12}}{\partial x_1}\right)_{\mathrm{e}} \mathrm{d}x_1 + \left(\frac{\partial r_{12}}{\partial x_2}\right)_{\mathrm{e}} \mathrm{d}x_2 + \left(\frac{\partial r_{12}}{\partial y_1}\right)_{\mathrm{e}} \mathrm{d}y_1 + \left(\frac{\partial r_{12}}{\partial y_2}\right)_{\mathrm{e}} \mathrm{d}y_2, \tag{2.337}$$

where the subscript "e" means that the derivatives are taken at the equilibrium position. The derivatives are obtained using Eq. (2.336) as

$$\begin{cases} \left(\dfrac{\partial r_{12}}{\partial x_1}\right)_{\mathrm{e}} = \left(\dfrac{x_1 - x_2}{r_{12}}\right)_{\mathrm{e}}, & \left(\dfrac{\partial r_{12}}{\partial x_2}\right)_{\mathrm{e}} = -\left(\dfrac{x_1 - x_2}{r_{12}}\right)_{\mathrm{e}}, \\ \left(\dfrac{\partial r_{12}}{\partial y_1}\right)_{\mathrm{e}} = \left(\dfrac{y_1 - y_2}{r_{12}}\right)_{\mathrm{e}}, & \left(\dfrac{\partial r_{12}}{\partial y_2}\right)_{\mathrm{e}} = -\left(\dfrac{y_1 - y_2}{r_{12}}\right)_{\mathrm{e}}, \end{cases} \tag{2.338}$$

and Fig. 2.26 clearly shows that

$$\sin\left(\frac{\theta_{\mathrm{e}}}{2}\right) = \left(\frac{x_1 - x_2}{r_{12}}\right)_{\mathrm{e}}, \qquad \cos\left(\frac{\theta_{\mathrm{e}}}{2}\right) = \left(\frac{y_1 - y_2}{r_{12}}\right)_{\mathrm{e}}. \tag{2.339}$$

Since we are describing small displacements within a molecule, we will change the differential symbol "d" into "Δ", replacing $\mathrm{d}r_{12}$ by Δr_{12}, and $\mathrm{d}x_1$, $\mathrm{d}x_2$, $\mathrm{d}y_1$, and $\mathrm{d}y_2$ by Δx_1, Δx_2, Δy_1, and Δy_2, respectively. This turns Eq. (2.337) into

$$\Delta r_{12} = s\Delta x_1 + c\Delta y_1 - s\Delta x_2 - c\Delta y_2, \tag{2.340}$$

and similarly gives us

$$\Delta r_{13} = -s\Delta x_1 + c\Delta y_1 + s\Delta x_3 - c\Delta y_3 \tag{2.341}$$

for r_{13}, where

$$s = \sin\left(\frac{\theta_{\mathrm{e}}}{2}\right) = \left(\frac{x_1 - x_2}{r_{12}}\right)_{\mathrm{e}} = -\left(\frac{x_1 - x_3}{r_{13}}\right)_{\mathrm{e}}, \tag{2.342}$$

$$c = \cos\left(\frac{\theta_{\mathrm{e}}}{2}\right) = \left(\frac{y_1 - y_2}{r_{12}}\right)_{\mathrm{e}} = \left(\frac{y_1 - y_3}{r_{13}}\right)_{\mathrm{e}}. \tag{2.343}$$

The square of r_{23}, which is the distance between atom 2 and atom 3, is

$$r_{23}^2 = (x_2 - x_3)^2 + (y_2 - y_3)^2 = (x_2 - x_3)^2, \tag{2.344}$$

and relates to r_{12} and r_{13} by the equation

$$r_{23}^2 = r_{12}^2 + r_{13}^2 - 2r_{12}r_{13}\cos\theta. \tag{2.345}$$

By differentiating both sides of Eq. (2.344), we can derive

$$r_{23}\,\mathrm{d}r_{23} = -2r_{\mathrm{e}}s\,\mathrm{d}x_2 + 2r_{\mathrm{e}}s\,\mathrm{d}x_3, \tag{2.346}$$

where r_e is the equilibrium internuclear distance $r_\mathrm{e} = r_{12,\mathrm{e}} = r_{13,\mathrm{e}}$. Similarly, by differentiating both sides of Eq. (2.345), we obtain

$$r_{23}\,\mathrm{d}r_{23} = 2r_\mathrm{e}s^2(\mathrm{d}r_{12} + \mathrm{d}r_{13}) + 2r_\mathrm{e}^2 sc\,\mathrm{d}\theta. \tag{2.347}$$

Having replaced "d" by "Δ", we can equate Eqs. (2.346) and (2.347), solve it in terms of $\Delta\theta$, then substitute Eqs. (2.340) and (2.341) into it, to derive

$$\Delta\theta = \frac{1}{r_\mathrm{e}}(-2s\Delta y_1 - c\Delta x_2 + s\Delta y_2 + c\Delta x_3 + s\Delta y_3). \tag{2.348}$$

Applying Eqs. (2.340), (2.341), and (2.348) into the matrix representation of Eq. (2.317), $\boldsymbol{s} = \boldsymbol{B}\boldsymbol{\eta}$, we derive

$$\boldsymbol{B} = \begin{pmatrix} \frac{s}{\sqrt{m_1}} & \frac{c}{\sqrt{m_1}} & 0 & \frac{-s}{\sqrt{m_2}} & \frac{-c}{\sqrt{m_2}} & 0 & 0 & 0 & 0 \\ \frac{-s}{\sqrt{m_1}} & \frac{c}{\sqrt{m_1}} & 0 & 0 & 0 & 0 & \frac{s}{\sqrt{m_3}} & \frac{-c}{\sqrt{m_3}} & 0 \\ 0 & \frac{\frac{-2s}{r_\mathrm{e}}}{\sqrt{m_1}} & 0 & \frac{\frac{-c}{r_\mathrm{e}}}{\sqrt{m_2}} & \frac{\frac{s}{r_\mathrm{e}}}{\sqrt{m_2}} & 0 & \frac{\frac{c}{r_\mathrm{e}}}{\sqrt{m_3}} & \frac{\frac{s}{r_\mathrm{e}}}{\sqrt{m_3}} & 0 \end{pmatrix}. \tag{2.349}$$

Therefore, the $\boldsymbol{G}$ matrix is represented as

$$\boldsymbol{G} = \boldsymbol{B}^t\boldsymbol{B} = \begin{pmatrix} \mu_1 + \mu_2 & \mu_1\cos\theta_\mathrm{e} & -\mu_1\frac{\sin\theta_\mathrm{e}}{r_\mathrm{e}} \\ \mu_1\cos\theta_\mathrm{e} & \mu_1 + \mu_3 & -\mu_1\frac{\sin\theta_\mathrm{e}}{r_\mathrm{e}} \\ -\mu_1\frac{\sin\theta_\mathrm{e}}{r_\mathrm{e}} & -\mu_1\frac{\sin\theta_\mathrm{e}}{r_\mathrm{e}} & \frac{1}{r_\mathrm{e}^2}(\mu_2 + \mu_3) + \frac{2}{r_\mathrm{e}^2}\mu_1(1 - \cos\theta_\mathrm{e}) \end{pmatrix}, \tag{2.350}$$

where

$$\mu_1 = \frac{1}{m_1}, \quad \mu_2 = \frac{1}{m_2}, \quad \mu_3 = \frac{1}{m_3}. \tag{2.351}$$

Since we are dealing with a symmetric triatomic molecule SO_2, $\mu_2 = \mu_3$. Also, from the symmetry of the molecule, the $\boldsymbol{F}$ matrix becomes

$$\boldsymbol{F} = \begin{pmatrix} f_{11} & f_{12} & f_{13} \\ f_{12} & f_{11} & f_{13} \\ f_{13} & f_{13} & f_{33} \end{pmatrix}, \tag{2.352}$$

where

$$\begin{cases} f_{11} = f(\Delta r_{12}, \Delta r_{12}) = f(\Delta r_{13}, \Delta r_{13}), \\ f_{12} = f(\Delta r_{12}, \Delta r_{13}) = f(\Delta r_{13}, \Delta r_{12}), \\ f_{13} = f(\Delta r_{12}, \Delta\theta) = f(\Delta\theta, \Delta r_{12}) \\ \qquad = f(\Delta r_{13}, \Delta\theta) = f(\Delta\theta, \Delta r_{13}), \\ f_{33} = f(\Delta\theta, \Delta\theta). \end{cases} \tag{2.353}$$

Adopting the force constants $f_{11} = 10.01 \times 10^2$ N/m, $f_{12} = 2.40 \times 10^0$ N/m, $\frac{f_{13}}{r_\mathrm{e}} = 1.89 \times 10^1$ N/m, and $\frac{f_{33}}{r_\mathrm{e}^2} = 7.93 \times 10^1$ N/m, and the geometrical parameters $\theta_\mathrm{e} =$

119.3° and $r_e = 1.431$ Å, we can calculate the $\boldsymbol{G}$ matrix in Eq. (2.350) and, in turn, the matrix product of $\boldsymbol{GF}$. By solving Eq. (2.333) using the $\boldsymbol{GF}$ matrix, we obtain the following three eigenvalues:

$$\omega_1^2 = 4.707 \times 10^{28}\ \mathrm{s}^{-2},$$
$$\omega_2^2 = 9.482 \times 10^{27}\ \mathrm{s}^{-2},$$
$$\omega_3^2 = 6.551 \times 10^{28}\ \mathrm{s}^{-2}.$$

Consequently, the eigen frequencies are derived as

$$\tilde{\nu}_1 = \frac{\omega_1}{2\pi c} = 1152\ \mathrm{cm}^{-1} \quad \text{(symmetric stretch)},$$
$$\tilde{\nu}_2 = \frac{\omega_2}{2\pi c} = 517\ \mathrm{cm}^{-1} \quad \text{(bending)},$$
$$\tilde{\nu}_3 = \frac{\omega_3}{2\pi c} = 1359\ \mathrm{cm}^{-1} \quad \text{(anti-symmetric stretch)}.$$

These values closely reproduce the observed vibrational frequencies of the normal modes, which has been introduced in Sect. 2.5.5. Here, we have derived the normal mode frequencies assuming that the elements of matrix $\boldsymbol{F}$ are given, but in the practical application of the GF matrix method to other molecules, we need to derive matrix $\boldsymbol{F}$ so as to reproduce the observed frequencies.

The eigenvectors associated with the derived eigen frequencies $\tilde{\nu}_1$, $\tilde{\nu}_2$, and $\tilde{\nu}_3$ are determined respectively, as

$$\begin{pmatrix} 0.6632 \\ 0.6632 \\ -0.3468 \end{pmatrix}, \quad \begin{pmatrix} 0.0156 \\ 0.0156 \\ 0.9998 \end{pmatrix}, \quad \begin{pmatrix} 0.7071 \\ -0.7071 \\ 0.0000 \end{pmatrix}.$$

This set of eigenvectors demonstrates that the normal coordinates $\{Q_i\}$ which give $\{\tilde{\nu}_i\}$ are represented by the internal coordinate system as

$$\begin{cases} Q_1 = (0.7478)\Delta r_{12} + (0.7478)\Delta r_{13} + (-0.0233)\Delta\theta, \\ Q_2 = (0.2594)\Delta r_{12} + (0.2594)\Delta r_{13} + (0.9922)\Delta\theta, \\ Q_3 = (0.7071)\Delta r_{12} + (-0.7071)\Delta r_{13}. \end{cases} \tag{2.354}$$

These eigenvectors show us that the normal mode vibration for $\tilde{\nu}_1$ is the symmetric stretch (the ν_1 mode), the one for $\tilde{\nu}_2$ is the bending (the ν_2 mode), and the one for $\tilde{\nu}_3$ is the anti-symmetric stretch (the ν_3 mode).

These normal coordinates can be related to the mass-weighted orthogonal coordinates by using the equation

$$\boldsymbol{s} = \boldsymbol{B}\boldsymbol{\eta}. \tag{2.355}$$

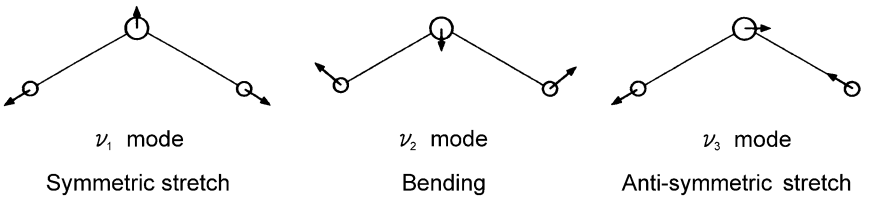

Fig. 2.27 The normal vibrational modes of SO_2

Specifically, by substituting Δr_{12}, Δr_{13}, and $\Delta\theta$ given respectively in Eqs. (2.340), (2.341), and (2.348) into Eq. (2.354), we can represent the displacements of the respective atoms along the x and y directions. We can follow the calculation as

$$\begin{cases} Q_1 = (0.78)\Delta y_1 + (-0.64)\Delta x_2 + (-0.39)\Delta y_2 + (0.64)\Delta x_3 + (-0.39)\Delta y_3, \\ Q_2 = (0.93)\Delta y_1 + (0.57)\Delta x_2 + (-0.47)\Delta y_2 + (-0.57)\Delta x_3 + (-0.47)\Delta y_3, \\ Q_3 = (1.22)\Delta x_1 + (-0.61)\Delta x_2 + (-0.36)\Delta y_2 + (-0.61)\Delta x_3 + (0.36)\Delta y_3. \end{cases} \tag{2.356}$$

How each atom is displaced in each vibration mode can be deduced by applying one of the Eckart conditions (cf. Sect. 2.5.6), that is,

$$\begin{aligned} & m_1\Delta x_1 + m_2\Delta x_2 + m_3\Delta x_3 = 0, \\ & m_1\Delta y_1 + m_2\Delta y_2 + m_3\Delta y_3 = 0, \\ & -m_1 y_{1,\mathrm{e}}\Delta x_1 + m_1 x_{1,\mathrm{e}}\Delta y_1 - m_2 y_{2,\mathrm{e}}\Delta x_2 + m_2 x_{2,\mathrm{e}}\Delta y_2 - m_3 y_{3,\mathrm{e}}\Delta x_3 \\ & \quad + m_3 x_{3,\mathrm{e}}\Delta y_3 = 0, \end{aligned}$$

to Eq. (2.356) and obtaining its inverse transformation, where the orthogonal coordinates $\{\xi_i\}$ is described using $\{Q_j\}$. The result can be illustrated as in Fig. 2.27.

Now, we can see from the normal coordinates given by Eq. (2.354) that Δr_{12} and Δr_{13} appear symmetrically. Taking this molecular symmetry into consideration, we can express the internal coordinates as

$$\Delta r_s = \frac{1}{\sqrt{2}}(\Delta r_{12} + \Delta r_{13}), \tag{2.357a}$$

$$\Delta r_a = \frac{1}{\sqrt{2}}(\Delta r_{12} - \Delta r_{13}), \tag{2.357b}$$

where the subscripts "s" and "a" stand for "symmetric" and "anti-symmetric", respectively.

Let us then describe the normal modes using the three displacement coordinates, Δr_s, Δr_a, and $\Delta\theta$. Equations (2.357a) and (2.357b) correspond to the internal coordinates being transformed as

$$\begin{pmatrix} \Delta r_s \\ \Delta\theta \\ \Delta r_a \end{pmatrix} = \begin{pmatrix} \frac{1}{\sqrt{2}} & \frac{1}{\sqrt{2}} & 0 \\ 0 & 0 & 1 \\ \frac{1}{\sqrt{2}} & -\frac{1}{\sqrt{2}} & 0 \end{pmatrix} \begin{pmatrix} \Delta r_{12} \\ \Delta r_{13} \\ \Delta\theta \end{pmatrix}. \tag{2.358}$$

Thus, letting

$$\boldsymbol{r} = \begin{pmatrix} \Delta r_s \\ \Delta\theta \\ \Delta r_a \end{pmatrix} \tag{2.359}$$

and

$$\boldsymbol{U} = \begin{pmatrix} \frac{1}{\sqrt{2}} & \frac{1}{\sqrt{2}} & 0 \\ 0 & 0 & 1 \\ \frac{1}{\sqrt{2}} & -\frac{1}{\sqrt{2}} & 0 \end{pmatrix}, \tag{2.360}$$

the transformation can be written as

$$\boldsymbol{r} = \boldsymbol{U}\boldsymbol{s}. \tag{2.361}$$

Also,

$$\boldsymbol{s} = \boldsymbol{U}^{-1}\boldsymbol{r}. \tag{2.362}$$

When we transform the eigenvector $\boldsymbol{s}^\circ$ derived from Eq. (2.333), or equivalently derived from

$$\boldsymbol{G}\boldsymbol{F}\boldsymbol{s}^\circ = \omega^2\boldsymbol{s}^\circ,$$

as

$$\boldsymbol{s}^\circ = \boldsymbol{U}^{-1}\boldsymbol{r}^\circ, \tag{2.363}$$

we obtain

$$\boldsymbol{G}\boldsymbol{F}\boldsymbol{U}^{-1}\boldsymbol{r}^\circ = \omega^2\boldsymbol{U}^{-1}\boldsymbol{r}^\circ,$$

and, consequently,

$$\boldsymbol{U}\boldsymbol{G}\boldsymbol{F}\boldsymbol{U}^{-1}\boldsymbol{r}^\circ = \omega^2\boldsymbol{r}^\circ. \tag{2.364}$$

Since $\boldsymbol{U}^{-1}\boldsymbol{U} = \boldsymbol{E}$, we can derive

$$\boldsymbol{U}\boldsymbol{G}\boldsymbol{U}^{-1}\boldsymbol{U}\boldsymbol{F}\boldsymbol{U}^{-1}\boldsymbol{r}^\circ = \omega^2\boldsymbol{r}^\circ. \tag{2.365}$$

This means that the normal modes can be obtained by transforming $\boldsymbol{G}$ and $\boldsymbol{F}$, respectively, into

$$\boldsymbol{G}' = \boldsymbol{U}\boldsymbol{G}\boldsymbol{U}^{-1}, \tag{2.366}$$

$$\boldsymbol{F}' = \boldsymbol{U}\boldsymbol{F}\boldsymbol{U}^{-1}, \tag{2.367}$$

and by solving

$$\boldsymbol{G}'\boldsymbol{F}'\boldsymbol{r}^\circ = \omega^2\boldsymbol{r}^\circ, \tag{2.368}$$

or in other words by diagonalizing the matrix product of $\boldsymbol{G}'\boldsymbol{F}'$.

Equations (2.366) and (2.367) allow us to derive $\boldsymbol{G}'$ and $\boldsymbol{F}'$ from the $\boldsymbol{G}$ in Eq. (2.350) and the $\boldsymbol{F}$ in Eq. (2.352), respectively, as

$$\boldsymbol{G}' = \boldsymbol{U}\boldsymbol{G}\boldsymbol{U}^{-1} = \begin{pmatrix} \mu_1(1+\cos\theta_\mathrm{e}) + \mu_2 & -\frac{\sqrt{2}}{r_\mathrm{e}}\mu_1 \sin\theta_\mathrm{e} & 0 \\ -\frac{\sqrt{2}}{r_\mathrm{e}}\mu_1 \sin\theta_\mathrm{e} & \frac{2}{r_\mathrm{e}^2}\mu_2 + \frac{2}{r_\mathrm{e}^2}\mu_1(1-\cos\theta_\mathrm{e}) & 0 \\ 0 & 0 & \mu_1(1-\cos\theta_\mathrm{e}) + \mu_2 \end{pmatrix}, \tag{2.369}$$

$$\boldsymbol{F}' = \boldsymbol{U}\boldsymbol{F}\boldsymbol{U}^{-1} = \begin{pmatrix} f_{11}+f_{12} & \sqrt{2}f_{13} & 0 \\ \sqrt{2}f_{13} & f_{33} & 0 \\ 0 & 0 & f_{11}-f_{12} \end{pmatrix}. \tag{2.370}$$

Looking at these matrices we notice that both $\boldsymbol{G}'$ and $\boldsymbol{F}'$ can be block-diagonalized into a 2×2 submatrix and a 1×1 submatrix. This means that $\boldsymbol{G}'\boldsymbol{F}'$ can also be block-diagonalized. The 1×1 submatrix can be seen as being diagonalized from the beginning, which allows us to immediately calculate $\tilde{\nu}_3 = 1359\ \mathrm{cm}^{-1}$ as an eigenfrequency.

The corresponding eigenvector is

$$\begin{pmatrix} 0 \\ 0 \\ 1.000 \end{pmatrix},$$

indicating that Eq. (2.357b) represents one of the normal modes. From the 2×2 submatrix, we obtain $\tilde{\nu}_1 = 1152\ \mathrm{cm}^{-1}$ and $\tilde{\nu}_2 = 517\ \mathrm{cm}^{-1}$, and the corresponding eigenvectors are represented respectively, as

$$\begin{pmatrix} 0.9379 \\ -0.3468 \\ 0.0000 \end{pmatrix}, \quad \begin{pmatrix} 0.0220 \\ 0.9998 \\ 0.0000 \end{pmatrix}.$$

This shows that these two normal modes can be approximated by Δr_s and $\Delta\theta$.

Problem 2.31

Derive the normal modes and normal coordinates of a water molecule (H_2O), using the structural parameters $r_\mathrm{e} = r_\mathrm{e}(\mathrm{O\text{–}H}) = 0.9575$ Å and $\theta_\mathrm{e} = \angle\mathrm{H\text{–}O\text{–}H} = 104.51°$, and the force constants

$$f_{11} = 7.68 \times 10^2\ \mathrm{N/m}, \qquad f_{12} = -8.2 \times 10^0\ \mathrm{N/m},$$
$$\frac{f_{13}}{r_\mathrm{e}} = 1.69 \times 10^1\ \mathrm{N/m}, \qquad \frac{f_{33}}{r_\mathrm{e}^2} = 7.07 \times 10^1\ \mathrm{N/m}.$$

Solution

As H_2O is a bent symmetric triatomic molecule like SO_2, we can apply the discussions above without modification. By calculating the $\boldsymbol{G}\boldsymbol{F}$ matrix and diagonalizing it, we can derive the three eigenvalues as

$$\omega_1^2 = 4.738 \times 10^{29}\ \mathrm{s}^{-2}, \quad \omega_2^2 = 9.014 \times 10^{28}\ \mathrm{s}^{-2}, \quad \omega_3^2 = 5.002 \times 10^{29}\ \mathrm{s}^{-2}.$$

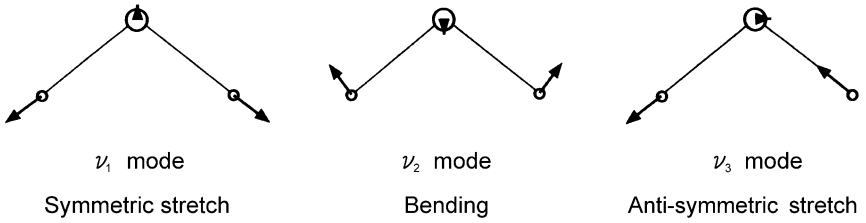

Fig. 2.28 The normal vibrational modes of H_2O

Then the eigenfrequencies can be obtained as

$$\tilde{\nu}_1 = 3655\ \text{cm}^{-1}, \quad \tilde{\nu}_2 = 1594\ \text{cm}^{-1}, \quad \tilde{\nu}_3 = 3755\ \text{cm}^{-1}.$$

These values agree well with the observed frequencies, $\tilde{\nu}_1 = 3652\ \text{cm}^{-1}$, $\tilde{\nu}_2 = 1592\ \text{cm}^{-1}$ and $\tilde{\nu}_3 = 3756\ \text{cm}^{-1}$. The eigenvectors corresponding to these frequencies are

$$\begin{pmatrix} 0.7069 \\ 0.7069 \\ -0.0227 \end{pmatrix}, \quad \begin{pmatrix} -0.0199 \\ -0.0199 \\ 0.9996 \end{pmatrix}, \quad \begin{pmatrix} 0.7071 \\ -0.7071 \\ 0.0000 \end{pmatrix},$$

respectively.

From Eq. (2.355), the normal coordinates Q_1, Q_2, and Q_3 can be represented using the displacement coordinates of atoms as

$$\begin{cases} Q_1 = (-0.82)\Delta y_1 + (0.58)\Delta x_2 + (0.41)\Delta y_2 + (-0.58)\Delta x_3 + (0.41)\Delta y_3, \\ Q_2 = (-1.63)\Delta y_1 + (-0.65)\Delta x_2 + (0.82)\Delta y_2 + (0.65)\Delta x_3 + (0.82)\Delta y_3, \\ Q_3 = (1.12)\Delta x_1 + (-0.56)\Delta x_2 + (-0.43)\Delta y_2 + (-0.56)\Delta x_3 + (0.43)\Delta y_3. \end{cases} \tag{2.371}$$

We can then apply the Eckart condition as in the case of SO_2 to derive the equations that describe these orthogonal coordinates using the normal coordinates, so that we see the displacements of each atom in the three different vibration modes as shown in Fig. 2.28. As the mass of a hydrogen atom is small, the displacements of the two hydrogen atoms become larger than that of the oxygen atom in the center. This is in marked contrast to the vibration of the SO_2 molecule illustrated in Fig. 2.27. □

2.5.9 Anharmonic Expansion of Potentials by Dimensionless Coordinates

In treating the vibration of a bent (non-linear) polyatomic molecule composed of n atoms in quantum mechanics, we can see from Eqs. (2.264) and (2.270) that its

vibrational Hamiltonian can be represented as the sum of the Hamiltonians of $3n-6$ harmonic oscillators that are independent from each other, as

$$H = \sum_{i=1}^{3n-6} H_i = \sum_{i=1}^{3n-6} \left(-\frac{\hbar^2}{2} \frac{\partial^2}{\partial Q_i^2} + \frac{1}{2} \omega_i^2 Q_i^2 \right). \tag{2.372}$$

However, as we have already learned in Sect. 2.5.5 through the example of SO_2, the vibrational potential along the Q_i coordinate is not harmonic in an exact sense, and neither are the $3n-6$ oscillators completely independent from each other.

These deviations from the harmonic potentials can be expressed by adding third-order terms such as $\alpha_{ijk} Q_i Q_j Q_k$ and higher-order terms. When introducing such high-order terms in the expansion of a vibrational potential, it is useful to make the coordinates dimensionless and let the expansion coefficients carry the dimension of energy. Since the vibrational energy is most often measured in terms of wave numbers (cm^{-1}) in experiments, we will represent the expansion coefficients in terms of wave numbers.

By dividing both sides of H_i in Eq. (2.372) by hc as

$$\frac{H_i}{hc} = -\frac{\hbar^2}{2hc} \frac{\partial^2}{\partial Q_i^2} + \frac{1}{2} \frac{\omega_i^2}{hc} Q_i^2, \tag{2.373}$$

which is represented in terms of wave numbers, and by introducing a dimensionless coordinate q_i, given as

$$q_i = \sqrt{\frac{hc\tilde{\nu}_i}{\hbar^2}}\, Q_i, \tag{2.374}$$

Eq. (2.373) becomes

$$\frac{H_i}{hc} = \frac{1}{2} \tilde{\nu}_i \left(-\frac{\partial^2}{\partial q_i^2} + q_i^2 \right), \tag{2.375}$$

where

$$\omega_i = 2\pi c \tilde{\nu}_i. \tag{2.376}$$

Therefore, the Hamiltonian given by Eq. (2.372) is expressed in terms of wave numbers as

$$\frac{H}{hc} = -\frac{1}{2} \sum_{i=1}^{3n-6} \tilde{\nu}_i \frac{\partial^2}{\partial q_i^2} + \frac{1}{2} \sum_{i=1}^{3n-6} \tilde{\nu}_i q_i^2, \tag{2.377}$$

in which the second summation represents the harmonic potential terms. When we expand the potential $V(\boldsymbol{q})$ by adding the anharmonic part to the harmonic part, as

$$\frac{V(\boldsymbol{q})}{hc} = \frac{1}{2} \sum_{i=1}^{3n-6} \tilde{\nu}_i q_i^2 + \sum \sum \sum_{i \leqq j \leqq k} k_{ijk} q_i q_j q_k + \sum \sum \sum \sum_{i \leqq j \leqq k \leqq l} k_{ijkl} q_i q_j q_k q_l + \cdots, \tag{2.378}$$

the Hamiltonian including the potential anharmonicities becomes

$$\frac{H}{hc} = \frac{1}{2}\sum_{i=1}^{3n-6}\tilde{\nu}_i\left(-\frac{\partial^2}{\partial q_i^2} + q_i^2\right) + \sum\sum_{i\leqq j\leqq k}\sum k_{ijk}q_i q_j q_k + \sum\sum_{i\leqq j\leqq k\leqq l}\sum\sum k_{ijkl}q_i q_j q_k q_l + \cdots. \tag{2.379}$$

The coefficients k_{ijk} and k_{ijkl} in Eq. (2.378) are called, respectively, the third-order and fourth-order anharmonic constants of the potential.

When the energies of vibrational levels are obtained from an observed spectrum, we can derive potential parameters in the Hamiltonian such as $\tilde{\nu}_i$, k_{ijk}, and k_{ijkl}. We will not go into details regarding the practical procedure to derive these parameters, as they are beyond the scope of this book, but a rough summary of it can be given as follows: First, the matrix elements for H/hc are evaluated using the wave functions represented as a product of harmonic oscillators, and the matrix is diagonalized. By comparing the eigenvalues thus derived from the calculations with the corresponding energies obtained in observations, the values of $\tilde{\nu}_i$, k_{ijk}, and k_{ijkl} are adjusted iteratively to improve the agreement between the observed and calculated energies. This procedure for parameter optimization is called the least-squares fit. We can draw a multi-dimensional potential energy surface using the resultant parameters. We can also draw multidimensional vibrational wave functions using the eigenvectors obtained simultaneously with the eigenenergies.

The vibrational wave functions for SO_2 derived by this procedure are shown in Fig. 2.29 as two-dimensional maps. This figure shows us how increases in the vibrational quantum numbers affect the wave function. The vertical and horizontal axes in each map represent the two S–O interatomic distances as dimensionless coordinates, which means that the diagonal line of 45° represents a normal coordinate for the symmetric stretch (ν_1) mode, and the line perpendicular to it represents a normal coordinate for the anti-symmetric stretch (ν_3) mode. We can see that, as a quantum number increases, the number of nodal lines perpendicularly crossing the corresponding normal coordinate increases. In order to derive the wave functions like those shown here, we need to know the shape of the multi-dimensional potential surface. That is to say that we need to determine potential parameters such as $\tilde{\nu}_i$, k_{ijk}, and k_{ijkl}.

When vibrational transitions are measured as infrared absorption, only a limited number of transitions can be observed because of the existence of the selection rules. In the case of SO_2, for example, only three transitions are allowed from the vibrational ground state $(v_1, v_2, v_3) = (0, 0, 0)$, namely the transitions to the three vibrational levels $(1, 0, 0)$, $(0, 1, 0)$, and $(0, 0, 1)$. The transition energies to these three levels can only allow us to determine three potential parameters at most, $\tilde{\nu}_1$, $\tilde{\nu}_2$, and $\tilde{\nu}_3$. In order to determine the third-order and fourth-order anharmonic constants, we need to know the energies of other vibrational levels distributed over a wide energy range. As one of the experimental methods to determine the third-order and the higher-order anharmonic constants, we need to know the energies of the other

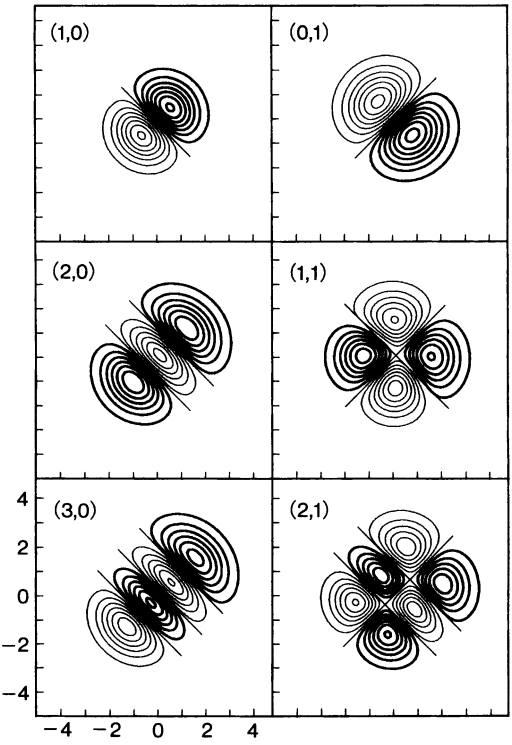

Fig. 2.29 Two-dimensional displays of the vibrational wave functions of SO_2. The vibrational levels are denoted using the quantum number of the symmetric stretch mode ν_1 and that of the anti-symmetric stretch mode ν_3 as (ν_1, ν_3). The abscissa represents the internuclear distance of one of the two S–O bonds, and the ordinate that of the other S–O bond, as dimensionless coordinates

vibrational levels distributed in a wide energy range. Here, we will take a look at one of the experimental methods for determining the third-order and higher-order anharmonic constants, which is called dispersed fluorescence spectroscopy.

In this method, molecules are irradiated with laser light (wave number $\tilde{\nu}_{\mathrm{ex}}$) in the visible or ultraviolet wavelength range, and excite them from the vibrational ground state in the electronic ground state to a particular vibrational level in the electronically excited state. After the excitation, molecules emit fluorescence and deexcite themselves to populate the vibrational ground and excited states in the electronic ground state. By measuring the wavelength distribution of the emitted fluorescence, we can determine the vibrational levels to which the molecules are populated. When molecules emit fluorescence with wavelength λ_{fl} (wave number $\tilde{\nu}_{\mathrm{fl}} = 1/\lambda_{\mathrm{fl}}$) and deexcite themselves to the level (v_1, v_2, v_3) whose vibrational energy represented in terms of wave numbers is $\tilde{\varepsilon}(v_1, v_2, v_3)$, the relation

$$\tilde{\nu}_{\mathrm{ex}} = \tilde{\nu}_{\mathrm{fl}} + \tilde{\varepsilon}(v_1, v_2, v_3) \tag{2.380}$$

is seen to exist, as schematically shown in Fig. 2.30. Therefore, by dispersing the emitted fluorescence using a monochromator equipped with a grating, we can obtain a spectrum whose abscissa corresponds to wavelengths or wave numbers. Spectra thus obtained are called dispersed fluorescence spectra. This method allows us, in principle, to measure a large number of vibrational transitions without being restricted by the selection rules in the absorption of infrared light.

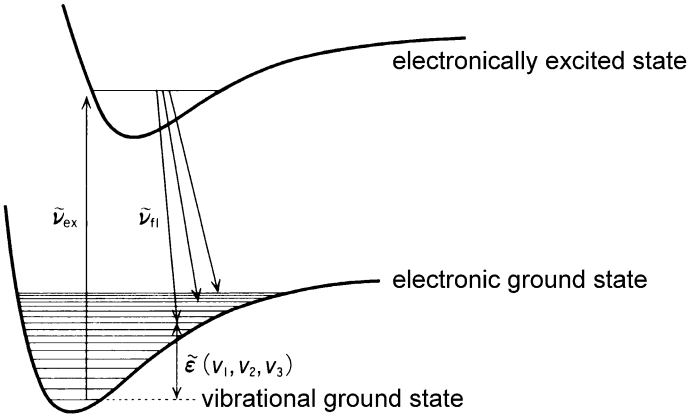

Fig. 2.30 A schematic diagram of the observation of vibrationally excited levels in dispersed fluorescence spectroscopy

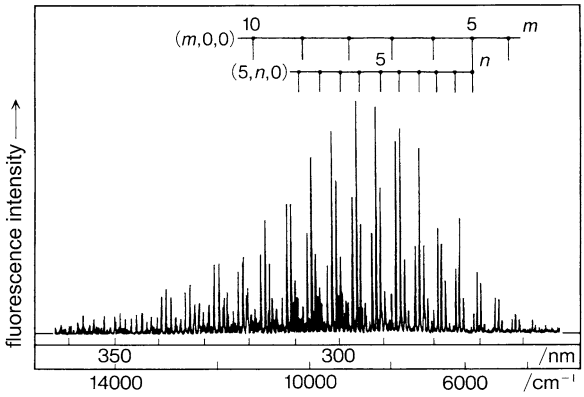

Fig. 2.31 An example of the dispersed fluorescence spectrum for SO_2 obtained by dispersing the fluorescence emitted from the vibrational ground state in the electronically excited state (the $\tilde{C}$ state). The wavelength measured by the abscissa represents the wavelength of the emitted fluorescence, and the wave number measured by the abscissa represents the vibrational term values, that is, the vibrational energy measured from the vibrational ground state in the electronic ground state

As a typical example, a dispersed fluorescence spectrum for SO_2 is shown in Fig. 2.31. This spectrum was observed when SO_2 was excited to the vibrational ground state (42573 cm^{-1}) in an electronically excited state called the $\tilde{C}$ state. The electronic ground state of polyatomic molecules is called the $\tilde{X}$ state, and the electronic states optically allowed from the $\tilde{X}$ state are usually referred to as the $\tilde{A}$ state, the $\tilde{B}$ state, the $\tilde{C}$ state, and so on, starting from the one with the lowest energy. The ordinate of Fig. 2.31 represents the intensity of the emitted fluorescence. Each of the individual fine peaks in this figure illustrates the fluorescence emitted with each transition to a vibrational level in the electronic ground state. By substituting

the observed wavelengths of the fluorescence peaks into Eq. (2.380), the energies of the vibrational levels can be obtained.

The anharmonic constants of a potential can be determined from this type of experimental data, and then, the wave functions of each of the vibrational levels can be obtained. The vibrational wave functions for SO_2 shown in Fig. 2.29 are those derived from the observed dispersed fluorescence spectra.

Chapter 3
Rotating Molecules

In Chap. 2, we have learned that molecules vibrate around their equilibrium geometrical structures. In the three-dimensional space, molecules not only vibrate but also rotate. This rotational motion is, in fact, also quantized. That is, the rotational energy of a freely rotating molecule in the gas phase takes only discrete values. This is greatly different from the rotational motion of a solid body in classical mechanics. An important aspect of the rotational motion is that it allows us to determine the geometrical structure of molecules. Knowing the energy difference between the discrete energy levels directly leads to the determination of the geometrical structure of a molecule. In this chapter, we will express the rotational energy of a molecule in classical mechanics and learn a procedure for treating it in quantum mechanics. In the course of learning this procedure, we will deepen our understanding of the quantum theory of angular momentum. We will further discuss the method for determining the geometrical structures of molecules based on data obtained from a rotational spectrum through a number of examples.

Summaries

3.1 Molecular Rotation and Molecular Structure

First, we will learn that we can describe quantized rotational energies using a constant, called a "rotational constant," in the case of diatomic molecules. Second, we will learn that a rotational constant gives us information about molecular structure, namely the internuclear distance. Finally, we will look at the example of linear triatomic molecules to learn how to determine molecular structures by the isotope substitution method.

3.2 The Angular Momentum of Molecular Rotation

We will study the quantum theory of angular momentum. We will seek to understand the commutation relation of angular momentum operators, as well as raising and lowering operators, and obtain the eigenvalues and eigenfunctions of angular momentum operators.

3.3 Molecular Rotation from the Point of View of Classical Mechanics

By treating a molecule as a rigid rotor and describing its rotational energy on the basis of classical mechanics, we will learn that they can be described by angular

K. Yamanouchi, *Quantum Mechanics of Molecular Structures*,
DOI 10.1007/978-3-642-32381-2_3,

velocity vectors and moment of inertia tensors. We will also discuss a classification of molecules based on the relative magnitudes of the three principal moments of inertia.

3.4 Molecular Rotation from the Point of View of Quantum Mechanics
We will quantize the molecular rotational energy described by classical mechanics. Then, we will learn the difference between angular momentum operators in the molecule-fixed coordinate system and those in the space-fixed coordinate system. Furthermore, we will deepen our understanding of the energy levels of symmetric top molecules and asymmetric top molecules.

3.5 Determination of Molecular Structures Based on Rotational Spectra
We will analyze the rotational spectra for symmetric top molecules and asymmetric top molecules to derive their rotational constants, and through these examples we will learn that molecular structure can be determined from rotational constants. In addition, a method of determining equilibrium structures will be introduced.

3.6 Rotating and Vibrating Molecules
Since there are rotational levels for each vibrational level, rotational structures are observed in the vibrational and electronic spectra. We will learn that we can determine rotational constants for vibrationally excited states and electronically excited states by analyzing the rotational structure.

3.1 Molecular Rotation and Molecular Structure

3.1.1 Microwave Spectroscopy

As we have seen in the previous chapter, molecular vibrational energy is quantized and takes discrete values. In many cases, vibrational motions are excited by irradiation of infrared (IR) light, and transition occurs from a low vibrational level to a high vibrational level. Therefore, from observing an absorption spectrum in the IR region we can not only tell which vibrational modes are excited but also identify the molecular species, as each molecular vibrational mode has its own vibrational frequency.

Another type of molecular motion besides vibration is "rotation." A molecule in the gas phase both vibrates and rotates, and the rotational energy is also discrete. Therefore, we can understand that the absorption of light causes a transition between rotational levels with different energies.

As has been introduced in Chap. 1, the spectra of electric waves reaching the Earth from outer space are characterized by sharp peaks appearing at constant intervals. The electric waves observed are emitted from "interstellar molecules" when transitions occur from their rotationally excited levels to their lower rotational energy levels. Such spectra are observed in a broad range of frequency spanning from 10 GHz to 50 GHz.

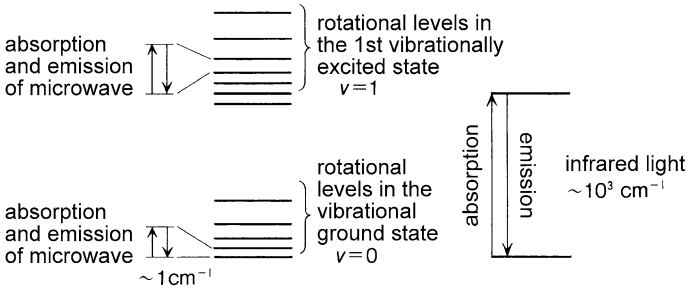

Fig. 3.1 Vibrational and rotational levels of a molecule and their transitions in IR and microwave regions

Choosing a typical frequency of light,

$$\nu = \frac{c}{\lambda} = 30\ \text{GHz} = 3 \times 10^{10}\ \text{Hz},$$

we can express the energy of the light in terms of wave numbers (cm^{-1}) as

$$\tilde{\nu} = \frac{1}{\lambda} = \frac{\nu}{c} \cong 1.0\ \text{cm}^{-1},$$

which gives us the wavelength λ as 1.0 cm. Electromagnetic waves whose wavelengths are around 1 cm are in the domain of electric waves and are called "microwaves." We can see that interstellar molecules emit electromagnetic waves in the microwave region as they are deexcited in the rotational motion.

In many cases, when molecular rotational transition occurs, the wavelength of the light that is absorbed or emitted falls in the microwave region. The research field concerned with observations of the absorption and emission of microwaves and the study of molecular rotation based on their spectra is called "microwave spectroscopy" or "rotational spectroscopy."

Since energy intervals between molecular vibrational levels is roughly about 1000 cm^{-1}, we can see that the intervals of rotational levels are only 10^{-3} to 10^{-2} times as large as those of vibrational levels. This is illustrated in Fig. 3.1.

3.1.2 The Quantum Theory of Molecular Rotation (Diatomic Molecules)

We will now learn that we can determine the structure of a diatomic molecule based on microwave spectroscopy. As shown by Eq. (2.1) in Chap. 2, the motion of a diatomic molecule AB in the three-dimensional space can be separated into the motion of the center of mass and the relative motion. The relative motion, as the equation shows, can be reconceptualized as the motion of a mass point whose position is specified by the position vector $\boldsymbol{r} = \boldsymbol{r}_B - \boldsymbol{r}_A$ and whose reduced mass is

$\mu = \frac{m_A m_B}{m_A + m_B}$, as illustrated in Fig. 3.2. This motion is described by the following Schrödinger equation:

$$-\frac{\hbar^2}{2\mu}\left(\frac{\partial^2}{\partial x^2} + \frac{\partial^2}{\partial y^2} + \frac{\partial^2}{\partial z^2}\right)\psi + V\psi = E\psi. \tag{3.1}$$

In the case of a diatomic molecule which rotates freely in space, $V(x, y, z) = 0$. If we use the Laplacian,

$$\nabla^2 = \frac{\partial^2}{\partial x^2} + \frac{\partial^2}{\partial y^2} + \frac{\partial^2}{\partial z^2}, \tag{3.2}$$

the Schrödinger equation for the freely rotating diatomic molecule can be given by

$$-\frac{\hbar^2}{2\mu}\nabla^2\psi(x, y, z) = E\psi(x, y, z). \tag{3.3}$$

As shown in Fig. 3.2, it is more natural to use the polar coordinate system (r, θ, ϕ) than the x-y-z coordinate system, as the mass point moves on a sphere. Here, r is called a radius, θ a polar angle, and ϕ an azimuthal angle or azimuth angle. The polar angle, θ, may also be called the zenith angle, the meridian angle or the colatitude. From Fig. 3.2, we can write

$$\begin{cases} x = r\sin\theta\cos\phi, \\ y = r\sin\theta\sin\phi, \\ z = r\cos\theta. \end{cases} \tag{3.4}$$

Let us now see the diatomic molecule as a rigid rotor, assuming that molecules do not vibrate, which means that the length of the vector $\boldsymbol{r}$, or the internuclear distance $r = |\boldsymbol{r}|$, is constant. Then, the mass point depicted in Fig. 3.2 will move on a sphere with the radius of r. Let us then consider how we can express ∇^2 in the polar coordinate system. By taking into account the fact that r is fixed and is not a variable, $\frac{\partial}{\partial x}$, $\frac{\partial}{\partial y}$, and $\frac{\partial}{\partial z}$ can be written as follows:

$$\begin{cases} \dfrac{\partial}{\partial x} = \left(\dfrac{\partial\theta}{\partial x}\right)\dfrac{\partial}{\partial\theta} + \left(\dfrac{\partial\phi}{\partial x}\right)\dfrac{\partial}{\partial\phi}, \\ \dfrac{\partial}{\partial y} = \left(\dfrac{\partial\theta}{\partial y}\right)\dfrac{\partial}{\partial\theta} + \left(\dfrac{\partial\phi}{\partial y}\right)\dfrac{\partial}{\partial\phi}, \\ \dfrac{\partial}{\partial z} = \left(\dfrac{\partial\theta}{\partial z}\right)\dfrac{\partial}{\partial\theta} + \left(\dfrac{\partial\phi}{\partial z}\right)\dfrac{\partial}{\partial\phi}. \end{cases} \tag{3.5}$$

As we can derive

$$\tan^2\theta = \frac{x^2 + y^2}{z^2} \tag{3.6}$$

and

$$\tan\phi = \frac{y}{x} \tag{3.7}$$

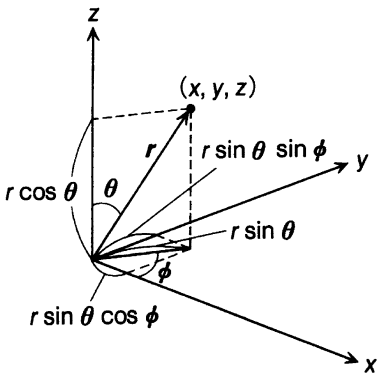

Fig. 3.2 Motion of a particle described in the three-dimensional polar coordinate system

from Eq. (3.4), we can obtain $\frac{\partial\theta}{\partial x}$, $\frac{\partial\theta}{\partial y}$, and $\frac{\partial\theta}{\partial z}$ by differentiating both sides of Eq. (3.6) with respect to x, y, and z, respectively, and similarly obtain $\frac{\partial\phi}{\partial x}$, $\frac{\partial\phi}{\partial y}$, and $\frac{\partial\phi}{\partial z}$ by differentiating both sides of Eq. (3.7) with respect to x, y, and z, respectively. Substituting these values into Eq. (3.5) and adding up the calculated results for $\frac{\partial^2}{\partial x^2}$, $\frac{\partial^2}{\partial y^2}$, and $\frac{\partial^2}{\partial z^2}$, we obtain

$$\nabla^2 = \frac{\Lambda}{r^2}, \tag{3.8}$$

where

$$\Lambda = \frac{1}{\sin\theta}\frac{\partial}{\partial\theta}\left(\sin\theta\frac{\partial}{\partial\theta}\right) + \frac{1}{\sin^2\theta}\frac{\partial^2}{\partial\phi^2}. \tag{3.9}$$

Thus, the Schrödinger equation (3.3) can be written in polar coordinates as

$$-\frac{\hbar^2}{2\mu}\frac{1}{r^2}\Lambda\psi = E\psi. \tag{3.10}$$

As shown later, it turns out that the Schrödinger equation

$$-\hbar^2\Lambda\psi = \varepsilon\psi \tag{3.11}$$

has the eigenvalue

$$\varepsilon = J(J+1)\hbar^2 \quad (J = 0, 1, 2\ldots), \tag{3.12}$$

where J is the rotational quantum number. From Eqs. (3.10) and (3.11), we can derive

$$2\mu r^2 E = J(J+1)\hbar^2, \tag{3.13}$$

which tells us that eigenenergy E depends on the rotational quantum number J. We will therefore express it as E_J. Furthermore, by using the moment of inertia I of the diatomic molecule, which is given as $I = \mu r^2$, we can write

$$E_J = \frac{\hbar^2}{2I}J(J+1). \tag{3.14}$$

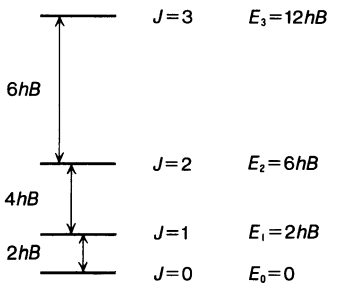

Fig. 3.3 Rotational energy levels of a diatomic molecule

When we represent this eigenenergy of rotation as

$$E_J = hBJ(J+1), \quad B = \frac{h}{8\pi^2 I}\ (\text{Hz}), \tag{3.15a}$$

B is called the rotational constant. In this instance, B is expressed in terms of s^{-1} or, in other words, Hz. We can also express B in terms of cm^{-1}, in which case,

$$E_J = hcBJ(J+1), \quad B = \frac{h}{8\pi^2 cI}\ (\text{cm}^{-1}). \tag{3.15b}$$

The Hz unit is used in microwave spectroscopy, but in infrared, visible, or ultraviolet spectroscopy, rotational constants are in most cases represented in units of cm^{-1}.

The rotational energy levels of the diatomic molecule, treated here as a rigid rotor, are plotted in Fig. 3.3. If transitions between rotational levels of the diatomic molecule are observed in the microwave region, we can determine the rotational constant of the molecule. For instance, if we observe a transition from the $J = 0$ level to the $J = 1$ level at ν_{obs} Hz, this signifies that

$$E_1 - E_0 = h\nu_{\text{obs}}.$$

Therefore, from Fig. 3.3, we can derive

$$2hB = h\nu_{\text{obs}},$$

which gives us $B = \nu_{\text{obs}}/2$. When B is determined, the moment of inertia can be obtained from Eq. (3.15a), so as long as the reduced mass μ is known, the internuclear distance r can be calculated. Thus, the internuclear distance of a diatomic molecule can be determined by observing its microwave absorption (or emission). This shows the advantage of the observation of rotational transitions in determining the geometrical structures of molecules.

To look at a concrete example, let us determine the geometrical structure of the carbon monoxide molecule $^{12}C^{16}O$. In the rotational spectrum of $^{12}C^{16}O$, the transition $J = 1 \leftarrow J = 0$ is observed at 115271.204 MHz. Hence, the rotational constant B is readily determined as $B = \nu_{\text{obs}}/2 = 57635.602$ MHz, and by using the values $m(^{12}C) = 12.0$ amu and $m(^{16}O) = 15.9949$ amu for the masses of ^{12}C and ^{16}O, respectively, the internuclear distance r is determined as $r = 1.13089 \times 10^{-10}$ m $=$ 1.13089 Å.

Furthermore, when B, the reduced mass μ, and the internuclear distance r are expressed in MHz (1 MHz $= 10^6$ Hz), atomic mass unit (amu), and Å, respectively, the following relationship holds, in correspondence with Eq. (3.15a):

$$\mu r^2 B = \frac{h}{8\pi^2} = 505379 \text{ amu Å MHz}. \tag{3.16}$$

Problem 3.1
Of the rotational transitions for $^{12}C^{16}O$, the transition $J = 7 \leftarrow J = 6$ is observed at 806651.719 MHz. Obtain the rotational constant and the internuclear distance r.

Solution
The energy difference between the two levels, $J = 7$ and $J = 6$, is written with the rotational constant as

$$E_7 - E_6 = 56hB - 42hB = 14hB.$$

Therefore,

$$B = \frac{806651.719}{14} = 57617.980 \text{ MHz}.$$

By using Eq. (3.16), we can derive $r = 1.1311$ Å. □

The rotational constant derived in the problem above is smaller than the one derived from the $J = 1 \leftarrow J = 0$ transition, if only slightly. This also causes the internuclear distance to be calculated as larger than in the case of $J = 1 \leftarrow J = 0$. Discussing the reason for this in detail is beyond the scope of this book, but in brief, it can be attributed to the phenomenon of centrifugal distortion, where the internuclear distance elongates with an increase in the rotational quantum number. It is known that the rotational energy E_J can be expanded as

$$E_J = hBJ(J+1) - hDJ^2(J+1)^2 + \cdots, \tag{3.17}$$

wherein the terms $-hDJ^2(J+1)^2$ and D are called the centrifugal distortion term and the centrifugal distortion constant, respectively.

It is known that, in expressing the rotational energy of the vibrational ground state of CO with the centrifugal distortion term incorporated, the following values allow us to reproduce the observed spectra:

$$B = 57635.970 \text{ MHz}, \quad D = 0.18358 \text{ MHz}.$$

When we use these constants to calculate the transition frequencies for $J = 1 \leftarrow J = 0$ and $J = 7 \leftarrow J = 6$, we obtain 115271.206 MHz and 806651.708 MHz, respectively, which are in good agreement with the observed values.

3.1.3 Rotational Energy Levels of Linear Molecules and Structure Determination by Means of Isotope Substitution

As long as linear molecules are treated as rigid rotors, we can apply to them the method of treatment for the rotation of diatomic molecules described in Sect. 3.1.2.

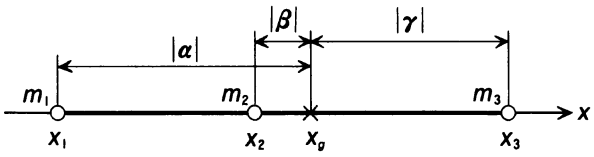

Fig. 3.4 Linear triatomic molecule

Let us then determine the rotational constant of interstellar molecules by examining the spectrum of microwave emission from the Taurus Dark Cloud, which has been introduced in Chap. 1, Fig. 1.8. As will be discussed in Sect. 3.4, the rotational energy of linear molecules can be written with rotational constant B, as in the case of diatomic molecules, as $E_J = hBJ(J+1)$. The series of strongest transition observed at nearly equal intervals is the rotational transition of HC_3N(H–C≡C–C≡N) from the $J+1$ level to the J level. The transition frequency from $J=4$ to $J=3$ is 36392.3 MHz, and from $J=5$ to $J=4$, 45490.3 MHz. Then, from $8B =$ 36392.3 MHz and $10B = 45490.3$ MHz, we can easily calculate $B = 4549.04$ MHz and $B = 4549.03$ MHz, respectively. We can also derive B without determining the assigned quantum number J, by regarding the observed, nearly equal intervals of the series as $2B$, and calculating $2B = 45490.3 - 36392.3$ MHz to obtain $B = 4549.0$ MHz. As the value of B is known to be 4549.058 MHz, we can see that the simple analyses above are appropriate.

However, obtaining the value of the rotational constant B alone does not allow us to determine the internuclear distance for each pair of atoms in a HC_3N molecule. This is also true of linear triatomic molecules, which are the linear molecules containing the smallest number of atoms. For example, OCS, a linear triatomic molecule, exhibits the transition $J = 2 \leftarrow J = 1$ at 24325.9 MHz. Here, the interval between $J=2$ and $J=1$ is $4hB$ ($= hB \times 2 \times 3 - hB \times 1 \times 2$), and the moment of inertia I can be obtained as $I = 83.101$ amu Å^2. However, the molecular structure of a linear triatomic molecule cannot be said to have been determined unless both of the two internuclear distances have been obtained, which means that additional information is needed.

Let us take a triatomic molecule that consists of atoms 1, 2, and 3, with masses m_1, m_2, and m_3, respectively, aligned on the x axis, as shown in Fig. 3.4. Denoting the x coordinates of the three atoms as x_1, x_2, and x_3, respectively, and that of the mass center as x_g, the moment of inertia of this linear triatomic molecule is written as

$$I = m_1\alpha^2 + m_2\beta^2 + m_3\gamma^2, \tag{3.18}$$

where

$$\begin{cases} \alpha = x_1 - x_g, \\ \beta = x_2 - x_g, \\ \gamma = x_3 - x_g. \end{cases} \tag{3.19}$$

From the condition that the first-order moment around the center of mass disappears, we can write

$$m_1\alpha + m_2\beta + m_3\gamma = 0. \tag{3.20}$$

Let us then consider the case of the third atom being substituted with another isotope. If the third atomic mass in this isotope species changes to $m_3 + \Delta m_3$, the moment of inertia I_3^{iso} becomes

$$I_3^{\text{iso}} = m_1(\alpha - \delta x_g)^2 + m_2(\beta - \delta x_g)^2 + (m_3 + \Delta m_3)(\gamma - \delta x_g)^2, \tag{3.21}$$

where $\delta x_g = x_g^{\text{iso}} - x_g$, signifying that the position of the center of mass has shifted by δx_g from x_g to x_g^{iso}. In addition, from the condition that the first-order moment disappears, we can write

$$m_1(\alpha - \delta x_g) + m_2(\beta - \delta x_g) + (m_3 + \Delta m_3)(\gamma - \delta x_g) = 0. \tag{3.22}$$

Modifying Eq. (3.22) by using Eq. (3.20), we obtain the expression

$$\Delta m_3 \gamma = (M + \Delta m_3)\delta x_g, \tag{3.23}$$

where M,

$$M = m_1 + m_2 + m_3, \tag{3.24}$$

is the total mass of the molecule before the isotope substitution. Calculating $I_3^{\text{iso}} - I$ with Eq. (3.23), we can derive

$$\begin{aligned} I_3^{\text{iso}} - I &= \Delta m_3 \gamma^2 - 2\Delta m_3 \gamma \delta x_g + (M + \Delta m_3)\delta x_g^2 \\ &= \Delta m_3 \gamma^2 - \frac{\Delta m_3^2}{(M + \Delta m_3)}\gamma^2 \\ &= \mu_3 \gamma^2 \end{aligned} \tag{3.25}$$

where

$$\mu_3 = \frac{M \Delta m_3}{M + \Delta m_3}. \tag{3.26}$$

Therefore, $\gamma = x_3 - x_g$ can be derived from $I_3^{\text{iso}} - I$. Once γ is obtained, α and β can be calculated from Eqs. (3.18) and (3.20), and internuclear distances $x_2 - x_1$ and $x_3 - x_2$ can be determined from Eq. (3.19).

Let us apply the same procedure as above to OCS. Here, we will treat O, C, and S as atoms 1, 2, and 3, respectively. The previously shown transition, $J = 2 \leftarrow J = 1$, is that of the normal species $^{16}O^{12}C^{32}S$. When measuring the spectrum of $^{16}O^{12}C^{34}S$, the transition $J = 2 \leftarrow J = 1$ is observed at 23731.3 MHz. As this frequency corresponds to $4B^{\text{iso}}$, we can obtain $I_3^{\text{iso}} = 85.184$ amu Å. Using $m(^{32}S) = 31.9721$ amu and $m(^{34}S) = 33.9679$ amu for the masses of ^{32}S and ^{34}S, respectively, we can determine γ from Eq. (3.25) as $|\gamma| = 1.0383$ Å. Following the above-stated procedure, we can obtain $r_{CO} = 1.163$ Å and $r_{CS} = 1.560$ Å.

When we examine the process through which Eq. (3.25) is derived, we realize that the same equation as the one for the third atom can be derived for the first and second atoms. In the case of OCS, α can be directly obtained by determining the value of I_1^{iso} for the isotope species with ^{18}O substituted for ^{16}O. Similarly, β can be derived directly from the value of I_2^{iso} determined for the isotope species with ^{13}C substituted for ^{12}C. Furthermore, from the three values α, β and γ, we can

determine the two internuclear distances in OCS, r_{CO} and r_{CS}. Molecular structure determined through this isotope substitution method are called "r_s structure," where the subscript s stands for "substitution." The isotope substitution method is also used to determine the geometrical structure of polyatomic molecules other than linear molecules.

In this section, we have limited our discussion to the rotational energy of diatomic and linear triatomic molecules as seen as a rigid rotor. What, then, will be the forms of eigenfunctions corresponding to their eigenvalues? In the next section, we will treat the angular momentum in quantum mechanics in order to obtain the rotational wave function.

Problem 3.2
The transition $J = 2 \leftarrow J = 1$ of $^{16}O^{13}C^{32}S$ and $^{18}O^{12}C^{32}S$ are observed at 24247.5 MHz and 22819.3 MHz, respectively. Find the absolute values of α and β as defined in Eq. (3.19), and determine the molecular structure of OCS. Let the masses of ^{13}C and ^{18}O be $m(^{13}C) = 13.0034$ amu and $m(^{18}O) = 17.9992$ amu, respectively.

Solution
Using $I_2^{\text{iso}} = 83.3701$ amu Å^2 and Eq. (3.25), we can derive

$$|\beta| = \sqrt{\frac{I_2^{\text{iso}} - I}{\mu_2}} = \sqrt{\frac{0.2691}{0.9868}} = 0.5222 \text{ Å}.$$

Similarly, with $I_1^{\text{iso}} = 88.5880$ amu Å^2, we obtain

$$|\alpha| = \sqrt{\frac{I_1^{\text{iso}} - I}{\mu_1}} = \sqrt{\frac{0.4870}{1.9395}} = 1.6820 \text{ Å}.$$

As $|\gamma| = 1.0383$ Å has been given in the text, we can derive the following values, paying special attention to the position of the center of mass:

$$r_{CO} = |\alpha| - |\beta| = 1.160 \text{ Å},$$
$$r_{CS} = |\beta| + |\gamma| = 1.560 \text{ Å}.$$

These values are in good agreement with the previous results derived using only $^{16}O^{12}C^{32}S$ and $^{16}O^{12}C^{34}S$. □

3.2 The Angular Momentum of Molecular Rotation

In the preceding section, we took Eqs. (3.11) and (3.12) as a given premise, in solving the Schrödinger equation for the rotation of a diatomic molecule (Eq. (3.10)). In fact, the operator represented as $-\hbar\Lambda$ in Eq. (3.11) is equal to the square of the angular momentum operator in quantum mechanics. Thus, in this section, we will learn the quantum mechanics of angular momentum, to understand molecular rotation.

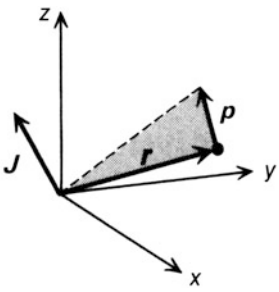

Fig. 3.5 The angular momentum vector $\boldsymbol{J}$ ($\boldsymbol{J}$ is perpendicular to the plane formed by $\boldsymbol{r}$ and $\boldsymbol{p}$)

3.2.1 Angular Momentum Operators

When a mass point m is moving around the origin with momentum $\boldsymbol{p} = m\boldsymbol{v}$ in the space-fixed x-y-z coordinate system as seen in Fig. 3.5, the angular momentum $\boldsymbol{J}$ of the movement of the mass point is expressed as

$$\boldsymbol{J} = \boldsymbol{r} \times \boldsymbol{p}, \tag{3.27}$$

where $\boldsymbol{r}$ is the position vector of the mass point. When $\boldsymbol{r} = (x, y, z)$ and $\boldsymbol{p} = (p_x, p_y, p_z)$, the x, y and z components of the angular momentum can be derived from

$$\boldsymbol{J} = \begin{vmatrix} \boldsymbol{i} & \boldsymbol{j} & \boldsymbol{k} \\ x & y & z \\ p_x & p_y & p_z \end{vmatrix} \tag{3.28}$$

as

$$\begin{cases} J_x = yp_z - zp_y, \\ J_y = zp_x - xp_z, \\ J_z = xp_y - yp_x. \end{cases} \tag{3.29}$$

Shifting the discussion to quantum mechanics by applying the substitutions

$$p_x = -\mathrm{i}\hbar\frac{\partial}{\partial x}, \quad p_y = -\mathrm{i}\hbar\frac{\partial}{\partial y}, \quad p_z = -\mathrm{i}\hbar\frac{\partial}{\partial z}, \tag{3.30}$$

the angular momentum operator in Eq. (3.29) can be expressed in quantum mechanics as

$$\begin{cases} J_x = -\mathrm{i}\hbar\left(y\dfrac{\partial}{\partial z} - z\dfrac{\partial}{\partial y}\right), \\ J_y = -\mathrm{i}\hbar\left(z\dfrac{\partial}{\partial x} - x\dfrac{\partial}{\partial z}\right), \\ J_z = -\mathrm{i}\hbar\left(x\dfrac{\partial}{\partial y} - y\dfrac{\partial}{\partial x}\right). \end{cases} \tag{3.31}$$

Let us now describe this in the polar coordinate system. Firstly, treating r as another variable number, we can obtain an equation corresponding to Eq. (3.5), thereby calculating $\frac{\partial}{\partial x}$, $\frac{\partial}{\partial y}$, and $\frac{\partial}{\partial z}$ as

$$\begin{cases} \dfrac{\partial}{\partial x} = \sin\theta\cos\phi\dfrac{\partial}{\partial r} + \dfrac{1}{r}\cos\theta\cos\phi\dfrac{\partial}{\partial\theta} - \dfrac{1}{r}\left(\dfrac{\sin\phi}{\sin\theta}\right)\dfrac{\partial}{\partial\phi}, \\ \dfrac{\partial}{\partial y} = \sin\theta\sin\phi\dfrac{\partial}{\partial r} + \dfrac{1}{r}\cos\theta\sin\phi\dfrac{\partial}{\partial\theta} + \dfrac{1}{r}\left(\dfrac{\cos\phi}{\sin\theta}\right)\dfrac{\partial}{\partial\phi}, \\ \dfrac{\partial}{\partial z} = \cos\theta\dfrac{\partial}{\partial r} - \dfrac{1}{r}\sin\theta\dfrac{\partial}{\partial\theta}, \end{cases} \tag{3.32}$$

and deriving J_x, J_y, and J_z as

$$\begin{cases} J_x = -\mathrm{i}\hbar\left(-\sin\phi\dfrac{\partial}{\partial\theta} - \cot\theta\cos\phi\dfrac{\partial}{\partial\phi}\right), \\ J_y = -\mathrm{i}\hbar\left(\cos\phi\dfrac{\partial}{\partial\theta} - \cot\theta\sin\phi\dfrac{\partial}{\partial\phi}\right), \\ J_z = -\mathrm{i}\hbar\dfrac{\partial}{\partial\phi}. \end{cases} \tag{3.33}$$

Secondly, the square of the total angular momentum $\boldsymbol{J}^2$, which is expressed as

$$\boldsymbol{J}^2 = J_x^2 + J_y^2 + J_z^2, \tag{3.34}$$

can be rewritten in terms of polar coordinates by using Eq. (3.33), as

$$\boldsymbol{J}^2 = -\hbar^2\left\{\frac{1}{\sin\theta}\frac{\partial}{\partial\theta}\left(\sin\theta\frac{\partial}{\partial\theta}\right) + \frac{1}{\sin^2\theta}\frac{\partial^2}{\partial\phi^2}\right\}. \tag{3.35}$$

This formula can be expressed with the operator Λ, which has been introduced in Eq. (3.9) for the rigid rotor of a diatomic molecule, as

$$\boldsymbol{J}^2 = -\hbar^2\Lambda. \tag{3.36}$$

Therefore, the Hamiltonian expressing the rotational motion of the rigid diatomic molecule is given as

$$H_{\mathrm{rot}} = -\frac{\hbar^2}{2\mu r^2}\Lambda = \frac{\boldsymbol{J}^2}{2\mu r^2} = \frac{\boldsymbol{J}^2}{2I}. \tag{3.37}$$

3.2.2 Commutation Relations of Angular Momentum Operators

When $\hat{A}$ and $\hat{B}$ are operators,

$$[\hat{A}, \hat{B}] = \hat{A}\hat{B} - \hat{B}\hat{A} \tag{3.38}$$

is called the commutator, and characterizes the operators. For example, when

$$[\hat{A}, \hat{B}] = 0, \tag{3.39}$$

this shows that $\hat{A}$ and $\hat{B}$ are commutative. In this case, operators $\hat{A}$ and $\hat{B}$ share the same system of eigenfunctions.

Let us then examine the commutation relation of the angular momentum operator, which has been obtained in Sect. 3.2.2. Here, we will use the x-y-z coordinate system rather than the polar coordinate system. Using Eq. (3.31) and the definition of the commutator in Eq. (3.38), we can write

$$\begin{aligned}[J_x, J_y] &= (-\mathrm{i}\hbar)^2 \left\{ \left(y\frac{\partial}{\partial z} - z\frac{\partial}{\partial y} \right) \left(z\frac{\partial}{\partial x} - x\frac{\partial}{\partial z} \right) \right. \\ &\quad \left. - \left(z\frac{\partial}{\partial x} - x\frac{\partial}{\partial z} \right) \left(y\frac{\partial}{\partial z} - z\frac{\partial}{\partial y} \right) \right\} \\ &= (-\mathrm{i}\hbar)^2 \left(y\frac{\partial}{\partial x} - x\frac{\partial}{\partial y} \right) \\ &= \mathrm{i}\hbar J_z. \end{aligned} \tag{3.40a}$$

Similarly, we can write

$$[J_y, J_z] = \mathrm{i}\hbar J_x, \tag{3.40b}$$

and

$$[J_z, J_x] = \mathrm{i}\hbar J_y. \tag{3.40c}$$

This commutation relation applies only to angular momenta in the space-fixed coordinate system. When a momentum is in the molecule-fixed coordinate system, as in the case discussed in Sect. 3.4.2, the sign of the right-hand side of its commutation relation becomes negative.

As shown in Eqs. (3.40a) through (3.40c), J_x, J_y, and J_z are not commutative with one another. However, the total angular momentum operator $\boldsymbol{J}^2$ commutates with J_x, as shown below. First,

$$\begin{aligned}\left[J_x, \boldsymbol{J}^2\right] &= \left[J_x, J_x^2 + J_y^2 + J_z^2\right] \\ &= \left[J_x, J_x^2\right] + \left[J_x, J_y^2\right] + \left[J_x, J_z^2\right]. \end{aligned} \tag{3.41}$$

Then, by using the property of the commutation operator,

$$\left[\hat{A}, \hat{B}^2\right] = [\hat{A}, \hat{B}]\hat{B} + \hat{B}[\hat{A}, \hat{B}], \tag{3.42}$$

and the commutation relation Eqs. (3.40a) through (3.40c) we can write

$$\begin{cases} \left[J_x, J_x^2\right] = 0, \\ \left[J_x, J_y^2\right] = [J_x, J_y]J_y + J_y[J_x, J_y] = \mathrm{i}\hbar J_z J_y + \mathrm{i}\hbar J_y J_z, \\ \left[J_x, J_z^2\right] = [J_x, J_z]J_z + J_z[J_x, J_z] = -\mathrm{i}\hbar J_y J_z - \mathrm{i}\hbar J_z J_y. \end{cases} \tag{3.43}$$

Substituting these values into Eq. (3.41), we obtain

$$\left[J_x, \boldsymbol{J}^2\right] = 0. \tag{3.44a}$$

We can similarly show that

$$\left[J_y, \boldsymbol{J}^2\right] = 0, \quad \left[J_z, \boldsymbol{J}^2\right] = 0. \tag{3.44b}$$

This signifies that, when J_α is J_x, J_y, or J_z, $\boldsymbol{J}^2$ and J_α share the same set of eigenfunctions.

3.2.3 Raising and Lowering Operators

Let us then consider the properties of the system of eigenfunctions shared by $\boldsymbol{J}^2$ and J_α, as well as the corresponding eigenvalues of $\boldsymbol{J}^2$ and J_α. In order to examine these issues, we will select J_z for J_α, and express the eigenfunction shared by $\boldsymbol{J}^2$ and J_z as $\psi(\lambda, m) = |\lambda, m\rangle$, whose eigenvalues are $\lambda\hbar^2$ and $m\hbar$, respectively, as shown below:

$$\boldsymbol{J}^2|\lambda, m\rangle = \lambda\hbar^2|\lambda, m\rangle \tag{3.45}$$

$$J_z|\lambda, m\rangle = m\hbar|\lambda, m\rangle. \tag{3.46}$$

Here, the values of λ and m are both unknown. We will therefore obtain the possible values of λ and m as follows.

First, instead of J_x and J_y, we will introduce operators J_+ and J_-, defining them as

$$J_+ \equiv J_x + \mathrm{i}J_y \tag{3.47a}$$

$$J_- \equiv J_x - \mathrm{i}J_y. \tag{3.47b}$$

We will now demonstrate that these $J_\pm$ operated on $|\lambda, m\rangle$, namely $J_\pm|\lambda, m\rangle$, is the eigenfunction of $\boldsymbol{J}^2$ and J_z. Operating $\boldsymbol{J}^2$ on $J_\pm|\lambda, m\rangle$, we can write

$$\begin{aligned}\boldsymbol{J}^2\big(J_\pm|\lambda, m\rangle\big) &= J_\pm\big(\boldsymbol{J}^2|\lambda, m\rangle\big) \\ &= J_\pm\big(\lambda\hbar^2|\lambda, m\rangle\big) \\ &= \lambda\hbar^2\big(J_\pm|\lambda, m\rangle\big),\end{aligned} \tag{3.48}$$

where the first line of equation is derived by the fact that Eqs. (3.44a) and (3.44b) give us $[\boldsymbol{J}^2, J_\pm] = 0$. Next, from the commutation relation of J_z and $J_\pm$ being

$$[J_z, J_\pm] = \pm\hbar J_\pm, \tag{3.49}$$

we can write

$$J_z J_\pm = J_\pm J_z \pm \hbar J_\pm. \tag{3.50}$$

Therefore, by operating J_z on $J_\pm|\lambda, m\rangle$, we can obtain

$$\begin{aligned}J_z\big(J_\pm|\lambda, m\rangle\big) &= J_\pm J_z|\lambda, m\rangle \pm \hbar J_\pm|\lambda, m\rangle \\ &= J_\pm m\hbar|\lambda, m\rangle \pm \hbar J_\pm|\lambda, m\rangle \\ &= (m \pm 1)\hbar\big(J_\pm|\lambda, m\rangle\big).\end{aligned} \tag{3.51}$$

We can see from Eqs. (3.48) and (3.51) that $J_\pm|\lambda, m\rangle$ are also eigenfunctions shared by $\boldsymbol{J}^2$ and J_z. Also, Eq. (3.51) signifies that by operating $J_\pm$ on $|\lambda, m\rangle$, the eigenvalue of J_z changes by $\pm\hbar$. For this, J_+ and J_- are referred to as the raising operator and the lowering operator, respectively.

Problem 3.3
Demonstrate Eq. (3.49).

Solution
In the case of J_+, by using Eqs. (3.40a) through (3.40c) and the definition given in Eqs. (3.47a) and (3.47b), we can write

$$\begin{aligned}[J_z, J_+] &= [J_z, J_x + \mathrm{i}J_y] \\ &= [J_z, J_x] + \mathrm{i}[J_z, J_y] \\ &= \mathrm{i}\hbar J_y + \mathrm{i}(-\mathrm{i}\hbar J_x) \\ &= \hbar(J_x + \mathrm{i}J_y) \\ &= \hbar J_+.\end{aligned}$$

In the case of J_-, we can similarly derive

$$[J_z, J_-] = -\hbar J_-. \qquad \square$$

Problem 3.4

(1) Show that $[J_+, J_-] = 2\hbar J_z$.
(2) Write $J_+J_- + J_-J_+$ using $\boldsymbol{J}^2$ and J_z.
(3) Based on the results of (1) and (2), write J_+J_- and J_-J_+ using $\boldsymbol{J}^2$ and J_z.

Solution

(1) Using the definition of the raising and lowering operators in Eqs. (3.47a) and (3.47b), we can write

$$\begin{aligned}[J_+, J_-] &= J_+J_- - J_-J_+ \\ &= -2\mathrm{i}(J_xJ_y - J_yJ_x) \\ &= 2\hbar J_z. \end{aligned} \tag{3.52}$$

(2) Similarly, $J_+J_- + J_-J_+$ can be calculated as

$$J_+J_- + J_-J_+ = 2\left(J_x^2 + J_y^2\right).$$

Therefore, by using $\boldsymbol{J}^2 = J_x^2 + J_y^2 + J_z^2$, we can obtain

$$J_+J_- + J_-J_+ = 2\left(\boldsymbol{J}^2 - J_z^2\right). \tag{3.53}$$

(3) By adding Eq. (3.52) to Eq. (3.53), and by subtracting Eq. (3.53) from Eq. (3.52), we obtain

$$J_+J_- = \boldsymbol{J}^2 - J_z(J_z - \hbar), \tag{3.54a}$$

and

$$J_-J_+ = \boldsymbol{J}^2 - J_z(J_z + \hbar), \tag{3.54b}$$

respectively. $\square$

3.2.4 Eigenvalues of Angular Momentum Operators

We will now calculate the square modulus of $J_{\pm}|\lambda, m\rangle$ that appeared in Sect. 3.2.3, that is, $|J_{\pm}|\lambda, m\rangle|^2$, which is the norm of $J_{\pm}|\lambda, m\rangle$.

Here, $J_{\pm}$ is not a Hermitian operator, but J_x and J_y are. We can use this to write

$$\int (J_{\pm}\psi_{\lambda m})^* \psi_{\lambda' m'} \, \mathrm{d}\tau = \int \psi^*_{\lambda m} (J_{\mp}\psi_{\lambda' m'}) \, \mathrm{d}\tau. \tag{3.55}$$

And thus, by setting $\psi_{\lambda' m'} = J_{\pm}\psi_{\lambda m}$ we obtain

$$\left|J_{\pm}|\lambda, m\rangle\right|^2 = \langle \lambda, m | J_{\mp} J_{\pm} | \lambda, m \rangle. \tag{3.56}$$

Then, as $J_{\mp}J_{\pm}$ can be calculated as

$$\begin{aligned} J_{\mp}J_{\pm} &= (J_x \mp \mathrm{i}J_y)(J_x \pm \mathrm{i}J_y) \\ &= \boldsymbol{J}^2 - J_z^2 \pm \mathrm{i}\{J_x J_y - J_y J_x\} \\ &= \boldsymbol{J}^2 - J_z(J_z \pm \hbar), \end{aligned} \tag{3.57}$$

we derive

$$\begin{aligned} \left|J_{\pm}|\lambda, m\rangle\right|^2 &= \langle \lambda, m | \boldsymbol{J}^2 - J_z(J_z \pm \hbar) | \lambda, m \rangle \\ &= \left\{\lambda - m(m \pm 1)\right\} \hbar^2 \langle \lambda, m | \lambda, m \rangle. \end{aligned} \tag{3.58}$$

As the norm of a wave function always has a positive or zero value, we can show from Eq. (3.58) that

$$\lambda - m(m \pm 1) \geqq 0$$

holds, and that, therefore,

$$\lambda \geqq m(m \pm 1) = m^2 \pm m \tag{3.59}$$

also holds.

As Eq. (3.51) demonstrates, each time the raising operator J_+ acts on $|\lambda, m\rangle$, m increases by 1. This can be illustrated as

$$|\lambda, m\rangle \overset{J_+}{\to} |\lambda, m+1\rangle \overset{J_+}{\to} |\lambda, m+2\rangle \overset{J_+}{\to} \cdots. \tag{3.60}$$

Similarly, with each instance of the lowering operator J_- acting on $|\lambda, m\rangle$, m decreases by 1. That is,

$$|\lambda, m\rangle \overset{J_-}{\to} |\lambda, m-1\rangle \overset{J_-}{\to} |\lambda, m-2\rangle \overset{J_-}{\to} \cdots. \tag{3.61}$$

However, Eq. (3.59) shows that the value of m cannot increase or decrease infinitely; it has upper and lower limits.

We will therefore write the maximum value of m as $m_{\max}$, and the minimum value of m as $m_{\min}$. Operating J_+ on $|\lambda, m_{\max}\rangle$, then, we can write

$$J_+|\lambda, m_{\max}\rangle = 0. \tag{3.62}$$

Operating J_- on $|\lambda, m_{\min}\rangle$, on the other hand, necessarily gives us

$$J_-|\lambda, m_{\min}\rangle = 0. \tag{3.63}$$

Therefore, from Eq. (3.62), we obtain

$$J_- J_+|\lambda, m_{\max}\rangle = 0, \tag{3.64}$$

into which Eq. (3.57) can be substituted to give us

$$\left\{\boldsymbol{J}^2 - J_z(J_z + \hbar)\right\}|\lambda, m_{\max}\rangle = 0. \tag{3.65}$$

Therefore, the fact that Eqs. (3.45) and (3.46) allow us to write

$$\left\{\lambda - m_{\max}(m_{\max} + 1)\right\}\hbar^2|\lambda, m_{\max}\rangle = 0 \tag{3.66}$$

signifies that

$$\lambda - m_{\max}(m_{\max} + 1) = 0 \tag{3.67}$$

holds. Similarly, from Eq. (3.63) we can calculate $J_+ J_-$ as

$$J_+ J_-|\lambda, m_{\min}\rangle = 0, \tag{3.68}$$

which leads us to

$$\lambda - m_{\min}(m_{\min} - 1) = 0. \tag{3.69}$$

Subtracting Eq. (3.67) from Eq. (3.69), we obtain

$$m_{\max}(m_{\max} + 1) - m_{\min}(m_{\min} - 1) = 0,$$

and by factorizing this we can write

$$(m_{\max} + m_{\min})(m_{\max} - m_{\min} + 1) = 0. \tag{3.70}$$

As $m_{\max} \geqq m_{\min}$, the content in the second set of parentheses in this formula is necessarily positive. Therefore,

$$m_{\max} + m_{\min} = 0 \tag{3.71}$$

needs to hold. Thus, when

$$j = m_{\max} = -m_{\min}, \tag{3.72}$$

it is shown from Eq. (3.67) that

$$\lambda = j(j + 1). \tag{3.73}$$

From Eq. (3.72), we can write

$$m_{\max} - m_{\min} = j + j = 2j. \tag{3.74}$$

As m increases by increments of 1 from $m_{\min}$ to $m_{\max}$, we know that $(m_{\max} - m_{\min})$ is a positive integer or zero. From Eq. (3.74), then, $2j$ is required to be a positive integer or zero. Therefore, the possible values for j are

$$j = 0, \frac{1}{2}, 1, \frac{3}{2}, \ldots, \tag{3.75}$$

making j one of three possibilities: zero, a positive integer, or a positive half-odd integer.

We can summarize what we have seen above using j instead of λ as follows. The angular momentum operator $\boldsymbol{J}^2$ and J_z share the same set of eigenfunctions $\{\psi_{jm} = |j, m\rangle\}$, and satisfy the relations

$$\boldsymbol{J}^2|j, m\rangle = j(j+1)\hbar^2|j, m\rangle \tag{3.76}$$

and

$$J_z|j, m\rangle = m\hbar|j, m\rangle \quad \big(m = -j, -(j-1), \ldots, j-1, j\big), \tag{3.77}$$

where j can take the values $j = 0, \frac{1}{2}, 1, \frac{3}{2}, \ldots$, and the number of different values that m can take in the set of eigenfunctions denoted as $\{|j, m\rangle\}$ is $2j+1$. This means that, when the quantum number j is rewritten as J, and by using Eqs. (3.36) and (3.37), the Schrödinger equation of the rigid rotor, Eq. (3.10), gives the eigenvalue of Eq. (3.14) and the eigenfunction of $|J, m\rangle$. Here, the rotational quantum number J is either zero or a positive integer. An example of the quantum number of the angular momentum becoming a half odd integer can be found in the case of the electron spin angular momentum ($J = \frac{1}{2}$). Half-odd angular numbers appear when we treat the electron spin angular momentum or the nuclear spin angular momentum.

3.2.5 Eigenfunctions of Angular Momentum Operators

Here, we will deepen our understanding of the concrete shape of the eigenfunction $|j, m\rangle$ introduced in Sect. 3.2.4. For the purpose of this discussion, j and m are treated as integers.

In the polar coordinate system, as J_z is expressed as

$$J_z = -\mathrm{i}\hbar\frac{\partial}{\partial\phi}, \tag{3.78}$$

Eq. (3.77) can be written as

$$-\mathrm{i}\hbar\frac{\partial}{\partial\phi}\psi_{jm} = m\hbar\psi_{jm}. \tag{3.79}$$

This equation shows that ψ_{jm} can be expressed as a function depending on θ multiplied by $\mathrm{e}^{\mathrm{i}m\phi}$, or as

$$\psi_{jm}(\theta, \phi) = P_{jm}(\cos\theta)\mathrm{e}^{\mathrm{i}m\phi}, \tag{3.80}$$

where the function depending on θ is expressed as $P_{jm}(\cos\theta)$, a function of $\cos\theta$, in order to simplify later discussions. Incidentally, the functions ψ_{jm} here are what are called spherical harmonics, and are often denoted as Y_{jm}.

To derive the shape of ψ_{jm}, we will express the raising and lowering operators

$$J_+ = J_x + \mathrm{i}J_y$$

and

$$J_- = J_x - \mathrm{i}J_y$$

in polar coordinates. As Eq. (3.33) gives us

$$J_x = -\mathrm{i}\hbar\left(-\sin\phi\frac{\partial}{\partial\theta} - \cot\theta\cos\phi\frac{\partial}{\partial\phi}\right)$$

and

$$J_y = -\mathrm{i}\hbar\left(\cos\phi\frac{\partial}{\partial\theta} - \cot\theta\sin\phi\frac{\partial}{\partial\phi}\right),$$

we can write

$$J_+ = \hbar\mathrm{e}^{\mathrm{i}\phi}\left(\frac{\partial}{\partial\theta} + \mathrm{i}\cot\theta\frac{\partial}{\partial\phi}\right), \tag{3.81}$$

and

$$J_- = \hbar\mathrm{e}^{-\mathrm{i}\phi}\left(-\frac{\partial}{\partial\theta} + \mathrm{i}\cot\theta\frac{\partial}{\partial\phi}\right). \tag{3.82}$$

As previously shown, operating J_+ on ψ_{jj} results in

$$J_+\psi_{jj} = 0, \tag{3.83}$$

because m cannot be larger than j. Therefore,

$$\hbar\mathrm{e}^{\mathrm{i}\phi}\left(\frac{\partial}{\partial\theta} + \mathrm{i}\cot\theta\frac{\partial}{\partial\phi}\right)\mathrm{e}^{\mathrm{i}j\phi}P_{jj}(\cos\theta) = 0, \tag{3.84}$$

which is a differential equation easily solved to yield

$$P_{jj}(\cos\theta) = C_j\sin^j\theta. \tag{3.85}$$

Problem 3.5
Solve the differential equation (3.84) given above, and demonstrate that it yields Eq. (3.85).

Solution
Performing the differentiation of Eq. (3.84) with respect to ϕ, we obtain

$$\frac{\partial P_{jj}}{\partial\theta} - j\cot\theta P_{jj} = 0.$$

By substituting $\sin\theta = x$, this can be written as

$$\mathrm{d}P_{jj} = j\frac{P_{jj}}{x}\mathrm{d}x,$$

from which we derive

$$P_{jj} = C_j x^j = C_j\sin^j\theta. \qquad \square$$

Therefore, from Eq. (3.80), we can write

$$\psi_{jj} = C_j\sin^j\theta\mathrm{e}^{\mathrm{i}j\phi}. \tag{3.86}$$

By using the normalization condition

$$\int_0^{\pi}\int_0^{2\pi} \psi_{jj}^{*}\psi_{jj}\sin\theta\,\mathrm{d}\theta\,\mathrm{d}\phi = 1,$$

we can obtain C_j as

$$|C_j| = \frac{1}{2^j\,j!}\left\{\frac{(2j+1)!}{4\pi}\right\}^{\frac{1}{2}}. \tag{3.87}$$

As ψ_{jj} has now been obtained, we operate the lowering operator J_- on it to obtain ψ_{jm-1} as

$$J_-\psi_{jm} = \sqrt{j(j+1)-m(m-1)}\hbar\psi_{jm-1}. \tag{3.88a}$$

By operating J_- succesively we can derive $\psi_{jm'}$ with smaller m' values. Here, Eq. (3.88a) can be derived from Eqs. (3.58) and (3.73). Correspondingly, a similar procedure gives us

$$J_+\psi_{jm} = \sqrt{j(j+1)-m(m+1)}\hbar\psi_{jm+1}. \tag{3.88b}$$

As what has been given in Eq. (3.58) is $|J_\pm\psi_{jm}|^2$, the right-hand sides of Eqs. (3.88a) and (3.88b) will be multiplied by a phase factor which takes the form of $\mathrm{e}^{\mathrm{i}\delta}$. Here, we have adopted the Condon-Shortley phase convention, wherein $\delta = 0$.

We will next obtain the concrete shape of ψ_{jm} for $j = 0$ and $j = 1$. When $j = 0$, m is necessarily also 0, and therefore, assuming that C_j takes a positive value, we can use Eqs. (3.86) and (3.87) to write

$$\psi_{00} = C_0\sin^0\theta\mathrm{e}^{\mathrm{i}\cdot 0\cdot\phi} = \frac{1}{\sqrt{4\pi}}. \tag{3.89}$$

This signifies that, when $j = 0$, the shape of the eigenfunction is spherically symmetric, and is independent of both θ and ϕ.

When $j = 1$, on the other hand, there are three possible eigenfunctions depending on the value of m, namely ψ_{11}, ψ_{10}, and ψ_{1-1}. From Eqs. (3.86) and (3.87), we can write

$$\psi_{11} = -\frac{1}{2}\sqrt{\frac{3\cdot 2}{4\pi}}\sin\theta\mathrm{e}^{\mathrm{i}\phi} = -\sqrt{\frac{3}{8\pi}}\sin\theta\mathrm{e}^{\mathrm{i}\phi}. \tag{3.90}$$

From Eq. (3.88a), the relation

$$J_-\psi_{11} = \sqrt{1\cdot 2-1\cdot 0}\hbar\psi_{10} = \sqrt{2}\hbar\psi_{10} \tag{3.91}$$

can be obtained, while operating Eq. (3.82) on ψ_{11} gives us

$$\begin{aligned} J_-\psi_{11} &= \hbar\mathrm{e}^{-\mathrm{i}\phi}\left(-\frac{\partial}{\partial\theta}+\mathrm{i}\cot\theta\frac{\partial}{\partial\phi}\right)\psi_{11} \\ &= \hbar\cdot 2\sqrt{\frac{3}{8\pi}}\cos\theta. \end{aligned} \tag{3.92}$$

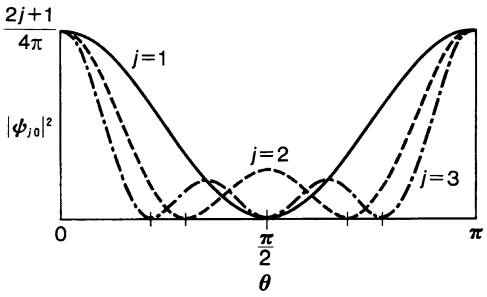

Fig. 3.6 The squared modulus of the eigenfunction of an angular momentum operator as a function of the polar angle θ

From Eqs. (3.91) and (3.92), we can derive

$$\psi_{10} = \sqrt{\frac{3}{4\pi}} \cos\theta. \tag{3.93}$$

By operating J_- on this eigenfunction again, we can obtain

$$\psi_{1-1} = \sqrt{\frac{3}{8\pi}} \sin\theta \mathrm{e}^{-\mathrm{i}\phi}. \tag{3.94}$$

Here, we can verify that the positive and negative signs on ψ_{11} and ψ_{1-1} indeed satisfy the relation of spherical harmonics,

$$\psi^*_{jm} = (-1)^m \psi_{j-m}.$$

In order to visualize the shape of the wave functions, we will now plot $|\psi_{10}|^2$ as a function of θ. As Eq. (3.93) allows us to write

$$|\psi_{10}|^2 = \frac{3}{4\pi} \cos^2\theta,$$

the shape of $|\psi_{10}|^2$ as θ varies from 0 to π is as shown in Fig. 3.6. Thus, we can see that this is a function which has a node at $\theta = 90° = \frac{\pi}{2}$.

In determining the angular momentum of a diatomic molecule rotating freely in space, or that of an electron in a hydrogenic atom in a space with no external field, the z axis chosen as the quantization axis can be oriented in any direction. Furthermore, in the case of $j = 1$, the three eigenfunctions ψ_{11}, ψ_{10}, and ψ_{1-1} of the square of the total angular momentum operator $\boldsymbol{J}^2$ give us the same eigenvalue $\hbar^2 j(j+1) = 2\hbar^2$, showing that they are triply degenerated $(2j + 1 = 3)$.

When we calculate linear combinations of ψ_{11} and ψ_{1-1} as

$$\psi_x = \frac{1}{-\sqrt{2}}(\psi_{11} - \psi_{1-1}) = \sqrt{\frac{3}{4\pi}} \sin\theta \cos\phi \tag{3.95}$$

and

$$\psi_y = \frac{1}{-\sqrt{2}\mathrm{i}}(\psi_{11} + \psi_{1-1}) = \sqrt{\frac{3}{4\pi}} \sin\theta \sin\phi, \tag{3.96}$$

their distributions extend in the directions of the x and y axes, and are shaped as the distribution of ψ_{10} rotated into the directions of the x and y axes, respectively.

For a larger value of j, too, we can determine ψ_{jm} in a similar manner. We can see that the number of nodes in the wave functions increases as j becomes larger. For cases of ψ_{j0} $(m = 0)$ we obtain

$$\psi_{20} = \sqrt{\frac{5}{16\pi}}\left(3\cos^2\theta - 1\right) \tag{3.97}$$

and

$$\psi_{30} = \sqrt{\frac{7}{16\pi}}\left(5\cos^3\theta - 3\cos\theta\right). \tag{3.98}$$

When we plot the square moduli of these eigenfunctions as functions of θ, we see that, as shown in Fig. 3.6, these functions have two and three nodes, respectively, in the range of $0 \leqq \theta \leqq \pi$.

In discussing the angular momentum of an electron in a hydrogenic atom, the orbitals of the electron for $j = 0, 1, 2, 3$ are called the s, p, d, and f orbitals, respectively. For instance, when the orbital angular momentum of the electron is 0 the electron is in the s orbital, and when the orbital angular momentum is 1 the electron is in the p orbital.

Among the spherical harmonics ψ_{jm}, the ones for $m = 0$ can be written with the Legendre polynomial $P_j(\cos\theta)$ as

$$\psi_{j0}(\theta, \phi) = \sqrt{\frac{2j+1}{4\pi}} P_j(\cos\theta). \tag{3.99}$$

The Legendre polynomial can be defined by the Rodrigues formula,

$$P_j(x) = \frac{1}{2^j j!}\frac{\mathrm{d}^j}{\mathrm{d}x^j}\left(x^2 - 1\right)^j, \tag{3.100}$$

and is known to be the solution to the Legendre equation,

$$\left\{\left(1 - x^2\right)\frac{\mathrm{d}^2}{\mathrm{d}x^2} - 2x\frac{\mathrm{d}}{\mathrm{d}x} + j(j+1)\right\} P_j(x) = 0. \tag{3.101}$$

Problem 3.6
$\psi_{jm} = |j, m\rangle$ is the eigenfunction of $\boldsymbol{J}^2$. Using the fact that $\boldsymbol{J}^2$ is given in Eq. (3.35) as

$$\boldsymbol{J}^2 = -\hbar^2\left\{\frac{1}{\sin\theta}\frac{\partial}{\partial\theta}\left(\sin\theta\frac{\partial}{\partial\theta}\right) + \frac{1}{\sin^2\theta}\frac{\partial^2}{\partial\phi^2}\right\},$$

find the equation that $\Theta_{jm}(\theta)$ satisfies when the variables are separated as

$$\psi_{jm} = \Theta_{jm}(\theta)\Phi_m(\phi).$$

Solution
From Eq. (3.80) and the normalization condition for $\Phi_m(\phi)$, it is obvious that $\Phi_m(\phi) = \frac{1}{\sqrt{2\pi}}\mathrm{e}^{\mathrm{i}m\phi}$. Using the relation $\boldsymbol{J}^2|j, m\rangle = j(j+1)\hbar^2|j, m\rangle$, we can obtain

$$-\left\{\frac{1}{\sin\theta}\frac{\partial}{\partial\theta}\left(\sin\theta\frac{\partial}{\partial\theta}\right) - \frac{m^2}{\sin^2\theta}\right\}\Theta_{jm}(\theta) = j(j+1)\Theta_{jm}(\theta). \tag{3.102}$$

□

Problem 3.7
For $m = 0$, show that the equation satisfied by $\Theta_{jm}(\theta)$, as calculated in Problem 3.6, is identical to the Legendre equation (3.101). Here, let $\cos\theta = x$.

Solution
By setting $m = 0$ in Eq. (3.102) and by using $-\sin\theta \mathrm{d}\theta = \mathrm{d}x$, the equation satisfied by $\Theta_{jm}(\theta)$ becomes Eq. (3.101). □

3.3 Molecular Rotation from the Point of View of Classical Mechanics

In this section, we will first define a molecule-fixed coordinate system by Euler angles. Next, we will derive the rotational energy of a polyatomic molecule in classical mechanics, in order to understand that rotational kinetic energy is represented by moments of inertia with respect to the three principal axes of inertia. Then, we will calculate the angular momentum in the molecule-fixed coordinate system.

3.3.1 Molecular Rotation and Euler Angles

In Sects. 3.1 and 3.2, we have learned that, when diatomic and linear molecules can be treated as rigid rotors, we can represent their rotational level energies as Eq. (3.15a), $E_J = hBJ(J+1)$, based on the quantum theory of angular momentum. We have also seen that eigenfunctions $\psi_{Jm} = |J, m\rangle$ are functions called the spherical harmonics. These results, however, are only applicable in cases where a molecule rotates around an axis that includes the center of mass and is perpendicular to the molecular axis on which the atoms are located. For example, in the case of a methylchloride molecule, CH_3Cl, as illustrated in Fig. 3.7(a), not only a rotation around the axis that is perpendicular to the C–Cl bond axis but also another rotational motion around the C–Cl bond axis is possible. Thus, we can conceptualize a CH_3Cl molecule rotating in a free space as simultaneously undergoing the two kinds of rotational motion around these two axes. In another case, with a H_2O molecule, we can think of rotations around three axes, x, y, and z, as shown in Fig. 3.7(b), as comprising the rotational motion of the molecule. We can then visualize the overall rotation, as a complex rotational motion resulting from the superposition of these three rotations. Thus, we can see that our discussion in the previous section falls short of allowing us to handle the rotations of non-linear polyatomic molecules in general.

Additionally, in describing a rotational motion around a molecular axis, using a molecule-fixed coordinate system instead of a space-fixed coordinate system will help us simplify matters and draw a clearer picture. For this, we need to transform the Hamiltonian of the molecular rotation from one in the space-fixed coordinate system to one in the molecule-fixed coordinate system.

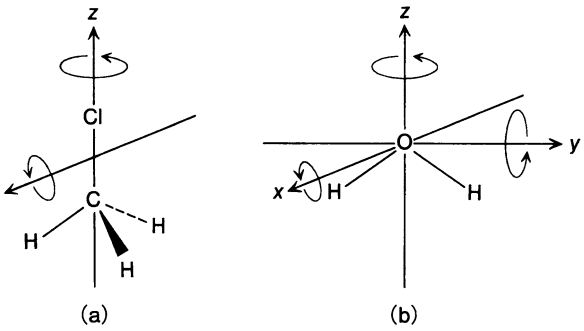

Fig. 3.7 Rotational motions of (**a**) CH_3Cl and (**b**) H_2O

Let us now think about a molecule which consists of n atoms, whose masses are m_i and coordinates $\boldsymbol{R}_i$ $(i = 1, \ldots, n)$. Here, the coordinate system is a space-fixed coordinate system whose origin coincides with the center of mass of the molecule. In this case, the kinetic energy of the rotational motion can be written as

$$T = \sum_{i=1}^{n} \frac{1}{2} m_i \dot{\boldsymbol{R}}_i^2. \tag{3.103}$$

Next, we will describe $\boldsymbol{R}_i$ in a molecule-fixed coordinate system that rotates together with the molecule, and whose origin, again, coincides with the molecule's center of mass. In this molecule-fixed coordinate system, when the coordinate of the i-th atom is given by $\boldsymbol{r}_i$, $\boldsymbol{r}_i$ and $\boldsymbol{R}_i$ are related as

$$\boldsymbol{r}_i = \boldsymbol{S}\boldsymbol{R}_i, \tag{3.104}$$

where the 3×3 matrix $\boldsymbol{S}$ expresses a rotation. Therefore, the kinetic energy T becomes

$$T = \sum_{i=1}^{n} \frac{1}{2} m_i \left(\dot{\boldsymbol{S}}^{-1} \boldsymbol{r}_i\right) \cdot \left(\dot{\boldsymbol{S}}^{-1} \boldsymbol{r}_i\right), \tag{3.105}$$

in which $\boldsymbol{S}^{-1}$ is the inverse of $\boldsymbol{S}$. Also, $\boldsymbol{r}_i$ does not depend on time, as it is the coordinate of an atom in the molecule expressed as a molecule-fixed coordinate. Thus the time dependence of the molecular rotation is expressed by matrix $\boldsymbol{S}$.

Let us then describe the rotational matrix $\boldsymbol{S}$ using three Euler angles, α, β, and γ. Starting from the coordinate system S described by the space-fixed axes x, y, and z, first we define the x' and y' axes by rotating S around the z axis by an angle of α $(0 \leqq \alpha < 2\pi)$, as shown in Fig. 3.8(a). We thus obtain coordinate system S', which is described by the new axes x', y', and z'. Here, the z' axis is identical to the z axis.

Next, as shown in Fig. 3.8(b), we define the z'' and x'' axes by rotating S' around the y' axis by an angle of β $(0 \leqq \beta < \pi)$, to obtain coordinate system S'', described by the new axes x'', y'', and z'', where the y'' axis is identical to the y' axis.

Finally, as shown in Fig. 3.8(c), we define the x''' and y''' axes by rotating S'' around the z'' axis by an angle of γ $(0 \leqq \gamma < 2\pi)$. Thus, we obtain coordinate

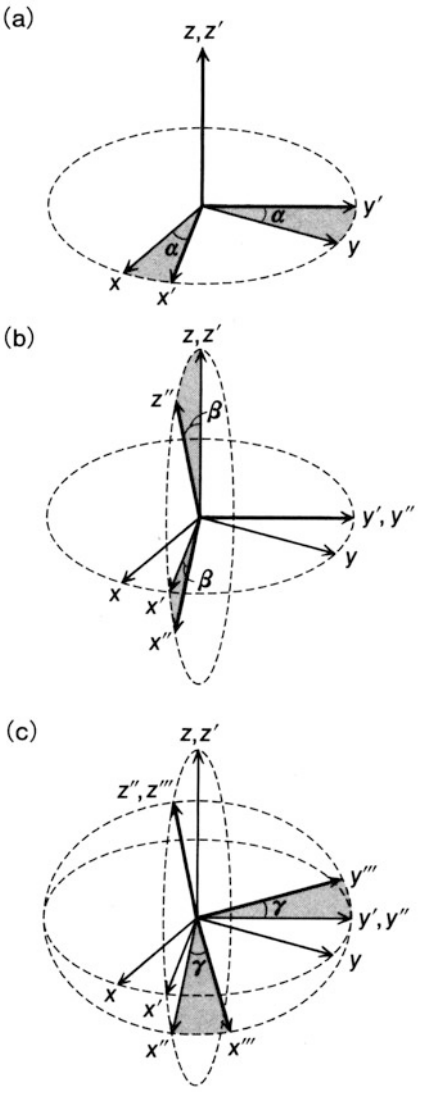

Fig. 3.8 The transformation of a coordinate system by the Euler angles α, β and γ

system S''', described by the new axes x''', y''', and z'''. Here, the z''' axis is identical to the z'' axis.

We will now consider the x''', y''', and z''' axes as the coordinate axes of a molecule-fixed coordinate system, and refer to them as the a, b, and c axes, respectively. To summarize, the space-fixed coordinate system S is transformed into a molecule-fixed coordinate system S''' by being rotated by the Euler angles α, β and γ. This also means that we can express the overall motion of the molecule as changes in the angles α, β and γ per a unit of time, and thereby obtain the kinetic energy of the rotation.

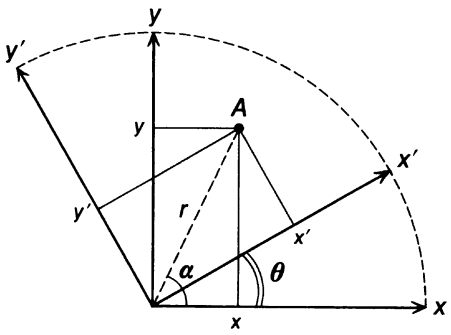

Fig. 3.9 The rotation of a two-dimensional coordinate system

3.3.2 Matrix Representation of the Coordinate Rotation

Here, we will express the coordinate transformation by Euler angles introduced above by a matrix representation. Before we begin, let us consider the case of a point (x, y) in an x-y coordinate system being transformed into a point (x', y') in an x'-y' coordinate system by the rotation of the x and y axes on a two-dimensional plane. When we define r as the distance between the origin of a coordinate system and point (x, y), as shown in Fig. 3.9, the coordinates of this point, A, are given by

$$\begin{cases} x = r\cos\alpha, \\ y = r\sin\alpha. \end{cases} \tag{3.106}$$

When the new coordinate system x'-y' is the x-y coordinate system rotated around its origin by an angle of θ, the x'-y' coordinates of point A are written as

$$\begin{cases} x' = r\cos(\alpha - \theta), \\ y' = r\sin(\alpha - \theta). \end{cases} \tag{3.107}$$

The rotation by the angle of θ is described using the addition theorem as

$$\begin{pmatrix} x' \\ y' \end{pmatrix} = \begin{pmatrix} \cos\theta & \sin\theta \\ -\sin\theta & \cos\theta \end{pmatrix} \begin{pmatrix} x \\ y \end{pmatrix}. \tag{3.108}$$

We will now turn our attention to the rotation by Euler angles α, β and γ discussed above. In each of these steps the two coordinate axes, which are orthogonal to each other, are rotated on their plane. The first rotation is represented by a 3×3 matrix as

$$\boldsymbol{A} = \begin{pmatrix} \cos\alpha & \sin\alpha & 0 \\ -\sin\alpha & \cos\alpha & 0 \\ 0 & 0 & 1 \end{pmatrix}, \tag{3.109}$$

the second rotation as

$$\boldsymbol{B} = \begin{pmatrix} \cos\beta & 0 & -\sin\beta \\ 0 & 1 & 0 \\ \sin\beta & 0 & \cos\beta \end{pmatrix}, \tag{3.110}$$

and the third rotation as

$$\boldsymbol{C} = \begin{pmatrix} \cos\gamma & \sin\gamma & 0 \\ -\sin\gamma & \cos\gamma & 0 \\ 0 & 0 & 1 \end{pmatrix}. \tag{3.111}$$

Therefore, the rotational matrix $\boldsymbol{S}$ in Eq. (3.104) can be expressed as a product of these three rotations as

$$\boldsymbol{S} = \boldsymbol{C}\boldsymbol{B}\boldsymbol{A}. \tag{3.112}$$

The actual expression of $\boldsymbol{S}$, then, is

$$\boldsymbol{S} = \begin{pmatrix} \cos\beta\cos\alpha\cos\gamma & \cos\beta\sin\alpha\cos\gamma & -\sin\beta\cos\gamma \\ \quad -\sin\alpha\sin\gamma & \quad +\cos\alpha\sin\gamma & \\ -\cos\beta\cos\alpha\sin\gamma & -\cos\beta\sin\alpha\sin\gamma & \sin\beta\sin\gamma \\ \quad -\sin\alpha\cos\gamma & \quad +\cos\alpha\cos\gamma & \\ \sin\beta\cos\alpha & \sin\beta\sin\alpha & \cos\beta \end{pmatrix}. \tag{3.113}$$

Matrices representing rotations, such as $\boldsymbol{A}$, $\boldsymbol{B}$, or $\boldsymbol{C}$, are characterized by their transposed matrices being identical to the inverse of the original matrices, that is, ${}^t\boldsymbol{A} = \boldsymbol{A}^{-1}$, ${}^t\boldsymbol{B} = \boldsymbol{B}^{-1}$, and ${}^t\boldsymbol{C} = \boldsymbol{C}^{-1}$. The transposed matrix of $\boldsymbol{A}$, for example, can be written as

$${}^t\boldsymbol{A} = \begin{pmatrix} \cos\alpha & -\sin\alpha & 0 \\ \sin\alpha & \cos\alpha & 0 \\ 0 & 0 & 1 \end{pmatrix}, \tag{3.114}$$

which coincides with the matrix $\boldsymbol{A}$ inverted as $\alpha \to -\alpha$. This signifies that ${}^t\boldsymbol{A}$ corresponds to the operation of rotating a coordinate system by the angle of α in the inverse direction of $\boldsymbol{A}$. Thus, ${}^t\boldsymbol{A}\boldsymbol{A}$ expresses an operation where the coordinate system is rotated clockwise by angle α and then counterclockwise by angle α, which returns it to its original position. This can be confirmed through calculation as

$$\begin{aligned} {}^t\boldsymbol{A}\boldsymbol{A} &= \begin{pmatrix} \cos\alpha & -\sin\alpha & 0 \\ \sin\alpha & \cos\alpha & 0 \\ 0 & 0 & 1 \end{pmatrix} \begin{pmatrix} \cos\alpha & \sin\alpha & 0 \\ -\sin\alpha & \cos\alpha & 0 \\ 0 & 0 & 1 \end{pmatrix} \\ &= \begin{pmatrix} 1 & 0 & 0 \\ 0 & 1 & 0 \\ 0 & 0 & 1 \end{pmatrix} = \boldsymbol{E}. \end{aligned} \tag{3.115}$$

We have thus shown that the transpose of $\boldsymbol{S}$ is identical to the inverse of $\boldsymbol{S}$, that is,

$${}^t\boldsymbol{S} = \boldsymbol{S}^{-1}. \tag{3.116}$$

Indeed, we can see that

$$\begin{aligned} {}^t\boldsymbol{S}\boldsymbol{S} &= {}^t(\boldsymbol{C}\boldsymbol{B}\boldsymbol{A})(\boldsymbol{C}\boldsymbol{B}\boldsymbol{A}) \\ &= {}^t\boldsymbol{A}\,{}^t\boldsymbol{B}\,{}^t\boldsymbol{C}\boldsymbol{C}\boldsymbol{B}\boldsymbol{A} \\ &= \boldsymbol{A}^{-1}\boldsymbol{B}^{-1}\boldsymbol{C}^{-1}\boldsymbol{C}\boldsymbol{B}\boldsymbol{A} \\ &= \boldsymbol{E}. \end{aligned} \tag{3.117}$$

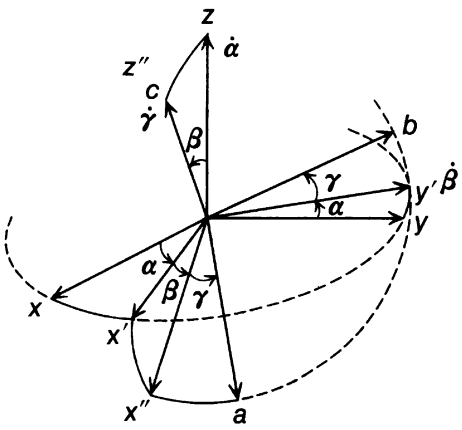

Fig. 3.10 Euler angles and their time derivatives

Therefore, by operating ${}^t\boldsymbol{S}$ from the left on Eq. (3.104), the position vector $\boldsymbol{R}_i = (x_i, y_i, z_i)$ for the i-th atom in the molecule in the space-fixed coordinate system can be derived from its position vector $\boldsymbol{r}_i = (a_i, b_i, c_i)$ in the molecule-fixed coordinate system as

$$\boldsymbol{R}_i = {}^t\boldsymbol{S}\boldsymbol{r}_i, \tag{3.118}$$

namely,

$$\begin{pmatrix} x_i \\ y_i \\ z_i \end{pmatrix} = {}^t\boldsymbol{S} \begin{pmatrix} a_i \\ b_i \\ c_i \end{pmatrix}. \tag{3.119}$$

From Eq. (3.105), we can obtain the kinetic energy of the rotation of the molecule as

$$\begin{aligned} T &= \sum_{i=1}^{n} \frac{1}{2} m_i \left({}^t\dot{\boldsymbol{S}}\boldsymbol{r}_i\right) \cdot \left({}^t\dot{\boldsymbol{S}}\boldsymbol{r}_i\right) \\ &= \sum_{i=1}^{n} \frac{1}{2} m_i \left({}^t\boldsymbol{r}_i \dot{\boldsymbol{S}}^t\dot{\boldsymbol{S}}\boldsymbol{r}_i\right). \end{aligned} \tag{3.120}$$

3.3.3 The Kinetic Energy and Angular Momentum of the Rotation of a Molecule

Let us now consider a space-fixed coordinate system in which a molecule-fixed coordinate system is rotating around its a axis with an angular velocity of ω_a. Here, ω_a can be written using the time derivatives of Euler angles $\dot{\boldsymbol{\alpha}}$, $\dot{\boldsymbol{\beta}}$, $\dot{\boldsymbol{\gamma}}$, as shown in Fig. 3.10, as a sum of their projections to the a axis as

$$\begin{aligned}\omega_a &= (\dot{\boldsymbol{\alpha}})_a + (\dot{\boldsymbol{\beta}})_a + (\dot{\boldsymbol{\gamma}})_a \\ &= -\dot{\boldsymbol{\alpha}} \sin\beta\cos\gamma + \dot{\boldsymbol{\beta}} \sin\gamma, \end{aligned} \tag{3.121}$$

where $\dot{\boldsymbol{\alpha}}$, whose magnitude is $|\dot{\boldsymbol{\alpha}}| \equiv \dot{\alpha} = \frac{\partial\alpha}{\partial t}$, represents the vector in the direction of the axis of the rotation α, that is, the vector in the direction of the z axis, $\dot{\boldsymbol{\beta}}$, whose magnitude is $|\dot{\boldsymbol{\beta}}| \equiv \dot{\beta} = \frac{\partial\beta}{\partial t}$, represents the vector in the direction of the y' axis, and $\dot{\boldsymbol{\gamma}}$, whose magnitude is $|\dot{\boldsymbol{\gamma}}| \equiv \dot{\gamma} = \frac{\partial\gamma}{\partial t}$, represents the vector in the direction of the z'' (or c) axis. Similarly,

$$\omega_b = \dot{\alpha}\sin\beta\sin\gamma + \dot{\beta}\cos\gamma \tag{3.122}$$

$$\omega_c = \dot{\alpha}\cos\beta + \dot{\gamma}. \tag{3.123}$$

From these angular velocities, ω_a, ω_b, and ω_c, we can obtain

$$\boldsymbol{S}\dot{\boldsymbol{S}}^{-1} = \begin{pmatrix} 0 & -\omega_c & \omega_b \\ \omega_c & 0 & -\omega_a \\ -\omega_b & \omega_a & 0 \end{pmatrix}. \tag{3.124}$$

Problem 3.8
Derive Eq. (3.124).

Solution
From

$${}^t\dot{\boldsymbol{S}} = {}^t\dot{\boldsymbol{A}}\,{}^t\boldsymbol{B}\,{}^t\boldsymbol{C} + {}^t\boldsymbol{A}\,{}^t\dot{\boldsymbol{B}}\,{}^t\boldsymbol{C} + {}^t\boldsymbol{A}\,{}^t\boldsymbol{B}\,{}^t\dot{\boldsymbol{C}}, \tag{3.125}$$

we can express $\boldsymbol{S}\,{}^t\dot{\boldsymbol{S}}$ as

$$\begin{aligned}\boldsymbol{S}\,{}^t\dot{\boldsymbol{S}} &= \boldsymbol{C}\boldsymbol{B}\boldsymbol{A}\,{}^t\dot{\boldsymbol{A}}\,{}^t\boldsymbol{B}\,{}^t\boldsymbol{C} + \boldsymbol{C}\boldsymbol{B}\boldsymbol{A}\,{}^t\boldsymbol{A}\,{}^t\dot{\boldsymbol{B}}\,{}^t\boldsymbol{C} + \boldsymbol{C}\boldsymbol{B}\boldsymbol{A}\,{}^t\boldsymbol{A}\,{}^t\boldsymbol{B}\,{}^t\dot{\boldsymbol{C}} \\ &= \boldsymbol{C}\boldsymbol{B}\boldsymbol{A}\,{}^t\dot{\boldsymbol{A}}\,{}^t\boldsymbol{B}\,{}^t\boldsymbol{C} + \boldsymbol{C}\boldsymbol{B}\,{}^t\dot{\boldsymbol{B}}\,{}^t\boldsymbol{C} + \boldsymbol{C}\,{}^t\dot{\boldsymbol{C}}, \end{aligned} \tag{3.126}$$

wherein the first, second, and third terms can be written using Eqs. (3.109), (3.110), and (3.111), as

$$\boldsymbol{C}\boldsymbol{B}\boldsymbol{A}\,{}^t\dot{\boldsymbol{A}}\,{}^t\boldsymbol{B}\,{}^t\boldsymbol{C} = \begin{pmatrix} 0 & -\cos\beta & \sin\gamma\sin\beta \\ \cos\beta & 0 & \cos\gamma\sin\beta \\ -\sin\beta\sin\gamma & -\sin\beta\cos\gamma & 0 \end{pmatrix}\dot{\alpha}, \tag{3.127}$$

$$\boldsymbol{C}\boldsymbol{B}\,{}^t\dot{\boldsymbol{B}}\,{}^t\boldsymbol{C} = \begin{pmatrix} 0 & 0 & \cos\gamma \\ 0 & 0 & -\sin\gamma \\ -\cos\gamma & \sin\gamma & 0 \end{pmatrix}\dot{\beta}, \tag{3.128}$$

$$\boldsymbol{C}\,{}^t\dot{\boldsymbol{C}} = \begin{pmatrix} 0 & -1 & 0 \\ 1 & 0 & 0 \\ 0 & 0 & 0 \end{pmatrix}\dot{\gamma}, \tag{3.129}$$

respectively. Substituting these matrices into Eq. (3.126) and using Eqs. (3.121), (3.122), and (3.123), we can obtain Eq. (3.124) as

$$\boldsymbol{S}\dot{\boldsymbol{S}}^{-1} = \boldsymbol{S}^t\dot{\boldsymbol{S}} = \begin{pmatrix} 0 & -\dot{\alpha}\cos\beta - \dot{\gamma} & \dot{\alpha}\sin\beta\sin\gamma + \dot{\beta}\cos\gamma \\ \dot{\alpha}\cos\beta + \dot{\gamma} & 0 & \dot{\alpha}\sin\beta\cos\gamma - \dot{\beta}\sin\gamma \\ -\dot{\alpha}\sin\beta\sin\gamma - \dot{\beta}\cos\gamma & -\dot{\alpha}\sin\beta\cos\gamma + \dot{\beta}\sin\gamma & 0 \end{pmatrix}$$

$$= \begin{pmatrix} 0 & -\omega_c & \omega_b \\ \omega_c & 0 & -\omega_a \\ -\omega_b & \omega_a & 0 \end{pmatrix}. \qquad \square$$

We will now use Eq. (3.124) to derive the kinetic energy T given in Eq. (3.120). First, from Eq. (3.117), we can write

$$\begin{aligned} \dot{\boldsymbol{S}}^t\dot{\boldsymbol{S}} &= \dot{\boldsymbol{S}}\big({}^t\boldsymbol{S}\boldsymbol{S}\big)^t\dot{\boldsymbol{S}} \\ &= \big(\dot{\boldsymbol{S}}^t\boldsymbol{S}\big)\big(\boldsymbol{S}^t\dot{\boldsymbol{S}}\big) \\ &= {}^t\big(\boldsymbol{S}^t\dot{\boldsymbol{S}}\big)\big(\boldsymbol{S}^t\dot{\boldsymbol{S}}\big). \end{aligned} \tag{3.130}$$

Next, from Eq. (3.124), we obtain

$$\boldsymbol{S}^t\dot{\boldsymbol{S}}\boldsymbol{r}_i = \begin{pmatrix} -\omega_c b_i + \omega_b c_i \\ \omega_c a_i - \omega_a c_i \\ -\omega_b a_i + \omega_a b_i \end{pmatrix}. \tag{3.131}$$

Thus, from Eqs. (3.130) and (3.131), we can derive the kinetic energy of the rotation motion, T (in Eq. (3.120)), as

$$\begin{aligned} T &= \sum_{i=1}^{n} m_i \left\{ \frac{1}{2}\big(b_i^2 + c_i^2\big)\omega_a^2 + \frac{1}{2}\big(c_i^2 + a_i^2\big)\omega_b^2 + \frac{1}{2}\big(a_i^2 + b_i^2\big)\omega_c^2 \right. \\ &\quad \left. - a_i b_i \omega_a \omega_b - b_i c_i \omega_b \omega_c - c_i a_i \omega_c \omega_a \right\} \\ &= \frac{1}{2} I_{aa}\omega_a^2 + \frac{1}{2} I_{bb}\omega_b^2 + \frac{1}{2} I_{cc}\omega_c^2 + I_{ab}\omega_a\omega_b \\ &\quad + I_{bc}\omega_b\omega_c + I_{ca}\omega_c\omega_a, \end{aligned} \tag{3.132}$$

where

$$\begin{cases} I_{aa} = \sum m_i\big(b_i^2 + c_i^2\big), \\ I_{bb} = \sum m_i\big(c_i^2 + a_i^2\big), \\ I_{cc} = \sum m_i\big(a_i^2 + b_i^2\big), \\ I_{ab} = -\sum m_i a_i b_i, \\ I_{bc} = -\sum m_i b_i c_i, \\ I_{ca} = -\sum m_i c_i a_i. \end{cases} \tag{3.133}$$

When a 3×3 matrix $\boldsymbol{I}$, called the inertia tensor, or the moment of inertia tensor, is given by

$$\boldsymbol{I} = \begin{pmatrix} I_{aa} & I_{ab} & I_{ca} \\ I_{ab} & I_{bb} & I_{bc} \\ I_{ca} & I_{bc} & I_{cc} \end{pmatrix}, \tag{3.134}$$

and vector $\boldsymbol{\omega}$ is written as

$$\boldsymbol{\omega} = \begin{pmatrix} \omega_a \\ \omega_b \\ \omega_c \end{pmatrix}, \tag{3.135}$$

the kinetic energy of rotation represented by Eq. (3.132) can be expressed as

$$T = \frac{1}{2} {}^t\boldsymbol{\omega} \boldsymbol{I} \boldsymbol{\omega}. \tag{3.136}$$

Generally speaking, the inertia tensor $\boldsymbol{I}$ has off-diagonal matrix elements, but we can choose the a, b, and c axes of the molecule-fixed coordinate system in such a way as to render the inertia tensor diagonal. When chosen in this manner, the a, b, and c axes of the molecule-fixed coordinate system are called the principal axes of inertia, and the three diagonal elements in this case are called the principal moments of inertia. Representing the principal moments of inertia around the principal axes of inertia a, b, and c as I_A, I_B, and I_C, and choosing the a, b, and c axes so that

$$I_A \leqq I_B \leqq I_C, \tag{3.137}$$

the kinetic energy of the rotational motion can be written as

$$T = \frac{1}{2}\left(I_A \omega_a^2 + I_B \omega_b^2 + I_C \omega_c^2\right). \tag{3.138}$$

As the angular momenta in this molecule-fixed coordinate system are defined as

$$J_a = \frac{\partial T}{\partial \omega_a}, \quad J_b = \frac{\partial T}{\partial \omega_b}, \quad J_c = \frac{\partial T}{\partial \omega_c}, \tag{3.139}$$

we obtain

$$J_a = I_A \omega_a, \quad J_b = I_B \omega_b, \quad J_c = I_C \omega_c. \tag{3.140}$$

Thus, the kinetic energy can be expressed using the angular momenta as

$$T = \frac{J_a^2}{2I_A} + \frac{J_b^2}{2I_B} + \frac{J_c^2}{2I_C}. \tag{3.141}$$

3.3.4 Classification of Molecules by Values of the Moments of Inertia

The various shapes taken by polyatomic molecules can be categorized by the values of the three principal moments of inertia introduced in Sect. 3.3.3 into four types: symmetric top molecules, spherical top molecules, linear molecules, and asymmetric top molecules. Each will be explained below.

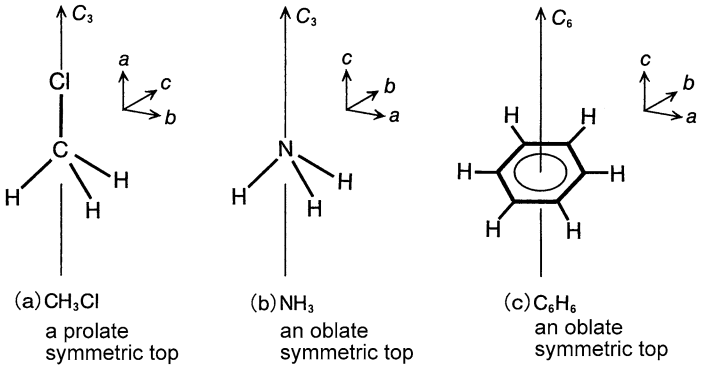

Fig. 3.11 Examples of symmetric tops

Symmetric Top Molecules

A symmetric top is a molecule whose rotational symmetry is equal to or higher than a 3-fold axis, which makes two of its three moments of inertia, I_A, I_B, and I_C, equal to each other. A 3-fold axis is a rotational axis around which the molecule is rotated by an angle of $\frac{2\pi}{3}$ radian $= 120°$ to coincide completely with its original shape. This axis is represented as C_3. Both (a) CH_3Cl and (b) NH_3 in Fig. 3.11 are an example of a symmetric top, which has a 3-fold axis C_3.

An n-fold axis, represented as C_n, is an axis around which the molecule is rotated by an angle of $\frac{2\pi}{n}$ radian to coincide completely with its original shape. Figure 3.11(c) illustrates C_6H_6, a symmetric top with a C_6 axis, or a 6-fold axis. As we can clearly see in Fig. 3.11, there are two more principal axes of inertia that are orthogonal with the C_3 or C_6 axis. In the case of CH_3Cl, the moment of inertia around the C_3 axis is smaller than that around either of the other two principal axes of inertia which are orthogonal with the C_3 axis. From this and Eq. (3.137), we can determine that

$$I_A < I_B = I_C, \tag{3.142a}$$

and that the C_3 axis coincides with the a axis. Such a symmetric top molecule is called a prolate symmetric top.

When the rotational constants are defined by following the definition in Eq. (3.15a) as

$$A = \frac{h}{8\pi^2 I_A}, \quad B = \frac{h}{8\pi^2 I_B}, \quad C = \frac{h}{8\pi^2 I_C}, \tag{3.143}$$

$$A > B = C \tag{3.142b}$$

holds for prolate symmetric tops. In this case, A and B are used as the rotational constants, as C, being equal to B, does not need to be expressed.

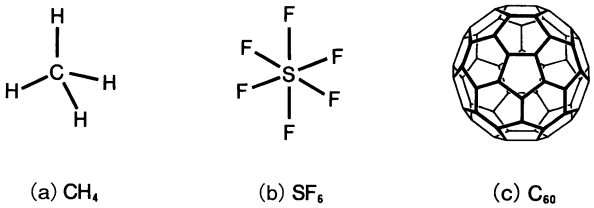

Fig. 3.12 Examples of spherical tops

In the case of NH_3 and C_6H_6, on the other hand, the moment of inertia around the C_3 or C_6 axis is larger than that around either of the other two principal axes of inertia which are orthogonal with the C_3 or C_6 axis. That is,

$$I_A = I_B < I_C. \tag{3.144a}$$

Therefore, the C_3 axis and the C_6 axis each coincides with the c axis of the molecule. Such symmetric tops are called oblate symmetric tops. With the rotational constants of an oblate symmetric top, the relationship

$$A = B > C \tag{3.144b}$$

holds, and therefore the two rotational consonants, B and C, are used to represent the rotational constants.

Spherical Top Molecules

A molecule with even higher symmetry, wherein all three principal moments of inertia are equal, is called a spherical top. Thus, in a spherical top,

$$I_A = I_B = I_C, \tag{3.145a}$$

and the rotation constants satisfy

$$A = B = C. \tag{3.145b}$$

The rotational constant of this molecule is represented by B. Examples of spherical tops include CH_4, SF_{16}, and C_{60}, illustrated in Fig. 3.12.

Linear Molecules

Described in terms of principal moments of inertia, a linear molecule is a molecule for which $I_A = 0$ and $I_B = I_C$ both hold. This is true of diatomic molecules as well. In this case, rotational constant A is not defined, and the two other rotational constants are equal, or $B = C$. Here, too, B is used to represent the rotational constant. Examples of linear molecules include CO_2, OCS, N_2O, HCN, C_3O_2, and HC_3N.

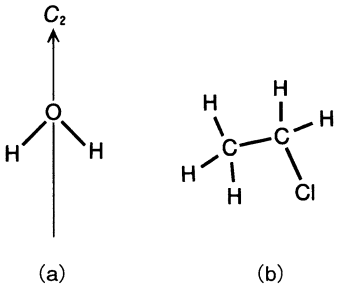

Fig. 3.13 Examples of asymmetric tops: H_2O, an asymmetric top with a C_2 axis (**a**), and CH_3CH_2Cl, an asymmetric top that has no C_2 axis (**b**)

Asymmetric Top Molecules

A molecule that does not fall into any of the above categories is called an asymmetric top, and the values of all three of its principal moments of inertia will be different. That is,

$$I_A < I_B < I_C, \tag{3.146a}$$

or, to write this in terms of rotational constants,

$$A > B > C. \tag{3.146b}$$

As illustrated in Fig. 3.13, examples of molecules classified as asymmetric tops include those which only have C_2-rotational axes and those which do not even have the C_2-rotational axes. For instance, H_2O, SO_2, C_6H_5Cl, $C_6H_5NH_2$, and CH_3CH_2Cl are all asymmetric top molecules. Among these, H_2O, SO_2, and C_6H_5Cl have a C_2 axis, but for each of these three molecular species the values of principal moments of inertia around the a, b, and c axes are all different.

Table 3.1 shows the rotational constants of a few molecular species that are representative of asymmetric top, symmetric top, and spherical top molecules.

3.4 Molecular Rotation from the Point of View of Quantum Mechanics

3.4.1 Quantum Mechanical Hamiltonians of Molecular Rotations

In the previous section, we have learned that the energy of the rotational motion of a rigid rotor is given by Eq. (3.141),

$$T = \frac{J_a^2}{2I_A} + \frac{J_b^2}{2I_B} + \frac{J_c^2}{2I_C},$$

in classical mechanics. Let us now turn to the issue of the quantization of kinetic energy, and derive the eigenenergy and eigenfunction of the molecular rotation.

Table 3.1 Examples of asymmetric tops, symmetric tops, and spherical tops, and their rotational constants[a]

	A/cm^{-1}	B/cm^{-1}	C/cm^{-1}
Asymmetric top molecules			
H_2O	27.878	14.512	9.285
SO_2	2.02736	0.34417	0.293535
CH_3CHO	1.8877	0.33901	0.30354
C_4H_4O	0.315117	0.308434	0.155804
Symmetric top molecules (Prolate top)			
$CH_3{}^{35}Cl$	5.097	0.443401	–
C_2H_6	2.681	0.6621	–
Symmetric top molecules (Oblate top)			
NH_3	–	9.94406	6.2521
NF_3	–	0.356283	0.19477
C_6H_6	–	0.1896	0.0948
Spherical top molecule			
CH_4	–	5.2412	–

[a]To convert the rotational constants from the cm^{-1} unit into the MHz unit, multiply them by 29979.2458

First, from Eq. (3.143), we can rewrite Eq. (3.141) using the rotational constants as

$$T = \frac{2\pi}{\hbar} A J_a^2 + \frac{2\pi}{\hbar} B J_b^2 + \frac{2\pi}{\hbar} C J_c^2. \tag{3.147}$$

We can treat this molecular rotation in quantum mechanics by expressing J_a, J_b, and J_c as angular momentum operators and solving the Schrödinger equation,

$$H\psi = E\psi.$$

As what we have in mind is a rigid rotor that rotates freely in the three-dimensional space, the potential term V in the Hamiltonian

$$H = T + V$$

is zero. That is, by solving the equation

$$T\psi = E\psi \tag{3.148}$$

we can derive the eigenenergy E and the eigenfunction ψ.

The question that remains, then, is which coordinate system to use to represent J_a, J_b, and J_c. In the previous section, we have derived the molecule-fixed a-b-c coordinate system, which rotates with the molecules, by rotating the space-fixed x-y-z system by Euler angles α, β, and γ. Therefore, it is natural to describe the molecular angular momentum using Euler angles α, β, and γ.

As shown in Fig. 3.10, the vector $\dot{\boldsymbol{\alpha}}$, which represents the time derivative of α, is parallel to the rotational axis around which the rotation by α occurs, that is, the

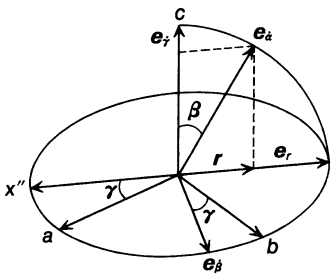

Fig. 3.14 Euler angles and the *a*-*b*-*c* coordinate system

z axis. Let us now define the unit vector pointing in this direction as $\boldsymbol{e}_{\dot\alpha}$. We will similarly define the unit vectors pointing in the directions of $\dot{\boldsymbol{\beta}}$ and $\dot{\boldsymbol{\gamma}}$, which represent the time derivatives of β and γ, respectively, and are on the y' axis and the z'' axis, respectively, as $\boldsymbol{e}_{\dot\beta}$ and $\boldsymbol{e}_{\dot\gamma}$, respectively.

Now, we can use the Schmidt orthogonalization to produce a unit vector $\boldsymbol{e}_r$ in the *a*-*b* plane so that it is orthogonal to $\boldsymbol{e}_{\dot\beta}$. Then we can describe $\boldsymbol{r}$, the projection vector of $\boldsymbol{e}_{\dot\alpha}$ in the *a*-*b* plane, as

$$\boldsymbol{r} = \boldsymbol{e}_{\dot\alpha} - (\boldsymbol{e}_{\dot\alpha} \cdot \boldsymbol{e}_{\dot\gamma})\boldsymbol{e}_{\dot\gamma}, \tag{3.149}$$

as illustrated in Fig. 3.14. Since

$$\boldsymbol{e}_{\dot\alpha} \cdot \boldsymbol{e}_{\dot\gamma} = |\boldsymbol{e}_{\dot\alpha}||\boldsymbol{e}_{\dot\gamma}| \cos\beta = \cos\beta, \tag{3.150}$$

vector $\boldsymbol{r}$ satisfies the relationship

$$\boldsymbol{r} \cdot \boldsymbol{r} = 1 - (\boldsymbol{e}_{\dot\alpha} \cdot \boldsymbol{e}_{\dot\gamma})^2 = \sin^2\beta, \tag{3.151}$$

and therefore the unit vector $\boldsymbol{e}_r$, which points in the direction of the vector $\boldsymbol{r}$, becomes

$$\begin{aligned} \boldsymbol{e}_r &= \frac{\boldsymbol{r}}{|\boldsymbol{r}|} = \frac{\boldsymbol{r}}{\sin\beta} \\ &= \left(\frac{1}{\sin\beta}\right)\boldsymbol{e}_{\dot\alpha} - \left(\frac{\cos\beta}{\sin\beta}\right)\boldsymbol{e}_{\dot\gamma}. \end{aligned} \tag{3.152}$$

Defining the unit vectors in the directions of the a axis and the b axis as $\boldsymbol{a}$ and $\boldsymbol{b}$, respectively, we can describe $\boldsymbol{a}$ and $\boldsymbol{b}$ from Fig. 3.14 as

$$\begin{aligned} \boldsymbol{a} &= -(\cos\gamma)\boldsymbol{e}_r + (\sin\gamma)\boldsymbol{e}_{\dot\beta} \\ &= \left(-\frac{\cos\gamma}{\sin\beta}\right)\boldsymbol{e}_{\dot\alpha} + \left(\frac{\cos\beta\cos\gamma}{\sin\beta}\right)\boldsymbol{e}_{\dot\gamma} + (\sin\gamma)\boldsymbol{e}_{\dot\beta}, \end{aligned} \tag{3.153a}$$

$$\boldsymbol{b} = \left(\frac{\sin\gamma}{\sin\beta}\right)\boldsymbol{e}_{\dot\alpha} - \left(\frac{\cos\beta\sin\gamma}{\sin\beta}\right)\boldsymbol{e}_{\dot\gamma} + (\cos\gamma)\boldsymbol{e}_{\dot\beta}. \tag{3.153b}$$

At the same time, $\boldsymbol{c}$, the unit vector pointing in the direction of the c axis, can be written as

$$\boldsymbol{c} = \boldsymbol{e}_{\dot\gamma}. \tag{3.153c}$$

If we define J_a, J_b, and J_c as the projection of the total angular momentum $\boldsymbol{J}$ onto the a, b, and c axes, respectively, they can be described as

$$J_a = \boldsymbol{a} \cdot \boldsymbol{J}, \quad J_b = \boldsymbol{b} \cdot \boldsymbol{J}, \quad J_c = \boldsymbol{c} \cdot \boldsymbol{J}. \tag{3.154}$$

$\boldsymbol{J}$, in turn, can be described with the Euler angle as

$$J_\alpha = \boldsymbol{e}_{\dot{\alpha}} \cdot \boldsymbol{J}, \quad J_\beta = \boldsymbol{e}_{\dot{\beta}} \cdot \boldsymbol{J}, \quad J_\gamma = \boldsymbol{e}_{\dot{\gamma}} \cdot \boldsymbol{J}. \tag{3.155}$$

Thus by substituting Eqs. (3.153a) through (3.153c) into Eq. (3.154) and by using Eq. (3.155) we can represent J_a, J_b, and J_c by J_α, J_β, and J_γ. Now, in order to shift the discussion into quantum mechanics, we will describe J_α, J_β, and J_γ as the quantum mechanical angular momentum operators

$$J_\alpha = -\mathrm{i}\hbar\frac{\partial}{\partial\alpha}, \quad J_\beta = -\mathrm{i}\hbar\frac{\partial}{\partial\beta}, \quad J_\gamma = -\mathrm{i}\hbar\frac{\partial}{\partial\gamma}, \tag{3.156}$$

and obtain the representations of J_a, J_b, and J_c in quantum mechanics,

$$J_a = -\mathrm{i}\hbar\left\{\left(-\frac{\cos\gamma}{\sin\beta}\right)\frac{\partial}{\partial\alpha} + \left(\frac{\cos\beta\cos\gamma}{\sin\beta}\right)\frac{\partial}{\partial\gamma} + \sin\gamma\frac{\partial}{\partial\beta}\right\}, \tag{3.157a}$$

$$J_b = -\mathrm{i}\hbar\left\{\left(\frac{\sin\gamma}{\sin\beta}\right)\frac{\partial}{\partial\alpha} - \left(\frac{\cos\beta\sin\gamma}{\sin\beta}\right)\frac{\partial}{\partial\gamma} + \cos\gamma\frac{\partial}{\partial\beta}\right\}, \tag{3.157b}$$

$$J_c = -\mathrm{i}\hbar\frac{\partial}{\partial\gamma}. \tag{3.157c}$$

It must be noted here that the a, b, and c axes at this point only represent the molecule-fixed right-hand coordinate system, and not necessary the principal axes of inertia.

It is when we substitute J_a, J_b, and J_c in Eqs. (3.157a) through (3.157c) into the rotational kinetic energy represented by the principal inertia axis system given as Eq. (3.141) and Eq. (3.147), that is,

$$T = \frac{J_a^2}{2I_A} + \frac{J_b^2}{2I_B} + \frac{J_c^2}{2I_C} = \frac{2\pi}{\hbar}AJ_a^2 + \frac{2\pi}{\hbar}BJ_b^2 + \frac{2\pi}{\hbar}CJ_c^2,$$

that the a, b, and c axes come to coincide with the principal inertia axis system. Still, the a-b-c coordinate system made to coincide with the principal inertia axis system may not necessary fulfill the conventional relationship $A \geqq B \geqq C$. Therefore, the discussion here is valid for all possible size relationships between A, B, and C.

Having derived the quantum-mechanical representation of the kinetic energy of the rotation of a rigid body, we are now ready to solve the Schrödinger equation (3.148). However, it is difficult to solve the Schrödinger equation for asymmetric top molecules, whose rotational constants A, B, and C are all different from each other. Therefore, we will first derive the concrete representation of the Schrödinger equation for a symmetric top molecule, a molecule with two equal rotational constants, in order to facilitate our understanding of the quantum mechanics of a rigid body rotation.

Supposing that the two rotational constants A and B among A, B, and C, take the same value, that is, $A = B$, the kinetic energy can be described as

$$T = \frac{2\pi}{\hbar} B \boldsymbol{J}^2 + \frac{2\pi}{\hbar}(C - B) J_c^2, \tag{3.158}$$

whereas if we suppose B and C take the same value, that is, $B = C$, it will be written as

$$T = \frac{2\pi}{\hbar} B \boldsymbol{J}^2 + \frac{2\pi}{\hbar}(A - B) J_a^2. \tag{3.159}$$

As Eqs. (3.157a) through (3.157c) show us that the representation of J_c is simpler than that of J_a or J_b, we will choose to use Eq. (3.158) to describe T. Incidentally, when the relationship $A \geqq B \geqq C$ is satisfied, Eq. (3.158) is suited for describing an oblate top molecule, and Eq. (3.159) for describing a prolate top molecule.

First, we evaluate $\boldsymbol{J}^2$ by using Eqs. (3.157a) through (3.157c), and obtain

$$\begin{aligned} \boldsymbol{J}^2 &= J_a^2 + J_b^2 + J_c^2 \\ &= (-\mathrm{i}\hbar)^2 \left\{ \frac{\partial^2}{\partial \beta^2} + \cot\beta \frac{\partial}{\partial \beta} + \frac{1}{\sin^2\beta}\left(\frac{\partial^2}{\partial \alpha^2} + \frac{\partial^2}{\partial \gamma^2} \right) - \frac{2\cos\beta}{\sin^2\beta} \frac{\partial^2}{\partial \alpha \partial \gamma} \right\}. \end{aligned} \tag{3.160}$$

The first two terms in the { } bracket can be described as

$$\frac{\partial^2}{\partial \beta^2} + \cot\beta \frac{\partial}{\partial \beta} = \frac{1}{\sin\beta} \frac{\partial}{\partial \beta}\left(\sin\beta \frac{\partial}{\partial \beta} \right). \tag{3.161}$$

Thus by adopting Eq. (3.158) and using Eqs. (3.157c) and (3.160), we can derive the Schrödinger equation for a symmetric top molecule as

$$\begin{aligned} (-\mathrm{i}\hbar)^2 \Bigg[\frac{2\pi}{\hbar} B \Bigg\{ \frac{1}{\sin\beta} \frac{\partial}{\partial \beta}\left(\sin\beta \frac{\partial}{\partial \beta} \right) + \frac{1}{\sin^2\beta}\left(\frac{\partial^2}{\partial \alpha^2} + \frac{\partial^2}{\partial \gamma^2} \right) \\ - \frac{2\cos\beta}{\sin^2\beta} \frac{\partial^2}{\partial \alpha \partial \gamma} \Bigg\} + \frac{2\pi}{\hbar}(C - B) \frac{\partial^2}{\partial \gamma^2} \Bigg] \psi = E\psi. \end{aligned} \tag{3.162}$$

In Eq. (3.162), α and γ appear only in the form of $\frac{\partial}{\partial \alpha}$ and $\frac{\partial}{\partial \gamma}$. Therefore, we can easily separate the variables and derive

$$\psi_{jkm}(\alpha, \beta, \gamma) = N_{jkm} \Theta_{jkm}(\beta) \mathrm{e}^{\mathrm{i}m\alpha} \mathrm{e}^{\mathrm{i}k\gamma}, \tag{3.163}$$

where N_{jkm} is the normalization constant.

Substituting Eq. (3.163) into Eq. (3.162) and dividing both sides of this formula by $N_{jkm}\mathrm{e}^{\mathrm{i}m\alpha}\mathrm{e}^{\mathrm{i}k\gamma}$, we can derive the differential equation for $\Theta_{jkm}(\beta)$,

$$\begin{aligned} -hB \left\{ \frac{1}{\sin\beta} \frac{\partial}{\partial \beta}\left(\sin\beta \frac{\partial}{\partial \beta} \right) - \frac{(m - k\cos\beta)^2}{\sin^2\beta} \right\} \Theta_{jkm}(\beta) \\ = \left(E - hCk^2 \right) \Theta_{jkm}(\beta). \end{aligned} \tag{3.164}$$

The wave function of Eq. (3.163) with $\Theta_{jkm}(\beta)$ derived by solving Eq. (3.164) is the rotational wave function of the symmetric top molecule.

If $k = 0$, Eq. (3.164) becomes

$$-hB\left\{\frac{1}{\sin\beta}\frac{\partial}{\partial\beta}\left(\sin\beta\frac{\partial}{\partial\beta}\right)-\frac{m^2}{\sin^2\beta}\right\}\Theta_{j0m}(\beta)=E\Theta_{j0m}(\beta). \tag{3.165}$$

This formula corresponds to Eq. (3.102) as derived from the Schrödinger equation for the rotation of diatomic molecules or linear molecules, and is thought to give the eigenvalue $E=\frac{\hbar^2}{2I_B}j(j+1)$. Also, comparing it with Eq. (3.102), we see that $\Theta_{j0m}(\beta)$ in Eq. (3.165) corresponds to $\Theta_{jm}(\theta)$ in Eq. (3.102). This signifies that the physical meaning of the polar angle θ in the polar coordinate and that of the Euler angle β are the same. Indeed, as is apparent from the definitions of the polar angle θ and the azimuthal angle ϕ in Fig. 3.2 and from the definitions of the Euler angles in Fig. 3.8, α can be substituted by ϕ, and β by θ.

We have now reached an understanding of $\Theta_{j0m}(\beta)$. Turning our attention then to the question of deriving $\Theta_{jkm}(\beta)$ when $k \neq 0$, we learn that, as will be discussed in Sect. 3.4.3, we can derive representations of rotational wave functions of symmetric top molecules by using both the angular momentum operators in the molecule-fixed system and those in the space-fixed coordinate system without evaluating $\Theta_{jkm}(\beta)$ directly. Let us then study the angular momentum operators, J_a, J_b, and J_c, in the molecule-fixed coordinate system described as Eqs. (3.157a) through (3.157c).

3.4.2 *Angular Momenta of Overall Rotations in Molecule-Fixed Coordinate Systems*

The angular momentum operators J_a, J_b, and J_c in a molecule-fixed coordinate system derived in Sect. 3.4.1 can be characterized by their commutation relations with each other. The commutation relations among J_a, J_b, and J_c can be derived through their representations using Euler angles α, β, and γ in Eqs. (3.157a) through (3.157c). By carefully calculating J_aJ_b and J_bJ_a, we can derive the commutator of J_a and J_b as

$$\begin{aligned}[J_a, J_b] &\equiv J_aJ_b - J_bJ_a \\ &= (-\mathrm{i}\hbar)^2\frac{\partial}{\partial\gamma} \\ &= -\mathrm{i}\hbar J_c.\end{aligned} \tag{3.166a}$$

Similarly, we can derive

$$[J_b, J_c] = -\mathrm{i}\hbar J_a, \tag{3.166b}$$

$$[J_c, J_a] = -\mathrm{i}\hbar J_b. \tag{3.166c}$$

These commutation relations look similar to, but are different from those among the angular momentum operators J_x, J_y, and J_z in a space-fixed coordinate described in Eqs. (3.40a) through (3.40c) in Sect. 3.2.2,

$$\begin{cases} [J_x, J_y] = \mathrm{i}\hbar J_z, \\ [J_y, J_z] = \mathrm{i}\hbar J_x, \\ [J_z, J_x] = \mathrm{i}\hbar J_y. \end{cases}$$

Problem 3.9
Write the angular momentum operators in the space-fixed coordinate system, J_x, J_y, and J_z, using Euler angles α, β, and γ.

Solution
As in the case of the molecule-fixed coordinate system, we first derive the projection of the unit vector $\boldsymbol{e}_{\dot{\gamma}}$ to the x-y surface, and define a unit vector which points in this direction as $\boldsymbol{e}_r$, which is written as

$$\boldsymbol{e}_r = \frac{\boldsymbol{e}_{\dot{\gamma}} - (\cos\beta)\boldsymbol{e}_{\dot{\alpha}}}{\sin\beta}. \tag{3.167}$$

We can represent $\boldsymbol{x}$ and $\boldsymbol{y}$ by $\boldsymbol{e}_r$ and $\boldsymbol{e}_{\dot{\beta}}$ as

$$\boldsymbol{x} = (\boldsymbol{e}_r \cdot \boldsymbol{x})\boldsymbol{e}_r + (\boldsymbol{e}_{\dot{\beta}} \cdot \boldsymbol{x})\boldsymbol{e}_{\dot{\beta}} = (\cos\alpha)\boldsymbol{e}_r - (\sin\alpha)\boldsymbol{e}_{\dot{\beta}}, \tag{3.168a}$$

$$\boldsymbol{y} = (\sin\alpha)\boldsymbol{e}_r + (\cos\alpha)\boldsymbol{e}_{\dot{\beta}}. \tag{3.168b}$$

Using these equations, we can derive

$$\begin{aligned} J_x &= \boldsymbol{x} \cdot \boldsymbol{J} = \left\{(\cos\alpha)\boldsymbol{e}_r - (\sin\alpha)\boldsymbol{e}_{\dot{\beta}}\right\} \cdot (J_\alpha \boldsymbol{e}_{\dot{\alpha}} + J_\beta \boldsymbol{e}_{\dot{\beta}} + J_\gamma \boldsymbol{e}_{\dot{\gamma}}) \\ &= -\mathrm{i}\hbar\left\{\left(\frac{\cos\alpha}{\sin\beta}\right)\frac{\partial}{\partial\gamma} - \left(\frac{\cos\alpha\cos\beta}{\sin\beta}\right)\frac{\partial}{\partial\alpha} - \sin\alpha\frac{\partial}{\partial\beta}\right\}, \end{aligned} \tag{3.169a}$$

$$J_y = \boldsymbol{y} \cdot \boldsymbol{J} = -\mathrm{i}\hbar\left\{\left(\frac{\sin\alpha}{\sin\beta}\right)\frac{\partial}{\partial\gamma} - \left(\frac{\sin\alpha\cos\beta}{\sin\beta}\right)\frac{\partial}{\partial\alpha} + \cos\alpha\frac{\partial}{\partial\beta}\right\}, \tag{3.169b}$$

$$J_z = \boldsymbol{z} \cdot \boldsymbol{J} = -\mathrm{i}\hbar\frac{\partial}{\partial\alpha}. \tag{3.169c}$$

□

Problem 3.10
Using the solution to Problem 3.9, confirm the commutation relations among J_x, J_y, and J_z.

Solution
By calculating $[J_x, J_y] = J_x J_y - J_y J_x$ with close attention to the order of the differentiations, we can indeed obtain the relation $[J_x, J_y] = \mathrm{i}\hbar J_z$. Similarly, we can show that $[J_y, J_z] = \mathrm{i}\hbar J_x$, $[J_z, J_x] = \mathrm{i}\hbar J_y$. □

We will now obtain the eigenfunction and eigenvalue of the angular momentum in the molecule-fixed coordinate system by using the commutation relations among

its angular momentum operators, as we have done for the angular momentum in the space-fixed coordinate system in Sect. 3.2. In this instance, the role played by J_c corresponds to that of J_z in Sect. 3.2.

Defining operators J^+ and J^-, respectively, as in the case of the space-fixed coordinate system, as

$$J^+ \equiv J_a + \mathrm{i}J_b, \tag{3.170a}$$

$$J^- \equiv J_a - \mathrm{i}J_b, \tag{3.170b}$$

we can show that, for $\{|j,k\rangle\}$, the set of eigenfunctions shared by $\boldsymbol{J}^2$ and J_c,

$$\boldsymbol{J}^2|j,k\rangle = j(j+1)\hbar^2|j,k\rangle \tag{3.171}$$

$$J_c|j,k\rangle = k\hbar|j,k\rangle \quad \big(k=-j,-(j-1),\ldots,j-1,j\big) \tag{3.172}$$

$$J^{\pm}|j,k\rangle = \sqrt{j(j+1)-k(k\mp1)}\hbar|j,k\mp1\rangle. \tag{3.173}$$

Problem 3.11
Following the same procedures as has been used in Sect. 3.2, derive Eqs. (3.171) through (3.173). Pay close attention to the difference of the ± signs.

Solution
J_a, J_b, and J_c are not commutative with each other, but $\boldsymbol{J}^2 = J_a^2 + J_b^2 + J_c^2$ is commutative with J_a. In other words, we can show from the commutation relations (3.166a) through (3.166c) that

$$\big[J_a, \boldsymbol{J}^2\big] = \big[J_b, \boldsymbol{J}^2\big] = \big[J_c, \boldsymbol{J}^2\big] = 0. \tag{3.174}$$

This means that if we choose the c axis as the quantizing axis there will be $\{|\lambda,k\rangle\}$, a set of eigenfunctions shared by $\boldsymbol{J}^2$ and J_c, and that this can be described as

$$\boldsymbol{J}^2|\lambda,k\rangle = \lambda\hbar^2|\lambda,k\rangle,$$
$$J_c|\lambda,k\rangle = k\hbar|\lambda,k\rangle.$$

We can also show

$$\begin{aligned}\boldsymbol{J}^2\big(J^{\pm}|\lambda,k\rangle\big) &= J^{\pm}\big(\boldsymbol{J}^2|\lambda,k\rangle\big)\\ &= J^{\pm}\big(\lambda\hbar^2|\lambda,k\rangle\big)\\ &= \lambda\hbar^2\big(J^{\pm}|\lambda,k\rangle\big)\end{aligned} \tag{3.175}$$

and

$$\begin{aligned}J_c\big(J^{\pm}|\lambda,k\rangle\big) &= J^{\pm}J_c|\lambda,k\rangle \mp \hbar J^{\pm}|\lambda,k\rangle\\ &= J^{\pm}k\hbar|\lambda,k\rangle \mp \hbar J^{\pm}|\lambda,k\rangle\\ &= (k\mp1)\hbar\big(J^{\pm}|\lambda,k\rangle\big),\end{aligned} \tag{3.176}$$

in which we use $[J_c, J^{\pm}] = \mp\hbar J^{\pm}$, that is, $J_cJ^{\pm} - J^{\pm}J_c = \mp\hbar J^{\pm}$.

This shows that, while $J^{\pm}|\lambda, k\rangle$ is indeed the common eigenfunction for $\boldsymbol{J}^2$ and J_c, the eigenvalue for J_c increases and decreases by $\hbar$ when J^- and J^+, respectively, are operated on $|\lambda, k\rangle$. That is, J^+ acts as a lowering operator and J^- as a raising operator, as shown below:

$$|\lambda, k\rangle \xrightarrow{J^+} |\lambda, k-1\rangle \xrightarrow{J^+} |\lambda, k-2\rangle \xrightarrow{J^+} \cdots, \tag{3.177a}$$

$$|\lambda, k\rangle \xrightarrow{J^-} |\lambda, k+1\rangle \xrightarrow{J^-} |\lambda, k+2\rangle \xrightarrow{J^-} \cdots. \tag{3.177b}$$

Thus, we can see that the signs appearing in the raising and lowering operators in the molecule-fixed coordinate system are reversed from those of the raising and lowering operators in the space-fixed coordinate system.

Let us now evaluate the norm of $J^{\pm}|\lambda, k\rangle$, as we have done in the case of the space-fixed coordinate system. From

$$\begin{aligned} \left|J^{\pm}|\lambda, k\rangle\right|^2 &= \langle\lambda, k|J^{\mp}J^{\pm}|\lambda, k\rangle \\ &= \langle\lambda, k|\boldsymbol{J}^2 - J_c^2 \pm \hbar J_c|\lambda, k\rangle \\ &= \langle\lambda, k|\boldsymbol{J}^2 - J_c(J_c \mp \hbar)|\lambda, k\rangle \\ &= \left\{\lambda - k(k \mp 1)\right\}\hbar^2\langle\lambda, k|\lambda, k\rangle, \end{aligned} \tag{3.178}$$

we can derive

$$\lambda - k(k \mp 1) \geqq 0,$$

which can be rewritten as

$$\lambda \geqq k(k \mp 1) = k^2 \mp k.$$

This shows that there are upper and lower limits for k, which we will define as $k_{\max}$ and $k_{\min}$, respectively. Then, for both the raising and lowering operators, $J^-|\lambda, k_{\max}\rangle = 0$ and $J^+|\lambda, k_{\min}\rangle = 0$ hold. First, from $J^+J^-|\lambda, k_{\max}\rangle = \{\boldsymbol{J}^2 - J_c(J_c + \hbar)\}|\lambda, k_{\max}\rangle = 0$, we can derive

$$\lambda - k_{\max}(k_{\max} + 1) = 0. \tag{3.179}$$

Similarly, from $J^-J^+|\lambda, k_{\min}\rangle = \{\boldsymbol{J}^2 - J_c(J_c - \hbar)\}|\lambda, k_{\min}\rangle = 0$, we can derive

$$\lambda - k_{\min}(k_{\min} - 1) = 0. \tag{3.180}$$

Eliminating λ from Eqs. (3.179) and (3.180), we obtain

$$(k_{\max} + k_{\min})(k_{\max} - k_{\min} + 1) = 0.$$

Since $k_{\max} \geqq k_{\min}$, the value of the content of the second pair of parentheses necessarily becomes larger than 0, and therefore

$$k_{\max} + k_{\min} = 0$$

must hold. If we define j as

$$j = k_{\max} = -k_{\min},$$

then

$$\lambda = j(j+1),$$

and we know from $k_{\max} - k_{\min} = j - (-j) = 2j \geqq 0$ that $2j$ is either 0 or a positive integer. Thus, we have shown that

$$\begin{aligned} \boldsymbol{J}^2|j,k\rangle &= j(j+1)\hbar^2|j,k\rangle \\ J_c|j,k\rangle &= k\hbar|j,k\rangle \quad \big(k=-j,-(j-1),\ldots,j-1,j\big), \end{aligned}$$

and, from Eq. (3.178), that

$$J^{\pm}|j,k\rangle = \sqrt{j(j+1)-k(k\mp1)}\hbar|j,k\mp1\rangle.$$

Here, too, as in Eqs. (3.88a) and (3.88b), we have adopted the Condon-Shortley phase convention. □

3.4.3 *Energy Level Diagrams of Prolate and Oblate Top Molecules*

From the discussion in Sect. 3.4.1, we can conclude that the wave function of a symmetric top molecule can be represented as

$$|j,k,m\rangle = N_{jkm}\Theta_{jkm}(\theta)\mathrm{e}^{\mathrm{i}k\gamma}\mathrm{e}^{\mathrm{i}m\phi}, \tag{3.181}$$

and that this constitutes the system of eigenfunctions shared by $\boldsymbol{J}^2$ and by J_z and J_c, which are commutative with $\boldsymbol{J}^2$. To summarize,

$$\boldsymbol{J}^2|j,k,m\rangle = j(j+1)\hbar^2|j,k,m\rangle, \tag{3.182}$$

$$J_c|j,k,m\rangle = k\hbar|j,k,m\rangle, \tag{3.183}$$

$$J_z|j,k,m\rangle = m\hbar|j,k,m\rangle, \tag{3.184}$$

$$(J_a \pm \mathrm{i}J_b)|j,k,m\rangle = \sqrt{j(j+1)-k(k\mp1)}\hbar|j,k\mp1,m\rangle, \tag{3.185}$$

$$(J_x \pm \mathrm{i}J_y)|j,k,m\rangle = \sqrt{j(j+1)-m(m\pm1)}\hbar|j,k,m\pm1\rangle. \tag{3.186}$$

From Eqs. (3.185) and (3.186), we can see that as long as we are provided with a state in which $k = m = 0$, or in other words $|j,0,0\rangle$, we can obtain the eigenfunction $|j,k,m\rangle$ by applying the raising and lowering operators. That is to say, if $k > 0$ and $m > 0$,

$$|j,k,m\rangle = N_{jkm}^{(+,+)}(J_a - \mathrm{i}J_b)^k(J_x + \mathrm{i}J_y)^m|j,0,0\rangle, \tag{3.187a}$$

$$|j,-k,m\rangle = N_{jkm}^{(-,+)}(J_a + \mathrm{i}J_b)^k(J_x + \mathrm{i}J_y)^m|j,0,0\rangle, \tag{3.187b}$$

$$|j,k,-m\rangle = N_{jkm}^{(+,-)}(J_a - \mathrm{i}J_b)^k(J_x - \mathrm{i}J_y)^m|j,0,0\rangle, \tag{3.187c}$$

$$|j,-k,-m\rangle = N_{jkm}^{(-,-)}(J_a + \mathrm{i}J_b)^k(J_x - \mathrm{i}J_y)^m|j,0,0\rangle, \tag{3.187d}$$

where $N_{jkm}^{(+,+)}$ and the other corresponding coefficients are normalization constants.

Let us then calculate the wave function $|j,0,0\rangle$. As we have learned in Sect. 3.4.1, $\Theta_{j0m}(\theta) = \Theta_{jm}(\theta)$, and therefore, from Eq. (3.181), we can derive

$$|j,0,0\rangle = N_{j00}\Theta_{j0}(\theta). \tag{3.188}$$

As shown in Sect. 3.2.5, the spherical harmonics ψ_{jm} can be written as

$$\psi_{jm} = \Theta_{jm}(\theta)\Phi_m(\phi) = \frac{1}{\sqrt{2\pi}}\Theta_{jm}(\theta)\mathrm{e}^{\mathrm{i}m\phi}, \tag{3.189}$$

which allows us to use Eq. (3.99) to derive the normalized wave function

$$|j,0,0\rangle = \Theta_{j0}(\theta) = \sqrt{j+\frac{1}{2}}P_j(\cos\theta). \tag{3.190}$$

When we operate Eq. (3.158), the rotational Hamiltonian for symmetric top molecules, that is,

$$H = T = \frac{2\pi}{\hbar}B\boldsymbol{J}^2 + \frac{2\pi}{\hbar}(C-B)J_c^2, \tag{3.191}$$

on $|j,k,m\rangle$, we can obtain from Eqs. (3.182) and (3.183)

$$H|j,k,m\rangle = \left\{hBj(j+1) + h(C-B)k^2\right\}|j,k,m\rangle. \tag{3.192}$$

Therefore, the eigenenergy can be expressed as

$$E_{jk} = hBj(j+1) + h(C-B)k^2. \tag{3.193}$$

This shows that $|j,k,m\rangle$ is indeed the eigenfunction of the Hamiltonian for symmetric top molecules.

The quantization axis c can be set to the principal axis of inertia a by making the cyclic permutation

$$\begin{aligned} a &\longrightarrow b, \\ b &\longrightarrow c, \\ c &\longrightarrow a. \end{aligned}$$

Then, the substitution $(j,k) \to (J,K_a)$ under the condition $A > B = C$ yields the eigenenergy of the prolate symmetric top molecule as

$$E_{JK_a} = hBJ(J+1) + h(A-B)K_a^2. \tag{3.194}$$

In order to set the quantization axis c to the principal axis of inertia c, on the other hand, the substitution $(j,k) \to (J,K_c)$ is made to Eq. (3.193) to yield the eigenenergy

$$E_{JK_c} = hBJ(J+1) + h(C-B)K_c^2. \tag{3.195}$$

If the condition $A = B > C$ is satisfied, Eq. (3.195) represents the eigenenergy of an oblate top molecule. The eigenenergies of symmetric top molecules described as Eqs. (3.194) and (3.195) can be schematically shown as Fig. 3.15. Commonly, both K_a and K_c are simply written as K.

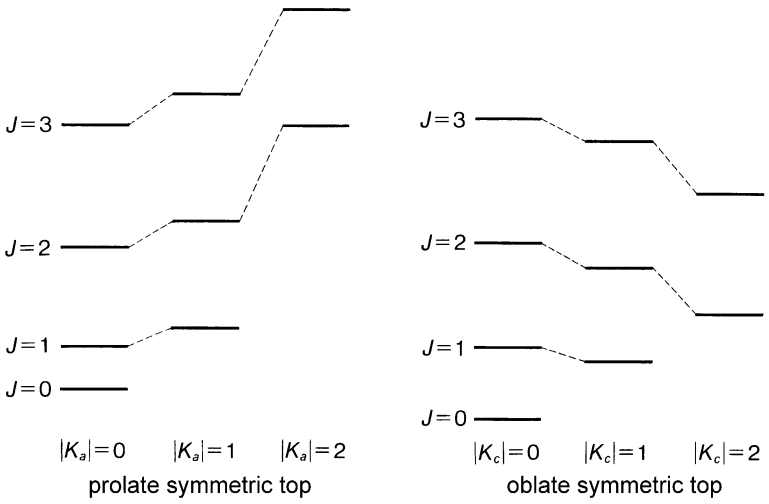

Fig. 3.15 The eigenenergy diagrams of a symmetric top molecule

3.4.4 Energy Levels of Diatomic and Linear Molecules

We have already learned that the rotational level energies of diatomic molecules and linear molecules are expressed using the quantum number J of a total angular momentum by Eq. (3.15a), that is,

$$E_J = hBJ(J+1).$$

Then, as we did in the previous subsection, let us treat diatomic molecules and linear molecules using a molecule-fixed coordinate system. If we define the inertia axis connecting the atoms as the a axis, as long as we regard these atoms as mass points we cannot define the rotation around the a axis. Therefore, we will only treat the rotational motion around the b axis and that around the c axis. For these rotations, it is obvious that

$$I_B = I_C \tag{3.196}$$

holds. Therefore, the Hamiltonian of the rotational motion can be written as

$$H = T = \frac{J_b^2}{2I_B} + \frac{J_c^2}{2I_C} = \frac{2\pi}{\hbar} B\left(J_b^2 + J_c^2\right). \tag{3.197}$$

Because the total angular momentum $\boldsymbol{J}$ of the rotation of a rigid body is written as

$$\boldsymbol{J}^2 = J_b^2 + J_c^2, \tag{3.198}$$

Eq. (3.197) is expressed as

$$H = \frac{2\pi}{\hbar} B\boldsymbol{J}^2. \tag{3.199}$$

When we compare this Eq. (3.199) with the Hamiltonian of a symmetric top molecule expressed as Eqs. (3.158) and (3.159), we see that Eq. (3.199) is obtained by setting $J_a = 0$ or $J_c = 0$ in the Hamiltonian of a symmetric top molecule. This is clearly shown in Eq. (3.165), that is, the wave function $|J, 0, M\rangle$, obtained by the replacements $j \to J$, $k = 0$, and $m \to M$ in Eq. (3.181) representing the wave function of a symmetric top molecule, can be regarded as the wave function of a diatomic molecule or a linear molecule. From Eq. (3.182), we obtain

$$\boldsymbol{J}^2|J, 0, M\rangle = J(J+1)\hbar^2|J, 0, M\rangle. \tag{3.200}$$

Therefore, the eigenenergy can be written as

$$E_J = hBJ(J+1). \tag{3.201}$$

As we have already learned, if we specify one value for J, there will be $(2J + 1)$ rotational wave functions $|J, 0, M\rangle$ with different M values $(M = -J, -J + 1, \ldots, J + 1, J)$. The level energies of these $(2J + 1)$ functions can be expressed as in Eq. (3.201), regardless of the value of M. We describe this situation as the energy level specified by J being $(2J + 1)$-fold degenerate, or as the degeneracy of the energy level being $2J + 1$.

3.4.5 Energy Levels of Spherical Top Molecules

The moment of inertia of a spherical top molecule fulfill the relationship $I_A = I_B = I_C$, and the Hamiltonian of the rotational motion can be written as

$$H = T = \frac{1}{2I_B}\left(J_a^2 + J_b^2 + J_c^2\right) = \frac{2\pi}{\hbar} B\boldsymbol{J}^2. \tag{3.202}$$

Therefore, we can obtain its eigenfunction as $|J, K, M\rangle$ by making the replacements

$$j \to J, \quad k \to K, \quad m \to M$$

in Eq. (3.181), which gives us

$$H|J, K, M\rangle = hBJ(J+1)|J, K, M\rangle. \tag{3.203}$$

Each state specified by one J value has a $(2J + 1)$-fold degeneracy with respect to M, as well as a $(2J + 1)$-fold degeneracy with respect to K. Consequently, the total degeneracy becomes $(2J + 1)^2$.

3.4.6 Energy Levels of Asymmetric Top Molecules

We are now ready to derive the rotational energy levels of an asymmetric molecule whose three rotational constants have different values. Let $A > B > C$. What is immediately clear is that the eigenfunction of a symmetric top molecule, $|J, K, M\rangle$,

cannot simply be regarded as the eigenfunction of an asymmetric top molecule as it is. We will then describe the state which has the total angular momentum $\boldsymbol{J}$ as one of the linear combinations of $|J, K, M\rangle$ as

$$\psi_J = \sum_K \sum_M |J, K, M\rangle, \tag{3.204}$$

and look for wave functions that can diagonalize the matrix of the rotational Hamiltonian

$$H = \frac{2\pi}{\hbar} A J_a^2 + \frac{2\pi}{\hbar} B J_b^2 + \frac{2\pi}{\hbar} C J_c^2. \tag{3.205}$$

To this end, we first describe H in terms of $\boldsymbol{J}^2$, J_c^2, J^+, and J^-. As the definitions of J^+ and J^- given in Eqs. (3.170a) and (3.170b) allow us to represent J^+J^+ and J^-J^- as

$$\begin{aligned} J^+J^+ &= (J_a + \mathrm{i}J_b)(J_a + \mathrm{i}J_b) \\ &= J_a^2 + \mathrm{i}J_aJ_b + \mathrm{i}J_bJ_a - J_b^2, \\ J^-J^- &= (J_a - \mathrm{i}J_b)(J_a - \mathrm{i}J_b) \\ &= J_a^2 - \mathrm{i}J_aJ_b - \mathrm{i}J_bJ_a - J_b^2, \end{aligned}$$

we can derive

$$\begin{aligned} J^+J^+ + J^-J^- &= \left(J^+\right)^2 + \left(J^-\right)^2 \\ &= 2\left(J_a^2 - J_b^2\right). \end{aligned} \tag{3.206}$$

Then, let p, q, and r be such coefficients that the Hamiltonian can be written as

$$H = \frac{2\pi}{\hbar} p\boldsymbol{J}^2 + \frac{2\pi}{\hbar} q J_c^2 + \frac{2\pi}{\hbar} r\left\{\left(J^+\right)^2 + \left(J^-\right)^2\right\}. \tag{3.207}$$

Using Eq. (3.206) and the equation $\boldsymbol{J}^2 = J_a^2 + J_b^2 + J_c^2$, the Hamiltonian of Eq. (3.207) can be described using J_a^2, J_b^2, and J_c^2 as

$$H = \frac{2\pi}{\hbar}(p + 2r)J_a^2 + \frac{2\pi}{\hbar}(p - 2r)J_b^2 + \frac{2\pi}{\hbar}(p + q)J_c^2. \tag{3.208}$$

When we compare Eq. (3.208) with Eq. (3.205), we can see that A, B, and C can be written using p, q, and r as

$$A = p + 2r, \quad B = p - 2r, \quad C = p + q, \tag{3.209}$$

which means that p, q, and r can be written in terms of A, B, and C as

$$p = \frac{1}{2}(A + B), \quad q = C - \frac{1}{2}(A + B), \quad r = \frac{1}{4}(A - B). \tag{3.210}$$

By substituting these equations into Eq. (3.207), we obtain the rotational Hamiltonian

$$H = \frac{2\pi}{\hbar}\left(\frac{A + B}{2}\right)\boldsymbol{J}^2 + \frac{2\pi}{\hbar}\left(C - \frac{A + B}{2}\right)J_c^2 + \frac{2\pi}{\hbar}\left(\frac{A - B}{4}\right)\left\{\left(J^+\right)^2 + \left(J^-\right)^2\right\}. \tag{3.211}$$

Once we describe the rotational Hamiltonian in this form, its Hamiltonian matrix can readily be evaluated using the $|J, K, M\rangle$ basis set.

As the Hamiltonian is three-dimensionally isotropic, and its $|J, K, M\rangle$ consequently has a $(2J+1)$-fold degeneracy with respect to M, we need not specify the M in the evaluation of the Hamiltonian matrix. Thus, we can simply write $|J, K, M\rangle$ as $|J, K\rangle$. Also, as K is given as an eigenvalue of J_c, we can write K as K_c, and $|J, K\rangle$ as $|J, K_c\rangle$. Then, from Eqs. (3.182), (3.183), and (3.185), we can evaluate the necessary matrix elements as

$$\langle J, K_c|\boldsymbol{J}^2|J, K_c\rangle = J(J+1)\hbar^2, \tag{3.212}$$

$$\langle J, K_c|J_c^2|J, K_c\rangle = K_c^2\hbar^2, \tag{3.213}$$

$$\begin{aligned}&\langle J, K_c+2|J^-J^-|J, K_c\rangle \\ &\quad = \langle J, K_c|J^+J^+|J, K_c+2\rangle \\ &\quad = \sqrt{J(J+1)-K_c(K_c+1)}\cdot\sqrt{J(J+1)-(K_c+1)(K_c+2)}\hbar^2,\end{aligned} \tag{3.214}$$

$$\begin{aligned}&\langle J, K_c-2|J^+J^+|J, K_c\rangle \\ &\quad = \langle J, K_c|J^-J^-|J, K_c-2\rangle \\ &\quad = \sqrt{J(J+1)-K_c(K_c-1)}\cdot\sqrt{J(J+1)-(K_c-1)(K_c-2)}\hbar^2.\end{aligned} \tag{3.215}$$

What this signifies is that, given the three rotational constants A, B, and C, we can evaluate the matrix element $\langle J', K_c'|H|J, K_c\rangle$, and by diagonalizing the Hamiltonian matrix, in turn, obtain the eigenvalues and eigenfunctions of any given asymmetric top molecule.

3.4.7 Calculating the Rotational Energy Levels of an Asymmetric Top Molecule for $J = 0$ and $J = 1$

Now we will evaluate the actual matrix elements as obtained above in Sect. 3.4.6, and derive the rotational energy levels of an asymmetric top molecule for cases where $J = 0$ and $J = 1$.

(i) $J = 0$

When $J = 0$, $K_c = 0$ is required, and therefore the eigenfunction becomes

$$|J, K_c\rangle = |0, 0\rangle. \tag{3.216}$$

The Hamiltonian matrix is a one-by-one matrix consisting of the sole matrix element $\langle 0, 0|H|0, 0\rangle$. Naturally, its eigenenergy is

$$E = \langle 0, 0|H|0, 0\rangle = 0. \tag{3.217}$$

(ii) $J = 1$

When $J = 1$, K_c can take one of three values, $K_c = -1, 0, 1$, so that we can evaluate the Hamiltonian matrix elements using the following three basis functions:

$$|J, K_c\rangle = |1, 1\rangle, |1, 0\rangle, |1, -1\rangle.$$

The diagonal elements are generated from the operators $\boldsymbol{J}^2$ and J_c^2, so that

$$\begin{aligned}\langle 1, 1|H|1, 1\rangle &= \frac{2\pi}{\hbar}\left(\frac{A+B}{2}\right)\langle 1, 1|\boldsymbol{J}^2|1, 1\rangle + \frac{2\pi}{\hbar}\left(C - \frac{A+B}{2}\right)\langle 1, 1|J_c^2|1, 1\rangle \\ &= \frac{2\pi}{\hbar}\left(\frac{A+B}{2}\right)2\hbar^2 + \frac{2\pi}{\hbar}\left(C - \frac{A+B}{2}\right)\hbar^2 \\ &= h\left(C + \frac{A+B}{2}\right) \end{aligned} \tag{3.218}$$

is obtained from Eq. (3.211).

Similarly,

$$\langle 1, -1|H|1, -1\rangle = h\left(C + \frac{A+B}{2}\right), \tag{3.219}$$

$$\langle 1, 0|H|1, 0\rangle = h(A+B) \tag{3.220}$$

can be obtained.

The off-diagonal elements can only exist between the basis functions whose K_c values differ by 2, that is, for $\Delta K_c = \pm 2$, so that

$$\begin{aligned}\langle 1, 1|H|1, -1\rangle &= \frac{2\pi}{\hbar}\left(\frac{A-B}{4}\right)\langle 1, 1|J^- J^-|1, -1\rangle \\ &= h\left(\frac{A-B}{2}\right) \end{aligned} \tag{3.221}$$

is derived.

Also, similarly,

$$\langle 1, -1|H|1, 1\rangle = h\left(\frac{A-B}{2}\right) \tag{3.222}$$

is derived.

Based on the matrix evaluations above, we can describe the Hamiltonian matrix $\boldsymbol{H}_1$ for $J = 1$ as

$$\boldsymbol{H}_1 = h\left(\begin{array}{c|c|c} C + \frac{A+B}{2} & 0 & \frac{A-B}{2} \\ \hline 0 & A+B & 0 \\ \hline \frac{A-B}{2} & 0 & C + \frac{A+B}{2} \end{array}\right) \tag{3.223}$$

If we reorder the basis functions, $|1, 1\rangle, |1, 0\rangle, |1, -1\rangle$, so that they stand in the order of $|1, 0\rangle, |1, 1\rangle, |1, -1\rangle$, the Hamiltonian matrix is represented as

$$\boldsymbol{H}_1' = h\left(\begin{array}{c|cc} A+B & 0 & 0 \\ \hline 0 & C + \frac{A+B}{2} & \frac{A-B}{2} \\ 0 & \frac{A-B}{2} & C + \frac{A+B}{2} \end{array}\right), \tag{3.224}$$

and we can see that this is block-diagonalized. Therefore, $|J, K_c\rangle = |1, 0\rangle$ is already an eigenfunction, and its eigenenergy E_{10} is

$$E_{10} = h(A + B). \tag{3.225}$$

Next, by diagonalizing the remaining two-by-two matrix,

$$\boldsymbol{H}' = h \begin{pmatrix} C + \frac{A+B}{2} & \frac{A-B}{2} \\ \frac{A-B}{2} & C + \frac{A+B}{2} \end{pmatrix}, \tag{3.226}$$

we can derive

$$\boldsymbol{E}' = h \begin{pmatrix} B + C & 0 \\ 0 & A + C \end{pmatrix}, \tag{3.227}$$

where the two diagonal elements express the eigenvalues. The eigenfunction associated with the eigenvalue $h(B + C)$ is

$$\frac{1}{\sqrt{2}}\big(-|1, 1\rangle + |1, -1\rangle\big), \tag{3.228}$$

whereas that associated with the eigenvelue $h(A + C)$ is

$$\frac{1}{\sqrt{2}}\big(|1, 1\rangle + |1, -1\rangle\big). \tag{3.229}$$

The diagonalization process given above can be interpreted as the unitary transformation of a column vector whose elements are the two basis functions,

$$\begin{pmatrix} |1, 1\rangle \\ |1, -1\rangle \end{pmatrix},$$

by a unitary transformation matrix

$$\boldsymbol{U} = \frac{1}{\sqrt{2}} \begin{pmatrix} -1 & 1 \\ 1 & 1 \end{pmatrix}, \tag{3.230}$$

which causes the $\boldsymbol{H}'$ to be transformed into a diagonal matrix $\boldsymbol{E}'$. This process can be represented using these matrices as

$${}^t\boldsymbol{U}\boldsymbol{H}'\boldsymbol{U} = \boldsymbol{E}'. \tag{3.231}$$

The three eigenenergies obtained by the processes above can be sorted in decreasing order of energy as

$$h(A + B) > h(A + C) > h(B + C), \tag{3.232}$$

because $A > B > C$.

Our next task is to determine what to call those levels corresponding to the energy expressions derived above. Let us first consider gradually modifying the structure of the asymmetric top molecule so that it approaches an oblate symmetric top molecule, as illustrated in the right half of Fig. 3.16.

As $A = B$ holds in an oblate symmetric top molecule, we can conceptualize this as a case where the A and B in an asymmetric top molecule approach each

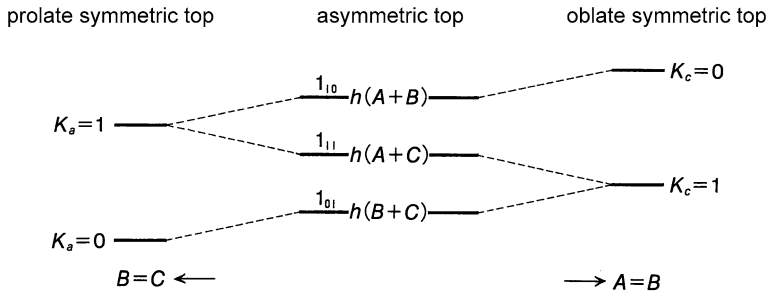

Fig. 3.16 The correlation diagram of level energies in asymmetric top molecules and symmetric top molecules (for $J = 1$)

other to the limit, so that they have the same value. This allows us to see the two rotational levels of an asymmetric top molecule whose eigenenergies are $h(B + C)$ and $h(A + C)$ and whose eigenfunctions are given by Eqs. (3.228) and (3.229), respectively, as having the same rotational energy, $h(B + C)$, at the one extreme where the molecule becomes an oblate symmetric top molecule. In other words, these two levels of the asymmetric top molecule correlate with the rotational level of an oblate top molecule, $|J, K_c\rangle = |1, 1\rangle$. Also, the rotational level of an asymmetric top molecule whose energy is $h(A+B)$ correlates with the rotational level $|J, K_c\rangle = |1, 0\rangle$ of an oblate top molecule. Indeed, if we assume that $A = B$, the eigenenergy of this level becomes $2hB$, which corresponds to $J = 1$, $K_c = 0$ being substituted into Eq. (3.195).

Let us now consider modifying the structure of an asymmetric top molecule so that it approximates a prolate symmetric top molecule. A prolate symmetric top molecule is one where $B = C$ holds, so it represents the case of the B and C in an asymmetric top molecule approaching each other to the point where they have the same value. This tells us that the two rotational levels of an asymmetric top molecule whose eigenenergies are $h(A + B)$ and $h(A + C)$ have the same rotational energy, $h(A + B)$, at the other extreme where the molecule becomes a prolate symmetric top molecule.

In the discussion above, the c axis is defined as the quantization axis along which K is defined as the projection of the total rotational angular momentum, in rewriting Eq. (3.205) as Eq. (3.211). The procedures above also stand exactly as they are when the cyclic permutation is performed on a, b, and c, that is, when $a \to b$, $b \to c$, and $c \to a$, and so the Hamiltonian of Eq. (3.205) can also be written as

$$H = \frac{2\pi}{\hbar}\left(\frac{B+C}{2}\right)\boldsymbol{J}^2 + \frac{2\pi}{\hbar}\left(A - \frac{B+C}{2}\right)J_a^2 + \frac{2\pi}{\hbar}\left(\frac{B-C}{4}\right)\left\{\left(J^+\right)^2 + \left(J^-\right)^2\right\}. \tag{3.233}$$

Let us then diagonalize the matrix elements of this Hamiltonian by representing them with the $|J, K\rangle$ basis set. For this, we simply need to repeat the above discussion using the cyclic permutation $a \to b$, $b \to c$, and $c \to a$, and thus we can readily see that the energy level for the eigenenergy $h(B + C)$ is represented as

$|J, K_a\rangle = |1, 0\rangle$, and that this directly correlates with the $|J, K_a\rangle = |1, 0\rangle$ of a prolate symmetric top molecule. Indeed, if we assume that $B = C$, then the eigenenergy becomes $2hB$, which corresponds to the result obtained when substituting $J = 1$ and $K_a = 0$ into Eq. (3.194). In addition, we can see that the rotational levels whose eigenenergies are $h(A + C)$ and $h(A + B)$ can be written, respectively, as

$$\frac{1}{\sqrt{2}}\big(-|1, 1\rangle + |1, -1\rangle\big), \tag{3.234}$$

$$\frac{1}{\sqrt{2}}\big(|1, 1\rangle + |1, -1\rangle\big). \tag{3.235}$$

This shows that the rotational energies of these two rotational levels for an asymmetric top molecule approach the same value, $h(A + B)$, as the B and C approach each other, ultimately constituting a prolate symmetric top molecule. In other words, these two levels of an asymmetric top molecule correlate with the rotational level $|J, K_a\rangle = |1, 1\rangle$ of a prolate top molecule. This is what is illustrated in the left half of Fig. 3.16.

To summarize, when $J = 1$,

- the level whose eigenenergy is given by $h(A + B)$ correlates with $K_a = 1$ and $K_c = 0$,
- the level whose eigenenergy is given by $h(A + C)$ correlates with $K_a = 1$ and $K_c = 1$, and
- the level whose eigenenergy is given by $h(B + C)$ correlates with $K_a = 0$ and $K_c = 1$.

Therefore, it is reasonable to call these three energy levels 1_{10}, 1_{11}, and 1_{01}, so that the K_a and K_c values are expressed in the subscripts of the quantum number for the total rotational angular momentum, as $J_{K_a K_c}$. That is, the rotational level energies for an asymmetric top molecule with $J = 1$ can be given as

$$\begin{aligned} E(1_{10}) &= h(A + B), \\ E(1_{11}) &= h(A + C), \\ E(1_{01}) &= h(B + C). \end{aligned} \tag{3.236}$$

When τ is defined as

$$\tau \equiv K_a - K_c, \tag{3.237}$$

its values are $\tau = 1, 0, -1$ for the three levels $J_{K_a K_c} = 1_{10}, 1_{11}, 1_{01}$, respectively. Therefore, we sometimes specify these rotational levels using τ, as $J_\tau = 1_1, 1_0, 1_{-1}$.

3.4.8 Wang's Transformation

As shown in the preceding subsection using the specific case of $J = 1$, the Hamiltonian matrix evaluated by the $|J, K\rangle$ basis functions has off-diagonal elements between $|J, K\rangle$ and $|J, K \pm 2\rangle$. This turns the Hamiltonian matrix into a tridiagonal matrix. Therefore, in order to transform $|J, K\rangle$ and $|J, -K\rangle$ into

$$\frac{1}{\sqrt{2}}\big(-|J,K\rangle+|J,-K\rangle\big), \tag{3.238}$$

$$\frac{1}{\sqrt{2}}\big(|J,K\rangle+|J,-K\rangle\big), \tag{3.239}$$

let us now introduce a matrix represented as

$$\boldsymbol{U}_J=\frac{1}{\sqrt{2}}\begin{pmatrix} \ddots & & & & & & \iddots \\ & -1 & 0 & 0 & 0 & 1 & \\ & 0 & -1 & 0 & 1 & 0 & \\ & 0 & 0 & \sqrt{2} & 0 & 0 & \\ & 0 & 1 & 0 & 1 & 0 & \\ & 1 & 0 & 0 & 0 & 1 & \\ \iddots & & & & & & \ddots \end{pmatrix}. \tag{3.240}$$

This matrix is called Wang's matrix, and the transformation of a set of basis functions by this matrix is called Wang's transformation. This transformation is a unitary transformation of the $|J,K\rangle$ basis functions specified by a given value J and $(2J+1)$ different values for K $(=-J,-J+1,\ldots,J)$.

When $J=1$, the transformation matrix $\boldsymbol{U}_1$ is

$$\boldsymbol{U}_1=\frac{1}{\sqrt{2}}\begin{pmatrix} -1 & 0 & 1 \\ 0 & \sqrt{2} & 0 \\ 1 & 0 & 1 \end{pmatrix}. \tag{3.241}$$

The Hamiltonian matrix $\boldsymbol{H}_1$ in Eq. (3.223) is diagonalized by this transformation as

$${}^t\boldsymbol{U}_1\boldsymbol{H}_1\boldsymbol{U}_1=\boldsymbol{U}_1\boldsymbol{H}_1\boldsymbol{U}_1=\begin{pmatrix} B+C & 0 & 0 \\ 0 & A+B & 0 \\ 0 & 0 & C+A \end{pmatrix}. \tag{3.242}$$

Note here that ${}^t\boldsymbol{U}_J=\boldsymbol{U}_J$ holds, as $\boldsymbol{U}_J$ is a symmetric matrix.

When $J\geqq 2$, Wang's transformation does not lead directly to diagonalization, but block diagonalization can be achieved, which facilitates the eigenvalue problem. Let us look at this by solving the next problem.

Problem 3.12

Letting $J=2$, and using the representation in which the quantization axis is set as the c axis, derive the Hamiltonian matrix for the rotational motion of a molecule. Then, block-diagonalize the Hamiltonian matrix by carrying out Wang's basis transformation.

Solution

As shown in Eq. (3.210), we can represent p, q, and r using A, B, and C as

$$p=\frac{1}{2}(A+B),\quad q=C-\frac{1}{2}(A+B),\quad r=\frac{1}{4}(A-B),$$

and therefore the Hamiltonian matrix can be written as

$$\boldsymbol{H} = h\begin{pmatrix} 6p+4q & 0 & 2\sqrt{6}r & 0 & 0 \\ 0 & 6p+q & 0 & 6r & 0 \\ 2\sqrt{6}r & 0 & 6p & 0 & 2\sqrt{6}r \\ 0 & 6r & 0 & 6p+q & 0 \\ 0 & 0 & 2\sqrt{6}r & 0 & 6p+4q \end{pmatrix}, \tag{3.243}$$

which shows it to be a tridiagonal matrix.

When we use Wang's basis transformation matrix for $J = 2$,

$$\boldsymbol{U}_2 = \frac{1}{\sqrt{2}}\begin{pmatrix} -1 & 0 & 0 & 0 & 1 \\ 0 & -1 & 0 & 1 & 0 \\ 0 & 0 & \sqrt{2} & 0 & 0 \\ 0 & 1 & 0 & 1 & 0 \\ 1 & 0 & 0 & 0 & 1 \end{pmatrix}, \tag{3.244}$$

in calculating $\boldsymbol{H}' = \boldsymbol{U}_2\boldsymbol{H}\boldsymbol{U}_2$, we obtain

$$\boldsymbol{H}' = h\begin{pmatrix} 6p+4q & 0 & 0 & 0 & 0 \\ 0 & 6p+q-6r & 0 & 0 & 0 \\ 0 & 0 & 6p & 0 & 4\sqrt{3}r \\ 0 & 0 & 0 & 6p+q+6r & 0 \\ 0 & 0 & 4\sqrt{3}r & 0 & 6p+4q \end{pmatrix}. \tag{3.245}$$

By changing the order of the basis functions that are not diagonalized, the block-diagonalized Hamiltonian matrix can be simplified as

$$\boldsymbol{H}' = h\begin{pmatrix} \boxed{A+B+4C} & 0 & 0 & 0 & 0 \\ 0 & \boxed{A+4B+C} & 0 & 0 & 0 \\ 0 & 0 & \boxed{4A+B+C} & 0 & 0 \\ 0 & 0 & 0 & \boxed{\begin{matrix} A+B+4C & \sqrt{3}(A-B) \\ \sqrt{3}(A-B) & 3(A+B) \end{matrix}} & \\ 0 & 0 & 0 & & \end{pmatrix}. \tag{3.246}$$

This clearly shows that three out of five eigenenergies can be determined by Wang's transformation alone, namely as $A+B+4C$, $A+4B+C$, and $4A+B+C$. □

The results obtained in Problem 3.12 show us that we have to diagonalize the 2×2 sub-matrix in Eq. (3.246) in order to derive the two remaining eigenenergies for $J = 2$. This diagonalization can be easily performed, and the two eigenvalues are obtained as

$$h\left\{2(A+B+C) \pm 2\sqrt{(B-C)^2 + (A-C)(A-B)}\right\}.$$

When we examine the relative level energies of these five rotational eigenstates under the condition $A > B > C$, and derive the K_a and K_c values assigned to the

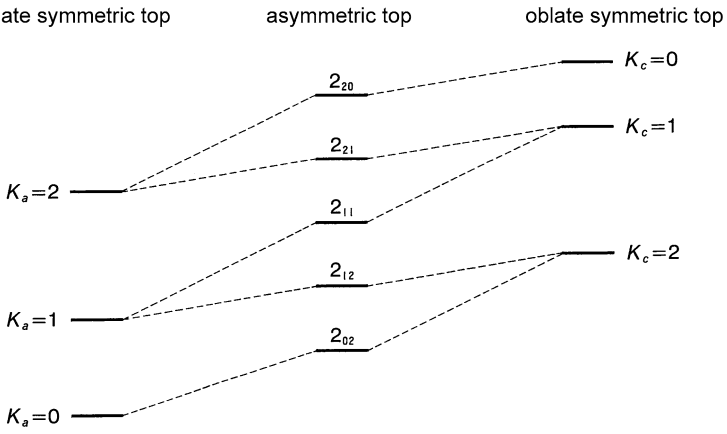

Fig. 3.17 The correlation diagram of level energies in asymmetric top molecules and symmetric top molecules (for $J = 2$)

respective levels in the same way as we did for $J = 1$, we obtain the rotational eigenenergies for $J = 2$ in decreasing order of the energy as

$$\begin{cases} E(2_{20}) = h\left\{2(A+B+C) + 2\sqrt{(B-C)^2 + (A-C)(A-B)}\right\}, \\ E(2_{21}) = h(4A+B+C), \\ E(2_{11}) = h(A+4B+C), \\ E(2_{12}) = h(A+B+4C), \\ E(2_{02}) = h\left\{2(A+B+C) - 2\sqrt{(B-C)^2 + (A-C)(A-B)}\right\}. \end{cases} \tag{3.247}$$

The correlation diagram for $J = 2$ is thus as shown in Fig. 3.17.

Table 3.2 summarizes the level energies for an asymmetric top molecule as represented using rotational constants. The rotational level energies for $J = 3$ are also included in the table.

3.4.9 Symmetry in the Rotational Levels of an Asymmetric Top Molecule

Wang's transformation turns the Hamiltonian matrix of an asymmetric top molecule into four sub-matrices, and each is characterized by the different parity for its $K_a K_c$, as *ee*, *eo*, *oo*, or *oe*, where "*e*" stands for "even" and "*o*" for "odd". This classification of rotational levels can be seen in the block-diagonalized Hamiltonian given in Eq. (3.246) as well as in the labeling with $K_a K_c$ shown in Eq. (3.247). Let us then examine how this classification into four groups by the parity combinations of $K_a K_c$ is reflected in the symmetry of the wave functions for an asymmetric top molecule.

We will first consider a C_2 rotation, or a rotation by 180 degrees, of an asymmetric top molecule around the a axis, which is one of the three principal axes of

Table 3.2 Rotational level energies for an asymmetric top molecule

$J_{K_a K_c}$	$E(J_{K_a K_c})/h$
0_{00}	0
1_{10}	$A+B$
1_{11}	$A+C$
1_{01}	$B+C$
2_{20}	$2A+2B+2C+2\sqrt{(B-C)^2+(A-C)(A-B)}$
2_{21}	$4A+B+C$
2_{11}	$A+4B+C$
2_{12}	$A+B+4C$
2_{02}	$2A+2B+2C-2\sqrt{(B-C)^2+(A-C)(A-B)}$
3_{30}	$5A+5B+2C+2\sqrt{4(A-B)^2+(A-C)(B-C)}$
3_{31}	$5A+2B+5C+2\sqrt{4(A-C)^2-(A-B)(B-C)}$
3_{21}	$2A+5B+5C+2\sqrt{4(B-C)^2+(A-B)(A-C)}$
3_{22}	$4A+4B+4C$
3_{12}	$5A+5B+2C-2\sqrt{4(A-B)^2+(A-C)(B-C)}$
3_{13}	$5A+2B+5C-2\sqrt{4(A-C)^2-(A-B)(B-C)}$
3_{03}	$2A+5B+5C-2\sqrt{4(B-C)^2+(A-B)(A-C)}$

the molecule. When this rotation occurs, the molecule-fixed rotational angular momenta are transformed as $J_a \to J_a$, $J_b \to -J_b$, and $J_c \to -J_c$. Note here that the signs of two of the rotational angular momenta have been reversed. The rotational Hamiltonian, on the other hand, as expressed by Eq. (3.147), stays constant during this symmetry operation. The same applies when the C_2 rotation is performed around the b axis or the c axis. Therefore, we will now write the three types of symmetry operations where a molecule is rotated by $180^\circ = \frac{2\pi}{2}$ radians around the a, b, and c axes as C_2^a, C_2^b, and C_2^c, and examine how the rotational wave functions are transformed by these three operations.

First, let us consider the operation C_n^c, whereby the rotational wave functions of a symmetric top molecule is affected by a rotation of $\frac{2\pi}{n}$ around the c axis. As shown in Eq. (3.181), the wave functions of a symmetric top molecule are given as

$$|J, K, M\rangle = N_{JKM}\Theta_{JKM}(\theta)\mathrm{e}^{\mathrm{i}K\gamma}\mathrm{e}^{\mathrm{i}M\phi} \tag{3.248}$$

and therefore the C_n^c rotation is represented as $\gamma \to \gamma + \frac{2\pi}{n}$, which gives us

$$\begin{aligned} C_n^c|J, K, M\rangle &= N_{JKM}\Theta_{JKM}(\theta)\mathrm{e}^{\mathrm{i}K(\gamma+\frac{2\pi}{n})}\mathrm{e}^{\mathrm{i}M\phi} \\ &= \left(\mathrm{e}^{\mathrm{i}\frac{2\pi}{n}}\right)^K|J, K, M\rangle \\ &= \varepsilon_n^K|J, K, M\rangle, \end{aligned} \tag{3.249}$$

where ε_n is defined as $\varepsilon_n = \mathrm{e}^{\mathrm{i}\frac{2\pi}{n}}$. This can then be re-written as

$$C_n^c|J, K_C, M\rangle = \varepsilon_n^{K_C}|J, K_C, M\rangle. \tag{3.250}$$

Table 3.3 A character table for the D_2 point group (symmetry group V)

	E	C_2^a	C_2^b	C_2^c	$K_a K_c$
A	1	1	1	1	ee
B_a	1	1	-1	-1	eo
B_b	1	-1	1	-1	oo
B_c	1	-1	-1	1	oe

We can also see that, by replacing the c axis with the a axis,

$$C_n^a|J, K_A, M\rangle = \varepsilon_n^{K_A}|J, K_A, M\rangle \tag{3.251}$$

will be readily obtained.

For the case where $n = 2$, which is the case of a C_2 rotation, we obtain

$$\varepsilon_2 = \mathrm{e}^{\mathrm{i}\pi} = \cos\pi + \mathrm{i}\sin\pi = -1.$$

Therefore, we can derive

$$C_2^c|J, K_C, M\rangle = (-1)^{K_C}|J, K_C, M\rangle, \tag{3.252}$$

$$C_2^a|J, K_A, M\rangle = (-1)^{K_A}|J, K_A, M\rangle. \tag{3.253}$$

We can see that the rotational wave function $J_{K_a K_c}$ of an asymmetric top molecule, too, can be transformed by the C_2^c and C_2^a operations as, respectively,

$$C_2^c|J, K_a, K_c\rangle = (-1)^{K_c}|J, K_a, K_c\rangle, \tag{3.254}$$

$$C_2^a|J, K_a, K_c\rangle = (-1)^{K_a}|J, K_a, K_c\rangle. \tag{3.255}$$

In operating C_2^a, for example, the wave function does not change its sign if K_a is even, and it does if K_a is odd. Furthermore, as

$$C_2^b = C_2^c C_2^a \tag{3.256}$$

stands, the rotational wave function $|J, K_a, K_c\rangle$ can be transformed by C_2^b as

$$C_2^b|J, K_a, K_c\rangle = (-1)^{K_a + K_c}|J, K_a, K_c\rangle. \tag{3.257}$$

The results of these rotational operations are summarized in Table 3.3 in the form of a character table, which indicates whether the signs of the wave functions with the parities of ee, eo, oo, and oe are changed or not upon the operations C_2^a, C_2^b, and C_2^c. In this table, "1" stands for the sign remaining the same, and "-1" for the sign being changed. The operation E represents the identity operation, whereby nothing is changed.

Generally speaking, the symmetry of a molecule is classified using a type of groups called point groups. Table 3.3 is a character table for the D_2 point group, which characterizes the symmetry of the rotational Hamiltonian of an asymmetric top molecule. This group has four symmetry species, A, B_a, B_b, and B_c, and as shown in this character table, ee levels are classified into the A symmetry species, eo levels into the B_a symmetry species, oo levels into the B_b symmetry species, and oe levels into the B_c symmetry species. This signifies that even for molecules

with low symmetry, such as those belonging to the C_2 point group or to the C_1 point group, we can classify the symmetry of their rotational wave functions into one of these four symmetry species shown for the D_2 point group. This point group is also called the symmetry group V. In the case of $J = 2$, which we looked at earlier, the five rotational levels that have been derived, 2_{20}, 2_{21}, 2_{11}, 2_{12}, and 2_{01}, are classified into the A, B_a, B_b, B_c, and A symmetry species, respectively.

3.5 Determination of Molecular Structures Based on Rotational Spectra

In Sect. 3.4, we have learned that the energy levels of symmetric top molecules and asymmetric top molecules can be written using rotational constants. This means that, if we can find out the energy spacing between two energy levels, we can obtain the rotational constant, which in turn gives us the moment of inertia. As explained in Sect. 3.1 during our discussion of diatomic and linear molecules, we can determine the molecular structure when the moment of inertia is given. In this section we will determine the molecular structures of symmetric top molecules and asymmetric top molecules from the analysis of the rotational spectra.

3.5.1 Molecular Structures of Symmetric Top Molecules

Let us take the example of a tetra-atomic molecule of the XY_3 type. Molecules such as NH_3, PH_3, NF_3 fall under this category. Arranging the atoms as shown in Fig. 3.18, we represent the distance between X and Y as 'r' and the bond angle $\angle Y{-}X{-}Y$ as 'θ'. If we assume this molecule to be an oblate symmetric top and take the C_3 axis as the c axis, the moment of inertia around the two axes of inertia perpendicular to the c axis (the a axis and the b axis), I_B $(=I_A)$, can be described by r and θ as

$$I_B = 2m_Y r^2 \sin^2\frac{\theta}{2} + \frac{m_X m_Y}{M} r^2 \left(3 - 4\sin^2\frac{\theta}{2}\right), \tag{3.258}$$

where m_X and m_Y are the masses of atoms X and Y, respectively, and M represents the mass of the whole molecule,

$$M = m_X + 3m_Y. \tag{3.259}$$

Similarly, the moment of inertia around the c axis, I_C, can be written as

$$I_C = 4m_Y r^2 \sin^2\frac{\theta}{2}. \tag{3.260}$$

By converting the moments of inertia I_B and I_C into rotational constants B and C using the definitions given in Eq. (3.143), we can derive the rotational energy E_{JK} from Eq. (3.195).

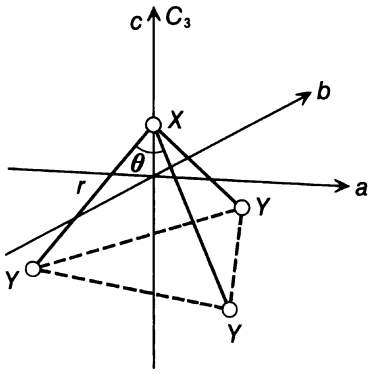

Fig. 3.18 Molecular structure of an XY_3-type oblate symmetric top molecule

Table 3.4 Frequencies of rotational transitions for $^{14}NF_3$ and $^{15}NF_3$

Transition		Transition frequency/MHz	B/MHz
$^{14}NF_3$			
$J = 1 \leftarrow 0$	$F = 1 \leftarrow 1$	21360.34	10681.09
	$2 \leftarrow 1$	21362.60	
	$0 \leftarrow 1$	21365.60	
$^{15}NF_3$			
$J = 1 \leftarrow 0$		21258.92	10629.46

In the case of $^{14}NF_3$ molecules, the transition in the microwave region from the $J = 0$, $K = 0$ level to the $J = 1$, $K = 0$ level is observed as shown in the upper column of Table 3.4. With $^{14}NF_3$ molecules, the rotational energy level of $J = 1$ splits slightly into three different levels because of an interaction called the nuclear quadrupole interaction, which causes the transition from $J = 0$ to $J = 1$ to be observed as three adjacent transitions, as shown in the table.

A detailed explanation of the nuclear quadrupole interaction is beyond the scope of this textbook, but to put it briefly, this is the interaction between the nuclear quadrupole moment of the nitrogen atom nucleus and the electric field gradient at the nuclear position. This interaction only appears when the nuclear spin I satisfies $I \geqq 1$. In such cases, the energy level is labeled by the quantum number F for the total angular momentum $\boldsymbol{F}$, which is a sum of the angular momentum $\boldsymbol{J}$ of the molecular rotation and the angular momentum $\boldsymbol{I}$ of the nuclear spin of the nitrogen nucleus. As each level has a degeneracy of $2F + 1$, if we take there to be no nuclear quadrupole interaction then the transition frequency for $J = 1 \leftarrow J = 0$ is given by the weighted average of the transition frequency for $F = 2 \leftarrow 1$, $F = 1 \leftarrow 1$ and $F = 0 \leftarrow 1$, where the weighting factor is $5 : 3 : 1$. This can be calculated as $\bar{\nu} = 21362.18$ MHz.

It is known that the selection rule for the rotational transition of a symmetric top molecule is written as

$$\Delta J = 0, \pm 1, \quad \Delta K = 0. \tag{3.261}$$

Here, ΔJ and ΔK can be written as $\Delta J = J' - J''$, $\Delta K = K' - K''$, and they stand for the changes in J and K accompanying the transition from a lower energy level with the rotational quantum numbers J'' and K'' to a higher energy level with the rotational quantum numbers J' and K'. As seen here, it is conventional in molecular spectroscopy to express a pair of levels related by a transition with a double prime ($''$) marking the quantum number for the lower energy level and a prime ($'$) marking the quantum number for the higher energy level.

Of the two rules in Eq. (3.261), we can easily understand the selection rule $\Delta K = 0$. The dipole moment vector $\boldsymbol{\mu}$ of a symmetric top molecule points in the direction of the a axis if it is a prolate symmetric top molecule, or in the direction of the c axis if it is an oblate symmetric top molecule. Thus it is not affected by the rotation around its axis by the Euler angle γ. On the other hand, K is the projection of the angular momentum on this molecular axis, and appears as a part of $\mathrm{e}^{\mathrm{i}K\gamma}$ in the wave function. Therefore, of the matrix element representing the dipole transition in Eq. (2.87), Chap. 2, the part that is dependent on γ will be $\int_0^{2\pi} \mathrm{e}^{-\mathrm{i}K'\gamma} \mathrm{e}^{\mathrm{i}K''\gamma} \, \mathrm{d}\gamma$. This integral has a non-zero value only when $\Delta K = K' - K'' = 0$. It is thus shown that the selection rule $\Delta K = 0$ stands.

Using Eq. (3.195) to calculate ν, the frequency of the microwave absorbed by the transition, we obtain

$$\begin{aligned} h\nu &= E_{J'K'} - E_{J''K''} \\ &= hBJ'\left(J'+1\right) - hBJ''\left(J''+1\right) \end{aligned} \tag{3.262}$$

from $K' = K''$. This demonstrates that the selection rule $\Delta K = 0$ allows us to determine the rotational constant B from observation results, but not the rotational constant C. As $J'' = 0$, $J' = 1$ in this example, Eq. (3.262) can be rewritten here as $h\nu = E_{10} - E_{00} = 2hB$, which gives us the rotational constant as $B(^{14}\mathrm{NF_3}) = 10681.09$ MHz when we apply the $\bar{\nu}$ obtained as the weighted average.

However, as shown in Eq. (3.258), being given the rotational constant B, and thus I_B, is not sufficient for us to determine both r and θ independently. Therefore, let us now consider using the isotope substitution method adopted to determine the molecular structure of OCS in Sect. 3.1.3.

As shown in the lower column of Table 3.4, in the case of $^{15}\mathrm{NF_3}$ the transition of $J = 1 \leftarrow J = 0$ is observed. Despite also having a nitrogen nucleus, here the molecule does not exhibit the type of split observed in $^{14}\mathrm{NF_3}$, because with $^{15}\mathrm{N}$ the nuclear spin is $I = \frac{1}{2}$ and this precludes the nuclear quadrupole interaction. Therefore, the rotational constant B is straightforwardly obtained as $B(^{15}\mathrm{NF_3}) = 10629.46$ MHz.

By using these two rotational constants, we can derive two independent formulas corresponding to Eq. (3.258). If we define a and b as $a = r^2$ and $b = r^2 \sin^2 \frac{\theta}{2}$,

Table 3.5 Frequencies of rotational transitions for SO_2 in the $v_2 = 1$ state

$J'_{K'_a K'_c} - J''_{K''_a K''_c}$	Transition frequencies/MHz
1_{11}–0_{00}	70735.92
1_{11}–2_{02}	13457.92
2_{11}–2_{02}	54739.49
4_{04}–3_{13}	28138.55
4_{13}–4_{04}	60498.77

the two formulas can be seen as a set of simultaneous linear equations about a and b. We can solve this equation by the use of $m(\mathrm{F}) = 18.998405$ amu, $m(^{14}\mathrm{N}) = 14.003074$ amu, and $m(^{15}\mathrm{N}) = 15.000108$ amu, to obtain the parameters representing the molecular structure, or the structural parameters, as $r = 1.3711$ Å and $\theta = 102.16°$.

Problem 3.13
The rotational constant of an ammonia molecule at its vibrational ground state is given as

$$298115.37 \text{ MHz} \quad \text{for } ^{14}NH_3,$$
$$297388.12 \text{ MHz} \quad \text{for } ^{15}NH_3.$$

Determine the internuclear distance between the N atom and an H atom of an ammonia molecule, r(N–H), and the bond angle $\theta = \angle$H–N–H, using $m(\mathrm{H}) = 1.007825$ amu.

Solution
As in the case of NF_3, we can solve the simultaneous linear equations and obtain the structural parameters $r = 1.0156$ Å and $\theta = 107.28°$. □

3.5.2 Determining the Rotational Constants of Asymmetric Top Molecules

Taking SO_2 as an example of an asymmetric top molecule, we will determine its rotational constant from the rotational spectrum. When we measure the rotational spectrum of the vibrationally excited state ($v_2 = 1$) of the bending mode (v_2), the transition frequencies are obtained as shown in Table 3.5. Three of these transitions are shown in Fig. 3.19 with their rotational energy levels.

From the transition frequencies observed here and the rotational level energies expressed with rotational constants A, B, and C (listed in Table 3.2), we can obtain the three relations

$$A + C = 70735.92 \text{ MHz}, \tag{3.263}$$

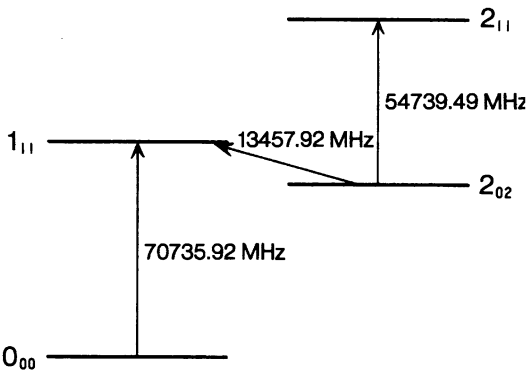

Fig. 3.19 Rotational levels and rotational transitions of SO_2

$$A + C - \left\{2(A + B + C) - 2\sqrt{Q}\right\} = 13457.92 \text{ MHz}, \tag{3.264}$$

$$A + 4B + C - \left\{2(A + B + C) - 2\sqrt{Q}\right\} = 54739.49 \text{ MHz}, \tag{3.265}$$

where

$$Q = (B - C)^2 + (A - C)(A - B). \tag{3.266}$$

With three unknown values, A, B, and C, appearing in these three independent formulas, we are able to determine A, B, and C. Solving these linear equations we immediately obtain $B = 10320.39$ MHz and $\sqrt{Q} = 52417.31$ MHz. When $A > C$,

$$A = \frac{A + C}{2} + \sqrt{\frac{1}{3}\left\{Q - \left(B - \frac{A + C}{2}\right)^2\right\}} \tag{3.267}$$

always holds, so by substituting B and Q into this equation we can derive

$$A = 61952.38 \text{ MHz},$$
$$C = 8783.54 \text{ MHz}.$$

In actuality, we utilize not only the rotational transitions as has been used here but also transition frequencies between levels with larger J values, and calculate the rotational constants A, B, and C by the method of least-squares. However, when using transitions between high-energy levels for analysis, we must account for the effect of centrifugal force operating on the molecule and causing it to deviate from the rigid rotor, by including the centrifugal distortion terms in the rotational Hamiltonian in addition to the part describing a rigid rotor.

The rotational constants of the $v_2 = 1$ state of SO_2, calculated with this method of least squares, are reported to be $A = 61954.69$ MHz, $B = 10320.28$ MHz, and $C = 8783.96$ MHz. We can confirm that the rotational constants calculated earlier using only three transitions are in good agreement with these literature values.

Problem 3.14

Methylhydrazine, CH_3NHNH_2, is known to have two rotational isomers called the inner form and the outer form. Their geometrical structures are shown in

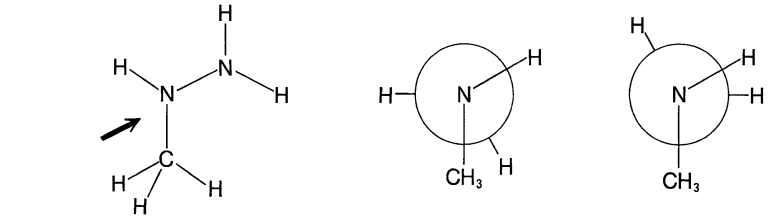

Fig. 3.20 Two rotational isomers of methylhydrazine

Table 3.6 Rotational transitions of the inner-form rotational isomer of methylhydrazine

Transitions	Transition frequencies/MHz[a]
a-type	
1_{01}–0_{00}	18221.65
2_{02}–1_{01}	36406.72
2_{11}–1_{10}	37600.94
2_{12}–1_{11}	35285.61
b-type	
1_{11}–0_{00}	45235.93
3_{03}–2_{12}	28625.69
c-type	
1_{11}–1_{01}	27014.22
2_{12}–2_{02}	25893.04
3_{13}–3_{03}	24279.69

[a]The rotational transitions exhibit a hyperfine structure associated with the small energy splitting of the rotational levels induced by the nuclear quadrupole couplings originating from two nitrogen nuclei, but only the central frequencies of the rotational transitions are listed in the table

Figs. 3.20(b) and 3.20(c) as the Newman projections along the N–N bond axis whose direction is represented by the arrow in Fig. 3.20(a). Rotational transition frequencies of the inner rotational isomer at its vibrational ground state have been obtained as shown in Table 3.6. Calculate the rotational constants A, B, and C.

Solution

Rotational isomers are isomers that can interchange each other with internal rotation around the N–N single bond. From Table 3.6, we can use the transitions 1_{01}–0_{00}, 2_{11}–1_{10}, and 1_{11}–0_{00} to write

$$B + C = 18221.65 \text{ MHz},$$
$$3B + C = 37600.94 \text{ MHz},$$
$$A + C = 45235.93 \text{ MHz}.$$

These equations allow us to calculate the rotational constants as $A = 36703.9$ MHz, $B = 9689.6$ MHz, and $C = 8532.0$ MHz. Rotational constants can also be derived from transitions other than these three. □

Let us now turn to an explanation of the a-type, b-type, and c-type transitions shown in Table 3.6. Paying attention to the parity of $K_a K_c$ at the rotational level $J_{K_a K_c}$, we realize that the a-type transitions are transitions that occur between ee and eo or between oo and oe. Similarly, the b-type transitions occur between oo and ee or between oe and eo, and the c-type transitions between ee and oe or between eo and oo.

As Eq. (2.87) shows in Chap. 2, the probability of an optical transition is proportional to the squared modulus of the matrix element wherein the dipole moment vector is sandwiched between the wave functions of the upper-state and the lower-state of the transitions. Therefore, the requirement for a transition to occur is that the matrix element $\langle J''_{K''_a K''_c} | \boldsymbol{\mu} | J'_{K'_a K'_c} \rangle$ not be 0 in the molecule-fixed coordinate system. This means that

$$\Gamma(J''_{K''_a K''_c}) \otimes \Gamma(\boldsymbol{\mu}) \otimes \Gamma(J'_{K'_a K'_c}) = A \quad \text{(totally symmetric species)} \tag{3.268}$$

is required, where Γ stands for a symmetry species listed in the character table for the D_2 point group given in Table 3.3.

Here, a product of symmetry species signifies the values on the character tables of the two symmetry species being multiplied with each other. For example, the symmetry species B_a has the character $(1\ 1\ -1\ -1)$, whereas B_b has $(1\ -1\ 1\ -1)$, as shown in Table 3.3. To obtain the symmetry species $B_a \otimes B_b$, we multiply the corresponding four sets of characters, which gives us $(1\ -1\ -1\ 1)$. According to Table 3.3, this character is that of the symmetry species B_c. This relationship is represented as $B_a \otimes B_b = B_c$.

The wave function takes the form of one of the symmetry species, A, B_a, B_b, or B_c, in accordance with the parity of $K_a K_c$. We also note that, when we represent $\boldsymbol{\mu}$ by its components in the directions of the a, b, and c axes as (μ_a, μ_b, μ_c), we can write $\Gamma(\mu_a) = B_a$, $\Gamma(\mu_b) = B_b$, and $\Gamma(\mu_c) = B_c$. This is because, as μ_a for instance is the component in the direction of the a axis, it does not change its sign with the C_2^a rotation (a 180° rotation around the a axis) but does change its sign with the C_2^b and C_2^c rotations. Therefore, by searching out the combinations of symmetry species satisfying the requirement of Eq. (3.268), we find the pairs of levels between which transitions occur to be as shown in Table 3.7.

For example, with $ee \leftrightarrow eo$, we can write

$$\begin{aligned} \Gamma(ee) \otimes \Gamma(\mu_a) \otimes \Gamma(eo) &= A \otimes B_a \otimes B_a \\ &= B_a \otimes B_a \\ &= A, \end{aligned} \tag{3.269}$$

which exhibits total symmetry and therefore shows us that an a-type transition is allowed between these two levels, but we also obtain

Table 3.7 Allowed transitions for asymmetric top molecules

a-type transition		
$\mu_a \neq 0$	$ee \leftrightarrow eo$	$oe \leftrightarrow oo$
(B_a)	$(A)\ (B_a)$	$(B_c)\ (B_b)$
b-type transition		
$\mu_b \neq 0$	$ee \leftrightarrow oo$	$oe \leftrightarrow eo$
(B_b)	$(A)\ (B_b)$	$(B_c)\ (B_a)$
c-type transition		
$\mu_c \neq 0$	$ee \leftrightarrow oe$	$eo \leftrightarrow oo$
(B_c)	$(A)\ (B_c)$	$(B_a)\ (B_b)$

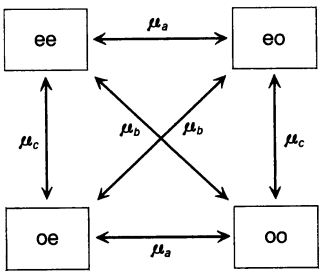

Fig. 3.21 Selection rules of $K_a K_c$ for the rotational transition of an asymmetric top molecule

$$\Gamma(ee) \otimes \Gamma(\mu_b) \otimes \Gamma(eo) = A \otimes B_b \otimes B_a = B_c, \tag{3.270}$$

which demonstrates that a b-type transition does not occur.

The six possibilities for transitions listed in Table 3.7 can be schematized as Fig. 3.21. In the case of methylhydrazine introduced in Problem 3.14, it is because the symmetry is low and μ_a, μ_b, and μ_c all take a non-zero value that the a-, b-, and c-type rotational transitions have all been observed. As in the case of symmetric top molecules, the selection rule for ΔJ shown in Eq. (3.261), $\Delta J = 0, \pm 1$, is satisfied.

In the case of the rotational transition of SO_2 (illustrated in Table 3.5), on the other hand, only the b-type transitions are observed. The reason for this is that the symmetry of the SO_2 molecule causes its dipole moment to point in the direction of the b axis, as shown in Fig. 3.22, which only allows μ_b a non-zero value (i.e., $\mu_b \neq 0$, $\mu_a = \mu_b = 0$). Incidentally, in the case of a nonpolar molecule, whose dipole moment is 0, no transition occurs between different rotational levels of the same vibrational state, because $\mu_a = \mu_b = \mu_c = 0$.

3.5.3 Molecular Structures of Asymmetric Top Molecules

Still using SO_2 as our example, we will now determine the molecular structure of an asymmetric top molecule from the three rotational constants A, B, and C.

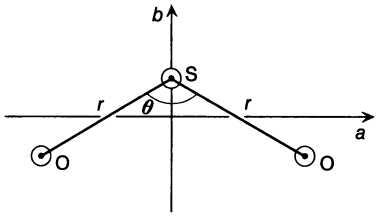

Fig. 3.22 Molecular structure of SO_2

Table 3.8 Rotational constants of SO_2 in the vibrational ground state and the vibrational excited states

	Vibrational ground state	$v_1 = 1$	$v_2 = 1$	$v_3 = 1$
A/MHz	60778.79	60809.84	61954.69	60158.77
B/MHz	10318.10	10267.96	10320.28	10283.25
C/MHz	8799.96	8757.13	8783.96	8767.08

Table 3.9 Rotational constants and moments of inertia for SO_2

(a) Vibrational ground state	A_0	B_0	C_0	
	60778.79	10318.10	8799.96	
	I_A	I_B	I_C	ΔI
	8.3151	48.9799	57.4297	0.1347
(b) Equilibrium structure	A_e	B_e	C_e	
	60485.33	10359.51	8845.82	
	I_A^e	I_B^e	I_C^e	ΔI
	8.3554	48.7841	57.1320	−0.0075

From the observed rotational spectra of SO_2 in its vibrational ground state and its vibrationally excited states, the rotational constants are obtained as shown in Table 3.8, following the same procedure as discussed in Sect. 3.5.2. As shown in this table, the rotational constants vary slightly with different vibrational levels. This is mainly due to the vibrational effects originating from harmonic vibration such as those of the anharmonicity of vibration. As we are about to see, these variations can be exploited to obtain the structure of the molecule at its equilibrium position, or the equilibrium structure. According to Eq. (3.143), the rotational constants for the vibrational ground state of SO_2 can be converted into the moments of inertia I_A, I_B, and I_C, as shown in Table 3.9(a).

When we express the molecular structure of SO_2 by the principal inertial axis system as shown in Fig. 3.22, the moments of inertia around the a axis and the b axis, I_A and I_B, are represented as

$$I_A = \frac{2m_O m_S}{M} r^2 \cos^2 \frac{\theta}{2}, \tag{3.271}$$

Table 3.10 Molecular structure of SO_2

(a) Vibrational ground state	r/Å	θ/deg	(b) Equilibrium structure	r/Å	θ/deg
(I_A, I_B)	1.4322	119.53	(I_A^e, I_B^e)	1.4309	119.31
(I_B, I_C)	1.4351	119.13	(I_B^e, I_C^e)	1.4307	119.34
(I_C, I_A)	1.4336	119.60	(I_C^e, I_A^e)	1.4308	119.31
Average	1.4336	119.42	Average	1.4308	119.32

$$I_B = 2m_O r^2 \sin^2 \frac{\theta}{2}, \tag{3.272}$$

respectively. Here, r is the internuclear distance between the S atom and an O atom, θ is the bond angle ∠O–S–O, m_O and m_S are the masses of an O atom and the S atom, respectively, and M is the total mass of the molecule, $2m_O + m_S$. We can also easily show that

$$I_C = \frac{2m_O m_S}{M} r^2 \cos^2 \frac{\theta}{2} + 2m_O r^2 \sin^2 \frac{\theta}{2}. \tag{3.273}$$

From Eqs. (3.271) through (3.273), we can see that

$$I_c = I_A + I_B. \tag{3.274}$$

Since I_A, I_B, and I_C are given as above, we have sufficient information to determine the necessary structural parameters. That is, as soon as two of these three values are given, we can obtain r and θ from the relations (3.271) through (3.273).

Let us then first examine whether the three moments of inertia satisfy the relation (3.274). When we define the inertial defect ΔI as

$$\Delta I = I_C - I_A - I_B, \tag{3.275}$$

Eq. (3.274) demands that $\Delta I = 0$. However, when we calculate from the observed moments of inertia shown in Table 3.9(a), the ΔI value for the vibrational ground state becomes $\Delta I = 0.1347$ amu Å^2, and not 0. It is known that in most cases with planar molecules, that is, molecules whose component atoms all reside on the same plane at the equilibrium position, the inertial defect does not become exactly 0 but rather takes a very small positive value.

That the inertial defect does not become 0 signifies that different structural parameters are drawn from different pairs of I_A, I_B, and I_C. Calculating the structural parameters, then, for all three combinations, (I_A, I_B), (I_B, I_C), and (I_C, I_A), using Eqs. (3.271) through (3.273), we obtain the figures shown in Table 3.10. The internuclear distance takes a value between $r = 1.432$ Å and $r = 1.435$ Å, with difference recognized at the third decimal place. The bond angle, on the other hand, takes a value between $\theta = 119.1°$ and $\theta = 119.6°$, and shows difference at the first decimal place.

We can obtain the average of these parameters as $r = 1.434$ Å and $\theta = 119.4°$, but considering the high precision of the rotational constants derived from measured spectra, we must be able to arrive at structural parameters of much higher precision.

The reason why there is a slight variation in the structural parameters derived from different pairs of moments of inertia is that there is a vibrational effect in the rotational constant for the vibrational ground state, too, because of zero-point vibration. Let us then remove the vibrational effect and calculate the three rotational constants for the equilibrium position, on the basis of the vibrational level dependence of rotational constants.

First, we will define the vibrational quantum number dependence of the rotational constants as

$$A_{\boldsymbol{v}} = A_{\mathrm{e}} - \sum_{i=1}^{3} \alpha_i^A \left(v_i + \frac{1}{2} \right), \tag{3.276}$$

$$B_{\boldsymbol{v}} = B_{\mathrm{e}} - \sum_{i=1}^{3} \alpha_i^B \left(v_i + \frac{1}{2} \right), \tag{3.277}$$

$$C_{\boldsymbol{v}} = C_{\mathrm{e}} - \sum_{i=1}^{3} \alpha_i^C \left(v_i + \frac{1}{2} \right), \tag{3.278}$$

and use the quantum numbers v_1, v_2, and v_3 of the ν_1, ν_2, and ν_3 modes to expand the equations. Here, $A_{\boldsymbol{v}}$, $B_{\boldsymbol{v}}$, and $C_{\boldsymbol{v}}$ are the rotational constants for the $\boldsymbol{v} = (v_1, v_2, v_3)$ level, whereas A_{e}, B_{e}, and C_{e} are the rotational constants free from vibrational effect in the equilibrium position; α_i^A, α_i^B, and α_i^C are referred to as vibration-rotation constants.

Problem 3.15

Calculate the rotational constants A_{e}, B_{e}, and C_{e} for the equilibrium position, as well as the vibration-rotation constants α_i^A, α_i^B, and α_i^C $(i = 1, 2, 3)$, by substituting the measured rotational constants shown in Table 3.8 into Eqs. (3.276) through (3.278).

Solution

We will first consider A_{e}, α_1^A, α_2^A, and α_3^A. From Eq. (3.276), we can write

$$A_{(0,\,0,\,0)} = A_{\mathrm{e}} - \left(\frac{1}{2}\alpha_1^A + \frac{1}{2}\alpha_2^A + \frac{1}{2}\alpha_3^A \right), \tag{3.279a}$$

$$A_{(1,\,0,\,0)} = A_{\mathrm{e}} - \left(\frac{3}{2}\alpha_1^A + \frac{1}{2}\alpha_2^A + \frac{1}{2}\alpha_3^A \right), \tag{3.279b}$$

$$A_{(0,\,1,\,0)} = A_{\mathrm{e}} - \left(\frac{1}{2}\alpha_1^A + \frac{3}{2}\alpha_2^A + \frac{1}{2}\alpha_3^A \right), \tag{3.279c}$$

$$A_{(0,\,0,\,1)} = A_{\mathrm{e}} - \left(\frac{1}{2}\alpha_1^A + \frac{1}{2}\alpha_2^A + \frac{3}{2}\alpha_3^A \right), \tag{3.279d}$$

which allows us to derive

$$A_{(0,\,0,\,0)} - A_{(1,\,0,\,0)} = \alpha_1^A \tag{3.280a}$$

Table 3.11 Vibration-rotation constants for SO_2

i	α_i^A/MHz	α_i^B/MHz	α_i^C/MHz
1	−31.05	50.14	42.83
2	−1175.90	−2.18	16.00
3	620.02	34.85	32.88

by subtracting Eq. (3.279b) from Eq. (3.279a), and similarly

$$A_{(0,\,0,\,0)} - A_{(0,\,1,\,0)} = \alpha_2^A, \tag{3.280b}$$

$$A_{(0,\,0,\,0)} - A_{(0,\,0,\,1)} = \alpha_3^A. \tag{3.280c}$$

Therefore, substituting the rotational constants in Table 3.8 into these equations, we obtain

$$\alpha_1^A = -31.05 \text{ MHz}, \quad \alpha_2^A = -1175.90 \text{ MHz}, \quad \alpha_3^A = 620.02 \text{ MHz},$$

which in turn can be substituted into Eq. (3.279a) to give us

$$A_\mathrm{e} = 60485.325 \text{ MHz}.$$

By similar procedures, we can calculate α_i^B, B_e, α_i^C, and C_e. The rotational constants and the vibration-rotation constants are shown in Tables 3.9(b) and 3.11, respectively. □

Translating the obtained values for A_e, B_e, and C_e into moments of inertia, we can calculate I_A^e, I_B^e, and I_C^e as shown in Table 3.9(b). When we use these figures to calculate the inertial defect, we arrive at $\Delta I^\mathrm{e} = -0.0075$ amu Å^2, whose absolute value is less than 6 % of the inertial defect for the vibrational ground state as calculated before. The structural parameter obtained for each of the combinations $(I_A^\mathrm{e}, I_B^\mathrm{e})$, $(I_B^\mathrm{e}, I_C^\mathrm{e})$, and $(I_C^\mathrm{e}, I_A^\mathrm{e})$, becomes close enough to the average,

$$r = 1.4308 \text{ Å}, \quad \theta = 119.32°,$$

that the difference is only recognized at the fourth and second decimal places, respectively. Thus, these average values can be taken as the molecular structure at the equilibrium position. Equilibrium structures obtained thus by offsetting the effect of the interaction between molecular vibration and rotation are called r_e structures. For instance, the r_e structure of SO_2 at the electronic ground state is written as $r_\mathrm{e} = 1.4308$ Å and $\theta_\mathrm{e} = 119.32°$. In contrast, a structure obtained from rotational constants for the vibrational ground state is called a r_0 structure.

As shown above, the value of inertial defect ΔI does not become exactly 0 even when we offset the effect of molecular vibration by applying Eqs. (3.276) through (3.278). This is because the inertial defect ΔI consists of three components originating from different interactions, and can be represented as

$$\Delta I = \Delta I_\mathrm{vib} + \Delta I_\mathrm{cent} + \Delta I_\mathrm{elec}. \tag{3.281}$$

Of these three components, ΔI_vib has the largest value; it is the contribution of the vibration-rotation interaction (the Coriolis interaction), and can be estimated as long

as the harmonic part of the vibrational potential is known. ΔI_{cent} is the contribution of centrifugal distortion, and ΔI_{elec} is the contribution of the interaction between intramolecular electrons and the rotation of the molecule. In the analysis above, the term ΔI_{vib} is corrected to become 0 during the procedure for obtaining A_{e}, B_{e}, and C_{e}. Consequently, we can think of ΔI as representing the slight contribution of the two components which remain uncorrected, that is, $\Delta I_{\text{cent}} + \Delta I_{\text{elec}}$.

In the case of methylhydrazine, which we focused on in Problem 3.14, there are many structural parameters that need to be specified in order to determine the full geometrical structure of the molecule. This is because the positions of the six hydrogen atoms must be specified, in addition to the internuclear distances for N–N and C–N, as well as the bond angle ∠N–N–C. This makes it impossible to determine the full molecular structure from the three rotational constants alone. Thus, in such cases, various types of approaches are taken to obtain the molecular structure with as high a precision as possible, such as employing the isotope substitution method or using the information on internuclear distances obtained by the gas electron diffraction method (to be discussed in the next chapter). Another approach is to reduce the number of structural parameters by assuming the bond lengths of all three C–H bonds in the methyl group to be equal. In yet another approach, we can obtain the theoretical equilibrium structure by using an *ab initio* molecular orbital calculation with a high reliability, and use its structural parameters as supplementary data in determining the other structural parameters from experimental data.

3.6 Rotating and Vibrating Molecules

In the previous section, we have determined rotational constants for each vibrational state by observing transitions between different rotational levels within the same vibrational state. However, information about rotational level energies can also be obtained from transitions between different vibrational levels, which are observed mainly in the IR region, as well as from transitions between different electronic states, which are observed mainly in the visible and UV regions. For example, the IR emission spectrum introduced in Fig. 1.7(a), Chap. 1, is composed of the observed transitions between rotational levels which belong to different vibrational states of CO_2.

In this section, we will examine molecular rotations in vibrationally excited states and electronically excited states by analyzing rotational structures observed in transitions between vibrational states in the same electronic state and those observed in transitions between vibrational states in two different electronic states.

3.6.1 Rotational Structures of Vibrational Transitions

An observation of the absorption spectrum of CO in the IR region from the vibrational ground state ($v = 0$) to the second excited state ($v = 2$) revealed a fine comb-like structure as shown in Fig. 3.23. This $v = 2 \leftarrow 0$ transition, called "overtone

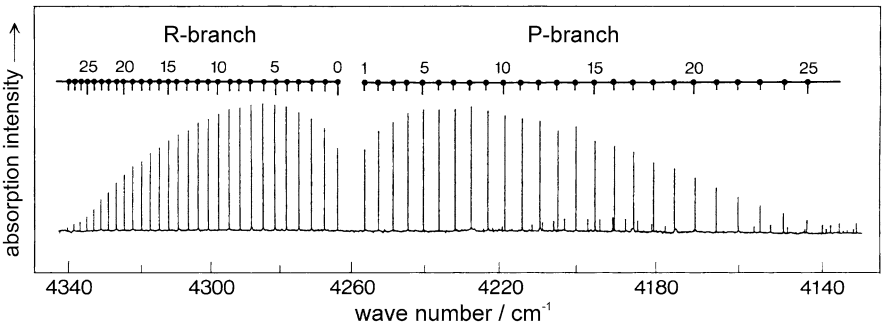

Fig. 3.23 An overtone ($v = 2 \leftarrow 0$) absorption spectrum of CO

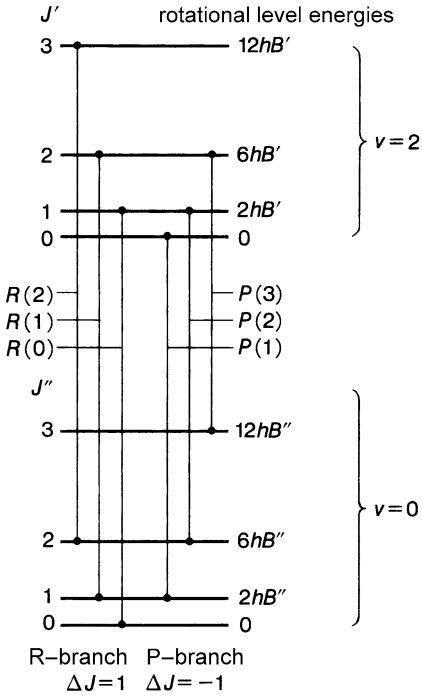

Fig. 3.24 Vibrational and rotational transitions of CO

absorption," is induced by the anharmonicity of molecular vibrations, as shown in Sect. 2.3.4. Worthy of note here is the comb-like structure that has appeared owing to the high resolution of the spectrum. Each of these transitions can be attributed as the transition from one rotational level in the $v = 0$ state to one in the $v = 2$ state.

The situation can be schematized as in Fig. 3.24; the spectrum is constructed of the R-branch, which spreads in the higher energy region according to the selection rule $\Delta J = J' - J'' = 1$, and the P-branch, which spreads in the lower energy region according to the selection rule $\Delta J = -1$. A number in parentheses, such as the 0

and 1 in $R(0)$ and $P(1)$, represents the rotational quantum number J'' of the lower level of the transition.

Such transitions between rotational levels found in a vibrational spectrum are called its rotational structure. In this case, the selection rule is described as $\Delta J = \pm 1$. The transitions that are not observed, such as $\Delta J = 0$ (Q-branch), $\Delta J = +2$ (S-branch), and $\Delta J = -2$ (O-branch), are called the forbidden transitions. The energy interval between $J'' = 0$ and $J' = 0$ is called the band center, or the energy of the band origin, and it is represented as $\tilde{\nu}_0$.

Taking a close look at Fig. 3.23 we realize that, in the case of the R-branch, as J'' becomes larger, the spacing in the comb-like peaks becomes gradually narrower toward the high-energy side, whereas in the case of the P-branch, as J'' becomes larger the spacing in the comb-like peaks becomes gradually wider toward the low-energy side. This phenomenon can be explained as follows.

The $R(J)$ transition is the transition from $J'' = J$ to $J' = J + 1$, and its wave number is calculated as

$$\begin{aligned}\tilde{\nu}\big[R(J)\big] &= \tilde{\nu}_0 + B'(J+1)(J+2) - B''J(J+1) \\ &= \tilde{\nu}_0 + \big(B' - B''\big)J(J+1) + 2B'(J+1),\end{aligned} \tag{3.282}$$

where the rotational constant is expressed in terms of cm^{-1}. Similarly, the wave number of the $P(J)$ transition is written as

$$\tilde{\nu}\big[P(J)\big] = \tilde{\nu}_0 + \big(B' - B''\big)J(J+1) - 2B'J. \tag{3.283}$$

The rotational constant B' in a vibrationally excited state is slightly smaller than B'' because of the anharmonicity of vibration. Therefore, $B' - B''$ is a negative value, if only a small one, and the amount of increases in $\tilde{\nu}[R(J)]$ steadily grows smaller as J increases. As for $\tilde{\nu}[P(J)]$, on the other hand, its amount of decreases steadily grows larger as J increases. In other words, the relationship $B' < B''$ makes the P-branch and the R-branch asymmetrical.

From this vibration-rotation spectrum, we can readily obtain the rotational constants B' and B''. For instance, since $R(0)$ and $P(2)$ have the common upper level $J' = 1$, it is clear from Fig. 3.24 that

$$\tilde{\nu}\big[R(0)\big] - \tilde{\nu}\big[P(2)\big] = 6B''. \tag{3.284}$$

Similarly, as $R(1)$ and $P(1)$ have the common lower level $J'' = 1$, we can write

$$\tilde{\nu}\big[R(1)\big] - \tilde{\nu}\big[P(1)\big] = 6B'. \tag{3.285}$$

Thus, we can calculate B'' and B' from the observed transition wave numbers using Eqs. (3.284) and (3.285). Such a method of obtaining the energy difference between two levels by use of two transition energies sharing the same level is called the combination difference method.

Of the overtone vibration-rotation transitions shown in Fig. 3.24, the wave numbers of the six transitions closest to the band origin are listed in Table 3.12, with the wave numbers of the vibration-rotation transition for the fundamental ($v = 1 \leftarrow 0$) provided as well.

Table 3.12 Vibration-rotation transitions of CO

Assignment	Transition wave numbers/cm^{-1}	
	$v = 1 \leftarrow 0$	$v = 2 \leftarrow 0$
$R(2)$	2154.5960	4271.1770
$R(1)$	2150.8564	4267.5425
$R(0)$	2147.0816	4263.8376
$P(1)$	2139.4265	4256.2176
$P(2)$	2135.5466	4252.3026
$P(3)$	2131.6320	4248.3180
$\tilde{\nu}_0$	2143.2715	4260.0626

Note: $\tilde{\nu}_0$ represents a wave number of the rotational band origin

In the case of linear molecules, when vibration excitation by IR absorption is induced by a transition moment perpendicular to the molecular axis, we can observe the Q-branch ($\Delta J = 0$) in addition to the P-branch ($\Delta J = -1$) and the R-branch ($\Delta J = 1$). For example, the broad emission-type peak observed at 667 cm^{-1} and the absorption-type peaks observed at 618 cm^{-1} and 721 cm^{-1} in the IR spectrum of CO_2 shown in Fig. 1.7(a), Chap. 1, correspond to the portions where Q-branch transitions are densely located.

Problem 3.16
Using the transition wave number listed in Table 3.12, calculate the rotational constants B_0, B_1, and B_2, of the three vibrational levels of CO, $v = 0, 1, 2$, respectively. Also calculate the wave numbers of the band origins for the two vibration-rotation transitions, $v = 1 \leftarrow 0$ and $v = 2 \leftarrow 0$.

Solution
From the transition $v = 1 \leftarrow 0$, we can determine B_0 and B_1 in the following manner:

$$\begin{aligned}\tilde{\nu}\big[R(0)\big] - \tilde{\nu}\big[P(2)\big] &= 2147.0816 - 2135.5466 \\ &= 11.5350\ \text{cm}^{-1},\end{aligned}$$

which is equal to $6B_0$ so that $B_0 = 1.92250\ \text{cm}^{-1}$, and

$$\begin{aligned}\tilde{\nu}\big[R(1)\big] - \tilde{\nu}\big[P(1)\big] &= 2150.8564 - 2139.4265 \\ &= 11.4299\ \text{cm}^{-1},\end{aligned}$$

which is equal to $6B_1$ so that $B_1 = 1.90498\ \text{cm}^{-1}$.

Similarly, from the transition $v = 2 \leftarrow 0$, we can determine B_0 and B_2 as

$$B_0 = \frac{1}{6}\big\{\tilde{\nu}\big[R(0)\big] - \tilde{\nu}\big[P(2)\big]\big\} = 1.92250\ \text{cm}^{-1},$$

$$B_2 = \frac{1}{6}\big\{\tilde{\nu}\big[R(1)\big] - \tilde{\nu}\big[P(1)\big]\big\} = 1.88748\ \text{cm}^{-1}.$$

Thus the three rotational constants are determined as $B_0 = 1.9225\ \mathrm{cm}^{-1}$, $B_1 = 1.9050\ \mathrm{cm}^{-1}$, and $B_2 = 1.8875\ \mathrm{cm}^{-1}$.

Next, the wave number of the band origin of the transition $v = 1 \leftarrow 0$, $\tilde{\nu}_0(1 \leftarrow 0)$, is calculated as

$$\begin{aligned}\tilde{\nu}_0(1 \leftarrow 0) &= \tilde{\nu}\big[P(1)\big] + 2B_0 \\ &= 2143.2715\ \mathrm{cm}^{-1}.\end{aligned}$$

Similarly, the wave number of the band origin of the transition $v = 2 \leftarrow 0$, $\tilde{\nu}_0(2 \leftarrow 0)$, is calculated as

$$\begin{aligned}\tilde{\nu}_0(2 \leftarrow 0) &= \tilde{\nu}\big[P(1)\big] + 2B_0 \\ &= 4260.0626\ \mathrm{cm}^{-1}.\end{aligned}$$

The wave numbers of these band origins can be immediately equated with the energy values of levels $v = 1$ and $v = 2$ as measured from $J'' = 0$ in the vibrational ground state. In other words, these wave numbers can be regarded as term values. □

Problem 3.17
Using the solution to Problem 3.16, answer the following questions.

(1) Using the obtained rotational constants B_0, B_1, and B_2, determine the equilibrium internuclear distance r_e of CO.
(2) Using the wave numbers of band origins, determine the Morse potential parameters, ω_e and $\omega_\mathrm{e}x_\mathrm{e}$, of CO.
(3) Using ω_e and $\omega_\mathrm{e}x_\mathrm{e}$, predict the dissociation energy D_0 and compare the result with the observed value, $D_0 = 11.09$ eV.

Solution

(1) For a diatomic molecule, too, the vibrational dependence of the rotational constant B_v can be described by the vibration-rotation constant α_e as has been shown in Eq. (3.277). That is, using the equilibrium rotational constant B_e, B_v can be expressed as

$$B_v = B_\mathrm{e} - \alpha_\mathrm{e}\left(v + \frac{1}{2}\right). \tag{3.286}$$

Therefore, $\alpha_\mathrm{e} = 0.01752\ \mathrm{cm}^{-1}$ can be derived from B_0 and B_1, and $\alpha_\mathrm{e} = 0.01750\ \mathrm{cm}^{-1}$ from B_1 and B_2. As these two numerical values are mostly in agreement, we can conclude that Eq. (3.286) is valid. Adopting the mean value $\alpha_\mathrm{e} = 0.01751\ \mathrm{cm}^{-1}$ for α_e, B_e is calculated as $B_\mathrm{e} = 1.9313\ \mathrm{cm}^{-1}$. We can convert this figure into a moment of inertia to determine the equilibrium internuclear distance as $r_\mathrm{e} = 1.1283$ Å, by applying the formula $I = \mu r_\mathrm{e}^2$.

(2) Using Eq. (2.174), which has been introduced in Sect. 2.3.8, we can derive

$$\begin{aligned}\tilde{\nu}_0(1 \leftarrow 0) &= E_1 - E_0 = \omega_\mathrm{e} - 2\omega_\mathrm{e}x_\mathrm{e}, \\ \tilde{\nu}_0(2 \leftarrow 0) &= E_2 - E_0 = 2\omega_\mathrm{e} - 6\omega_\mathrm{e}x_\mathrm{e}.\end{aligned}$$

By substituting the values of the band origins into these equations, the Morse parameters can be determined as

$$\omega_e = 2169.752 \text{ cm}^{-1},$$
$$\omega_e x_e = 13.240 \text{ cm}^{-1}.$$

(3) From Eq. (2.177), $D_e = 88893.95 \text{ cm}^{-1}$. From Eq. (2.173), $D_0 = D_e - \frac{\omega_e}{2} + \frac{\omega_e x_e}{4} = 87812.384 \text{ cm}^{-1}$, which can be converted into the eV unit as $D_0 = 10.89$ eV. This is in good agreement with the observed value. Therefore, we can conclude that the Morse potential is a good approximation of the interatomic potential of CO.

Incidentally, as B_0 is the expectation value of $B = \frac{h}{8\pi^2 \mu r^2}$ at $v = 0$, B_0 can be written as

$$B_0 = \frac{h}{8\pi^2 \mu} \langle \psi_0 | \frac{1}{r^2} | \psi_0 \rangle. \tag{3.287}$$

□

3.6.2 Rotational Structures of Electronic Transitions

As has been introduced in the first chapter, the electronically excited state of a molecule also contains different vibrational levels, each of which, in turn, contains different rotational levels. When a molecule absorbs visible or ultraviolet light and is excited to their electronically excited state, a transition occurs in most cases to both the vibrationally and rotationally excited states. To take an example, Fig. 3.25 shows the rotational structure observed when SO_2 is excited from the vibrational ground state in the electronic ground state (which is called the $\tilde{X}$ state) to the vibrational level $(v_1, v_2, v_3) = (1, 3, 0)$ in the electronically excited state (which is called the $\tilde{C}$ state).

Converting the wave number of this spectral region into a wavelength, it corresponds to approximately 224 nm, which is in the UV wavelength region. From the assignment of the rotational transitions shown in the figure in the form of $J'_{K'_a K'_c} - J''_{K''_a K''_c}$, we can confirm that the selection rule $\Delta J = 0, \pm 1$ is satisfied. Furthermore, when we focus on the parity of $K_a K_c$, we realize that only the a-type transitions, which have the form $eo \leftrightarrow ee$ or $oe \leftrightarrow oo$, are observed. This means that the dipole moment of the electronic transition is pointing in the direction of the a axis. Of the observed transitions between different rotational levels, the ones with low J values are listed in Table 3.13.

As shown in Table 3.9(a), the rotational constants A'', B'', and C'' for the vibrational ground state in the electronic ground state $\tilde{X}$, that is, $(v_1, v_2, v_3) = (0, 0, 0)$, have already been determined from the rotational spectra in the microwave region. Therefore, using the transition wave numbers given in Table 3.13, we can determine the rotational constants A', B', and C' for $\tilde{C}(1, 3, 0)$ and the wave number of the band origin $\tilde{\nu}_0$.

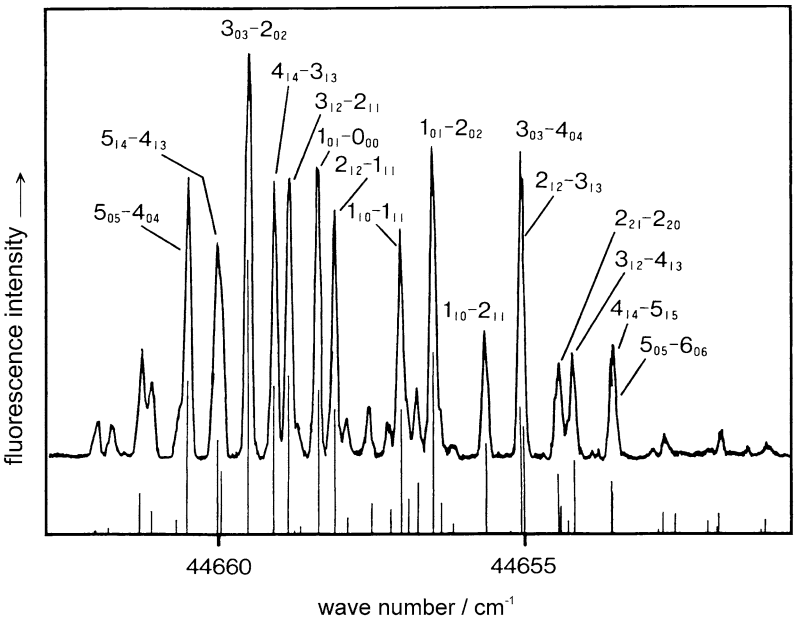

Fig. 3.25 The rotational structure of the $\tilde{C}(1,3,0) - \tilde{X}(0,0,0)$ transitions for SO_2

Table 3.13 The rotational structure of the $\tilde{C}(1,3,0)$–$\tilde{X}(0,0,0)$ transition for SO_2

Assignment $J'_{K'_a K'_c}$–$J''_{K''_a K''_c}$	Transition wave numbers/cm^{-1}
3_{03}–2_{02}	44659.542
3_{12}–2_{11}	44658.871
1_{01}–0_{00}	44658.388
2_{12}–1_{11}	44658.097
1_{10}–1_{11}	44656.998
2_{12}–2_{11}	44656.721
1_{01}–2_{02}	44656.470
1_{10}–2_{11}	44655.624
2_{12}–3_{13}	44655.062
2_{21}–2_{20}	44654.468

Problem 3.18

Using the transition wave numbers listed in Table 3.13, determine the rotational constants A', B', and C' for $\tilde{C}(1,3,0)$ and the wave number of the band origin $\tilde{\nu}_0$.

Solution

Using the expressions given in Table 3.2, we will describe the transition wave number using the rotational constants and $\tilde{\nu}_0$. Averaging the value of C' obtained from

$2_{12} - 1_{11}$ and $1_{10} - 1_{11}$ and that obtained from $2_{12} - 2_{11}$ and $1_{10} - 2_{11}$, we can take $C' = 0.2745\ \mathrm{cm}^{-1}$. Similarly, we can obtain $A' = 1.207\ \mathrm{cm}^{-1}$ from $2_{21} - 2_{20}$ and $1_{01} - 0_{00}$, and $B' = 0.3419\ \mathrm{cm}^{-1}$ from $3_{12} - 2_{11}$ and $2_{12} - 2_{11}$. The values of B' and C' determined here, along with the transition wave number of $1_{01} - 0_{00}$, allow us to calculate the wave number of the band origin as $\tilde{\nu}_0 = 44657.77\ \mathrm{cm}^{-1}$. □

The vertical lines shown below the observed peaks in Fig. 3.25 are the calculated spectra based on the rotational constants A', B', and C' obtained in Problem 3.18. We can see that the calculated spectra successfully reproduce not only the transition wave numbers but even the peak intensities.

By applying an analysis similar to that of Problem 3.18 to the rotational structure of the $\tilde{C}(0, 0, 0) - \tilde{X}(0, 0, 0)$ transition of SO_2, the rotational constants for the vibrational ground state $\boldsymbol{v} = (0, 0, 0)$ of the electronically excited state $\tilde{C}$ are calculated as

$$A_0 = 1.15053\ \mathrm{cm}^{-1}, \quad B_0 = 0.34744\ \mathrm{cm}^{-1}, \quad C_0 = 0.26543\ \mathrm{cm}^{-1}.$$

Taking A_0 and B_0 from these rotational constants and calculating the internuclear distance r between the S atom and the O atom, as well as the bond angle $\theta = \angle$O–S–O in the same manner as in Sect. 3.5.3, the r_0 structure is determined as $r = 1.560$ Å and $\theta = 104.3°$. When we compare these structural parameters with the r_0 structure of the electronic ground state $\tilde{X}$, which has previously been determined, it becomes clear that the internuclear distance increases by 0.126 Å, and the bond angle decreases by 15.1°, with the electronic excitation.

As shown here, we can determine the term values of different vibrational levels and the rotational constants for the electronically excited state through the analysis of rotational structures. Therefore, by measuring molecular spectra in visible and UV regions with a sufficiently high energy resolution required to resolve rotational structures, we can determine molecular structures and derive information on the shapes of the potential energy surfaces in the electronically excited state.

Chapter 4
Scattering Electrons

One of the ways to determine the geometrical structure of gaseous molecules is the gas electron diffraction method. In this method, highly accelerated electron beams are shot into molecules. After colliding with the target molecules, the electrons are scattered. Information on the distances between atoms in the molecules is clearly imprinted in the spatial interference patterns of this scattered wave. This phenomenon of electron scattering can also be described by quantum mechanics. Therefore in this section, we will first learn the framework of quantum mechanics for dealing with the scattering phenomenon. Then, after learning the mechanism of electron scattering caused by atoms, we will discuss the case of electrons being scattered by molecules and learn how molecular structures are reflected in the interference patterns of scattered electrons, thereby reaching an understanding of the method for determining molecular structures by the analysis of interference patterns. In addition, we will learn the effect of molecular vibration on interference patterns, and understand the difference between the molecular structure obtained from the analysis of rotational structure in spectra introduced in the previous chapter and that obtained from the gas electron diffraction method.

Summaries

4.1 Scattering Electron Waves

We will learn here that accelerated electron beams have the characteristics of a wave, and that, when atoms or molecules are irradiated with an electron beam, its scattering state can be described as the sum of the incident plane wave and the scattering spherical wave. We will also discuss how to define scattering amplitudes, scattering differential cross sections, and scattering total cross sections, using probability current densities.

4.2 Electron Scattering by Atoms

The Schrödinger equation for scattering electrons will be used to write the wave function representing a scattering state. In addition, we will describe the scattering amplitude of an electron being scattered by atoms according to the Born approximation.

K. Yamanouchi, *Quantum Mechanics of Molecular Structures*,
DOI 10.1007/978-3-642-32381-2_4,

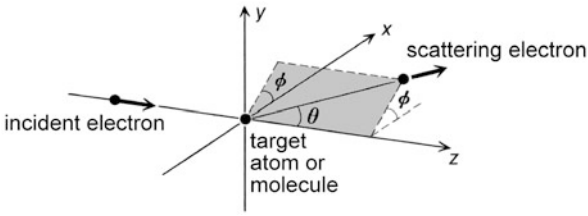

Fig. 4.1 Electron scattering by an atom or a molecule

4.3 Electron Scattering by Molecules
We will look at electron scattering caused by diatomic molecules aligned in a specific spatial direction and that caused by diatomic molecules taking random orientations, so as to reach the understanding that the geometrical structures of molecules and the degree of molecular alignment can be determined from the interference patterns of scattered electrons.

4.4 Phase Shift of the Scattering Electron Wave
By solving the Schrödinger equation for scattering using the partial wave expansion method, we will understand that when electrons are scattered by atoms the scattered wave is drawn in by the atoms to cause a phase shift. From the behavior of partial waves near the interaction region, we will derive the partial wave expansion of the scattering amplitude, and see that the scattering amplitude of electron scattered by atoms is written as a complex function.

4.5 The Effect of Molecular Vibration
As molecules vibrate, the distribution of internuclear distances has a width called the mean amplitude, and the intensity of the interference pattern of an electron beam scattered by the molecules decreases as the scattering angle increases. We will also derive the mean amplitude of diatomic molecules and see that this value increases as temperature rises.

4.6 Electron Beam Scattering by Polyatomic Molecules We will learn that the interference terms of electron scattered by molecules are given as the molecular scattering curve, and that the radial distribution curve is obtained by a Fourier transform of the molecular scattering curve. Also by looking at the example of the molecular scattering curve we will learn how internuclear distances are determined from the molecular scattering curve, and understand the effects that molecular vibration and phase shift have on molecular scattering curves. In addition, we will see that even in the case of relatively complex molecules with rotational isomers, not only their geometrical structures but also the abundance ratios of the isomers can be determined by using the gas electron diffraction method.

4.1 Scattering Electron Waves

Let us consider a situation in which, as in Fig. 4.1, accelerated electrons travel along the z axis and collide with atoms or molecules located at the origin, thereby being scattered along the polar angle θ and azimuthal angle ϕ. Considering the interpretation of wave functions in terms of probability, when the wave function of an electron

is represented as $\psi(\boldsymbol{r}, t)$, the scattering problem needs to be regarded as the question of how the probability $\rho(\boldsymbol{r}, t)$, written as

$$\rho(\boldsymbol{r}, t) \equiv \left|\psi(\boldsymbol{r}, t)\right|^2, \tag{4.1}$$

changes according to time.

As seen in Sect. 2.4, the time-dependent Schrödinger equation is represented as

$$\mathrm{i}\hbar\frac{\partial\psi}{\partial t} = -\frac{\hbar^2}{2m_\mathrm{e}}\nabla^2\psi + V\psi, \tag{4.2}$$

where m_e is the mass of the electron. When we differentiate $\rho(\boldsymbol{r}, t)$ by t, we obtain

$$\begin{aligned}\frac{\partial}{\partial t}\rho(\boldsymbol{r}, t) &= \frac{\partial}{\partial t}\left\{\psi^*(\boldsymbol{r}, t)\psi(\boldsymbol{r}, t)\right\} \\ &= \frac{\partial\psi^*}{\partial t}\psi + \psi^*\frac{\partial\psi}{\partial t}.\end{aligned} \tag{4.3}$$

Substituting Eq. (4.2) and its complex conjugate into Eq. (4.3), we can write

$$\begin{aligned}\frac{\partial\rho}{\partial t} &= \frac{1}{\mathrm{i}\hbar}\left(\frac{\hbar^2}{2m_\mathrm{e}}\nabla^2\psi^* - V\psi^*\right)\psi + \frac{1}{\mathrm{i}\hbar}\psi^*\left(-\frac{\hbar^2}{2m_\mathrm{e}}\nabla^2\psi + V\psi\right) \\ &= \frac{\hbar}{2m_\mathrm{e}\mathrm{i}}\left\{\left(\nabla^2\psi^*\right)\psi - \psi^*\left(\nabla^2\psi\right)\right\} \\ &= \frac{\hbar}{2m_\mathrm{e}\mathrm{i}}\nabla\cdot\left\{\left(\nabla\psi^*\right)\psi - \psi^*\left(\nabla\psi\right)\right\},\end{aligned} \tag{4.4}$$

where $\nabla\psi$ is a vector quantity which can also be represented as grad ψ, and is given as

$$\nabla\psi = \left(\frac{\partial\psi}{\partial x}, \frac{\partial\psi}{\partial y}, \frac{\partial\psi}{\partial z}\right). \tag{4.5}$$

In general, for a vector $\boldsymbol{a} = (a_x, a_y, a_z)$, $\nabla\cdot\boldsymbol{a}$, which can also be represented as div $\boldsymbol{a}$, is given as

$$\nabla\cdot\boldsymbol{a} = \frac{\partial a_x}{\partial x} + \frac{\partial a_y}{\partial y} + \frac{\partial a_z}{\partial z}.$$

Therefore, $\nabla\cdot(\nabla\psi)$ is written as

$$\nabla\cdot(\nabla\psi) = \frac{\partial^2\psi}{\partial x^2} + \frac{\partial^2\psi}{\partial y^2} + \frac{\partial^2\psi}{\partial z^2}, \tag{4.6}$$

and is equal to $\nabla^2\psi$. When we define a vector $\boldsymbol{j}$, called the probability current density, as

$$\boldsymbol{j} = \frac{\hbar}{2m_\mathrm{e}\mathrm{i}}\left(\psi^*\nabla\psi - \psi\nabla\psi^*\right), \tag{4.7}$$

Eq. (4.4) becomes

$$\frac{\partial \rho}{\partial t} + \operatorname{div} \boldsymbol{j} = 0. \tag{4.8}$$

The probability current density is also simply called the current density or the flux density. This is known as the equation of continuity and expresses the conservation of the probability, that is, this equation signifies that the probability with which the number of electrons increases (or decreases) in a given region is equal to the probability with which they enter (or exit) the region through the boundary.

Next, when we consider an electron making free one-dimensional movements, the wavelength λ describing the characteristics of the wave is related to p, the momentum of the electron as defined when seeing it as a particle, by the formula of de Broglie, that is,

$$\lambda = \frac{h}{p} = \frac{h}{m_{\mathrm{e}} v}. \tag{4.9}$$

In experiments of gas electron diffraction, electrons are accelerated at the acceleration voltage of tens of kV. In this case, the kinetic energy acquired by an electron when it is accelerated by the electric field generated at the voltage potential difference of V can be written as

$$\frac{1}{2} m_{\mathrm{e}} v^2 = eV, \tag{4.10}$$

where e is the charge (the elementary charge) and v the velocity of the electron. From the formula of de Broglie, the wavelength of the electron can be represented as

$$\lambda = \frac{h}{p} = \frac{h}{m_{\mathrm{e}} v} = \frac{h}{\sqrt{2 m_{\mathrm{e}} e V}}. \tag{4.11}$$

For example, when the acceleration voltage is 40 kV, we can use the values $e = 1.602176462 \times 10^{-19}$ C, $m_{\mathrm{e}} = 9.10938188 \times 10^{-31}$ kg, and $h = 6.62606876 \times 10^{-34}$ J s to arrive at $\lambda = 0.06132$ Å. Although, as will be discussed in Problem 4.1, we will need to apply relativistic corrections if we are to obtain a more precise value for the wavelength.

When we define a 3-dimensional wave vector $\boldsymbol{k}$ using the momentum vector $\boldsymbol{p}$ as

$$\boldsymbol{k} = \frac{\boldsymbol{p}}{\hbar}, \tag{4.12}$$

$\boldsymbol{k}$ can be written as

$$\boldsymbol{k} = (k_x, k_y, k_z) = \left(\frac{2\pi}{\lambda_x}, \frac{2\pi}{\lambda_y}, \frac{2\pi}{\lambda_z} \right). \tag{4.13}$$

A plane wave with the constant wavelength λ which propagates along the $\boldsymbol{k}$ direction is represented as

$$\begin{aligned}\psi_{\boldsymbol{k}} &= \exp\{\mathrm{i}(\boldsymbol{k}\cdot\boldsymbol{r}-\omega t)\}\\ &= \mathrm{e}^{\mathrm{i}k_x x}\mathrm{e}^{\mathrm{i}k_y y}\mathrm{e}^{\mathrm{i}k_z z}\mathrm{e}^{-\mathrm{i}\omega t}.\end{aligned} \tag{4.14}$$

When the wave fronts lined up at the interval of the wavelength λ travel in the direction of $\boldsymbol{k}$, a given pair of adjacent wave fronts will cross the x axis, y axis, and z axis each at two points separated by the distance of λ_x, λ_y and λ_z, respectively, as shown in Fig. 4.2. When the direction of the vector $\boldsymbol{k}$ coincides with the z axis, we can regard the three wavelengths as $\lambda_x \to \infty$, $\lambda_y \to \infty$, and $\lambda_z \to \lambda$, and therefore we can represent a plane wave propagating along the z axis as

$$\psi_z = \exp\{\mathrm{i}(kz-\omega t)\} = \mathrm{e}^{\mathrm{i}kz}\mathrm{e}^{-\mathrm{i}\omega t}. \tag{4.15}$$

After being scattered by a target atom or molecule, on the other hand, the plane wave of an electron is considered to expand spherically. Thus for an electron wave propagating through a region whose distance from the target position, r, is sufficiently large, where its movement is in the direction of polar angle θ and azimuthal angle ϕ, the wavelength has to be the same as before, while the shape of the wave is written as $\exp\{\mathrm{i}(kr-\omega t)\}$. At the same time, however, the probability with which an electron is found in the volume element $r^2\sin\theta\,\mathrm{d}r\,\mathrm{d}\theta\,\mathrm{d}\phi$ in polar coordinates needs to be constant. This necessitates the square modulus of ψ_s, which is the wave function of the scattering wave, to decrease inversely proportional to r^2 as r increases. That is, the wave function of an electron scattered along the direction of θ, ϕ is represented as that of a spherical wave which has the following shape:

$$\psi_\mathrm{s} \propto \frac{1}{r}\exp\{\mathrm{i}(kr-\omega t)\}. \tag{4.16}$$

Generally speaking, the intensity distribution of the scattering wave can be thought to depend on the directions θ and ϕ, so the scattering amplitude dependent on the directions θ and ϕ is expressed as $f(\theta,\phi)$. When r is sufficiently large, or $r \to \infty$, the asymptotic form of this function can be written as

$$\psi_\mathrm{s} \sim \frac{f(\theta,\phi)}{r}\mathrm{e}^{\mathrm{i}kr}\mathrm{e}^{-\mathrm{i}\omega t}. \tag{4.17}$$

The function $f(\theta,\phi)$ is called scattering amplitude, and has a dimension of length as seen from Eq. (4.17).

From the above discussion, we see that the state in which an electron beam propagating along the z axis is scattered and expanding as an outgoing spherical wave is written as the sum of Eqs. (4.15) and (4.17), that is,

$$\psi \sim \mathrm{e}^{\mathrm{i}kz} + \frac{f(\theta,\phi)}{r}\mathrm{e}^{\mathrm{i}kr}. \tag{4.18}$$

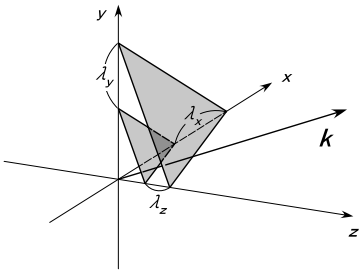

Fig. 4.2 A plane wave with the wave vector $\boldsymbol{k}$

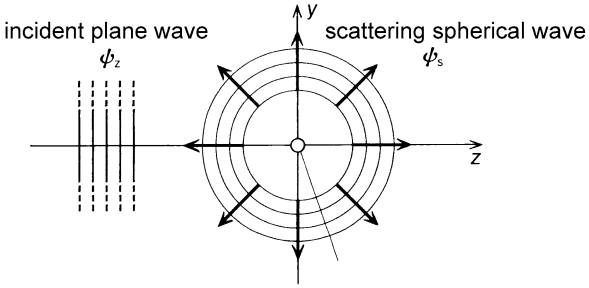

Fig. 4.3 The waves of an electron beam in a scattering state

In Eq. (4.18), however, the factor $\mathrm{e}^{-\mathrm{i}\omega t}$ is omitted. As is clear from the explanations so far, the first term of this equation represents the component of the incident plane wave advancing straight along one direction, and the second term represents the component of the scattered spherical wave propagating outwards along the directions appointed by θ and ϕ. An illustration is given in Fig. 4.3.

Let us now calculate the probability current densities of the two respective components by following Eq. (4.7). First, by substituting $\mathrm{e}^{\mathrm{i}kz}$ for ψ in Eq. (4.7), we obtain the probability current density propagating along the z axis as

$$\begin{aligned}\boldsymbol{j}_z &= \frac{\hbar}{2m_\mathrm{e}\mathrm{i}}\left\{\mathrm{e}^{-\mathrm{i}kz}\left(0,0,\frac{\partial \mathrm{e}^{\mathrm{i}kz}}{\partial z}\right)-\mathrm{e}^{\mathrm{i}kz}\left(0,0,\frac{\partial \mathrm{e}^{-\mathrm{i}kz}}{\partial z}\right)\right\}\\ &= \frac{\hbar}{2m_\mathrm{e}\mathrm{i}}(2\mathrm{i}k)\boldsymbol{e}_z\\ &= \frac{\hbar k}{m_\mathrm{e}}\boldsymbol{e}_z,\end{aligned} \tag{4.19}$$

where $\boldsymbol{e}_z$ is the unit vector for the direction of the z axis, and can be expressed as $\boldsymbol{e}_z = (0, 0, 1)$. Next, by substituting the second term in Eq. (4.18) for ψ in Eq. (4.7), we can calculate the probability current density propagating in the direction of $\boldsymbol{r}$, which in turn is defined by θ and ϕ, as

$$\boldsymbol{j}_r = \frac{\hbar}{2m_\mathrm{e}\mathrm{i}}\left\{\frac{f^*(\theta,\phi)}{r}\mathrm{e}^{-\mathrm{i}kr}\boldsymbol{e}_r\frac{\partial}{\partial r}\left(\frac{f(\theta,\phi)}{r}\mathrm{e}^{\mathrm{i}kr}\right)\right.$$

$$- \frac{f(\theta,\phi)}{r} \mathrm{e}^{\mathrm{i}kr} \boldsymbol{e}_r \frac{\partial}{\partial r} \left(\frac{f^*(\theta,\phi)}{r} \mathrm{e}^{-\mathrm{i}kr} \right) \Bigg\}$$

$$= \frac{\hbar k}{m_\mathrm{e}} \frac{|f(\theta,\phi)|^2}{r^2} \boldsymbol{e}_r, \tag{4.20}$$

where $\boldsymbol{e}_r$ is the unit vector for the direction of $\boldsymbol{r}$.

The ratio of the probability current density scattered into the differential solid angle of the direction (θ, ϕ) plotted against the probability current density of the incident wave, which propagates along the z axis, can be written as

$$\mathrm{d}\sigma = \frac{|\boldsymbol{j}_r|}{|\boldsymbol{j}_z|} r^2 \,\mathrm{d}\Omega = \frac{|f(\theta,\phi)|^2}{r^2} r^2 \,\mathrm{d}\Omega$$

$$= \left| f(\theta,\phi) \right|^2 \mathrm{d}\Omega. \tag{4.21}$$

Thus,

$$\frac{\mathrm{d}\sigma}{\mathrm{d}\Omega} = \left| f(\theta,\phi) \right|^2, \tag{4.22}$$

where $f(\theta, \phi)$ has the dimension of the length and $\frac{\mathrm{d}\sigma}{\mathrm{d}\Omega}$ has the dimension of the cross-section. This is why $\frac{\mathrm{d}\sigma}{\mathrm{d}\Omega}$ is known as a differential cross-section. The value obtained by integrating the differential cross-section for the entire ranges of θ and ϕ,

$$\sigma = \int \frac{\mathrm{d}\sigma}{\mathrm{d}\Omega} \mathrm{d}\Omega = \int_0^\pi \int_0^{2\pi} \left| f(\theta,\phi) \right|^2 \sin\theta \,\mathrm{d}\theta \,\mathrm{d}\phi, \tag{4.23}$$

expresses the ratio of the wave being scattered, and this is called the total cross-section. One of the main themes for this chapter is to derive the scattering amplitude $f(\theta, \phi)$ for the process in which an electron beam is scattered after colliding with either an atom or a molecule.

Problem 4.1

According to the theory of relativity, when m_e represents the stationary mass of an electron, the mass of this electron moving at the velocity of v is expressed as $\frac{m_\mathrm{e}}{\sqrt{1-\beta^2}}$, where $\beta = \frac{v}{c}$ and c is the speed of light.

(1) Taking into account the theory of relativity, find the wavelength of an electron accelerated by the accelerating voltage of V.
(2) Calculate the wavelength of the electrons accelerating at voltage 40 kV, comparing your result to the one obtained from the formula which does not account for the relativistic corrections.

Solution

(1) The relativistic energy of the electrons before being accelerated is $m_\mathrm{e}c^2$, and that of the electron after being accelerated is $\frac{m_\mathrm{e}c^2}{\sqrt{1-\beta^2}}$. As the amount of energy

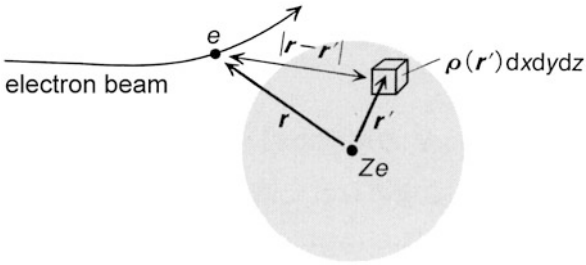

Fig. 4.4 Electron beam scattering by an atom

given to the electron by the electric field is eV, we can write

$$\frac{m_e c^2}{\sqrt{1-\beta^2}} - m_e c^2 = eV. \tag{4.24}$$

The wavelength of the accelerated electron is given as

$$\lambda = \frac{h}{m_e v}\sqrt{1-\beta^2} = \frac{h}{m_e c}\sqrt{\frac{1}{\beta^2} - 1}. \tag{4.25}$$

Once we eliminate β^2 from Eqs. (4.24) and (4.25), we obtain

$$\lambda = \frac{h}{\sqrt{2m_e eV}\cdot\sqrt{1+\frac{eV}{2m_e c^2}}}. \tag{4.26}$$

This is the wavelength of the electrons after applying relativistic corrections.

(2) When $V = 40$ kV, we can calculate the component $\left(1+\frac{eV}{2m_e c^2}\right)^{-\frac{1}{2}}$ in Eq. (4.26) as 0.98099. Thus, the wavelength is obtained as $\lambda = 0.06016$ Å. This tells us that the relativistic effect shortens the wavelength λ by about 1.9 %. □

4.2 Electron Scattering by Atoms

4.2.1 The Schrödinger Equation for Scattering

Let us first think about the case where an accelerated electron is scattered by an atom, as shown in Fig. 4.4. As the electron approaches the atom, the electron becomes increasingly influenced by the potential represented as $V(\boldsymbol{r})$ at the position vector $\boldsymbol{r}$, because of their Coulomb interaction with the atomic nuclei and with the electrons in the atom. The potential $V(\boldsymbol{r})$ can be described as follows:

$$V(\boldsymbol{r}) = -\frac{Ze^2}{4\pi\varepsilon_0 r} + \frac{e^2}{4\pi\varepsilon_0}\int \frac{\rho(\boldsymbol{r}')}{|\boldsymbol{r}-\boldsymbol{r}'|}\,\mathrm{d}\boldsymbol{r}'. \tag{4.27}$$

The first term in Eq. (4.27) represents the attractive potential between the incident electron and a nucleus in the target atom whose charge number is Z, whereas the second term expresses the repulsive potential between the incident electron and the electrons in the target atom. Here, $r = |\boldsymbol{r}|$, and $\rho(\boldsymbol{r}')$ represents the density of electrons at the position vector $\boldsymbol{r}'$; ε_0 is the vacuum permittivity. This whole scattering process is described by a wave function $\psi(\boldsymbol{r})$, which is the solution for the Schrödinger equation of electron motion given as

$$-\frac{\hbar^2}{2m_\mathrm{e}}\nabla^2\psi(\boldsymbol{r}) + V(\boldsymbol{r})\psi(\boldsymbol{r}) = E\psi(\boldsymbol{r}). \tag{4.28}$$

The wave number k in the solution for Eq. (4.28) fulfills

$$k^2 = \frac{2m_\mathrm{e}E}{\hbar^2} > 0. \tag{4.29}$$

Thus we can rewrite Eq. (4.28) using

$$U(\boldsymbol{r}) = \frac{2m_\mathrm{e}}{\hbar^2}V(\boldsymbol{r}) \tag{4.30}$$

as

$$\left(\nabla^2 + k^2\right)\psi_k(\boldsymbol{r}) = U(\boldsymbol{r})\psi_k(\boldsymbol{r}), \tag{4.31}$$

where ψ is represented as ψ_k because it will be characterized by k.

Let $G(\boldsymbol{k}, \boldsymbol{r})$ be a function of $\boldsymbol{k}$ and $\boldsymbol{r}$ which satisfies

$$\left(\nabla^2 + k^2\right)G(\boldsymbol{k}, \boldsymbol{r}) = \delta(\boldsymbol{r}), \tag{4.32}$$

where $\delta(\boldsymbol{r})$ is a delta function and satisfies either

$$\int f(\boldsymbol{r})\delta(\boldsymbol{r})\,\mathrm{d}\boldsymbol{r} = f(0) \tag{4.33a}$$

or

$$\int f(\boldsymbol{r})\delta\left(\boldsymbol{r} - \boldsymbol{r}'\right)\mathrm{d}\boldsymbol{r} = f\left(\boldsymbol{r}'\right) \tag{4.33b}$$

for any given function $f(\boldsymbol{r})$.

By using the function $G(\boldsymbol{k}, \boldsymbol{r})$, the solution for Eq. (4.31), $\psi_k(\boldsymbol{r})$, is represented as

$$\psi_k(\boldsymbol{r}) = \mathrm{e}^{\mathrm{i}\boldsymbol{k}\cdot\boldsymbol{r}} + \int G\left(\boldsymbol{k}, \boldsymbol{r} - \boldsymbol{r}'\right)U\left(\boldsymbol{r}'\right)\psi_k\left(\boldsymbol{r}'\right)\mathrm{d}\boldsymbol{r}'. \tag{4.34}$$

Problem 4.2

Show that $\psi_k(\boldsymbol{r})$ in Eq. (4.34) is the solution for the Schrödinger equation (4.31).

Solution
The first term $e^{i\boldsymbol{k}\cdot\boldsymbol{r}}$ in Eq. (4.34) is the plane wave propagating toward wave vector $\boldsymbol{k}$. As the scattering state is represented as the superposition of the incident wave and the scattering wave, we can assume that the integral of the second term represents the scattering wave. Substituting the first term of Eq. (4.34) into the left side of Eq. (4.31), we obtain

$$\begin{aligned}\left(\nabla^2+k^2\right)e^{i\boldsymbol{k}\cdot\boldsymbol{r}} &= \left(\nabla^2+k^2\right)e^{ik_x x+ik_y y+ik_z z}\\ &= \left\{-\left(k_x^2+k_y^2+k_z^2\right)+k^2\right\}e^{i\boldsymbol{k}\cdot\boldsymbol{r}}\\ &= 0.\end{aligned} \tag{4.35}$$

Next, by substituting the second term of Eq. (4.34) into the left side of Eq. (4.31) and by using

$$\delta\left(\boldsymbol{r}-\boldsymbol{r}'\right)=\delta\left(\boldsymbol{r}'-\boldsymbol{r}\right), \tag{4.36}$$

a feature of a delta function, we can arrive at

$$\begin{aligned}&\left(\nabla^2+k^2\right)\int G\left(\boldsymbol{k},\boldsymbol{r}-\boldsymbol{r}'\right)U\left(\boldsymbol{r}'\right)\psi_k\left(\boldsymbol{r}'\right)\mathrm{d}\boldsymbol{r}'\\ &\quad=\int\left(\nabla^2+k^2\right)G(\boldsymbol{k},\boldsymbol{r}-\boldsymbol{r}')U\left(\boldsymbol{r}'\right)\psi_k\left(\boldsymbol{r}'\right)\mathrm{d}\boldsymbol{r}'\\ &\quad=\int\delta\left(\boldsymbol{r}-\boldsymbol{r}'\right)U\left(\boldsymbol{r}'\right)\psi_k\left(\boldsymbol{r}'\right)\mathrm{d}\boldsymbol{r}'\\ &\quad=U(\boldsymbol{r})\psi_k(\boldsymbol{r}).\end{aligned} \tag{4.37}$$

Therefore, the $\psi_k(\boldsymbol{r})$ in Eq. (4.34) fulfills Eq. (4.31). □

When we think of the plane wave propagating along the z axis as the incident wave, as we did in the previous section, its wave vector can be written as $\boldsymbol{k}=(0,0,k)$, so the first term in Eq. (4.34) becomes

$$e^{i\boldsymbol{k}\cdot\boldsymbol{r}}=e^{ikz}. \tag{4.38}$$

It is also known that, when expressing the outgoing scattered spherical wave, the function $G(\boldsymbol{k},\boldsymbol{r})$, introduced in Eq. (4.32), is given as

$$G(\boldsymbol{k},\boldsymbol{r})=-\frac{1}{4\pi}\frac{e^{ikr}}{r}. \tag{4.39}$$

Under this condition, $\psi_k(\boldsymbol{r})$ can be written as

$$\begin{aligned}\psi_k(\boldsymbol{r}) &= e^{ikz}+\int G\left(\boldsymbol{k},\boldsymbol{r}-\boldsymbol{r}'\right)U\left(\boldsymbol{r}'\right)\psi_k\left(\boldsymbol{r}'\right)\mathrm{d}\boldsymbol{r}'\\ &= e^{ikz}-\int\frac{1}{4\pi}\frac{e^{ik|\boldsymbol{r}-\boldsymbol{r}'|}}{|\boldsymbol{r}-\boldsymbol{r}'|}U\left(\boldsymbol{r}'\right)\psi_k\left(\boldsymbol{r}'\right)\mathrm{d}\boldsymbol{r}'.\end{aligned} \tag{4.40}$$

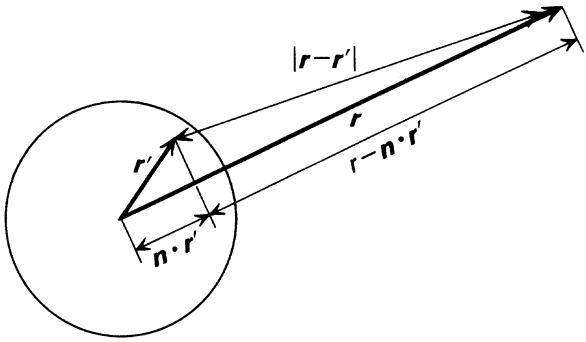

Fig. 4.5 Explanation for $|\boldsymbol{r}-\boldsymbol{r}'| \sim r - \boldsymbol{n}\cdot\boldsymbol{r}'$

Here, the magnitude of $\boldsymbol{r}'$ can be thought of as being only about the size of the atomic radius, which is considerably shorter than the distance between the origin and the observation point (about 0.1 to 1 m). Thus, as shown in Fig. 4.5, we can regard $|\boldsymbol{r}-\boldsymbol{r}'|$ as

$$\left|\boldsymbol{r}-\boldsymbol{r}'\right| \sim r - \boldsymbol{n}\cdot\boldsymbol{r}', \tag{4.41}$$

where $\boldsymbol{n}$ is the unit vector for the direction of $\boldsymbol{r}$. Similarly, its reciprocal can be approximated as

$$\frac{1}{|\boldsymbol{r}-\boldsymbol{r}'|} \sim \frac{1}{r}. \tag{4.42}$$

Thus the $\psi_k(\boldsymbol{r})$ in Eq. (4.40) is represented as

$$\psi_k(\boldsymbol{r}) = \mathrm{e}^{\mathrm{i}kz} - \frac{1}{4\pi r}\mathrm{e}^{\mathrm{i}kr}\int \mathrm{e}^{-\mathrm{i}k\boldsymbol{n}\cdot\boldsymbol{r}'}U\left(\boldsymbol{r}'\right)\psi_k\left(\boldsymbol{r}'\right)\mathrm{d}\boldsymbol{r}'. \tag{4.43}$$

When we compare the $\psi_k(\boldsymbol{r})$ in Eq. (4.43) with the $\psi(\boldsymbol{r})$ given by Eq. (4.18) in the previous section, we notice that the first term of $\psi_k(\boldsymbol{r})$ is the incident plane wave, whose wave number is $k = \frac{2\pi}{\lambda}$ (at wavelength λ), and that the second term is the scattering wave. This scattering wave represents the spherical wave expanding from the scattering center, and its wavelength does not differ from that of the incident plane wave.

This type of scattering is called elastic scattering. On the other hand, the type of scattering where the scattered electron beam changes its wavelength is called inelastic scattering. The contribution of the inelastic scattering is small, however, so in this chapter we will only discuss the elastic scattering.

From the correspondence between Eq. (4.18) and Eq. (4.43), we can see that the scattering amplitude $f(\theta,\phi)$ can be represented as

$$f(\theta,\phi) = f(\theta) = -\frac{1}{4\pi}\int \mathrm{e}^{-\mathrm{i}k\boldsymbol{n}\cdot\boldsymbol{r}'}U\left(\boldsymbol{r}'\right)\psi_k\left(\boldsymbol{r}'\right)\mathrm{d}\boldsymbol{r}', \tag{4.44}$$

where $U(\boldsymbol{r})$, having spherical symmetry, depends on the magnitude of $\boldsymbol{r}$, $r = |\boldsymbol{r}|$. Thus, we will henceforth represent $U(\boldsymbol{r})$ as $U(r)$. Also, as the scattering process has axial symmetry around the z axis, the scattering amplitude does not depend on

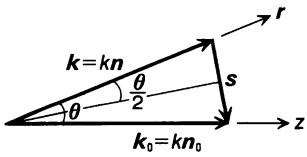

Fig. 4.6 The wave vector of the incident wave ($\boldsymbol{k}_0$) and the wave vector of the scattering wave ($\boldsymbol{k}$)

the azimuthal angle ϕ, which allows us to write the scattering amplitude as $f(\theta)$. While the solution to the process where an electron beam is scattered by an atom seems to have already been given in Eq. (4.43), the solution $\psi_k(\boldsymbol{r}')$ is a part of the integral of the scattering amplitude $f(\theta)$. This means that we cannot calculate the scattering amplitude unless the $\psi_k(\boldsymbol{r}')$ is given in advance. In order to overcome this problem, let us now adopt an approximation called Born approximation.

4.2.2 *Representation of the Scattering Amplitude by Use of the Born Approximation*

When the scattering wave is weak and not largely changed from the incident wave by the potential, we can use an approximation where the $\psi_k(\boldsymbol{r}')$ in the integral of the scattering wave is substituted by the incident wave. In this approximation, by substituting $\mathrm{e}^{\mathrm{i}kz'}$ for $\psi_k(\boldsymbol{r}')$, the scattering amplitude in Eq. (4.44) is written as

$$f(\theta) = -\frac{1}{4\pi}\int \mathrm{e}^{-\mathrm{i}k\boldsymbol{n}\cdot\boldsymbol{r}'}U\left(r'\right)\mathrm{e}^{\mathrm{i}kz'}\,\mathrm{d}\boldsymbol{r}'. \tag{4.45}$$

When we represent the unit vector along the direction of the z axis as $\boldsymbol{n}_0$ and let $z' = \boldsymbol{n}_0 \cdot \boldsymbol{r}'$, the scattering amplitude $f(\theta)$ becomes

$$f(\theta) = -\frac{1}{4\pi}\int \mathrm{e}^{\mathrm{i}k(\boldsymbol{n}_0-\boldsymbol{n})\cdot\boldsymbol{r}'}U\left(r'\right)\mathrm{d}\boldsymbol{r}'. \tag{4.46}$$

Then, a vector $\boldsymbol{s}$ which can be expressed as

$$\boldsymbol{s} = k(\boldsymbol{n}_0 - \boldsymbol{n}) \tag{4.47}$$

is one whose direction coincides with that of $\boldsymbol{n}_0 - \boldsymbol{n}$ and whose magnitude is $2k\sin\frac{\theta}{2} = \frac{4\pi}{\lambda}\sin\frac{\theta}{2}$, as shown in Fig. 4.6. That is to say, we can write

$$s = |\boldsymbol{s}| = \frac{4\pi}{\lambda}\sin\frac{\theta}{2}. \tag{4.48}$$

The integral expressed in terms of $\boldsymbol{r}'$ which appears in Eq. (4.45) can be calculated either in the polar coordinate based on the original z axis or in the polar coordinate represented with the polar angle α and the azimuthal angle β by regarding the new direction of the axis, $\boldsymbol{n}_0 - \boldsymbol{n}$, as the z' axis, as shown in Fig. 4.7. In this

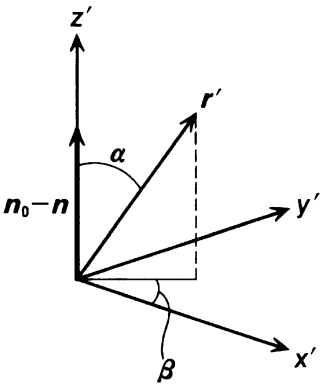

Fig. 4.7 A polar coordinate system whose z' axis is along the direction of $\boldsymbol{n}_0$–$\boldsymbol{n}$

new polar coordinate system, the $f(\theta)$ in Eq. (4.46) is written as

$$f(\theta) = -\frac{1}{4\pi}\int_0^\infty \int_0^\pi \int_0^{2\pi} \mathrm{e}^{\mathrm{i}sr'\cos\alpha} U(r') r'^2 \,\mathrm{d}r' \sin\alpha \,\mathrm{d}\alpha \,\mathrm{d}\beta$$
$$= -\frac{1}{2}\int_0^\infty \left(\int_0^\pi \mathrm{e}^{\mathrm{i}sr'\cos\alpha} \sin\alpha \,\mathrm{d}\alpha \right) U(r') r'^2 \,\mathrm{d}r'. \tag{4.49}$$

By calculating the integral given inside the round bracket ( ), we can obtain $f(\theta)$ as

$$f(\theta) = -\int_0^\infty \frac{\sin sr'}{sr'} U(r') r'^2 \,\mathrm{d}r'$$
$$= -\frac{2m_\mathrm{e}}{\hbar^2}\int_0^\infty \frac{\sin sr'}{sr'} V(r') r'^2 \,\mathrm{d}r'. \tag{4.50}$$

This is how to represent the scattering amplitude based on the Born approximation.

Problem 4.3
Derive Eq. (4.50) by performing the integration of given inside the round brackets ( ) in Eq. (4.49).

Solution
Letting the integral in ( ) be

$$I = \int_0^\pi \mathrm{e}^{\mathrm{i}sr'\cos\alpha} \sin\alpha \,\mathrm{d}\alpha, \tag{4.51}$$

and changing the variables from α to ζ using $\cos\alpha = \zeta$, which leads to $-\sin\alpha \,\mathrm{d}\alpha = \mathrm{d}\zeta$, we can write

$$I = \int_{-1}^1 \mathrm{e}^{\mathrm{i}sr'\zeta} \,\mathrm{d}\zeta = \frac{1}{\mathrm{i}sr'}\left(\mathrm{e}^{\mathrm{i}sr'} - \mathrm{e}^{-\mathrm{i}sr'}\right) = \frac{2\sin sr'}{sr'}. \tag{4.52}$$

By substituting this into Eq. (4.49) we can derive Eq. (4.50). □

4.2.3 Electron Scattering by Atoms

The scattering potential $V(r)$, as shown in Eq. (4.27), consists of two terms, the first of which corresponds to the attractive potential between the incident electron and the atomic nucleus, and the second to the repulsive potential between the incident electron and the electrons in the atom. By replacing these terms by $V_1(r)$ and $V_2(r)$, respectively, we can represent $V(r)$ as

$$V(r) = V_1(r) + V_2(r), \tag{4.53}$$

where

$$\begin{cases} V_1(r) = -\dfrac{Ze^2}{4\pi\varepsilon_0} \cdot \dfrac{1}{r}, & (4.54) \\ V_2(r) = \dfrac{e^2}{4\pi\varepsilon_0} \displaystyle\int \frac{\rho(\boldsymbol{r}')}{|\boldsymbol{r} - \boldsymbol{r}'|}\, \mathrm{d}\boldsymbol{r}'. & (4.55) \end{cases}$$

Let us now calculate the scattering amplitude by using specific forms for $V_1(r)$ and $V_2(r)$. First, we can substitute Eq. (4.53) into Eq. (4.46) by using the relationship given in Eq. (4.30), and write

$$f(\theta) = f_1(\theta) + f_2(\theta), \tag{4.56}$$

where

$$\begin{cases} f_1(\theta) = -\dfrac{1}{4\pi} \displaystyle\int \mathrm{e}^{\mathrm{i}k(\boldsymbol{n}_0 - \boldsymbol{n})\cdot\boldsymbol{r}'} \cdot \frac{2m_\mathrm{e}}{\hbar^2} V_1(r')\, \mathrm{d}\boldsymbol{r}', & (4.57) \\ f_2(\theta) = -\dfrac{1}{4\pi} \displaystyle\int \mathrm{e}^{\mathrm{i}k(\boldsymbol{n}_0 - \boldsymbol{n})\cdot\boldsymbol{r}'} \cdot \frac{2m_\mathrm{e}}{\hbar^2} V_2(r')\, \mathrm{d}\boldsymbol{r}'. & (4.58) \end{cases}$$

In evaluating these integrals, we can use the integral formula

$$\int \frac{\mathrm{e}^{\mathrm{i}\boldsymbol{n}\cdot\boldsymbol{r}'}}{|\boldsymbol{r} - \boldsymbol{r}'|}\, \mathrm{d}\boldsymbol{r}' = \frac{4\pi}{|\boldsymbol{n}|^2} \mathrm{e}^{\mathrm{i}\boldsymbol{n}\cdot\boldsymbol{r}}. \tag{4.59}$$

When we substitute $\boldsymbol{r} = \boldsymbol{0}$ and $\boldsymbol{n} = \boldsymbol{s}$ into Eq. (4.59), we obtain

$$\int \frac{\mathrm{e}^{\mathrm{i}\boldsymbol{s}\cdot\boldsymbol{r}'}}{r'}\, \mathrm{d}\boldsymbol{r}' = \frac{4\pi}{|\boldsymbol{s}|^2} \mathrm{e}^0 = \frac{4\pi}{s^2}, \tag{4.60}$$

and thus $f_1(\theta)$ can be immediately derived as

$$f_1(\theta) = \frac{Ze^2}{4\pi\varepsilon_0} \cdot \frac{2m_\mathrm{e}}{\hbar^2} \cdot \frac{1}{4\pi} \int \frac{\mathrm{e}^{\mathrm{i}\boldsymbol{s}\cdot\boldsymbol{r}'}}{r'}\, \mathrm{d}\boldsymbol{r}'$$

$$= \frac{2m_e e^2 Z}{4\pi\varepsilon_0 \hbar^2} \cdot \frac{1}{s^2}. \tag{4.61}$$

We can calculate $f_2(\theta)$ using Eq. (4.55) as

$$f_2(\theta) = -\frac{e^2}{4\pi\varepsilon_0} \cdot \frac{2m_e}{\hbar^2} \cdot \frac{1}{4\pi} \int \mathrm{e}^{\mathrm{i}k(\boldsymbol{n}_0 - \boldsymbol{n})\cdot \boldsymbol{r}'} \left(\int \frac{\rho(\boldsymbol{r}'')}{|\boldsymbol{r}' - \boldsymbol{r}''|} \,\mathrm{d}\boldsymbol{r}'' \right) \mathrm{d}\boldsymbol{r}', \tag{4.62}$$

but, by executing the integral in terms of $\boldsymbol{r}'$ first, we can also represent $f_2(\theta)$ as

$$f_2(\theta) = -\frac{e^2}{4\pi\varepsilon_0} \cdot \frac{2m_e}{\hbar^2} \cdot \frac{1}{4\pi} \int \rho(\boldsymbol{r}'') \left(\int \frac{\mathrm{e}^{\mathrm{i}k(\boldsymbol{n}_0 - \boldsymbol{n})\cdot \boldsymbol{r}'}}{|\boldsymbol{r}'' - \boldsymbol{r}'|} \,\mathrm{d}\boldsymbol{r}' \right) \mathrm{d}\boldsymbol{r}''. \tag{4.63}$$

By using Eq. (4.59) for the integral inside the round brackets ( ), we obtain

$$\begin{aligned} f_2(\theta) &= -\frac{2m_e e^2}{4\pi\varepsilon_0 \hbar^2} \int \rho(\boldsymbol{r}'') \frac{\mathrm{e}^{\mathrm{i}k(\boldsymbol{n}_0 - \boldsymbol{n})\cdot \boldsymbol{r}''}}{|k(\boldsymbol{n}_0 - \boldsymbol{n})|^2} \,\mathrm{d}\boldsymbol{r}'' \\ &= -\frac{2m_e e^2}{4\pi\varepsilon_0 \hbar^2} \int \rho(\boldsymbol{r}'') \frac{\mathrm{e}^{\mathrm{i}sr'' \cos\alpha}}{s^2} \,\mathrm{d}\boldsymbol{r}''. \end{aligned} \tag{4.64}$$

Here, we can use the spherical symmetry of $\rho(\boldsymbol{r})$ to express it as $\rho(r)$ and calculate the integral in the same way as we did in Problem 4.3, which gives us

$$\begin{aligned} f_2(\theta) &= -\frac{2m_e e^2}{4\pi\varepsilon_0 \hbar^2} \cdot \frac{1}{s^2} \int_0^\infty \int_0^\pi \int_0^{2\pi} \rho(r'') \mathrm{e}^{\mathrm{i}sr'' \cos\alpha} r''^2 \,\mathrm{d}r'' \sin\alpha \,\mathrm{d}\alpha \,\mathrm{d}\beta, \\ &= -\frac{2m_e e^2}{4\pi\varepsilon_0 \hbar^2} \cdot \frac{4\pi}{s^2} \int_0^\infty \rho(r'') \frac{\sin sr''}{sr''} r''^2 \,\mathrm{d}r'' \\ &= -\frac{2m_e e^2}{4\pi\varepsilon_0 \hbar^2} \cdot \frac{A(\theta)}{s^2} \end{aligned} \tag{4.65}$$

where $A(\theta)$ is represented as

$$A(\theta) = 4\pi \int_0^\infty \rho(r) \frac{\sin sr}{sr} r^2 \,\mathrm{d}r \tag{4.66}$$

and is called the atomic scattering factor or the atomic structure factor. From Eqs. (4.61) and (4.65) above, we can derive the scattering amplitude given in Eq. (4.56) as

$$f(\theta) = \frac{2m_e e^2}{4\pi\varepsilon_0 \hbar^2} \left(\frac{Z - A(\theta)}{s^2} \right). \tag{4.67}$$

As can be seen from the way in which it has been derived, $A(\theta)$ here represents the contribution of the scattering by the electrons distributed in the atom, and $Z - A(\theta)$ represents the fact that the nuclear charge Z is shielded by the amount of $A(\theta)$ in the direction θ.

Problem 4.4
Show that the atomic scattering factor $A(\theta)$ satisfies $A(0) = Z$ when the scattering angle is $\theta = 0$. Also, discuss how $A(\theta)$ and the scattering amplitude $f(\theta)$ behave as the value of θ increases.

Solution
Taking the limit of $\theta \to 0$ in Eq. (4.66) corresponds to $s = 2k \sin \frac{\theta}{2} \to 0$. As $\frac{\sin sr}{sr} \to 1$ in this case, we can write

$$A(0) = 4\pi \int_0^\infty \rho(r) r^2 \, \mathrm{d}r.$$

As this represents $\rho(r)$ being integrated over all space, it is equal to the total charge of all electrons, Z. On the other hand, when θ increases, s increases and so does the denominator of $\frac{\sin sr}{sr}$, so that $A(\theta)$ approaches 0. Thus, from Eq. (4.67), we can see that $f(\theta)$ becomes proportional to Z. □

Problem 4.5
Derive the differential cross-section of the elastic scattering.

Solution
As the differential cross-section $\frac{\mathrm{d}\sigma}{\mathrm{d}\Omega}$ given by $|f(\theta)|^2$ as shown in Eq. (4.22), we can use Eq. (4.67) to derive it as

$$\frac{\mathrm{d}\sigma}{\mathrm{d}\Omega} = \left(\frac{2m_\mathrm{e} e^2}{4\pi\varepsilon_0 \hbar^2} \right)^2 \left(\frac{Z - A(\theta)}{s^2} \right)^2.$$

Thus the differential cross-section is proportional to s^{-4}, which accounts for the rapid decrease of the diffraction intensity of an electron beam when s increases. □

4.3 Electron Scattering by Molecules

4.3.1 The Scattering Amplitude of Electron Scattering by a Molecule

Although atoms in molecules are connected by chemical bonds, the electron distribution around each nucleus can be regarded as almost the same as that around an isolated atom. Therefore, $V_\mathrm{mol}(\boldsymbol{r})$, the potential of electron scattering by a molecule, can be expressed as a sum of the spherically symmetric potentials for the electron scattering by atoms, which we have dealt with in Sect. 4.2. That is,

$$V_\mathrm{mol}(\boldsymbol{r}) = \sum_i V_i(\boldsymbol{r}), \tag{4.68}$$

where the origin of $\boldsymbol{r}$ is arbitrary and the value $\boldsymbol{r} - \boldsymbol{r}_i$, with $\boldsymbol{r}_i$ being the position vector of the i-th atom, corresponds to the $\boldsymbol{r}$ in Sect. 4.2. As is shown in Fig. 4.8, the

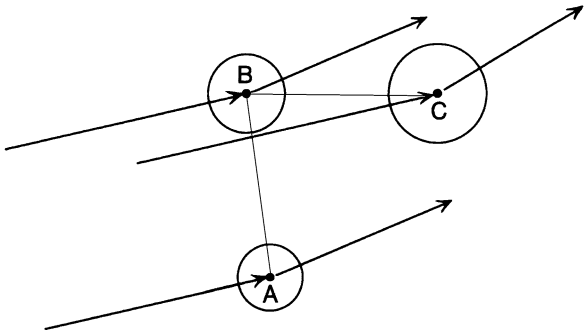

Fig. 4.8 Scattering of an electron beam by a triatomic molecule ABC

incident plane wave of an electron is scattered by each of the atoms in a molecule. Then, the scattered waves interfere with each other.

The scattering amplitude of an electron scattered by a molecule, $f_{\mathrm{mol}}(\theta)$, can be expressed as a sum of the scattering amplitudes of the electron scattered by the atoms, which have been given by Eq. (4.46). That is to say,

$$\begin{aligned} f_{\mathrm{mol}}(\theta) &= -\frac{1}{4\pi}\cdot\frac{2m_{\mathrm{e}}}{\hbar^2}\int \mathrm{e}^{\mathrm{i}\boldsymbol{s}\cdot\boldsymbol{r}'}V_{\mathrm{mol}}(\boldsymbol{r}')\,\mathrm{d}\boldsymbol{r}' \\ &= -\frac{1}{4\pi}\cdot\frac{2m_{\mathrm{e}}}{\hbar^2}\int \mathrm{e}^{\mathrm{i}\boldsymbol{s}\cdot\boldsymbol{r}'}\sum_i V_i(\boldsymbol{r}')\,\mathrm{d}\boldsymbol{r}' \\ &= \sum_i f_i(\theta)\mathrm{e}^{\mathrm{i}\boldsymbol{s}\cdot\boldsymbol{r}_i}. \end{aligned} \tag{4.69}$$

The function $f_i(\theta)$ is the scattering amplitude attributed to the i-th atom, and it can be expressed as

$$f_i(\theta) = \left(\frac{2m_{\mathrm{e}}e^2}{4\pi\varepsilon_0\hbar^2}\right)\left(\frac{Z_i - A_i(\theta)}{s^2}\right), \tag{4.70}$$

because $V_{\mathrm{mol}}(\boldsymbol{r}')$ in Eq. (4.69) can be written as

$$V_{\mathrm{mol}}(\boldsymbol{r}') = \sum_i\left(-\frac{Z_i e^2}{4\pi\varepsilon_0}\cdot\frac{1}{|\boldsymbol{r}'-\boldsymbol{r}_i|} + \frac{e^2}{4\pi\varepsilon_0}\int\frac{\rho_i(\boldsymbol{r}''-\boldsymbol{r}_i)}{|\boldsymbol{r}''-\boldsymbol{r}'|}\,\mathrm{d}\boldsymbol{r}''\right), \tag{4.71}$$

and the integral in Eq. (4.69) can be carried out as

$$\begin{aligned} \int\frac{\mathrm{e}^{\mathrm{i}\boldsymbol{s}\cdot\boldsymbol{r}'}}{|\boldsymbol{r}'-\boldsymbol{r}_i|}\mathrm{d}\boldsymbol{r}' &= \mathrm{e}^{\mathrm{i}\boldsymbol{s}\cdot\boldsymbol{r}_i}\int\frac{\mathrm{e}^{\mathrm{i}\boldsymbol{s}\cdot(\boldsymbol{r}'-\boldsymbol{r}_i)}}{|\boldsymbol{r}'-\boldsymbol{r}_i|}\,\mathrm{d}\boldsymbol{r}' \\ &= \mathrm{e}^{\mathrm{i}\boldsymbol{s}\cdot\boldsymbol{r}_i}\int\frac{\mathrm{e}^{\mathrm{i}\boldsymbol{s}\cdot\boldsymbol{r}'}}{|\boldsymbol{r}'|}\,\mathrm{d}\boldsymbol{r}' \end{aligned} \tag{4.72}$$

and

$$\int \mathrm{e}^{\mathrm{i}\boldsymbol{s}\cdot\boldsymbol{r}'}\left(\int \frac{\rho_i(\boldsymbol{r}''-\boldsymbol{r}_i)}{|\boldsymbol{r}''-\boldsymbol{r}'|}\,\mathrm{d}\boldsymbol{r}''\right)\mathrm{d}\boldsymbol{r}' = \int \rho_i(\boldsymbol{r}''-\boldsymbol{r}_i)\left\{\int \frac{\mathrm{e}^{\mathrm{i}\boldsymbol{s}\cdot\boldsymbol{r}'}}{|\boldsymbol{r}''-\boldsymbol{r}'|}\,\mathrm{d}\boldsymbol{r}'\right\}\mathrm{d}\boldsymbol{r}''$$
$$= \int \rho_i(\boldsymbol{r}''-\boldsymbol{r}_i)\frac{4\pi\,\mathrm{e}^{\mathrm{i}\boldsymbol{s}\cdot\boldsymbol{r}''}}{s^2}\,\mathrm{d}\boldsymbol{r}''$$
$$= \mathrm{e}^{\mathrm{i}\boldsymbol{s}\cdot\boldsymbol{r}_i}\int \rho_i(\boldsymbol{r}''-\boldsymbol{r}_i)\frac{4\pi\,\mathrm{e}^{\mathrm{i}\boldsymbol{s}\cdot(\boldsymbol{r}''-\boldsymbol{r}_i)}}{s^2}\,\mathrm{d}\boldsymbol{r}'' \quad (4.73)$$

in the same way as in the derivation of Eqs. (4.61) and (4.65).

4.3.2 The Scattering and Interference of an Electron Beam by a Diatomic Molecule

Let us first consider the simplest scenario, where an electron is scattered by a diatomic molecule. The scattering amplitude $f_{\mathrm{mol}}(\theta)$ can be expressed as

$$f_{\mathrm{mol}}(\theta) = \mathrm{e}^{\mathrm{i}\boldsymbol{s}\cdot\boldsymbol{r}_1} f_1(\theta) + \mathrm{e}^{\mathrm{i}\boldsymbol{s}\cdot\boldsymbol{r}_2} f_2(\theta) \quad (4.74)$$

by the formula (4.69). The scattering intensity $I(\theta)$ of the electron wave is given by the differential cross section $|f_{\mathrm{mol}}(\theta)|^2$, that is,

$$I(\theta) = \left|f_{\mathrm{mol}}(\theta)\right|^2 = f_1(\theta)^2 + f_2(\theta)^2 + 2f_1(\theta)f_2(\theta)\cos(\boldsymbol{s}\cdot\boldsymbol{r}_{12}), \quad (4.75)$$

where $\boldsymbol{r}_{12} = \boldsymbol{r}_2 - \boldsymbol{r}_1$, $r_{12} = |\boldsymbol{r}_{12}|$, and $f_1(\theta)$ and $f_2(\theta)$ are treated here as real functions given by Eq. (4.70). What should be noted in Eq. (4.75) is the existence of the third term. Whereas the first and second terms stand for the scattering by the respective atoms, and these terms are smooth functions which decay with the increase of θ, as shown in Problem 4.5, the third term oscillates when

$$\boldsymbol{s}\cdot\boldsymbol{r}_{12} = \frac{4\pi}{\lambda}\sin\frac{\theta}{2}\cdot r_{12}\cdot\cos\alpha \quad (4.76)$$

in the argument of the cosine function varies with θ. This third term represents the interference of the waves scattered by the two different atoms in the molecule. Here α stands for the angle between $\boldsymbol{s}$ and $\boldsymbol{r}_{12}$.

Problem 4.6
Prove that the scattering intensity $I(\theta)$ of an electron wave scattered by a diatomic molecule is given in the form of Eq. (4.75).

Solution
From Eq. (4.74), we can write

$$I(\theta) = \left|f_{\mathrm{mol}}(\theta)\right|^2 = f^*_{\mathrm{mol}}(\theta)f_{\mathrm{mol}}(\theta)$$
$$= \left(\mathrm{e}^{-\mathrm{i}\boldsymbol{s}\cdot\boldsymbol{r}_1} f_1^*(\theta) + \mathrm{e}^{-\mathrm{i}\boldsymbol{s}\cdot\boldsymbol{r}_2} f_2^*(\theta)\right)\cdot\left(\mathrm{e}^{\mathrm{i}\boldsymbol{s}\cdot\boldsymbol{r}_1} f_1(\theta) + \mathrm{e}^{\mathrm{i}\boldsymbol{s}\cdot\boldsymbol{r}_2} f_2(\theta)\right)$$

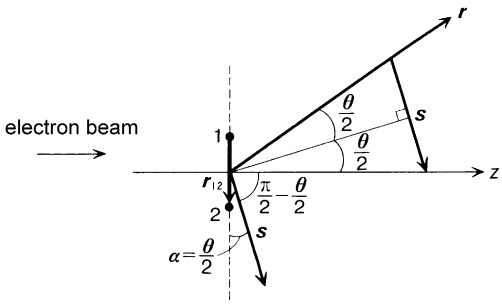

Fig. 4.9 An electron beam being propagated towards a diatomic molecule at an incident angle perpendicular to its molecular axis

$$= \left|f_1(\theta)\right|^2 + \left|f_2(\theta)\right|^2 + f_1^*(\theta) f_2(\theta) \mathrm{e}^{\mathrm{i}\boldsymbol{s}\cdot(\boldsymbol{r}_2-\boldsymbol{r}_1)} + f_1(\theta) f_2^*(\theta) \mathrm{e}^{-\mathrm{i}\boldsymbol{s}\cdot(\boldsymbol{r}_2-\boldsymbol{r}_1)}.$$

As in Eq. (4.70), the scattering amplitudes $f_1(\theta)$ and $f_2(\theta)$ are real functions. Therefore,

$$I(\theta) = f_1(\theta)^2 + f_2(\theta)^2 + 2 f_1(\theta) f_2(\theta) \cos(\boldsymbol{s} \cdot \boldsymbol{r}_{12}). \qquad \square$$

Let us now think about a specific condition where the molecular axis of a diatomic molecule is aligned along a direction perpendicular to the propagation direction of the electron beam. As seen in Fig. 4.9, $\alpha = \frac{\theta}{2}$, and

$$\boldsymbol{s} \cdot \boldsymbol{r}_{12} = \frac{4\pi}{\lambda} \sin\frac{\theta}{2} \cdot r_{12} \cdot \cos\frac{\theta}{2} = \frac{2\pi r_{12}}{\lambda} \sin\theta \tag{4.77}$$

can be obtained. This shows that the interference term oscillates with θ according to $\cos(\frac{2\pi r_{12}}{\lambda} \sin\theta)$.

When $r_{12} = 1$ Å and $\lambda = 0.05$ Å, we obtain $\boldsymbol{s} \cdot \boldsymbol{r}_{12} = 40\pi \sin\theta$. In this case, the interference term in the scattering intensity reaches its maxima when

$$40\pi \sin\theta = 0, 2\pi, 4\pi, 6\pi, \ldots,$$

that is, when

$$\theta = 0^\circ, 2.87^\circ, 5.74^\circ, 8.63^\circ, \ldots.$$

As a result of this interference, electrons arrive on a screen located 20 cm away from the scattering center with concentrated density at 1.00, 2.01, 3.03, ... cm above and below the center symmetrically. Therefore, when the molecules are spatially aligned, the interference pattern appears as horizontal stripes.

What is significant here is that the distance between these stripes depends on the internuclear distance r_{12}. This indicates that the internuclear distance can be determined by observing the distance between the interference stripes. Although the explanation here has been limited to a special condition in which diatomic molecules are aligned spatially along a specific direction, it demonstrates the basic principle underlying the determination of geometrical structures of all types of molecules by the electron diffraction method.

In a gaseous phase, diatomic molecules are randomly oriented under normal conditions. Therefore, the scattering intensity must be averaged by the integration over the entire spatial directions of the orientation of the molecular axis. When the third term of Eq. (4.75), that is, the interference term, is integrated over all space and then divided by 4π to calculate its average, defined as $I_{\mathrm{mol}}(\theta)$, we can write

$$\begin{aligned} I_{\mathrm{mol}}(\theta) &= 2f_1(\theta)f_2(\theta)\frac{1}{4\pi}\int_0^{\pi}\int_0^{2\pi}\cos(\boldsymbol{s}\cdot\boldsymbol{r}_{12})\sin\alpha\,\mathrm{d}\alpha\,\mathrm{d}\beta \\ &= 2f_1(\theta)f_2(\theta)\frac{1}{4\pi}\int_0^{2\pi}\mathrm{d}\beta\int_0^{\pi}\cos(sr_{12}\cos\alpha)\,\sin\alpha\,\mathrm{d}\alpha. \end{aligned} \tag{4.78}$$

Letting $\gamma = \cos\alpha$, as in the case of Eq. (4.51), we can write $d\gamma = -\sin\alpha\,\mathrm{d}\alpha$, and thus carry out the integral in terms of α as

$$\begin{aligned} \int_0^{\pi}\cos(sr_{12}\cos\alpha)\sin\alpha\,\mathrm{d}\alpha &= -\int_1^{-1}\cos(sr_{12}\gamma)\,\mathrm{d}\gamma \\ &= \left[\frac{\sin(sr_{12}\gamma)}{sr_{12}}\right]_{-1}^{1} \\ &= 2\frac{\sin sr_{12}}{sr_{12}}. \end{aligned} \tag{4.79}$$

Therefore, the total scattering intensity $I(\theta)$ for a diatomic molecule in a gaseous phase can be expressed as

$$I(\theta) = \left|f_1(\theta)\right|^2 + \left|f_2(\theta)\right|^2 + I_{\mathrm{mol}}(\theta), \tag{4.80}$$

$$I_{\mathrm{mol}}(\theta) = 2f_1(\theta)f_2(\theta)\frac{\sin sr_{12}}{sr_{12}}. \tag{4.81}$$

$I_{\mathrm{mol}}(\theta)$ is called the *molecular scattering intensity*.

As can be seen above, even if molecules are oriented randomly in all spatial directions, the interference term survives, causing a sinusoidal pattern in the scattering intensity, and becomes zero where $\sin sr_{12} = 0$. In this case, the interference pattern does not vary with the azimuthal angle ϕ, because the electron beam retains axial symmetry around the propagation direction. The same applies to cases of polyatomic molecules. Thus a pattern of concentric circles is observed in the case of a polyatomic molecule as well, as in Fig. 1.11(a) from Chap. 1, where we see an electron diffraction picture of carbon tetrachloride.

We will now define the distribution function of the orientation direction of the molecular axis of diatomic molecules in space as $P(\phi)$. The angle ϕ $(0 \leqq \phi \leqq \pi)$ stands for the polar angle where the z'' axis is fixed perpendicularly to the propagation direction of the electron beam. At the same time, the distribution around a given azimuthal angle is assumed to be random. Under this condition, the angular distribution function of molecules oriented in the direction of the z'' axis can be expressed

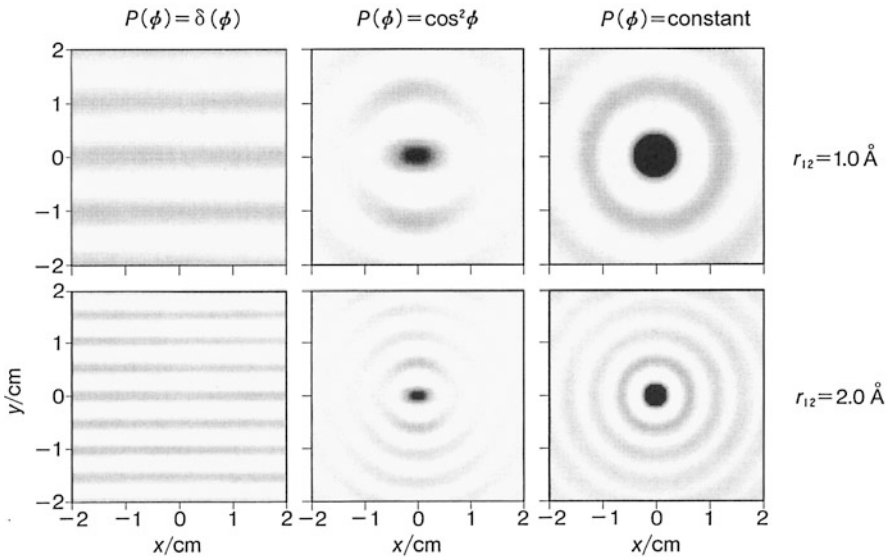

Fig. 4.10 Diffraction patterns of electron beams caused by aligned diatomic molecules and those caused by diatomic molecules with random orientations

using the delta function as $P(\phi) = \delta(\phi)$, whereas that of molecules facing random directions can be written as an isotropic distribution, that is, $P(\phi) = \text{constant}$.

Figure 4.10 shows the scattering patterns of electron beams accelerated to 40 kV for three different distribution functions of the direction of the axis of diatomic molecules. In this figure, only the interference term is depicted in the form of interference fringes to appear on a screen placed 20 cm away from the scattering center. The upper row of figures show the cases where the internuclear distance is $r_{12} = 1.0$ Å, and the lower row, those where $r_{12} = 2.0$ Å. The patterns shown in the middle column are those obtained when the distribution functions are given as $P(\phi) = \cos^2 \phi$.

As is clear from these figures, the interference patterns appear as horizontal stripes in the case of perfectly aligned (or oriented) molecules, and gradually approach the form of concentric circles as the degree of anisotropy in the alignment (or orientation) direction diminishes. This signifies that, if we can produce an ensemble of molecules with the tendency of being aligned (or oriented) along a specific direction by some experimental method, the degree of alignment (or orientation) of these molecules can be determined through the observation of their electron diffraction image. Indeed, it is known that such an ensemble of molecules whose molecular axes are aligned (or oriented) in space along a specific direction can be realized by irradiating molecules with linearly polarized intense laser light.

When we compare the images in the upper and lower rows of Fig. 4.10, we see that the intervals of the interference fringes in the lower row of figures is narrower by about half. This means that the intervals of the fringes decrease as the nuclear

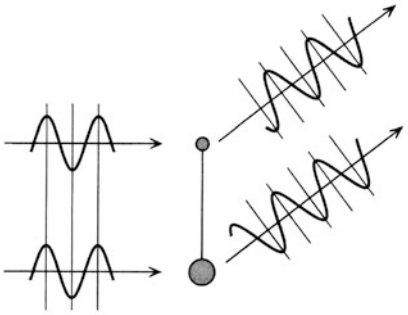

Fig. 4.11 The phase shifts of a scattered electron beam caused by the attractive potential

distance between an atomic pair increases. Therefore, the observation of the interference pattern directly leads us to the determination of the molecular structure. In other words, the structure of a molecule can be determined by its *halo*, which is what we call the interference pattern consisting of concentric circles recorded in electron diffraction experiments on gaseous molecules.

We must also note that, when we take into account scattered waves whose wave vectors have some components perpendicular to the page of Fig. 4.9, the interference patterns on the screen will not become perfectly horizontal stripes, but rather take the forms of hyperbolas that are convex downward when $y > 0$ and convex upward when $y < 0$. Nevertheless, as long as we are looking at 4 cm $\times$ 4 cm square regions on a screen 20 cm from the scattering center, the interference patterns can be seen as almost horizontal stripes.

4.4 Phase Shift of the Scattering Electron Wave

4.4.1 Partial-Wave Expansions of Scattered Waves

When an electron beam is scattered by a molecule, the waves resulting from simultaneous scatterings by different atoms in the molecule interfere with one another, creating ripples in the diffraction intensity. Although the electron diffraction pattern for a diatomic molecule, as shown in the previous section, are well represented by Eq. (4.81), a closer observation shows that the amplitude of the interference modulation becomes more suppressed than in Eq. (4.81) as the scattering angle θ or s increases. There are mainly two causes for this phenomenon. The first is the effect of molecular vibration, which is caused by the fact that the distance between atoms is not fixed but rather has a distribution with a range. This effect is explained in the next section. The second cause is that the phase shift of the scattered waves produced by the scattering by an atom varies by the atomic species. Simply put, the electron wave being scattered by a nucleus is pulled in by its attractive potential at the same time, causing a delay in the phase of the wave front. The heavier the atom, the larger the nuclear charge becomes, and consequentially so does the attractive potential. Thus the phase shifts grows larger as the atoms become heavier, as illustrated in Fig. 4.11. The phase shift effect appearing in the interference modulation

becomes larger when the difference between the charges of the two different nuclear species within a molecule becomes larger.

Let us now return to the Schrödinger equation (4.28), in order to understand the origin of the phase shift. From Eqs. (3.5) through (3.7), Eq. (3.8) can derived as

$$\nabla^2 = \frac{1}{r^2}\frac{\partial}{\partial r}\left(r^2\frac{\partial}{\partial r}\right) + \frac{\Lambda}{r^2}, \tag{4.82}$$

where r is also treated as a variable. Therefore, we can write Eq. (4.28) using the polar coordinate (r, θ, ϕ) as

$$-\frac{\hbar^2}{2m_e}\left\{\frac{1}{r^2}\frac{\partial}{\partial r}\left(r^2\frac{\partial}{\partial r}\right)\psi + \frac{\Lambda}{r^2}\psi\right\} + V(r)\psi = E\psi, \tag{4.83}$$

where Λ is given by Eq. (3.9) in Sect. 3.1. The solution of this equation, $\psi(r, \theta, \phi)$, is first rewritten as a product of $R(r)$, a function of the distance r, and $Y(\theta, \phi)$, a function of the angles θ and ϕ, so as to separate the variables. That is,

$$\psi(r, \theta, \phi) = R(r)Y(\theta, \phi). \tag{4.84}$$

Substituting Eq. (4.84) into Eq. (4.83) and dividing both sides of this equation by $R(r)Y(\theta, \phi)$, we obtain

$$-\frac{1}{r^2}\frac{\partial}{\partial r}\left(r^2\frac{\partial R(r)}{\partial r}\right)\frac{r^2}{R(r)} + \frac{2m_e r^2}{\hbar^2}\big(V(r) - E\big) = \frac{\Lambda Y(\theta, \phi)}{Y(\theta, \phi)}. \tag{4.85}$$

The left-hand side of this equation is a function of r only, and the right-hand side a function of θ and ϕ only. For this equation to always be satisfied, both of its sides need to be a constant. Letting this constant be α, the following two equations can be obtained from Eq. (4.85).

$$\Lambda Y(\theta, \phi) = \alpha Y(\theta, \phi), \tag{4.86}$$

$$-\frac{\hbar^2}{2m_e}\left\{\frac{1}{r^2}\frac{\mathrm{d}}{\mathrm{d}r}\left(r^2\frac{\mathrm{d}R(r)}{\mathrm{d}r}\right) + \frac{\alpha}{r^2}R(r)\right\} + V(r)R(r) = ER(r). \tag{4.87}$$

Here, as Eq. (4.87) is a differential equation in which the only variable is r, the partial differential has been changed into the ordinary differential. By comparing Eq. (3.11) in Sect. 3.1 with Eq. (4.86), we can write α as

$$\alpha = -l(l+1), \tag{4.88}$$

where l is either 0 or a positive integer. Therefore, the equation of the radial part to be solved is given by

$$-\frac{\hbar^2}{2m_e}\left\{\frac{1}{r^2}\frac{\mathrm{d}}{\mathrm{d}r}\left(r^2\frac{\mathrm{d}R(r)}{\mathrm{d}r}\right) - \frac{l(l+1)}{r^2}R(r)\right\} + V(r)R(r) = ER(r). \tag{4.89}$$

This equation shows that a radial eigenfunction $R(r)$ is determined for each value of l. Thus we will hereafter write $R(r)$ as $R_l(r)$.

In the case of $E < 0$, Eq. (4.89) would represent a bound state where electrons are bound in the potential $V(r)$. If $V(r)$ is the Coulomb attractive potential, the equation represents the radial equation of an electron in a hydrogen-like atom. However, as long as we are dealing with the scattering of an electron, $E > 0$ holds, as shown from Eq. (4.29).

Next, we will simplify Eq. (4.89) by turning it into an equation of $f_l(r)$ by the substitution of $R_l(r) = \frac{f_l(r)}{r}$, which gives us

$$-\frac{\hbar^2}{2m_e}\left\{\frac{\mathrm{d}^2 f_l(r)}{\mathrm{d}r^2} - \frac{l(l+1)}{r^2} f_l(r)\right\} + V(r) f_l(r) = E f_l(r). \tag{4.90a}$$

The same equation can be written using Eqs. (4.29) and (4.30) as

$$\left\{\frac{\mathrm{d}^2}{\mathrm{d}r^2} - \frac{l(l+1)}{r^2} - U(r) + k^2\right\} f_l(r) = 0. \tag{4.90b}$$

In order to explore the function form of $f_l(r)$, let us first look at its behavior at $r \to 0$. $U(r)$ is the potential determined by the Coulomb attractive force between the electron and the nucleus, and therefore never diverges at a rate faster than $\frac{1}{r}$. Therefore, around the origin, that is, when $r \to 0$, the term of $\frac{1}{r^2}$ plays a dominant role and Eq. (4.90b) becomes

$$\frac{\mathrm{d}^2 f_l(r)}{\mathrm{d}r^2} - \frac{l(l+1)}{r^2} f_l(r) \sim 0. \tag{4.91}$$

For f_l to behave like r^α around the origin, the equation

$$\alpha(\alpha - 1) - l(l+1) = 0 \tag{4.92}$$

needs to be satisfied. This can be factorized, and $\alpha = l + 1, -l$ are obtained. As the wave function $R_l(r)$ is finite, $f_l(r) = r R_l(r)$ has to be $f_l(r) \to 0$ at $r \to 0$, which means that the function behaves near the origin as

$$f_l(r) \propto r^{l+1}. \tag{4.93}$$

At $r \to \infty$, on the other hand, the charge of the nucleus is shielded by the electrons and thus $U(r)$ can be considered to become $U(r) \to 0$ more rapidly than the term $\frac{l(l+1)}{r^2}$. In this case, Eq. (4.90b) satisfies

$$\frac{\mathrm{d}^2 f_l(r)}{\mathrm{d}r^2} + \left\{k^2 - \frac{l(l+1)}{r^2}\right\} f_l(r) \sim 0. \tag{4.94}$$

It has already been shown in Sect. 3.2 that the solution of the Schrödinger equation of the angular part, Eq. (4.86), is given by the spherical harmonics $Y_{lm}(\theta, \phi)$. When we treat the scattering of an electron beam by atoms, the axial symmetry around the electron beam axis is preserved, and therefore the wave function of the angular part does not depend on the azimuthal angle ϕ but instead becomes a function of the polar angle θ only. This means that the wave function of the angular part

can be represented by Y_{l0}, which is obtained by substituting $m = 0$ into Y_{lm}. Here, Y_{l0} and the Legendre polynomial are converted into each other by the relation

$$P_l(\cos\theta) = \sqrt{\frac{4\pi}{2l+1}} Y_{l0}(\theta, \phi). \tag{4.95}$$

Generally, the solution of the Schrödinger equation (4.28) can also be represented as

$$\psi(r, \theta) = \frac{1}{r} \sum_{l=0}^{\infty} f_l(r) P_l(\cos\theta), \tag{4.96}$$

using the expansion by the Legendre polynomial. This type of expansion involves the superposition of wave functions of different orbital angular momenta, and is called the partial wave expansion.

Problem 4.7
Derive Eq. (4.90b), the radial equation in terms of $f_l(r)$, by substituting the equation of the partial wave expansion, Eq. (4.96), into the Schrödinger equation (4.31).

Solution
Following Eq. (4.82), we can express the ∇^2 in Eq. (4.31) by a polar coordinate as

$$\left\{ \frac{1}{r^2} \frac{\partial}{\partial r} \left(r^2 \frac{\partial}{\partial r} \right) + \frac{\Lambda}{r^2} + k^2 \right\} \psi(r, \theta) = U(r) \psi(r, \theta), \tag{4.97}$$

wherein the $U(\boldsymbol{r})$ from Eq. (4.31) is represented as $U(r)$ because it is a spherically symmetric potential. Substituting Eq. (4.96) into the $\psi(r, \theta)$ in Eq. (4.97) we obtain

$$\sum_{l=0}^{\infty} \frac{1}{r} P_l(\cos\theta) \left\{ \frac{\mathrm{d}^2}{\mathrm{d}r^2} - \frac{l(l+1)}{r^2} - U(r) + k^2 \right\} f_l(r) = 0, \tag{4.98}$$

where

$$-\Lambda P_l(\cos\theta) = l(l+1) P_l(\cos\theta), \tag{4.99}$$

derived from Eqs. (3.36), (3.76), and (3.99), has been used. When Eq. (4.98) is multiplied by $P_l(\cos\theta)$ and integrated, using the orthogonal relation of the Legendre polynomial $P_l(\cos\theta)$, that is,

$$\int_{-1}^{1} P_m(x) P_n(x)\, \mathrm{d}x = \frac{2}{2n+1} \delta_{mn}, \tag{4.100}$$

Eq. (4.90b),

$$\left\{ \frac{\mathrm{d}^2}{\mathrm{d}r^2} - \frac{l(l+1)}{r^2} - U(r) + k^2 \right\} f_l(r) = 0,$$

is readily obtained. □

4.4.2 The Behavior of Partial Waves in the Asymptotic Region

Equation (4.94), which partial waves need to satisfy in the asymptotic region, is known to have two linearly independent solutions, $s_l(kr)$ and $c_l(kr)$. Using the spherical Bessel function $j_l(kr)$ and the spherical Neumann function $n_l(kr)$, these solutions can be represented as

$$s_l(kr) = krj_l(kr), \tag{4.101a}$$

$$c_l(kr) = -krn_l(kr). \tag{4.101b}$$

The actual forms of these functions for $l = 0, 1, 2, 3$ are written by substituting $kr = x$ as follows:
When $l = 0$,

$$s_0(x) = \sin x, \tag{4.102a}$$

$$c_0(x) = \cos x. \tag{4.102b}$$

When $l = 1$,

$$s_1(x) = \frac{\sin x}{x} - \cos x, \tag{4.103a}$$

$$c_1(x) = \frac{\cos x}{x} + \sin x. \tag{4.103b}$$

When $l = 2$,

$$s_2(x) = \left(\frac{3}{x^2} - 1\right)\sin x - \frac{3\cos x}{x}, \tag{4.104a}$$

$$c_2(x) = \left(\frac{3}{x^2} - 1\right)\cos x + \frac{3\sin x}{x}. \tag{4.104b}$$

When $l = 3$,

$$s_3(x) = \left(\frac{15}{x^2} - 6\right)\frac{\sin x}{x} - \left(\frac{15}{x^2} - 1\right)\cos x, \tag{4.105a}$$

$$c_3(x) = \left(\frac{15}{x^2} - 6\right)\frac{\cos x}{x} + \left(\frac{15}{x^2} - 1\right)\sin x. \tag{4.105b}$$

The behavior of these functions is illustrated in Fig. 4.12. As this figure shows, $s_l(x)$ always starts from the origin, or in other words $s_l(0) = 0$, and as x becomes larger the form of the function approaches that of a sin function. We also note that the sinusoidal part of the waves shifts to the right as l becomes larger, but the spacing between the waves for an adjacent pair of values of l seems to reach a constant where x is large.

On the other hand, $c_l(x)$ diverges to positive infinity $(+\infty)$ around the origin except when $l = 0$. Where x is large, however, the behavior of this function is similar to that of $s_l(x)$, although the phases of the waves of $s_l(x)$ and $c_l(x)$ seem to differ by $\frac{\pi}{2}$.

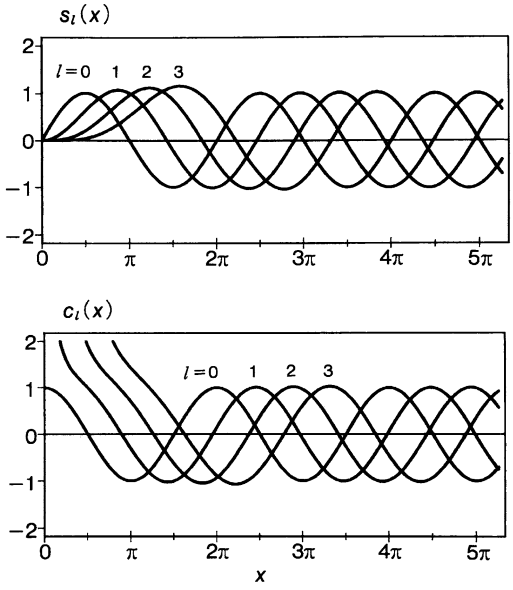

Fig. 4.12 The shapes of $s_l(x)$ and $c_l(x)$ for $l = 0, 1, 2, 3$

In the same way as the eigenfunctions of hydrogen-like atoms whose orbital angular momenta become $l = 0, 1, 2, \ldots$ are called the s orbital, the p orbital, the d orbital, ..., respectively, the partial waves representing the scattering states whose orbital angular momenta are $l = 0, 1, 2, \ldots$ are called the s wave, the p wave, the d wave, ..., respectively.

The asymptotic forms of the spherical Bessel function $j_l(x)$ and the spherical Neumann function $n_l(x)$ at $x \to \infty$ are known to be

$$j_l(x) \sim \frac{1}{x} \sin\left(x - \frac{\pi}{2} l\right), \tag{4.106a}$$

$$n_l(x) \sim -\frac{1}{x} \cos\left(x - \frac{\pi}{2} l\right), \tag{4.106b}$$

which tells us that the asymptotic forms of $s_l(x)$ and $c_l(x)$, as defined by Eqs. (4.101a) and (4.101b) are

$$s_l(x) \sim \sin\left(x - \frac{\pi}{2} l\right), \tag{4.107a}$$

$$c_l(x) \sim \cos\left(x - \frac{\pi}{2} l\right), \tag{4.107b}$$

at $x \to \infty$. This corresponds with the behaviors of $s_l(x)$ and $c_l(x)$ in the region of large x values in Fig. 4.12.

Problem 4.8
For $l = 0$ and $l = 1$, prove that $s_l(kr)$ and $c_l(kr)$ are solutions of the second-order differential equation of $f_l(x)$, Eq. (4.94).

Solution
In the case of $l = 0$, Eq. (4.94) is written as

$$\frac{\mathrm{d}^2}{\mathrm{d}r^2} f_0(r) + k^2 f_0(r) = 0, \tag{4.108}$$

whose solutions are obviously $s_0(kr) = \sin kr$ and $c_0(kr) = \cos kr$.

In the case of $l = 1$, Eq. (4.94) becomes

$$\frac{\mathrm{d}^2}{\mathrm{d}r^2} f_1(r) - \frac{2}{r^2} f_1(r) + k^2 f_1(r) = 0. \tag{4.109}$$

Substituting

$$f_1(r) = s_1(kr) = \frac{\sin kr}{kr} - \cos kr$$

into Eq. (4.109), we obtain

$$\begin{aligned} \frac{\mathrm{d}^2}{\mathrm{d}r^2} f_1(r) &= \frac{\mathrm{d}}{\mathrm{d}r}\left(\frac{\cos kr}{r} - \frac{\sin kr}{kr^2} + k \sin kr\right) \\ &= \frac{2}{r^2} f_1(r) - k^2 f_1(r), \end{aligned}$$

which shows us that $s_1(kr)$ is one of the solutions.

With $f_1(r) = c_1(kr)$, too, we can similarly prove that Eq. (4.109) will be satisfied. □

4.4.3 The Partial Wave Expansion of Plane Waves

Equation (4.94) is one which $f_l(r)$, the partial wave expansion of the scattering state expression $\psi(r, \theta)$, has to satisfy when $U(r)$ is sufficiently small, or in other words where the effect of the potential no longer reaches. It is also an equation with $U(r) = 0$, that is, an equation that needs to be satisfied by a wave being propagated which is not affected by any potentials, which is to say, a plane wave, $\mathrm{e}^{\mathrm{i}kz}$.

Let us then consider the expansion of $\mathrm{e}^{\mathrm{i}kz} = \mathrm{e}^{\mathrm{i}kr\cos\theta}$ with partial waves $s_l(kr)$ and $c_l(kr)$. First, as in Eq. (4.96), we expand $\mathrm{e}^{\mathrm{i}kz}$ using the Legendre polynomial $P_l(\cos\theta)$ as

$$\mathrm{e}^{\mathrm{i}kz} = \frac{1}{r} \sum_{l=0}^{\infty} g_l(r) P_l(\cos\theta). \tag{4.110}$$

In order to obtain $g_l(r)$, we multiply both sides of Eq. (4.110) by $P_l(\cos\theta)$ and integrate the equation, then use the orthogonal relation of Eq. (4.100) to derive

$$I = \int_{-1}^{1} \mathrm{e}^{\mathrm{i}kr\cos\theta} P_l(\cos\theta)\,\mathrm{d}(\cos\theta) = \frac{2}{2l+1}\cdot\frac{g_l(r)}{r}. \tag{4.111}$$

Letting $t = \cos\theta$, the integral I is written as

$$I = \int_{-1}^{1} \mathrm{e}^{\mathrm{i}krt} P_l(t)\,\mathrm{d}t. \tag{4.112}$$

By repeating the partial integration, the power series expansion of $\frac{1}{kr}$ is obtained as

$$\begin{aligned} I &= \frac{1}{\mathrm{i}kr}\left[\mathrm{e}^{\mathrm{i}krt} P_l(t)\right]_{-1}^{1} - \frac{1}{\mathrm{i}kr}\int_{-1}^{1} \mathrm{e}^{\mathrm{i}krt}\frac{\mathrm{d}P_l(t)}{\mathrm{d}t}\,\mathrm{d}t \\ &= \frac{1}{\mathrm{i}kr}\left[\mathrm{e}^{\mathrm{i}krt} P_l(t)\right]_{-1}^{1} - \frac{1}{(\mathrm{i}kr)^2}\left[\mathrm{e}^{\mathrm{i}krt}\frac{\mathrm{d}P_l(t)}{\mathrm{d}t}\right]_{-1}^{1} + \frac{1}{(\mathrm{i}kr)^2}\int_{-1}^{1} \mathrm{e}^{\mathrm{i}krt}\frac{\mathrm{d}^2P_l(t)}{\mathrm{d}t^2}\,\mathrm{d}t \\ &= \cdots. \end{aligned} \tag{4.113}$$

The behavior of this equation at $r \to \infty$ is dominated by its first term, in which the order of $\frac{1}{kr}$ is the lowest. Thus, at $r \to \infty$ we can write

$$\begin{aligned} I &\sim \frac{1}{\mathrm{i}kr}\left[\mathrm{e}^{\mathrm{i}krt} P_l(t)\right]_{-1}^{1} \\ &= \frac{1}{\mathrm{i}kr}\left\{\mathrm{e}^{\mathrm{i}kr} - (-1)^l \mathrm{e}^{-\mathrm{i}kr}\right\}, \end{aligned} \tag{4.114}$$

using the fact that the Legendre polynomial becomes

$$P_l(1) = 1, \quad P_l(-1) = (-1)^l \tag{4.115}$$

for $x = 1, -1$. As $\mathrm{e}^{\mathrm{i}x} = \cos x + \mathrm{i}\sin x$, we can also write

$$\mathrm{e}^{\mathrm{i}\pi l} = (-1)^l, \quad \mathrm{e}^{\mathrm{i}\frac{\pi}{2}l} = \mathrm{i}^l, \tag{4.116}$$

which can be used to change Eq. (4.114) into

$$\begin{aligned} I &\sim \frac{1}{\mathrm{i}kr}\left(\mathrm{e}^{\mathrm{i}kr} - \mathrm{e}^{\mathrm{i}\pi l}\mathrm{e}^{-\mathrm{i}kr}\right) \\ &= \frac{1}{\mathrm{i}kr}\mathrm{e}^{\mathrm{i}\frac{\pi}{2}l}\left\{\mathrm{e}^{\mathrm{i}(kr-\frac{\pi}{2}l)} - \mathrm{e}^{-\mathrm{i}(kr-\frac{\pi}{2}l)}\right\} \\ &= \frac{2}{kr}\mathrm{i}^l \sin\left(kr - \frac{\pi}{2}l\right). \end{aligned} \tag{4.117}$$

That is to say,

$$g_l(r) \sim \frac{2l+1}{k} \mathrm{i}^l \sin\left(kr - \frac{\pi}{2}l\right), \tag{4.118}$$

which tells us that the asymptotic form of $g_l(r)$ is proportional to the asymptotic form of $s_l(kr)$. We also know from the expansion in Eq. (4.110) that $g_l(r)$ at $r = 0$ is required to be $g_l(0) = 0$. Thus, $g_l(r)$ is shown to be a function proportional not to $c_l(kr)$ but to $s_l(kr)$, as

$$g_l(r) = \frac{2l+1}{k} \mathrm{i}^l s_l(kr). \tag{4.119}$$

Substituting this equation back into the original expansion equation (4.110), we can represent the plane wave $\mathrm{e}^{\mathrm{i}kz}$ as

$$\mathrm{e}^{\mathrm{i}kz} = \frac{1}{kr} \sum_{l=0}^{\infty} (2l+1) \mathrm{i}^l s_l(kr) P_l(\cos\theta). \tag{4.120}$$

This can also be expressed with the spherical Bessel function $j_l(kr)$ as

$$\mathrm{e}^{\mathrm{i}kz} = \sum_{l=0}^{\infty} (2l+1) \mathrm{i}^l j_l(kr) P_l(\cos\theta). \tag{4.121}$$

Equations (4.120) and (4.121) are known as the partial wave expansion of the plane wave.

4.4.4 The Partial Wave Expansion of Scattering Amplitudes

We are now ready to calculate the asymptotic form of $\psi(r, \theta)$ for scattering states where $U(r) \neq 0$, thus deriving the partial wave expansion of the scattering amplitude $f(\theta)$. In the asymptotic region of $r \to \infty$, the solution of Eq. (4.94), $f_l(r)$, is represented as the superposition of $s_l(kr)$ and $c_l(kr)$, that is,

$$f_l(r) \sim A_l s_l(kr) + B_l c_l(kr). \tag{4.122}$$

When C_l is a constant and δ_l is within the range $-\frac{\pi}{2} \leqq \delta_l \leqq \frac{\pi}{2}$, letting

$$A_l = C_l \cos\delta_l, \tag{4.123a}$$

$$B_l = C_l \sin\delta_l, \tag{4.123b}$$

we can rewrite $f_l(r)$ as

$$f_l(r) \sim C_l\big(\cos\delta_l s_l(kr) + \sin\delta_l c_l(kr)\big)$$

$$\sim C_l\left\{\cos\delta_l \sin\left(kr-\frac{\pi}{2}l\right)+\sin\delta_l\cos\left(kr-\frac{\pi}{2}l\right)\right\}$$
$$= C_l \sin\left(kr-\frac{\pi}{2}l+\delta_l\right), \tag{4.124}$$

wherein the second line is derived from the first by using the asymptotic forms of $s_l(kr)$ and $c_l(kr)$ given in Eqs. (4.107a) and (4.107b), respectively. The δ_l appearing in this equation is the phase shift of the scattering state with the orbital angular momentum l. Using this asymptotic form of $f_l(r)$, the asymptotic form of the Legendre expansion equation (4.96) at $r\to\infty$ can be obtained as

$$\psi(r,\theta)\sim\frac{1}{r}\sum_{l=0}^{\infty}C_l\sin\left(kr-\frac{\pi}{2}l+\delta_l\right)P_l(\cos\theta). \tag{4.125}$$

Our next task is to obtain the constant C_l. To this end, let us think about representing the asymptotic form in Eq. (4.125) by the sum of a term that depends on $\mathrm{e}^{\mathrm{i}kr}$ and another that depends on $\mathrm{e}^{-\mathrm{i}kr}$ as

$$\frac{1}{r}C_l\sin\left(kr-\frac{\pi}{2}l+\delta_l\right)=C_l\frac{1}{2\mathrm{i}r}\left\{\mathrm{e}^{\mathrm{i}kr}\mathrm{e}^{-\mathrm{i}\frac{\pi}{2}l}\mathrm{e}^{\mathrm{i}\delta_l}-\mathrm{e}^{-\mathrm{i}kr}\mathrm{e}^{\mathrm{i}\frac{\pi}{2}l}\mathrm{e}^{-\mathrm{i}\delta_l}\right\}$$
$$=\left(\frac{C_l}{2\mathrm{i}r}\mathrm{e}^{-\mathrm{i}\frac{\pi}{2}l}\mathrm{e}^{\mathrm{i}\delta_l}\right)\mathrm{e}^{\mathrm{i}kr}-\left(\frac{C_l}{2\mathrm{i}r}\mathrm{e}^{\mathrm{i}\frac{\pi}{2}l}\mathrm{e}^{-\mathrm{i}\delta_l}\right)\mathrm{e}^{-\mathrm{i}kr}, \tag{4.126}$$

so $\psi(r,\theta)$ is represented as

$$\psi(r,\theta)\sim\sum_{l=0}^{\infty}\left\{\left(\frac{C_l}{2\mathrm{i}r}\mathrm{e}^{-\mathrm{i}\frac{\pi}{2}l}\mathrm{e}^{\mathrm{i}\delta_l}\right)\mathrm{e}^{\mathrm{i}kr}-\left(\frac{C_l}{2\mathrm{i}r}\mathrm{e}^{\mathrm{i}\frac{\pi}{2}l}\mathrm{e}^{-\mathrm{i}\delta_l}\right)\mathrm{e}^{-\mathrm{i}kr}\right\}P_l(\cos\theta). \tag{4.127}$$

In the meantime, the asymptotic form of the scattering state is derived as

$$\psi(r,\theta)\sim\mathrm{e}^{\mathrm{i}kz}+\frac{f(\theta)}{r}\mathrm{e}^{\mathrm{i}kr}, \tag{4.128}$$

in accordance with Eq. (4.18). As the first term of this equation is expanded as Eq. (4.120), the asymptotic form of the coefficient of the term of $P_l(\cos\theta)$ is represented by the sum of $\mathrm{e}^{\mathrm{i}kr}$ and $\mathrm{e}^{-\mathrm{i}kr}$ as

$$\frac{1}{kr}(2l+1)\mathrm{i}^l\sin\left(kr-\frac{\pi}{2}l\right)$$
$$=\left\{\frac{(2l+1)\mathrm{i}^l}{2\mathrm{i}kr}\mathrm{e}^{-\mathrm{i}\frac{\pi}{2}l}\right\}\mathrm{e}^{\mathrm{i}kr}-\left\{\frac{(2l+1)\mathrm{i}^l}{2\mathrm{i}kr}\mathrm{e}^{\mathrm{i}\frac{\pi}{2}l}\right\}\mathrm{e}^{-\mathrm{i}kr}, \tag{4.129}$$

and Eq. (4.128) is rewritten as

$$\psi(r,\theta) \sim \sum_{l=0}^{\infty} \left\{ \left\{ \frac{(2l+1)\mathrm{i}^l}{2\mathrm{i}kr} \mathrm{e}^{-\mathrm{i}\frac{\pi}{2}l} \right\} \mathrm{e}^{\mathrm{i}kr} - \left\{ \frac{(2l+1)\mathrm{i}^l}{2\mathrm{i}kr} \mathrm{e}^{\mathrm{i}\frac{\pi}{2}l} \right\} \mathrm{e}^{-\mathrm{i}kr} \right\} P_l(\cos\theta) + \frac{f(\theta)}{r} \mathrm{e}^{\mathrm{i}kr}. \tag{4.130}$$

For Eqs. (4.127) and (4.130) to be consistent with each other, the terms in these two equations that depend on $\mathrm{e}^{-\mathrm{i}kr}$ need to be equal. Thus by equalizing the coefficients of the two $\mathrm{e}^{-\mathrm{i}kr}$ terms for all values of l, we can write

$$\frac{C_l}{2\mathrm{i}r} \mathrm{e}^{\mathrm{i}\frac{\pi}{2}l} \mathrm{e}^{-\mathrm{i}\delta_l} = \frac{(2l+1)\mathrm{i}^l}{2\mathrm{i}kr} \mathrm{e}^{\mathrm{i}\frac{\pi}{2}l}$$

and thus derive

$$C_l = \frac{(2l+1)\mathrm{i}^l}{k} \mathrm{e}^{\mathrm{i}\delta_l}. \tag{4.131}$$

Substituting this back into the Legendre expansion in Eq. (4.125), we obtain

$$\psi(r,\theta) \sim \frac{1}{kr} \sum_{l=0}^{\infty} (2l+1)\mathrm{i}^l \mathrm{e}^{\mathrm{i}\delta_l} \sin\left(kr - \frac{\pi}{2}l + \delta_l \right) P_l(\cos\theta). \tag{4.132}$$

This is the partial wave expansion of the asymptotic form of the scattering state.

We can also use the fact that the coefficients of $\mathrm{e}^{\mathrm{i}kr}$ in Eq. (4.127) and those of $\mathrm{e}^{\mathrm{i}kr}$ in Eq. (4.130) are equal to write

$$\sum_{l=0}^{\infty} \left\{ \frac{C_l}{2\mathrm{i}r} \mathrm{e}^{-\mathrm{i}\frac{\pi}{2}l} \mathrm{e}^{\mathrm{i}\delta_l} \right\} P_l(\cos\theta) = \sum_{l=0}^{\infty} \left\{ \frac{(2l+1)\mathrm{i}^l}{2\mathrm{i}kr} \mathrm{e}^{-\mathrm{i}\frac{\pi}{2}l} \right\} P_l(\cos\theta) + \frac{f(\theta)}{r}, \tag{4.133}$$

which can be rearranged using

$$\frac{C_l}{2\mathrm{i}r} \mathrm{e}^{-\mathrm{i}\frac{\pi}{2}l} \mathrm{e}^{\mathrm{i}\delta_l} - \frac{(2l+1)\mathrm{i}^l}{2\mathrm{i}kr} \mathrm{e}^{-\mathrm{i}\frac{\pi}{2}l} = \frac{(2l+1)}{2\mathrm{i}kr} \left(\mathrm{e}^{2\mathrm{i}\delta_l} - 1 \right) = \frac{(2l+1)}{kr} \mathrm{e}^{\mathrm{i}\delta_l} \sin\delta_l$$

to derive $f(\theta)$ as a sum in terms of l, as

$$f(\theta) = \frac{1}{k} \sum_{l=0}^{\infty} (2l+1) \mathrm{e}^{\mathrm{i}\delta_l} \sin\delta_l P_l(\cos\theta). \tag{4.134}$$

This equation is the partial wave expansion of the scattering amplitude expressed using the phase shift.

Let us now derive the total cross section σ using the scattering amplitude that has just been obtained. From the definition given in Eq. (4.23),

$$\begin{aligned}\sigma &= \int \left| f(\theta) \right|^2 \mathrm{d}\Omega \\ &= \int_0^{\pi} \int_0^{2\pi} \left| f(\theta) \right|^2 \sin\theta \, \mathrm{d}\theta \, \mathrm{d}\phi,\end{aligned}$$

so we can substitute Eq. (4.134) into this and derive

$$\begin{aligned}\sigma &= \frac{1}{k^2} \sum_{l=0}^{\infty} (2l+1)^2 \sin^2 \delta_l \frac{2}{2l+1} 2\pi \\ &= \frac{4\pi}{k^2} \sum_{l=0}^{\infty} (2l+1) \sin^2 \delta_l. \end{aligned} \tag{4.135}$$

Representing the partial cross section as

$$\sigma_l = \frac{4\pi}{k^2} (2l+1) \sin^2 \delta_l, \tag{4.136}$$

the total cross section is written as

$$\sigma = \sum_{l=0}^{\infty} \sigma_l. \tag{4.137}$$

When we substitute $\theta = 0$ into the scattering amplitude in Eq. (4.134), we obtain

$$f(0) = \frac{1}{k} \sum_{l=0}^{\infty} (2l+1) \mathrm{e}^{\mathrm{i}\delta_l} \sin \delta_l, \tag{4.138}$$

of which the imaginary part is expressed as

$$\mathrm{Im}\, f(0) = \frac{1}{k} \sum_{l=0}^{\infty} (2l+1) \sin^2 \delta_l, \tag{4.139}$$

where $\mathrm{Im}\, z$ stands for the imaginary part of z. By comparing this to Eq. (4.135), we can derive

$$\sigma = \frac{4\pi}{k} \mathrm{Im}\, f(0). \tag{4.140}$$

Equation (4.140) shows that the imaginary part of the forward scattering amplitude, that is, the scattering amplitude at $\theta = 0$, can be multiplied by $\frac{4\pi}{k}$ to become equal to the total cross section, and this equation is known as the equation representing the optical theorem.

4.4.5 Phase Shift in Electron Diffraction

As is evident from the discussion above, when we describe an electron wave scattered by atoms by the sum of partial waves with different values of the orbital angular momentum, each partial wave has a different phase shift δ_l, depending on the value of l. The total scattering amplitude, then, is represented as the sum of the complex scattering amplitudes each characterized by δ_l. This means that the total scattering amplitude can also be expressed as a complex function, as

$$f(\theta) = \left|f(\theta)\right| e^{i\eta(\theta)}. \tag{4.141}$$

When $A = \mathrm{Re}\, f(\theta)$ and $B = \mathrm{Im}\, f(\theta)$, where $\mathrm{Re}\, z$ stands for the real part of a complex number z, we can write $|f(\theta)|^2$ and $\tan\eta(\theta)$ as

$$\left|f(\theta)\right|^2 = A^2 + B^2, \tag{4.142}$$

$$\tan\eta(\theta) = \frac{B}{A}. \tag{4.143}$$

Problem 4.9
Prove the following two equations:

$$\mathrm{Re}\, f(\theta) = \frac{1}{2k}\sum_{l=0}^{\infty}(2l+1)\sin 2\delta_l P_l(\cos\theta), \tag{4.144a}$$

$$\mathrm{Im}\, f(\theta) = \frac{1}{2k}\sum_{l=0}^{\infty}(2l+1)(1-\cos 2\delta_l) P_l(\cos\theta). \tag{4.144b}$$

Solution
Extracting the real part and the imaginary part of Eq. (4.134), we can write

$$\mathrm{Re}\, f(\theta) = \frac{1}{k}\sum_{l=0}^{\infty}(2l+1)\cos\delta_l \sin\delta_l P_l(\cos\theta),$$

$$\mathrm{Im}\, f(\theta) = \frac{1}{k}\sum_{l=0}^{\infty}(2l+1)\sin^2\delta_l P_l(\cos\theta).$$

As $\sin 2\delta_l = 2\cos\delta_l \sin\delta_l$ and $1 - \cos 2\delta_l = 2\sin^2\delta_l$, we can see that Eqs. (4.144a) and (4.144b) hold. □

As is shown from the explanation so far, in order to obtain the complex scattering amplitude $f(\theta)$, which is expressed as Eq. (4.141), we need to solve the Schrödinger equation given by Eqs. (4.90a) and (4.90b) for each value of l, and calculate the corresponding phase shift δ_l. Then, using all of these δ_l values, we add up the partial waves until the values of A and B cease to be affected, that is, where they can be considered to reach convergence. Using these A and B, we can calculate $f(\theta)$. In

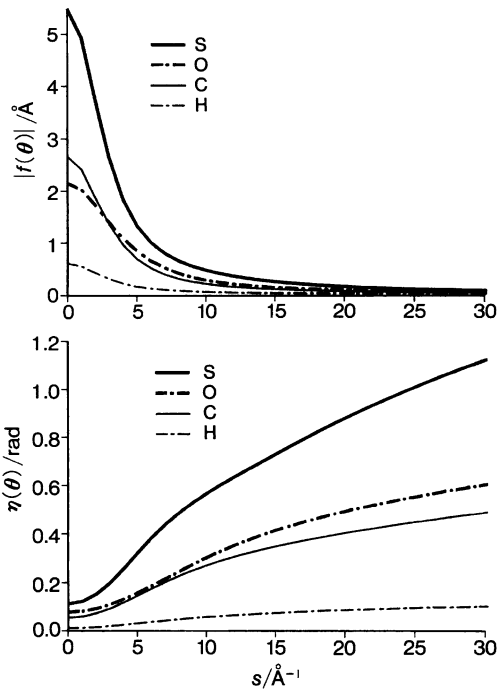

Fig. 4.13 The absolute values of the scattering amplitudes ($|f(\theta)|$) and the phase shifts ($\eta(\theta)$)

the case of an electron beam accelerated by 40 keV, it is known that adding up the partial waves for up to $l = 250$ gives us the convergence at a precision level of six figures.

As the potential $U(r)$ obviously differs for different atomic species, so do the phase shift δ_l and, thus, the value of $\eta(\theta)$. Figure 4.13 plots the values $|f(\theta)|$ and $\eta(\theta)$ of some atomic species as a function of the scattering parameter s. As is evident from the s dependence of $f(\theta)$ shown in Eq. (4.67), $|f(\theta)|$ rapidly decreases when s increases. We can also see from this figure that $\eta(\theta)$ increases monotonically when s increases, and that heavier atoms have larger $\eta(\theta)$ values, which reflects the extent of the pull on the waves being larger in heavier atoms.

Since the scattering amplitude is given as Eq. (4.141) in a complex representation, the scattering amplitude of the electron beam in the case of a scattering by a diatomic molecule, where the scattering amplitudes of atoms 1 and 2 are given by

$$\begin{cases} f_1(\theta) = \left|f_1(\theta)\right| \mathrm{e}^{\mathrm{i}\eta_1(\theta)}, \\ f_2(\theta) = \left|f_2(\theta)\right| \mathrm{e}^{\mathrm{i}\eta_2(\theta)}, \end{cases} \tag{4.145}$$

is calculated as

$$\begin{aligned} I(\theta) &= \left|f_{\mathrm{mol}}(\theta)\right|^2 \\ &= \left|f_1(\theta)\right|^2 + \left|f_2(\theta)\right|^2 + \left|f_1(\theta)\right| \cdot \left|f_2(\theta)\right| \mathrm{e}^{\mathrm{i}(\eta_1 - \eta_2)} \mathrm{e}^{\mathrm{i}\boldsymbol{s}\cdot(\boldsymbol{r}_1 - \boldsymbol{r}_2)} \end{aligned}$$

$$+\left|f_1(\theta)\right|\cdot\left|f_2(\theta)\right|\mathrm{e}^{-\mathrm{i}(\eta_1-\eta_2)}\mathrm{e}^{-\mathrm{i}\boldsymbol{s}\cdot(\boldsymbol{r}_1-\boldsymbol{r}_2)}$$

$$=\left|f_1(\theta)\right|^2+\left|f_2(\theta)\right|^2+2\left|f_1(\theta)\right|\cdot\left|f_2(\theta)\right|\cos\left\{(\eta_1-\eta_2)-\boldsymbol{s}\cdot\boldsymbol{r}_{12}\right\}, \quad (4.146)$$

using Eq. (4.74). By taking the third term of Eq. (4.146), which is an interference term, and integrating it over all space then taking the average, as we did to derive Eq. (4.81), we can obtain the molecular scattering intensity I_{mol} as

$$I_{\mathrm{mol}}(\theta)=2\left|f_1(\theta)\right|\cdot\left|f_2(\theta)\right|\cos(\eta_1-\eta_2)\frac{\sin sr_{12}}{sr_{12}}. \quad (4.147)$$

Problem 4.10
Calculate the $I_{\mathrm{mol}}(\theta)$ in Eq. (4.147) using Eq. (4.146).

Solution
Letting $\eta_1-\eta_2=\Delta\eta$, we can write

$$\cos\left\{(\eta_1-\eta_2)-\boldsymbol{s}\cdot\boldsymbol{r}_{12}\right\}=\cos\Delta\eta\cos(\boldsymbol{s}\cdot\boldsymbol{r}_{12})+\sin\Delta\eta\sin(\boldsymbol{s}\cdot\boldsymbol{r}_{12}).$$

When the second term of this equation integrated over all space and averaged is named I_2, we can derive

$$\begin{aligned}I_2&=\frac{1}{4\pi}\int_0^{2\pi}\mathrm{d}\beta\int_0^{\pi}\sin\Delta\eta\sin(sr_{12}\cos\alpha)\sin\alpha\,\mathrm{d}\alpha\\&=-\frac{1}{2}\sin\Delta\eta\int_1^{-1}\sin(sr_{12}\gamma)\,\mathrm{d}\gamma\\&=0.\end{aligned}$$

Therefore, we see that $I_{\mathrm{mol}}(\theta)$ is Eq. (4.78) multiplied by $\cos\Delta\eta$, which gives us Eq. (4.147). □

4.5 The Effect of Molecular Vibration

4.5.1 Mean Square Amplitudes

As described at the beginning of the previous section, the effect of molecular vibration appears in the diffraction pattern of an electron beam scattered by molecules. In this section, we will examine how the molecular scattering intensity described by Eq. (4.147) changes under the influence of molecular vibration.

As we have learned in Chap. 2, a molecule vibrates around its equilibrium internuclear distance. When we regard a diatomic molecule, as an approximation, as a harmonic oscillator in its vibrational ground state ($v=0$, where v is the vibrational quantum number), Eq. (2.54) from Sect. 2.2 allows us to write its molecular vibrational wave function as

$$\psi_0(\xi)=N_0H_0(\xi)\exp\left(-\frac{\xi^2}{2}\right). \quad (4.148)$$

As shown from Eq. (2.113) in Sect. 2.2, the expectation value of x^2 in this ground state is

$$\langle x^2 \rangle_{v=0} = \int \psi_0^* x^2 \psi_0 \, \mathrm{d}x = \langle 0|x^2|0\rangle = \frac{1}{2\beta}, \tag{4.149}$$

where x represents the displacement from the equilibrium internuclear distance r_e. We call $\langle x^2 \rangle_{v=0}$ the mean square amplitude for the vibrational ground state, and represent it as l_0^2. That is to say,

$$l_0^2 = \frac{1}{2\beta} = \frac{\hbar}{2\mu\omega} \quad \left(\beta = \frac{1}{2l_0^2}\right). \tag{4.150}$$

Using this mean square amplitude for the zero-point vibration, the eigenfunction for $v = 0$ can be described as

$$\psi_0(x) = \left(\frac{\beta}{\pi}\right)^{\frac{1}{4}} \exp\left(-\frac{x^2}{4l_0^2}\right). \tag{4.151}$$

Therefore, the distribution function for x can be written as

$$P_0(x) = \left|\psi_0(x)\right|^2 = \left(\frac{\beta}{\pi}\right)^{\frac{1}{2}} \exp\left(-\frac{x^2}{2l_0^2}\right) = \frac{1}{\sqrt{2\pi l_0^2}} \exp\left(-\frac{x^2}{2l_0^2}\right). \tag{4.152}$$

In the thermal equilibrium at temperature T, the ratio of the number of molecules which have the quantum number v with respect to the total number of molecules can be given by the Boltzmann distribution as

$$w_v = \frac{\exp\left(-\frac{v\hbar\omega}{kT}\right)}{\sum\limits_{n=0}^{\infty} \exp\left(-\frac{n\hbar\omega}{kT}\right)}, \tag{4.153}$$

so that, at temperature T, we can write the distribution function $P(x, T)$ as

$$P(x, T) = \sum_{v=0}^{\infty} w_v \left|\psi_v(x)\right|^2. \tag{4.154}$$

It is known that $P(x, T)$ is given by the same type of equation as the one for $v = 0$, Eq. (4.151), as

$$P(x, T) = \frac{1}{\sqrt{2\pi l_\mathrm{h}^2}} \exp\left(-\frac{x^2}{2l_\mathrm{h}^2}\right), \tag{4.155}$$

where l_h^2 is described as

$$l_\mathrm{h}^2 = l_0^2 \coth\left(\frac{\hbar\omega}{2kT}\right), \tag{4.156}$$

and stands for the mean square amplitude at temperature T.

We can prove that the mean square amplitude l_{h}^2 at temperature T is given by Eq. (4.156) as follows. First, by following the Boltzmann distribution, we can describe l_{h}^2 as the weighted sum of $\langle v|x^2|v\rangle$, which are the expectation values of x^2 at the eigenstate whose vibrational quantum number is v, so that

$$l_{\mathrm{h}}^2 = \langle x^2 \rangle_T = \sum_{v=0}^{\infty} w_v \langle v|x^2|v\rangle. \tag{4.157}$$

As Eq. (2.113) gives us

$$\langle v|x^2|v\rangle = \frac{2v+1}{2\beta}, \tag{4.158}$$

we can obtain

$$l_{\mathrm{h}}^2 = \frac{\sum_v \left(\frac{2v+1}{2\beta} \cdot \mathrm{e}^{-v\gamma}\right)}{\sum_v \mathrm{e}^{-v\gamma}}, \tag{4.159}$$

where $\gamma = \frac{\hbar\omega}{kT}$. As we can write

$$\sum_v \mathrm{e}^{-v\gamma} = \frac{1}{1-\mathrm{e}^{-\gamma}}, \tag{4.160}$$

we can differentiate both sides of this equation and derive

$$\sum_v v\mathrm{e}^{-v\gamma} = \frac{\mathrm{e}^{-\gamma}}{(1-\mathrm{e}^{-\gamma})^2}. \tag{4.161}$$

By substituting Eqs. (4.160) and (4.161) into Eq. (4.159), we can arrive at

$$\begin{aligned} l_{\mathrm{h}}^2 &= \frac{1}{2\beta}\left(\frac{2\mathrm{e}^{-\gamma}}{1-\mathrm{e}^{-\gamma}} + 1\right) \\ &= \frac{1}{2\beta}\left(\frac{\mathrm{e}^{\frac{\gamma}{2}} + \mathrm{e}^{-\frac{\gamma}{2}}}{\mathrm{e}^{\frac{\gamma}{2}} - \mathrm{e}^{-\frac{\gamma}{2}}}\right) \\ &= l_0^2 \coth\left(\frac{\hbar\omega}{2kT}\right), \end{aligned} \tag{4.162}$$

which shows that Eq. (4.156) stands. Note here that the square root of the mean square amplitude l_{h} is called the mean amplitude. In the case of diatomic molecules, l_{h} is in the range between 0.03 Å and 0.08 Å at room temperature (see Table 4.1).

Problem 4.11
Using the values given in Table 4.1 for the frequency $\tilde{\nu}$, calculate the mean amplitude at the vibrational ground state, l_0, and the mean amplitude at temperature $T = 300$ K, l_{h}, for diatomic molecules H_2, HCl, N_2, NO, O_2, Cl_2, and Br_2.

Table 4.1 Mean amplitudes of diatomic molecules

	$\tilde{\nu}/\mathrm{cm}^{-1}$	$l_0/$Å	$l_\mathrm{h}/$Å (300 K)
H_2	4401	0.0872	0.0872
HCl	2991	0.0758	0.0758
N_2	2359	0.0319	0.0319
NO	1904	0.0344	0.0344
O_2	1580	0.0365	0.0365
Cl_2	559.7	0.0415	0.0441
Br_2	323.2	0.0361	0.0448

Solution

Using μ amu, the reduced mass, and $\tilde{\nu}$ cm^{-1}, the vibrational frequency, of the diatomic molecule, we can write

$$l_0^2 = \frac{1}{2\beta} = \frac{h}{8\pi^2 \mu c \tilde{\nu}} = \frac{16.8576}{\mu \tilde{\nu}} \text{ Å}^2,$$

$$l_\mathrm{h}^2 = l_0^2 \coth\left(\frac{hc\tilde{\nu}}{2kT}\right) = l_0^2 \coth\left(\frac{0.71938\tilde{\nu}}{T}\right) \text{ Å}^2.$$

Thus, by adopting the values of $\tilde{\nu}$ given in Table 4.1, we can obtain l_0 and l_h at $T = 300$ K as shown in the table. We can see from the results that l_h is nearly equal to l_0 at room temperature in the case of diatomic molecules with relatively high vibrational frequencies, whereas l_h becomes larger than l_0 in diatomic molecules with lower vibrational frequencies. □

When the internuclear distance r_{12} has the probability distribution $P(x, T)$ shown by Eq. (4.155) around the equilibrium internuclear distance r_e, the molecular scattering intensity $I_\mathrm{mol}(\theta, r_{12})$ is averaged by this distribution function. That is, the averaged molecular scattering intensity $\langle I_\mathrm{mol}(\theta)\rangle$ can be written as

$$\left\langle I_\mathrm{mol}(\theta)\right\rangle = \int_{-\infty}^{\infty} P(x, T) I_\mathrm{mol}(\theta, r_\mathrm{e} + x)\, \mathrm{d}x, \tag{4.163}$$

where $r_{12} = r_\mathrm{e} + x$. Let us then derive the representation of $\langle I_\mathrm{mol}(\theta)\rangle$ by substituting the molecular scattering intensity $I_\mathrm{mol}(\theta)$ given by Eq. (4.147) into Eq. (4.163).

In this case, $\langle I_\mathrm{mol}(\theta)\rangle$ can be described as

$$\left\langle I_\mathrm{mol}(\theta)\right\rangle = 2\left|f_1(\theta)\right| \cdot \left|f_2(\theta)\right| \cos(\eta_1 - \eta_2) \cdot \frac{1}{\sqrt{2\pi l_\mathrm{h}^2}} \int_{-\infty}^{\infty} \exp\left(-\frac{x^2}{2l_\mathrm{h}^2}\right) \frac{\sin s(r_\mathrm{e} + x)}{s(r_\mathrm{e} + x)}\, \mathrm{d}x. \tag{4.164}$$

Representing the integral part of this equation as I and letting $\beta_{\mathrm{h}} = \frac{1}{2l_{\mathrm{h}}^2}$, we can write

$$I = \int_{-\infty}^{\infty} \mathrm{e}^{-\beta_{\mathrm{h}} x^2} \frac{\sin s(r_{\mathrm{e}} + x)}{s(r_{\mathrm{e}} + x)} \,\mathrm{d}x. \tag{4.165}$$

Of course, x cannot be $-\infty$, but the spread of the Gaussian in the integrand, that is, the mean amplitude l_{h} (< 0.1 Å), is sufficiently small in comparison to r_{e} (which ranges between 1 and 2 Å), so that the integrand becomes 0 quickly enough before $r_{\mathrm{e}} + x$ becomes negative. Therefore, the integral range from $-\infty$ to $+\infty$ can be rationalized. Because $\frac{x}{r_{\mathrm{e}}}$ is sufficiently small, we can approximate the denominator in the integrand as

$$\frac{1}{s(r_{\mathrm{e}} + x)} = \frac{1}{sr_{\mathrm{e}}} \cdot \frac{1}{\left(1 + \frac{x}{r_{\mathrm{e}}}\right)} \sim \frac{1}{sr_{\mathrm{e}}} \left(1 - \frac{x}{r_{\mathrm{e}}}\right). \tag{4.166}$$

This allows us to describe the integral I using

$$I_1 = \frac{1}{sr_{\mathrm{e}}} \int_{-\infty}^{\infty} \mathrm{e}^{-\beta_{\mathrm{h}} x^2} \sin s(r_{\mathrm{e}} + x) \,\mathrm{d}x \tag{4.167}$$

and

$$I_2 = \frac{1}{sr_{\mathrm{e}}^2} \int_{-\infty}^{\infty} \mathrm{e}^{-\beta_{\mathrm{h}} x^2} x \sin s(r_{\mathrm{e}} + x) \,\mathrm{d}x \tag{4.168}$$

as

$$I = I_1 - I_2. \tag{4.169}$$

By performing the integration of I_1 and I_2, we obtain

$$I_1 = \sqrt{2\pi l_{\mathrm{h}}^2} \mathrm{e}^{-\frac{l_{\mathrm{h}}^2}{2} s^2} \cdot \frac{\sin sr_{\mathrm{e}}}{sr_{\mathrm{e}}} \tag{4.170}$$

and

$$I_2 = \sqrt{2\pi l_{\mathrm{h}}^2} \mathrm{e}^{-\frac{l_{\mathrm{h}}^2}{2} s^2} \cdot \frac{l_{\mathrm{h}}^2}{r_{\mathrm{e}}^2} \cos sr_{\mathrm{e}}. \tag{4.171}$$

From Eqs. (4.169) through (4.171), we can derive

$$\begin{aligned} I &= \sqrt{2\pi l_{\mathrm{h}}^2} \mathrm{e}^{-\frac{l_{\mathrm{h}}^2}{2} s^2} \cdot \frac{1}{sr_{\mathrm{e}}} \left(\sin sr_{\mathrm{e}} - \frac{sl_{\mathrm{h}}^2}{r_{\mathrm{e}}} \cos sr_{\mathrm{e}} \right) \\ &= \sqrt{2\pi l_{\mathrm{h}}^2} \mathrm{e}^{-\frac{l_{\mathrm{h}}^2}{2} s^2} \cdot \frac{1}{sr_{\mathrm{e}}} \sin \left(sr_{\mathrm{e}} - \frac{sl_{\mathrm{h}}^2}{r_{\mathrm{e}}} \right), \end{aligned} \tag{4.172}$$

where the relationship

$$\sin \left(sr_{\mathrm{e}} - \frac{sl_{\mathrm{h}}^2}{r_{\mathrm{e}}} \right) = \sin sr_{\mathrm{e}} \cos \frac{sl_{\mathrm{h}}^2}{r_{\mathrm{e}}} - \cos sr_{\mathrm{e}} \sin \frac{sl_{\mathrm{h}}^2}{r_{\mathrm{e}}}$$

$$\sim \sin sr_{\mathrm{e}} - \frac{sl_{\mathrm{h}}^2}{r_{\mathrm{e}}} \cos sr_{\mathrm{e}} \tag{4.173}$$

is used because, as s is at most 40 Å^{-1} and $l_{\mathrm{h}} \sim 0.04$ Å, we can regard $\frac{sl_{\mathrm{h}}^2}{r_{\mathrm{e}}}$ as being sufficiently small.

By substituting Eq. (4.172) back into Eq. (4.165), Eq. (4.164) can be described as

$$\left\langle I_{\mathrm{mol}}(\theta) \right\rangle = 2\left|f_1(\theta)\right| \cdot \left|f_2(\theta)\right| \mathrm{e}^{-\frac{l_{\mathrm{h}}^2}{2}s^2} \cdot \cos(\eta_1 - \eta_2) \cdot \frac{\sin s\left(r_{\mathrm{e}} - \frac{l_{\mathrm{h}}^2}{r_{\mathrm{e}}}\right)}{sr_{\mathrm{e}}}. \tag{4.174}$$

What this shows is that, due to the vibration of the molecule, there appears a damping factor $\mathrm{e}^{-\frac{l_{\mathrm{h}}^2}{2}s^2}$, whose value decreases as the parameter s increases, that is, as the scattering angle increases. The degree of damping increases as l_{h} increases.

Problem 4.12

By performing the integrals in Eqs. (4.167) and (4.168), derive Eqs. (4.170) and (4.171), using

$$\int_{-\infty}^{\infty} \mathrm{e}^{-\frac{x^2}{2l_{\mathrm{h}}^2}} \cos sx \, \mathrm{d}x = \sqrt{2\pi l_{\mathrm{h}}^2} \mathrm{e}^{-\frac{l_{\mathrm{h}}^2}{2}s^2}. \tag{4.175}$$

Solution

By taking into account whether the integrands are even or odd with respect to x, we can derive

$$\begin{aligned} I_1 &= \frac{1}{sr_{\mathrm{e}}} \int_{-\infty}^{\infty} \mathrm{e}^{-\beta_{\mathrm{h}}x^2} (\sin sr_{\mathrm{e}} \cos sx + \cos sr_{\mathrm{e}} \sin sx) \, \mathrm{d}x \\ &= \frac{\sin sr_{\mathrm{e}}}{sr_{\mathrm{e}}} \int_{-\infty}^{\infty} \mathrm{e}^{-\beta_{\mathrm{h}}x^2} \cos sx \, \mathrm{d}x. \end{aligned}$$

Similarly, we obtain

$$\begin{aligned} I_2 &= \frac{\cos sr_{\mathrm{e}}}{sr_{\mathrm{e}}^2} \int_{-\infty}^{\infty} \mathrm{e}^{-\beta_{\mathrm{h}}x^2} x \sin sx \, \mathrm{d}x \\ &= \frac{\cos sr_{\mathrm{e}}}{sr_{\mathrm{e}}^2} \left(\left[\frac{\mathrm{e}^{-\beta_{\mathrm{h}}x^2}}{-2\beta_{\mathrm{h}}} \sin sx \right]_{-\infty}^{\infty} + \int_{-\infty}^{\infty} \frac{\mathrm{e}^{-\beta_{\mathrm{h}}x^2}}{2\beta_{\mathrm{h}}} s \cos sx \, \mathrm{d}x \right) \\ &= \frac{l_{\mathrm{h}}^2}{r_{\mathrm{e}}^2} \cos sr_{\mathrm{e}} \int_{-\infty}^{\infty} \mathrm{e}^{-\beta_{\mathrm{h}}x^2} \cos sx \, \mathrm{d}x. \end{aligned}$$

When we apply Eq. (4.175) to I_1 and I_2, we can obtain Eqs. (4.170) and (4.171) by using $\beta_{\mathrm{h}} = \frac{1}{2l_{\mathrm{h}}^2}$. □

It is known that, due to the anharmonicity of vibrations, $\langle I_{\mathrm{mol}}(\theta)\rangle$ can be described using r_{a}, which will be introduced in Sect. 4.5.2, as

$$\left\langle I_{\mathrm{mol}}(\theta)\right\rangle = 2\left|f_1(\theta)\right| \cdot \left|f_2(\theta)\right| \mathrm{e}^{-\frac{l_{\mathrm{h}}^2}{2}s^2} \cos(\eta_1 - \eta_2) \frac{\sin s(r_{\mathrm{a}} - \kappa s^2)}{s r_{\mathrm{a}}}, \tag{4.176}$$

where κ is called the anharmonicity parameter and can be described using the parameter α in the Morse potential of Eq. (2.161) and the mean amplitude l_{h} as

$$\kappa = \frac{\alpha}{6} l_{\mathrm{h}}^4. \tag{4.177}$$

The value of α differs by the species of diatomic molecules, but usually ranges between 1.0 and 2.6 Å^{-1}, which renders the value of κ around 1×10^{-6} Å^3. As can be seen from Eq. (4.176), the effect of the anharmonicity remains small as long as s is not large.

4.5.2 The r_{a} Structure and the r_{g} Structure

We will now turn our attention to the physical meaning of the internuclear distance of a diatomic molecule obtained by the gas phase electron difraction method. When r represents the internuclear distance r_{12}, the internuclear distance r_{a} that is obtained from the observed molecular scattering intensity using Eq. (4.176) can be given as the inverse of

$$\left\langle \frac{1}{r} \right\rangle_T = \int_0^\infty \frac{P(r,T)}{r}\,\mathrm{d}r, \tag{4.178}$$

i.e., as

$$r_{\mathrm{a}} \equiv \left\langle \frac{1}{r} \right\rangle_T^{-1} = \left(\int_0^\infty \frac{P(r,T)}{r}\,\mathrm{d}r \right)^{-1}. \tag{4.179}$$

The molecular structure described by the structural parameter given by Eq. (4.179) is called the r_{a} structure. When Δr represents the small displacement from the equilibrium internuclear distance r_{e}, that is, when

$$r = r_{\mathrm{e}} + \Delta r, \tag{4.180}$$

the Taylor expansion of $\frac{1}{r}$ around r_{e} is

$$\frac{1}{r} = \frac{1}{r_{\mathrm{e}}\left(1 + \frac{\Delta r}{r_{\mathrm{e}}}\right)} \sim \frac{1}{r_{\mathrm{e}}} \left\{ 1 - \frac{\Delta r}{r_{\mathrm{e}}} + \left(\frac{\Delta r}{r_{\mathrm{e}}} \right)^2 \right\}, \tag{4.181}$$

and therefore we can derive

$$r_a \sim r_e \left\{ 1 - \frac{\langle \Delta r \rangle_T}{r_e} + \frac{\langle (\Delta r)^2 \rangle_T}{r_e^2} \right\}^{-1}$$

$$\sim r_e + \langle \Delta r \rangle_T - \frac{\langle (\Delta r)^2 \rangle_T}{r_e} \tag{4.182}$$

from the definition of r_a given in Eq. (4.179). Substituting Δr for x in the definition of the mean square amplitude given in Eq. (4.157), we obtain

$$r_a \sim r_e + \langle \Delta r \rangle_T - \frac{l_h^2}{r_e}. \tag{4.183}$$

From the above discussion, we can see how the effect of molecular vibration is included in the r_a structure obtained directly from observed data. However, what has a clearer physical meaning as the average of the internuclear distance is the average of r, defined as

$$r_g \equiv \langle r \rangle_T = \int_0^\infty P(r, T) r \, dr. \tag{4.184}$$

The molecular structure described by the structural parameter given by Eq. (4.184) is called the r_g structure.

As is immediately apparent, we can derive

$$r_g = \langle r_e + \Delta r \rangle_T = r_e + \langle \Delta r \rangle_T, \tag{4.185}$$

and thus we can use Eqs. (4.183) and (4.185) to obtain

$$r_g = r_a + \frac{l_h^2}{r_e} \sim r_a + \frac{l_h^2}{r_a}. \tag{4.186}$$

This equation allows us to transform a r_a structure obtained by an experiment into a r_g structure.

In the case of O_2 molecules, for example, we know that $r_a = 1.2118$ Å and $l_h = 0.0365$ Å at room temperature. We can apply these values to Eq. (4.186) and calculate the value of r_g as $r_g = 1.2129$ Å. As it is known that $r_e = 1.2074$ Å for O_2, we can also confirm that $r_g = 1.2129$ Å is obtained when this value of r_e is adopted in the calculation of the term l_h^2/r_e.

Problem 4.13

We notice that the centrifugal distortion effect, which increases the internuclear distance, is not taken into account in Eq. (4.185) for r_g or in Eq. (4.183) for r_a. For a diatomic molecule, describe this increase in the internuclear distance induced by the rotational effect, δr, using the absolute temperature T.

Solution

Letting the reduced mass of the diatomic molecule be μ, the internuclear distance stretched by the centrifugal distortion effect be $r_e + \delta r$, and the angular fre-

quency of the rotation be ω_{rot}, the kinetic energy of the rotation is represented as $\frac{1}{2}\mu(r_{\mathrm{e}}+\delta r)^2\omega_{\mathrm{rot}}^2$, and the rotational energy of the diatomic molecule at the thermal equilibrium is represented as $k_{\mathrm{B}}T$, where k_{B} is the Boltzmann constant. Therefore, we can write

$$k_{\mathrm{B}}T = \frac{1}{2}\mu(r_{\mathrm{e}}+\delta r)^2\omega_{\mathrm{rot}}^2. \tag{4.187}$$

In the meantime, if we define k as the force constant for the vibrational motion of the diatomic molecule, the restoring force is $-k\delta r$, where δr is the displacement of the internuclear distance. As the restoring force and the centrifugal force $\mu(r_{\mathrm{e}}+\delta r)\omega_{\mathrm{rot}}^2$ are balanced with each other, the sum of these two forces becomes zero. That is to say,

$$k\delta r = \mu(r_{\mathrm{e}}+\delta r)\omega_{\mathrm{rot}}^2. \tag{4.188}$$

From Eqs. (4.187) and (4.188), we can approximate

$$\begin{aligned} k_{\mathrm{B}}T &= \frac{1}{2}k\left\{\delta r\cdot r_{\mathrm{e}} + (\delta r)^2\right\} \\ &\sim \frac{1}{2}k\delta r\cdot r_{\mathrm{e}}, \end{aligned} \tag{4.189}$$

ignoring the term of $(\delta r)^2$ due to its smallness. Therefore, we can estimate δr as

$$\delta r = \frac{2k_{\mathrm{B}}T}{kr_{\mathrm{e}}}. \tag{4.190}$$

At room temperature, δr takes a value between 0.001 and 0.002 Å. We can derive the r_{g} in Eq. (4.185) in a form that includes δr as

$$r_{\mathrm{g}} = r_{\mathrm{e}} + \delta r + \langle\Delta r\rangle_T. \tag{4.191}$$

□

If molecular vibration had no anharmonicity, the relation $\langle\Delta r\rangle_T = 0$ would hold for Eq. (4.191). Thus, we would only have to use r_{g} and the correction term δr to obtain r_{e}. In reality, however, $\langle\Delta r\rangle_T$ becomes larger than δr due to the anharmonicity. As have learned in Chap. 2, the vibrational potential V of the diatomic molecule can be described as an expansion of the Morse potential given in Eq. (2.161), which gives us

$$V = \frac{1}{2}\mu\omega^2(\Delta r)^2 - \frac{1}{2}\alpha\mu\omega^2(\Delta r)^3 + \cdots. \tag{4.192}$$

In a stationary state, $\left\langle\frac{\partial V}{\partial(\Delta r)}\right\rangle_T$, the expectation value of the force acting on the system, $\frac{\partial V}{\partial(\Delta r)}$, becomes zero, as stated in Ehrenfest's theorem. By using the relation derived from this theorem, we can write

$$\langle\Delta r\rangle_T = \frac{3}{2}\alpha\left\langle(\Delta r)^2\right\rangle_T. \tag{4.193}$$

As $\langle(\Delta r)^2\rangle_T = l_h^2$, we can rewrite Eq. (4.191) as

$$r_g = r_e + \delta r + \frac{3}{2}\alpha l_h^2. \tag{4.194}$$

What this equation shows is that, when r_a and l_h^2 are obtained by a gas phase electron diffraction experiment, we can evaluate r_g by applying Eq. (4.186), and then obtain the equilibrium internuclear distance r_e by estimating δr using the force constant. In doing so, of course, as the force constant k is given by $k = \mu\omega^2$, all we need is the frequency of the molecular vibration.

Problem 4.14
Calculate the r_e of an O_2 molecule using Eq. (4.194), letting the Morse parameter be $\alpha = 2.476$ Å^{-1}, the force constant $k = 1.18 \times 10^3$ N m^{-1}, and the Boltzmann constant $k_B = 1.3806503 \times 10^{-23}$ J K^{-1}.

Solution
When we use $r_a = 1.2118$ Å as a good estimate of r_e in Eq. (4.190) and assume that $T = 300$ K, we obtain $\delta r = 0.00058$ Å. By using $l_h = 0.0365$ Å, we can derive $\langle\Delta r\rangle_T = 0.00495$ Å. As $r_g = 1.2129$ Å, we obtain $r_e = 1.2074$ Å. □

4.6 Electron Beam Scattering by Polyatomic Molecules

4.6.1 Molecular Scattering Curves and Radial Distribution Curves

From the discussions so far, it has been made clear that we can calculate the intensity of a diffracted wave caused by a molecule consisting of n atoms as

$$I \propto \sum_i^n \left|f_i(\theta)\right|^2 + \sum_{i\neq j}^n \sum^n \left\{\left|f_i(\theta)\right|\left|f_j(\theta)\right|\cos(\eta_i - \eta_j)\int_0^\infty P_{ij}(r_{ij})\frac{\sin sr_{ij}}{sr_{ij}}\,\mathrm{d}r_{ij}\right\}, \tag{4.195}$$

where

$$f_i(\theta) \propto \frac{Z_i - A_i(\theta)}{s^2}. \tag{4.196}$$

Describing I as a sum of two parts, the molecular scattering intensity I_{mol} and the rest which gives the background, so that

$$I = I_{mol} + I_B, \tag{4.197}$$

we can express I_B as the sum of the square of the absolute value of the scattering amplitude $f_i(\theta)$ caused by the atoms within a molecule, that is,

$$I_B = \sum_i^n \left|f_i(\theta)\right|^2. \tag{4.198}$$

When we define the ratio of I_{mol} to I_B as

$$M(s) = \frac{I_{\mathrm{mol}}}{I_B} = \frac{\sum_{i\neq j}^{n}\sum^{n} |f_i(\theta)||f_j(\theta)| \cos(\eta_i - \eta_j) \int_0^\infty P_{ij}(r_{ij}) \frac{\sin sr_{ij}}{sr_{ij}} \mathrm{d}r_{ij}}{\sum_{k}^{n} |f_k(\theta)|^2}, \quad (4.199)$$

$M(s)$ is represented as

$$M(s) = \sum_{i\neq j}^{n}\sum^{n} \frac{(Z_i - A_i(\theta))(Z_j - A_j(\theta))}{\sum_{k}^{n}(Z_k - A_k(\theta))^2} \cos(\eta_i - \eta_j) \int_0^\infty P_{ij}(r_{ij}) \frac{\sin sr_{ij}}{sr_{ij}} \mathrm{d}r_{ij}. \quad (4.200)$$

As $A_i(\theta)$ and $A_j(\theta)$ are small enough in comparison with Z_i and Z_j, and as we can regard the term of $\cos(\eta_i - \eta_j)$ as being close to 1, we can approximate $M(s)$, if r_{ij} is represented as $r_{ij} = r'$, as

$$M(s) = K \sum_{i\neq j}^{n}\sum^{n} Z_i Z_j \int_0^\infty P_{ij}(r') \frac{\sin sr'}{sr'} \mathrm{d}r', \quad (4.201)$$

where K is a proportionality constant which does not depend on s and $P_{ij}(r')$ stands for the distribution of the distance r' originating from the vibrational motion of the molecule. When we multiply this $M(s)$ by s, and Fourier transform it with $\sin sr$, the function $D(r)$ of r is calculated as

$$\begin{aligned} D(r) &= \int_0^\infty sM(s) \sin sr \, \mathrm{d}s \\ &= K \sum_{i\neq j}^{n}\sum^{n} Z_i Z_j \int_0^\infty \int_0^\infty \frac{P_{ij}(r')}{r'} \sin sr' \sin sr \, \mathrm{d}r' \, \mathrm{d}s. \end{aligned} \quad (4.202)$$

The Fourier sine transform of a given function $f(r)$ is generally describable as

$$g(s) = \int_0^\infty f(r') \sin sr' \, \mathrm{d}r', \quad (4.203)$$

and the Fourier inverse transformation of this function as

$$f(r) = \frac{2}{\pi} \int_0^\infty g(s) \sin sr \, \mathrm{d}s, \quad (4.204)$$

so that we can substitute Eq. (4.203) into Eq. (4.204) to obtain

$$f(r) = \frac{2}{\pi} \int_0^\infty \int_0^\infty f(r') \sin sr' \sin sr \, \mathrm{d}r' \, \mathrm{d}s. \quad (4.205)$$

When we define $f(r')$ as

$$f(r') = \frac{P_{ij}(r')}{r'} \quad (4.206)$$

and apply Eq. (4.205) to Eq. (4.202), we can derive

$$D(r) = \frac{\pi}{2} K \sum_{i \neq j}^{n} \sum^{n} P_{ij}(r) \frac{Z_i Z_j}{r}. \tag{4.207}$$

This $D(r)$ is called the radial distribution curve or the radial distribution function. Equations (4.207) and (4.202) tell us that we can calculate the radial distribution curve $D(r)$ by the Fourier transform of $sM(s)$, which expresses the contribution of the molecular scattering. We can obtain $sM(s)$, in turn, from Eq. (4.202) by using the relationship between Eqs. (4.203) and (4.204), as

$$sM(s) = \frac{2}{\pi} \int_0^\infty D\left(r'\right) \sin sr' \, \mathrm{d}r'. \tag{4.208}$$

This function, $sM(s)$, is called the molecular scattering curve. Equation (4.208) signifies that we can obtain $sM(s)$ as the Fourier inverse transformation of $D(r')$.

The radial distribution curve given by Eq. (4.207) is useful for us to gain an intuitive understanding of the contribution of an atom pair to diffraction intensity that is caused by molecular scattering: a peak appearing at the distance of r in the radial distribution curve show us that there are two atoms located at a specific internuclear distance r, and the height of this peak is proportional to the product of the nuclear charges of the two atoms in question, while being inversely proportional to the internuclear distance. Also, the width of the peak represents the mean amplitude.

In an actual analysis, we represent the molecular scattering intensity observed in the form of a molecular scattering curve $sM(s)$. We then calculate $M(s)$, expressed as Eq. (4.200), by using structural parameters such as the internuclear distance and the bond angle, and multiply it by s to yield $sM(s)$, which in turn is fitted to the observed $sM(s)$ by the least-squares method by using the structural parameters as variables.

In calculating $sM(s)$, the effect of molecular vibration also needs to be taken into consideration. In the case of a polyatomic molecule, as will be discussed in Sect. 4.6.3, molecular vibration is described as the superposition of all vibrations along the normal coordinate. Therefore, to know how large the probability distribution is for the internuclear distance of bonded and non-bonded atomic pairs, that is, to find out the degree of the mean amplitude, we have to calculate the normal mode vibration through a vibrational analysis such as the GF matrix method discussed in Sect. 2.5, and then add up the contributions of all vibrational modes affecting the probability distribution of the internuclear distance.

As an example, the molecular scattering curve $sM(s)$ for CO_2 and the radial distribution curve $D(r)$ obtained through a Fourier transform of this $sM(s)$ are shown in Fig. 4.14. In the radial distribution curve, we can see two peaks at around 1.2 Å and 2.3 Å, which respectively represent r(C=O), the internuclear distance for C=O, and $r(\mathrm{O}\cdots\mathrm{O})$, the internuclear distance for O···O. The dotted line "···" is used here to represent a non-bonded atom pair.

As Eq. (4.207) shows, we can think of the peak intensities in a radial distribution curve as being roughly proportional to $\frac{Z_i Z_j}{r}$. As $2r(\mathrm{C{=}O) \sim } r(\mathrm{O}\cdots\mathrm{O})$, the

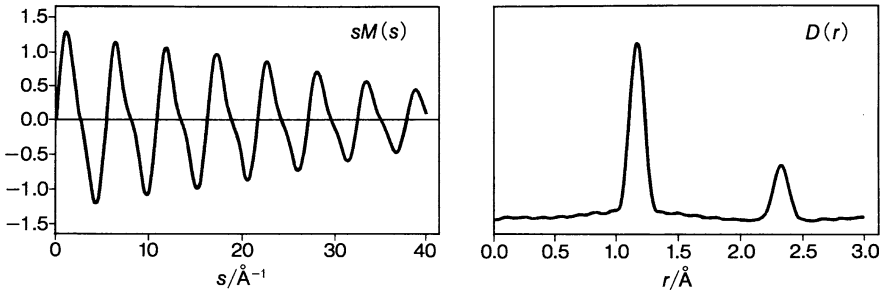

Fig. 4.14 The molecular scattering curve $sM(s)$ and the radial distribution curve $D(r)$ for CO_2

ratio of $I(\mathrm{C{=}O})$, the peak intensity at $r(\mathrm{C{=}O})$, to $I(\mathrm{O}\cdots\mathrm{O})$, the peak intensity at $r(\mathrm{O}\cdots\mathrm{O})$, becomes

$$I(\mathrm{C{=}O}) : I(\mathrm{O}\cdots\mathrm{O}) \sim 2 \cdot \frac{6 \cdot 8}{r(\mathrm{C{=}O})} : \frac{8 \cdot 8}{2r(\mathrm{C{=}O})}$$
$$= 3 : 1,$$

taking into account that there are two C=O bonds in the molecule. Indeed, this result is nearly equal to the ratio of the two peak intensities found in the radial distribution function in Fig. 4.14. What this radial distribution curve teaches us, then, is that there are two overlapping interference patterns constituting the molecular scattering curve, which are caused by atom pairs with different internuclear distances, and that the contribution of the interference pattern with the shorter internuclear distance is about three times as large as the contribution of that with the longer internuclear distance.

4.6.2 From a Molecular Scattering Curve to the Molecular Structure

Figure 4.15 shows the molecular scattering curve of CO_2 obtained from the electron diffraction image observed at room temperature. Let us now determine the molecular geometrical structure of CO_2 through a simple analysis.

First, we can determine s_0, the value of s for the zeros, where the molecular scattering curve intersects the horizontal axis in the figure, as listed in Table 4.2. This table shows us that all intervals between neighboring zeros are roughly equal, falling somewhere around 2.8 Å^{-1}. When we assume that the same cycle holds for smaller s values, the zero where $s = 8.03\ \text{Å}^{-1}$ can be counted as the third zero from the inside. Note here that regions of small-angle scattering, where s is even smaller, is blocked in order to prevent the electron beam traveling straight from hitting a detection instrument such as the photographic plate directly. This is why there is no data of the molecular scattering curve obtained for the small s region.

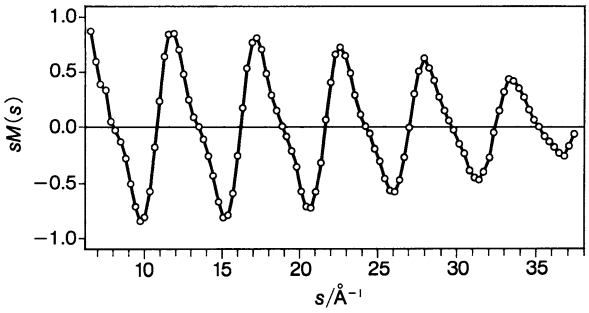

Fig. 4.15 The experimental molecular scattering curve of CO_2

Table 4.2 The position of the zeros s_0 in the molecular scattering curve and the internuclear distance r of CO_2

n	$s_0/\text{Å}^{-1}$	$r/\text{Å}$	n	$s_0/\text{Å}^{-1}$	$r/\text{Å}$
3	8.03	1.1737	9	24.20	1.1684
4	10.83	1.1603	10	27.04	1.1618
5	13.50	1.1636	11	29.72	1.1628
6	16.20	1.1636	12	32.45	1.1618
7	18.85	1.1666	13	35.17	1.1612
8	21.62	1.1625			

The zeros appearing at a regular interval of 2.8 Å^{-1} suggests that these zeros are ascribable to an interference pattern caused by a pair of atoms with a specific internuclear distance. Thus we will consider such an s value in the formula of the molecular scattering curve, Eq. (4.208), as to yield $\sin sr = 0$ as a zero. Then, $s_0 r = n\pi$ $(n = 1, 2, 3, \ldots)$, and therefore, from the value of the n-th zero, we can obtain

$$r = \frac{n}{s_0}\pi.$$

The r values calculated by this equation are also listed in Table 4.2. The r value is distributed around the region of 1.16 to 1.17 Å, and its average can be obtained as $r = 1.164$ Å. This figure corresponds well to the distance of the C=O bond in an CO_2 molecule at $T = 300$ K already calculated as $r_a(\text{C=O}) = 1.1640$ Å.

In the case of CO_2, interference caused by the non-bonded atom pair O···O has to be observed as well, as we learned in Fig. 4.14, which begs the question: Why do we not see the contribution from this atom pair in the molecular scattering curve? This puzzle can be solved when we look at Fig. 4.16, which charts the contributions of the two C=O pairs and of the one O···O pair in the molecular scattering curve of CO_2 calculated separately. As this figure shows, the positions of the zeros arising from C=O pairs correspond to the positions of the zeros arising from O···O. This is because, as $2r(\text{C=O}) \sim r(\text{O}\cdots\text{O})$ holds, the period of the sinusoidal molecular scattering curve caused by O···O is almost an exact half of the period of that caused by C=O.

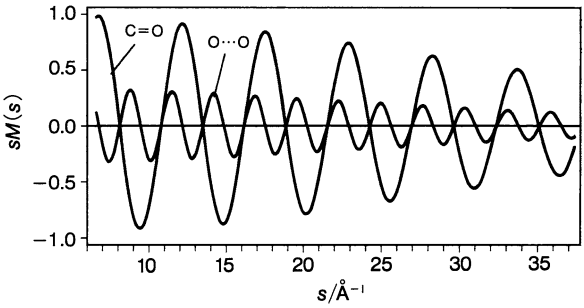

Fig. 4.16 Contributions of the C=O and O···O atom pairs constituting the molecular scattering curve of CO_2

Next, let us take CS_2 as an example to examine how the phase shift (see Sect. 4.4) and the effect of molecular vibration (see Sect. 4.5) are reflected in the molecular scattering curve.

Figure 4.17(a) shows the molecular scattering curve $sM(s)$ as calculated without taking either the phase shift or the molecular vibration into consideration. Next, when we include the phase shift $\cos(\eta_i - \eta_j)$, the shape of $sM(s)$ changes into Fig. 4.17(b). We can see here that, as discussed in Sect. 4.4, the phase shift decreases the amplitude of $sM(s)$ as the value of s increases. Figure 4.17(c), on the other hand, shows the case where phase shift is ignored, but the effect of molecular vibration is not, so that the terms of $e^{-\frac{l_h^2}{2}s^2}$ corresponding to the atom pairs C=S and S···S are included. This figure shows that the effect of molecular vibration decreases the amplitude of $sM(s)$ more rapidly than does the phase shift. Lastly, Fig. 4.17(d) shows the curve of $sM(s)$ which takes into account both the phase shift and the molecular vibration.

This last model of $sM(s)$ reproduces the observed curve of $sM(s)$. In the gas electron diffraction method, we determine molecular structures by taking account of both the effect of the phase shift and that of molecular vibration, then calculating $sM(s)$ with the internuclear distance and the bond angle regarded as structural parameters, and finally fitting the result to the observed $sM(s)$ by the least-squares method.

4.6.3 The Shrinkage Effect

In electron diffraction experiments, we can obtain the average values for the internuclear distance, as discussed in Sect. 4.5.2. The internuclear distances between bonded and non-bonded atom pairs obtained for linear triatomic molecules CO_2 and CS_2 at room temperature are represented as r_g structures in Table 4.3. This table shows that $r_g(O\cdots O)$ is less than twice the distance of $r_g(C{=}O)$, and that, similarly, $r_g(S\cdots S)$ is less than twice the distance of $r_g(C{=}S)$. The degree of shrinkage, that is,

$$\delta_g(CO_2) \equiv 2r_g(C{=}O) - r_g(O\cdots O) \tag{4.209}$$

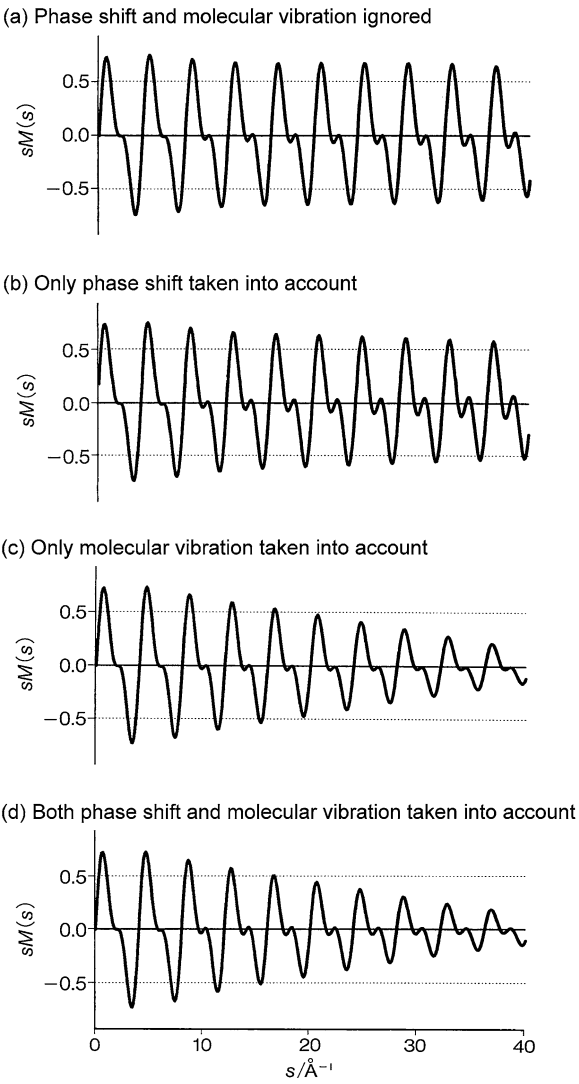

Fig. 4.17 The molecular scattering curve of CS_2

and

$$\delta_g(CS_2) \equiv 2r_g(C{=}S) - r_g(S\cdots S), \tag{4.210}$$

are both significantly larger than 0, considering that the precision of the structural parameters is somewhere around ± 0.001 Å. This shrinkage effect has first been explained by Morino and by Bastiansen's group, which is why it is also called the Morino-Bastiansen shrinkage effect. To understand this effect, we need to consider the fact that atom pairs within a molecule vibrate not only along the direction of its connection but also in a direction perpendicular to this stretching vibration, which gives the bending vibration.

Table 4.3 Shrinkage effects for CO_2 and CS_2 (unit: Å)

CO_2		CS_2	
$r_g(C{=}O)$	1.1642	$r_g(C{=}S)$	1.5592
$r_g(O\cdots O)$	2.3244	$r_g(S\cdots S)$	3.1126
$\delta_g(CO_2)$	0.0040	$\delta_g(CS_2)$	0.0058

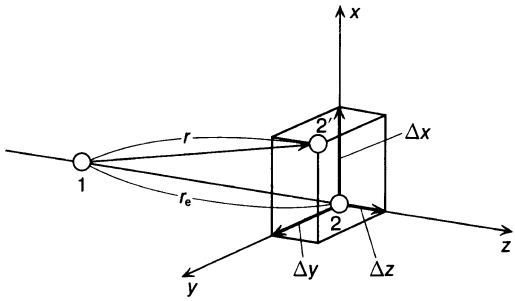

Fig. 4.18 The relative displacement of atom 2 with respect to atom 1 in a polyatomic molecule

Let us then derive the representation of the r_g structure in the case of a polyatomic molecule. The relative displacement of two atoms in a polyatomic molecule caused by molecular vibration is illustrated as Fig. 4.18. Letting the z axis run through the equilibrium position of atoms 1 and 2, and assuming that these two atoms are not necessarily connected by a direct chemical bond, we can represent the average of the internuclear distance r, r_g, by considering just the relative displacement of atom 2, whereby it moves to the position of $2'$, as

$$\begin{aligned} r_g &= \int_0^\infty P(r,T) r \, \mathrm{d}r \\ &= \left\langle \left\{ (\Delta x)^2 + (\Delta y)^2 + (r_e + \Delta z)^2 \right\}^{\frac{1}{2}} \right\rangle_T . \end{aligned} \tag{4.211}$$

As $(\Delta x)^2 + (\Delta y)^2 \ll (r_e + \Delta z)^2$, we can transform the above equation into

$$\begin{aligned} \left\{ (\Delta x)^2 + (\Delta y)^2 + (r_e + \Delta z)^2 \right\}^{\frac{1}{2}} &= (r_e + \Delta z) \left\{ 1 + \frac{(\Delta x)^2 + (\Delta y)^2}{(r_e + \Delta z)^2} \right\}^{\frac{1}{2}} \\ &\sim (r_e + \Delta z) \left\{ 1 + \frac{(\Delta x)^2 + (\Delta y)^2}{2(r_e + \Delta z)^2} \right\} \\ &\sim r_e + \Delta z + \frac{(\Delta x)^2 + (\Delta y)^2}{2 r_e}, \end{aligned} \tag{4.212}$$

and thus we can obtain

$$r_g = r_e + \langle \Delta z \rangle_T + \frac{\langle (\Delta x)^2 \rangle_T + \langle (\Delta y)^2 \rangle_T}{2 r_e} . \tag{4.213}$$

To add more precision, we can add δr, the stretch in the internuclear distance caused by the centrifugal force accompanying molecular rotation, into this equation, and express r_g as

$$r_g = r_e + \delta r + \langle \Delta z \rangle_T + \frac{\langle (\Delta x)^2 \rangle_T + \langle (\Delta y)^2 \rangle_T}{2r_e}. \tag{4.214}$$

Letting the part of this equation representing the vertical displacement be substituted by

$$K = \frac{\langle (\Delta x)^2 \rangle_T + \langle (\Delta y)^2 \rangle_T}{2r_e}, \tag{4.215}$$

we can write the $\delta_g(CO_2)$ in Eq. (4.209) as

$$\delta_g(CO_2) = 2K(C{=}O) - K(O \cdots O) \tag{4.216}$$

by using the fact that the terms of r_e, δr, and $\langle \Delta z \rangle_T$ on the right-hand side cancel each other out due to their additivity. This shows us that the shrinkage effect is only an apparent effect, which arises because the distance between C=O becomes seemingly longer due to the vertical displacement.

In the case of polyatomic molecules, we can obtain $\{Q_i\}$, a set of the normal coordinates represented by a linear combination of internal coordinates of displacement, by analyzing the normal mode of vibration as described in Sect. 2.5. This, then, also means that we can express an internal coordinate of displacement using $\{Q_i\}$. Thus we can express not only the coordinate of displacement along the z axis, which connects the intramolecular atom pair, but also that along a direction perpendicular to the z axis, by linear combinations of $\{Q_i\}$. Expanding Δz by $\{Q_i\}$, we can write

$$\Delta z = \sum_i L_i^z Q_i. \tag{4.217}$$

When we represent the vibrational quantum number of the i-th normal mode of vibration, Q_i, as v_i,

$$\begin{aligned} \langle Q_i Q_j \rangle_T &= \sum_{v_i} \sum_{v_j} w_{v_i v_j} \langle v_i v_j | Q_i Q_j | v_i v_j \rangle \\ &= \sum_{v_i} \sum_{v_j} w_{v_i v_j} \langle v_i | Q_i | v_i \rangle \langle v_j | Q_j | v_j \rangle \\ &= 0, \end{aligned} \tag{4.218}$$

$$\left\langle Q_i^2 \right\rangle_T = \sum_{v_i} w_{v_i} \langle v_i | Q_i^2 | v_i \rangle \neq 0, \tag{4.219}$$

where $i \neq j$ and the weight factors $w_{v_i v_j}$ and w_{v_i} follow the Boltzmann distribution. We can use Eq. (4.217) to calculate the $\langle (\Delta z)^2 \rangle_T$ corresponding to the average

square amplitude l_{h}^2 of the atom pair as

$$\begin{aligned}\langle(\Delta z)^2\rangle_T &= \left\langle\left(\sum_i L_i^z Q_i\right)\left(\sum_j L_j^z Q_j\right)\right\rangle_T \\ &= \sum_i \sum_j L_i^z L_j^z \langle Q_i Q_j\rangle_T \\ &= \sum_i \left(L_i^z\right)^2 \langle Q_i^2\rangle_T . \end{aligned} \tag{4.220}$$

Taking Eq. (2.269) from Sect. 2.5.5 into account, $\langle Q_i^2\rangle_T$ can be expressed in a similar manner as the average square amplitude of one-dimensional vibration given by Eq. (4.162) as

$$\langle Q_i^2\rangle_T = \frac{h}{8\pi^2 c\tilde{\nu}_i} \coth\left(\frac{\hbar\omega_i}{2kT}\right), \tag{4.221}$$

and therefore, when the form of Eq. (4.217) is given we can immediately calculate $\langle(\Delta z)^2\rangle_T$ by use of Eq. (4.220).

We can also expand Δx and Δy with the normal coordinate by using formulas corresponding to Eq. (4.217), and similarly calculate $\langle(\Delta x)^2\rangle_T$ and $\langle(\Delta y)^2\rangle_T$. Therefore, the contribution of the vertical displacement, K, can be evaluated by use of Eq. (4.215).

4.6.4 The r_α^0 Structure

As we learned in Chap. 4, we can determine the rotational constant of molecules by analyzing the rotational structure in the rotational spectrum or in the vibrational spectrum, and use this rotational constant to determine the molecular structure. The molecular structures obtained in this way are structures of molecules at their vibrational ground state (r_0 structures) or at their vibrationally excited state; these are different from the average structure (r_{g} structure) of an atom pair whose internuclear distance is at its thermal equilibrium, which can be obtained through the gas electron diffraction method.

We can imagine that by using both the high-precision rotational constant obtained through spectroscopy and the internuclear distance obtained directly by the electron diffraction method at the same time, we can determine the structure of a polyatomic molecule in more detail. To this end, we must first make the physical meanings of the molecular structures obtained by these two different methods the same. Only then can we consider the rotational constant and the molecular scattering curve as belonging in the same ballpark, and analyze them in conjunction with each other.

First of all, let us introduce the r_α structure defined as the distance between the average nuclear positions of two atoms in a polyatomic molecule at their thermal

equilibrium states. Again, by referring to Fig. 4.18 we can write

$$r_\alpha = \left\{ \langle \Delta x \rangle_T^2 + \langle \Delta y \rangle_T^2 + \left(r_\mathrm{e} + \langle \Delta z \rangle_T \right)^2 \right\}^{\frac{1}{2}} \tag{4.222}$$

by definition, and this gives us

$$r_\alpha \sim r_\mathrm{e} + \langle \Delta z \rangle_T + \frac{\langle \Delta x \rangle_T^2 + \langle \Delta y \rangle_T^2}{2 r_\mathrm{e}} \tag{4.223}$$

when treated in a similar manner as in Eq. (4.212). Here, we notice that $\langle \Delta x \rangle_T^2$ and $\langle \Delta y \rangle_T^2$ are both extremely small, in the order of 10^{-4} Å^2. Therefore, we can approximate this as

$$r_\alpha \sim r_\mathrm{e} + \langle \Delta z \rangle_T . \tag{4.224}$$

What this signifies is that the difference between an equilibrium internuclear distance and the distance between the average positions of the two nuclei is determined by the anharmonicity of the vibration in the direction of the line connecting the two atoms in question, and that we can neglect the contribution of the vibration in a direction perpendicular to this line. Thus, in the r_α structure, the shrinkage effect does not appear, and the additivity of internuclear distances holds. The average of the Δz in Eq. (4.224) is that at the thermal equilibrium state, but when we use the average of Δz at the vibrational ground state $\langle \Delta z \rangle_0$, we can obtain

$$r_\alpha^0 \sim r_\mathrm{e} + \langle \Delta z \rangle_0 , \tag{4.225}$$

which is called the r_α^0 structure. Also, when we describe the average of Δz at the vibrationally excited state as $\langle \Delta z \rangle_v$, we can obtain

$$r_v \sim r_\mathrm{e} + \langle \Delta z \rangle_v . \tag{4.226}$$

The parameters r_α^0 and r_v introduced here correspond to the structural parameters obtained by molecular spectroscopy. Let us then first show how r_α and r_g correspond to each other. From Eqs. (4.214) and (4.224), we can write

$$r_\alpha = r_\mathrm{g} - \frac{\langle (\Delta x)^2 \rangle_T + \langle (\Delta y)^2 \rangle_T}{2 r_\mathrm{e}} - \delta r , \tag{4.227}$$

which allows us to obtain the r_α structure from the r_g structure by using Eq. (4.227).

The parameter r_α^0 in Eq. (4.225) is defined as the limit value of r_α at $T \to 0$ K, that is,

$$r_\alpha^0 = \lim_{T \to 0\ \mathrm{K}} r_\alpha ,$$

and is also expressed as

$$r_\alpha^0 = r_\alpha - \left(\langle \Delta z \rangle_T - \langle \Delta z \rangle_0 \right), \tag{4.228}$$

from Eqs. (4.224) and (4.225). Therefore, to transform r_α to r_α^0, we have only to calculate $\langle \Delta z \rangle_T$ and $\langle \Delta z \rangle_0$ on the basis of the mean amplitude and the anharmonicity obtained by analyzing the normal modes of vibration and then substitute them into Eq. (4.228). When the two atoms are bonded, its anharmonicity can be described by the Morse parameter α as

$$r_\alpha^0 = r_\alpha - \frac{3}{2}\alpha\left(\left\langle (\Delta z)^2 \right\rangle_T - \left\langle (\Delta z)^2 \right\rangle_0\right), \tag{4.229}$$

from Eq. (4.193). As does the r_α structure, the r_α^0 structure has the additivity of the internuclear distance.

As the r_α^0 structure obtained here has the same physical meaning as the r_z structure obtained by spectroscopy, when we transform the structural parameter obtained by the electron diffraction method into an r_α^0 structure, the rotational constants calculated by using these structural parameters are equal to the rotational constants of the r_z structure, A_z, B_z, and C_z.

Let us then take the example of a diatomic molecule and represent the rotational constant B_z for its r_z structure using the rotational constant for its vibrational ground state, B_0. As shown in Eq. (3.287) from Sect. 3.6, the rotational constant B_0 can be represented as

$$\begin{aligned} B_0 &= \frac{h}{8\pi^2\mu}\left\langle 0\left|\frac{1}{r^2}\right|0\right\rangle \\ &= \frac{h}{8\pi^2\mu}\left\langle \frac{1}{r^2}\right\rangle_0 . \end{aligned} \tag{4.230}$$

When we let $r = r_e + \Delta r$ and expand $\frac{1}{r^2}$ by a Taylor expansion in terms of $\frac{\Delta r}{r_e}$, it becomes

$$\frac{1}{r^2} = \frac{1}{r_e^2}\left\{1 - 2\frac{\Delta r}{r_e} + 3\left(\frac{\Delta r}{r_e}\right)^2 - \cdots\right\}, \tag{4.231}$$

so by using the rotational constant for the equilibrium structure

$$B_e = \frac{h}{8\pi^2\mu r_e^2}, \tag{4.232}$$

we can write Eq. (4.230) as

$$B_0 = B_e\left\{1 - \frac{2\langle \Delta r\rangle_0}{r_e} + \frac{3\langle (\Delta r)^2\rangle_0}{r_e^2} - \cdots\right\}. \tag{4.233}$$

What we obtain when we stop this expansion at the second term is the rotational constant B_z, which corresponds to the r_z structure. That is, B_z can be represented as

$$B_z = \frac{h}{8\pi^2\mu r_z^2} = B_e\left(1 - \frac{2\langle \Delta r\rangle_0}{r_e}\right). \tag{4.234}$$

Problem 4.15
Using Eqs. (4.233) and (4.234), express the rotational constant B_z with B_0, B_e, and the vibrational frequency ν for the diatomic molecule treated as a harmonic oscillator.

Solution
From Eqs. (4.233) and (4.234), B_0 is represented as

$$B_0 \sim B_z + 3B_e \frac{\langle (\Delta r)^2 \rangle_0}{r_e^2}. \tag{4.235}$$

From Eq. (4.149), we can write

$$\left\langle (\Delta r)^2 \right\rangle_0 = \frac{1}{2\beta} = \frac{\hbar}{2\mu\omega}. \tag{4.236}$$

Substituting Eq. (4.236) into Eq. (4.235) and using $\omega = 2\pi\nu$, we can write

$$B_z = B_0 - \frac{3B_e^2}{\nu}. \tag{4.237}$$

Approximating $B_e \sim 1\ \mathrm{cm}^{-1}$ and $\nu \sim 1000\ \mathrm{cm}^{-1}$, we can estimate the rough value of $3B_e^2/\nu$ as $0.003\ \mathrm{cm}^{-1}$. □

As can be seen from the above problem, the anharmonicity of the potential does not affect the correction of B_0 to B_z in the case of diatomic molecules. The same can be said of polyatomic molecules. As we have learned with the example of SO_2 in Sect. 3.5, the rotational constant of a polyatomic molecule at the vibrational level $\boldsymbol{v} = (v_1, v_2, \ldots)$ is represented as

$$B_{\boldsymbol{v}} = B_e - \sum_i \alpha_i^B \left(v_i + \frac{g_i}{2} \right), \tag{4.238}$$

using the vibration-rotation constant α_i^B. The same type of formula holds for rotational constants $A_{\boldsymbol{v}}$ and $C_{\boldsymbol{v}}$. In Eq. (4.238), g_i stands for the degree of degeneracy for the i-th normal mode of vibration. Although we do not have enough space to go into detail in this book, let us note here that α_i^B is represented as the sum of the term that does not relate to the third-order anharmonic term, α_i^B (harmonic), and the term that does, α_i^B (anh). Therefore,

$$B_{\boldsymbol{v}} = B_e - \sum_i \alpha_i^B (\text{harmonic}) \left(v_i + \frac{g_i}{2} \right) - \sum_i \alpha_i^B (\text{anh}) \left(v_i + \frac{g_i}{2} \right) \tag{4.239}$$

holds. For the vibrational ground state, where $\boldsymbol{v} = (0, 0, \ldots)$, the rotational constant B_z corresponding to the r_α^0 structure is obtained by using just the harmonic part of the vibration-rotation constant and correcting it, as

$$B_z = B_0 + \frac{1}{2} \sum_i g_i \alpha_i^B (\text{harmonic}). \tag{4.240}$$

Table 4.4 Different structural parameters and their definitions

r_e	Equilibrium internuclear distance
r_α^0, r_z	Distance between the averaged nuclear positions in a vibrational ground state
r_α	Distance between the averaged nuclear positions at the thermal equilibrium
r_g	Averaged internuclear distance at the thermal equilibrium
r_a	Averaged internuclear distance defined by Eq. (4.179) at the thermal equilibrium
r_0	Effective distance between the nuclear positions obtained from rotational constants in the vibrational ground state
r_s	Effective distance between the nuclear positions obtained from the differences in the rotational constants of different isotopomers

From Eqs. (4.239) and (4.240), we can see that B_z is represented with B_e as

$$B_z = B_e - \frac{1}{2}\sum_i g_i \alpha_i^B (\text{anh}). \tag{4.241}$$

When we use the rotational constant to determine the molecular structure by the electron diffraction method, we treat the A_z, B_z, and C_z obtained as above as experimental values, along with the molecular scattering curve $sM(s)$ obtained by the electron diffraction method, and determine by the least-squares method the structural parameters, expressed as an r_α^0 structure, that reproduces both of them.

In Chap. 3, we have introduced the r_e structure, the r_0 structure (Sect. 3.5.3), and the r_s structure (Sect. 3.1.3). Now in Sects. 4.5 and 4.6, we have dealt with structural parameters that have different physical meanings, which are structures obtained by the electron diffraction method, expressed as r_a, r_g, r_α, and r_α^0 ($\sim r_z$). The physical meanings of these structural parameters are summarized in Table 4.4.

Needless to say, the clearest expression of a molecular structure is the structure at the equilibrium position, that is, the r_e structure. However, the r_e structure has only been obtained for molecules with particularly simple geometrical structures, such as diatomic molecules and triatomic molecules. When we obtain a molecular structure by the electron diffraction method, the r_g structure has a clear physical meaning with regards to the bonded atom pair, but it does not represent the bond angle at the thermal equilibrium state because there is a contribution of the vibration in the perpendicular direction. Therefore, a method usually adopted to express the structure at the thermal equilibrium state is to use the r_g structure to express the internuclear distance and the r_α structure to express the bond angle. As expressed by Eq. (4.225), the internuclear distance in the r_α^0 structure has the meaning of a projection of the average internuclear distance at the zero-point vibrational state to the direction connecting the equilibrium nuclear positions, and the bond angle in the r_α^0 structure also has the meaning of the average of the bond angle at the zero-point vibrational state. Another point of advantage of the r_α^0 structure is that this corresponds clearly to the rotational constant obtained by spectroscopy.

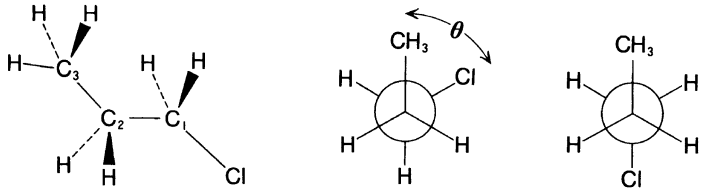

Fig. 4.19 The 1-chloropropane molecule and its two rotational isomers

The discussions above allow us to realize that molecular vibration plays an important role in describing the geometrical structure of molecules. While data obtained by molecular spectroscopy and those obtained by the electron diffraction method both give us information on molecular structures, the effect of molecular vibration is incorporated in different ways in these two methods. Therefore, after fully grasping the physical meaning of the respective structural parameters, we can better understand the meaning of molecular structures.

4.6.5 An Example of Structure Determination

Let us conclude by looking at an actual example of structure determination for the 1-chloropropane ($CH_3CH_2CH_2Cl$) molecule, shown in Fig. 4.19. In 1-chloropropane, an internal rotation around the C_1–C_2 bond axis is possible, and therefore two rotational isomers exist, called the gauche form and the anti form (Figs. 4.19(b) and (c)). These two isomers are known to coexist in the gas phase at room temperature.

As can be seen from Eq. (4.201), the contribution of an atom pair to the molecular scattering curve becomes larger the larger the product of the nuclear charges of the two atoms, $Z_i Z_j$, becomes, and the smaller the distance between these atoms becomes. In the case of 1-chloropropane, we can expect the contributions of the bonded atom pairs, C–Cl, C–C, and C–H, those of the atom pairs separated by one atom, C$\cdots$Cl and C$\cdots$C, and that of the two atoms at the ends of the molecule, C$\cdots$Cl, to be the ones to mainly show up in the molecular scattering curve.

Figure 4.20 shows the molecular scattering curve $sM(s)$ obtained by an experiment using an electron beam whose accelerating voltage is 40 kV. When this is transformed through the Fourier transform, we obtain the radial distribution curve $D(r)$, shown in Fig. 4.21.

As can be clearly seen in Fig. 4.21, each atom pair emerges as a peak in the radial distribution function. There are two peaks attributed to $C_3\cdots Cl$. This is because the molecular structures of the gauche form and the anti form are largely different, that is, the distance between $C_3\cdots Cl$ is about 3.15 Å in the gauche form while being about 4.1 Å in the anti form.

By taking the structural parameters describing the molecular structure as variables and analyzing $sM(s)$ through the least-squares method, not only can we determine the geometrical structure of the molecule, as has already been noted, but in the

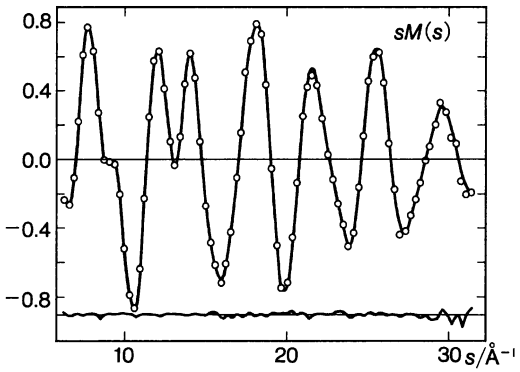

Fig. 4.20 The $sM(s)$ of 1-chloropropane. The values of the residual (observed value – calculated value) obtained as a result of the least-squares fit are given under the $sM(s)$. The residuals are constantly small, indicating that the observed curve is reproduced well

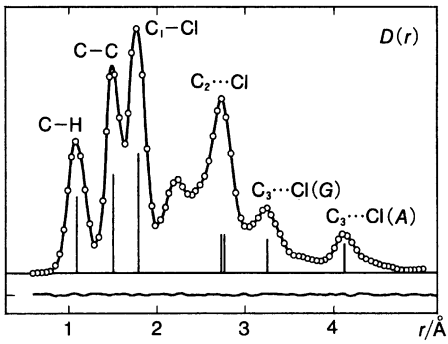

Fig. 4.21 The radial distribution function of 1-chloropropane. The residuals obtained as a result of the least-squares fit are given under the $D(r)$. G marks the gauche form and A the anti form

Table 4.5 Structural parameters of 1-chloropropane determined from the molecular scattering curve and the rotational constants

(1) Structural parameters common to the gauche and anti isomers (in Å unit)			
	r_z structure		r_g structure
r_z(C–H)	1.094	r_g(C–H)	1.113
r_z(C–C)	1.522	r_g(C–C)	1.525
r_z(C–Cl)	1.794	r_g(C–Cl)	1.796
(2) Structural parameters of the gauche isomer (r_z structure)			
∠ C–C–C	113.9°	∠ C–C–Cl	112.2°
θ	63.9°[a]		
(3) Structural parameters of the anti isomer (r_z structure)			
∠ C–C–C	111.3°	∠ C–C–Cl	111.3°

[a] θ represents the dihedral angle ∠ C–C–C–Cl shown in Fig. 4.19(b)

case of this particular molecular species we can also determine the abundance ratio of the two rotational isomers. Indeed, the peak intensities around 3.15 Å and 4.1 Å

directly reflect the abundance ratio, showing us that 62 % of the 1-chloropropane molecules in the gas phase at room temperature are the gauche form and 38 % are the anti form.

For this molecular species, the rotational constants A_0, B_0, and C_0 of each rotational isomer were obtained from the measurement of the rotational spectra. Therefore, in the same manner as has been described in Sect. 4.6.4, we have been able to determine the molecular structure with high precision by carrying out the least-squares analysis to simultaneously reproduce the two types of experimental data, that is, $sM(s)$ obtained by the electron diffraction method and the rotational constants obtained by the analysis of the rotational spectra. The structural parameters determined as a result are shown as the r_z structure in Table 4.5. The above-mentioned abundance ratio of the two isomers are also determined as one of the parameters in the course of this structure determination.

For Further Reading

Readers wishing to delve deeper into topics dealt with in this book are advised to look into the following literature.

To further your understanding on molecular spectroscopy, especially rotational spectroscopy, the following publications are recommended:

- H.W. Kroto, *Molecular Rotation Spectra*, Dover, New York, 1992.
- W. Gordy and R.L. Cook, *Microwave Molecular Spectra* 3rd ed. John Wiley & Sons, 1984.

For further reading on both vibrational and rotational spectra, you can turn to:

- W.S. Struve, *Fundamentals of Molecular Spectroscopy*, John Wiley & Sons, 1989.
- J.D. Graybeal, *Molecular Spectroscopy*, McGraw-Hill, 1988.

On electron diffraction you can refer to:

- Stereochemical Applications of Gas-Phase Electron Diffraction, Part A, in *The Electron Diffraction Technique*, Edited by I. Hargittai and M. Hargittai, VCH, 1988.

These publications will assist you in learning more about issues that this textbook has not been able to cover satisfactorily, such as molecular symmetry based on point groups, the interaction between molecular vibration and rotation, and the quantum theory of optical transitions.

For topics that have been treated in detail in this volume, such as the quantum mechanics of the harmonic oscillator (see Chap. 2), the quantum mechanics of the angular momentum (see Chap. 3), and the quantum mechanics of the scattering (see Chap. 4), a regular textbook on quantum mechanics should prove helpful for your understanding.

K. Yamanouchi, *Quantum Mechanics of Molecular Structures*,
DOI 10.1007/978-3-642-32381-2, © Springer-Verlag Berlin Heidelberg 2012

Figure Sources

Figures 1.5 and 1.7(a) in Chap. 1 have been reproduced with the kind permission of Dr. Toshihiro Ogawa. See

- H. Kobayashi, A. Shimota, K. Kondo, E. Okumura, Y. Kameda, H. Shimoda and T. Ogawa, *Applied Optics*, **38**, 6801 (1999).

for related discussions. Figure 1.8 has been based on Fig. 1 in

- M. Ohishi and M. Kaifu, *Faraday Discuss.*, **109**, 205 (1998),

with modifications added by assigning rotational transitions to the individual transition peaks.

Figure 2.11 in Chap. 2 and Fig. 3.23 in Chap. 3 have been created using spectra from

- "Tables of Wavenumbers for the Calibration of Infrared Spectrometers," 2nd ed., Compiled by A.R.H. Cole, International Union of Pure and Applied Chemistry, Pergamon (1977)

on pages 54 and 10, respectively.

Figure 2.31 in Chap. 2 is a modified reproduction of Fig. 1(a) from

- K. Yamanouchi, S. Takeuchi and S. Tsuchiya, *J. Chem. Phys.*, **92**, 4044 (1990),

and Fig. 3.25 in Chap. 3 is one of Fig. 2 from

- K. Yamanouchi, M. Okunishi, Y. Endo and S. Tsuchiya, *J. Mol. Struct.*, **352/353**; 541 (1995).

Figures 4.20 and 4.21 in Chap. 4 are made using Figs. 3 and 4, respectively, from

- K. Yamanouchi, M. Sugie, H. Takeo, C. Matsumura and K. Kuchitsu, *J. Phys. Chem.*, **88**, 2315 (1984).

Subject Index

A
a-type transitions, 182
Absorption bands, 69
All-trans-retinal, 4
Ammonia, 68, 179
Angular frequency, 28
Angular momentum operator, 128
Anharmonic constants, 114
Anharmonic couplings, 96
Anharmonic term, 50, 253
Anharmonicity, 61, 66, 96, 189
Anharmonicity of vibrations, 238
Anharmonicity parameter, 238
Annihilation operator, 58
Anti form, 255
Anti-symmetric stretch, 108, 114
Anti-symmetric stretch mode, 86
Anti-symmetric vibrational motion, 11
Asymmetric top, 152
Asymmetric triatomic molecule, 79
Asymptotic form, 201, 226, 227
Asymptotic solution, 29
Atmospheric environment, 8
Atomic mass unit, 125
Atomic scattering factor, 211
Atomic structure factor, 211
Attractive potential, 210
Average square amplitude, 250
Axial symmetry, 216
Azimuth angle, 122
Azimuthal angle, 122

B
b-type transitions, 182
Band origin, 193
Bending vibration, 11
Bent polyatomic molecule, 102
Bent triatomic molecule, 79, 95
Benzene, 5
β-carotene, 2
Black body radiation, 9
Block diagonalization, 171
Block-diagonalized, 111
Boltzmann constant, 240
Boltzmann distribution, 233
Bond angles, 101
Born approximation, 209
Born's probability interpretation, 42
Boundary condition, 27
Box-type potential, 6
Bra state, 43
Bracket notation, 43

C
c-type transitions, 182
Carbon dioxide, 9
Carbon tetrachloride, 15, 216
Caret, 27
Carotenoid, 2
Celestial bodies, 12
Center of mass, 23, 78
Centimeter-minus-one, 9
Centrifugal distortion, 125, 188, 239
Centrifugal distortion constant, 125
Centrifugal distortion term, 125
Centrifugal force, 249
Chemical bonds, 101, 212
1-chloropropane, 255
11-cis-retinal, 3
Classical equation of motion, 81
Colatitude, 122
Commutation relation, 131, 158
Complex conjugate, 38, 43
Condon-Shortley phase convention, 138

K. Yamanouchi, *Quantum Mechanics of Molecular Structures*,
DOI 10.1007/978-3-642-32381-2, © Springer-Verlag Berlin Heidelberg 2012

Conjugated system, 5
Coordinate operators, 41
Coriolis interaction, 187
Coulomb attractive potential, 220
Coulomb interaction, 204
Coupled oscillator, 81
Creation operator, 58
Cross section, 203
Cyanine, 2
Cyclic permutation, 169

D
d orbital, 223
d wave, 223
Damping factor, 237
Dark nebula, 12
De Broglie waves, 15
De-excitation, 10
Degrees of freedom, 78
Delta function, 205
Diagonal element, 41
Diagonalization, 89, 100
Diatomic molecule, 122
Differential cross-section, 203
Dipole moment, 41
Dipole moment vector, 178
Discrete levels, 18
Discrete value, 13
Dispersed fluorescence spectra, 115
Dispersed fluorescence spectroscopy, 115
Dissociation energy, 64
Double minimum potential, 70
Dunham-type expansion, 96
Dyes, 2

E
Eckart condition, 97, 109, 112
Ehrenfest's theorem, 240
Eigenenergy, 31, 36
Eigenfunction, 27, 36
Eigenvalue, 27, 36
Elastic scattering, 207
Electric field gradient, 177
Electric waves, 120
Electromagnetic radiation, 7
Electromagnetic waves, 7, 121
Electron diffraction, 14, 15, 17, 20
Electron diffraction method, 188
Electron diffraction photograph, 16
Electron scattering, 14, 15
Electron spin angular momentum, 136
Electronic ground state, 3, 20
Electronically excited state, 3, 14, 20, 115, 188
Emission and absorption, 8
Equilibrium internuclear distance, 22, 23, 64, 192, 235
Equilibrium position, 46, 81
Equilibrium rotational constant, 192
Euler angles, 142
Even function, 35, 72
Expectation value, 41, 45 52

F
Fermi doublet, 11
Fermi resonance, 11
Finite polynomial series, 34
Firefly, 3
First-order perturbation energy, 61
First-order perturbation theory, 62
First overtone, 49
Flavonoid, 2
Flavonol, 2
Forbidden transitions, 190
Force constant, 22, 33, 81
Forward scattering amplitude, 229
Fourier transform, 16, 243
Fourth-order anharmonic constants, 114
Freely rotating diatomic molecule, 122
Fundamental tone, 49

G
Gas electron diffraction, 200
Gas phase, 20
Gauche form, 255
Gauss-type function, 35
Gaussian, 35
Gaussian function, 71
Geometrical structure, 14, 18
$\boldsymbol{GF}$ matrix, 108
GF matrix method, 104, 105, 108, 243
Greenhouse effect, 10

H
Halo, 15, 218
Hamiltonian, 23, 91
Harmonic oscillator, 23, 32, 36, 93, 113, 232
Harmonic potential, 23, 33
Hermite differential equation, 34, 38
Hermite Gaussian function, 38, 46
Hermite polynomials, 34
Hermite recurrence formula, 37
Hermitian operator, 41, 45
Heteronuclear diatomic molecule, 32, 41, 78
Hierarchical nature, 14
Higher-order terms, 97
Highest Occupied Molecular Orbital, 6
HOMO, 6
Hydrogen-like atoms, 223

I
Incident plane wave, 202
Inelastic scattering, 207
Inertia tensor, 149
Inertial defect, 185, 187
Inflection point, 27
Infrared absorption, 32, 114
Infrared absorption spectrum, 69
Infrared light, 8
Infrared region, 14
Initial conditions, 24
Inner form, 180
Interatomic distance, 17
Interference pattern, 16
Internal coordinate system, 101
Internal coordinates, 101, 104
Internuclear distance, 16, 17, 122
Interstellar molecules, 120, 126
Interstellar spaces, 12
Interstellar substances, 12
Inversion motion, 68, 77
IR emission spectrum, 188
Isotope substitution method, 128, 178

K
Kekulé structural formulae, 5
Ket state, 43
Kinetic energy, 22, 81
Kronecker's delta, 48

L
Lagrange's equation, 23
Lagrangian, 23, 81, 97
Least-squares fit, 114
Least-squares method, 254
Legendre equation, 140
Legendre expansion, 227
Legendre polynomial, 140, 221
Linear polyatomic molecule, 79
Linear symmetric triatomic molecule, 84
Linear triatomic molecule, 79, 126
Lowering operator, 58, 132
Lowest Unoccupied Molecular Orbital, 6
Luciferin, 3
LUMO, 6

M
Mass point, 78
Mass-weighted Cartesian displacement coordinates, 81
Mass-weighted coordinates, 98
Mass-weighted orthogonal coordinate, 104
Matrix element, 41, 45
Mean square amplitude, 233
Meridian angle, 122
Methylchloride, 141
Methylhydrazine, 180
Microwave, 8, 121
Microwave emission, 126
Microwave spectroscopy, 121, 124
Molecular moment of inertia, 123
Molecular scattering curve, 17, 243
Molecular scattering intensity, 216, 235
Molecular spectroscopy, 17
Molecular structures, 17
Molecule-fixed coordinate system, 131, 141
Moment of inertia, 13, 124, 150
Moment of inertia tensor, 149
Monochromator, 115
Morino-Bastiansen shrinkage effect, 247
Morse oscillator, 63
Morse potential, 63, 238
Morse potential curve, 68
Morse potential parameters, 192
Multi-dimensional potential surface, 114

N
n-dimensional space, 51
Newman projection, 181
Newton's equation of motion, 24
Node, 35, 72
Non-bonded atom pairs, 17
Normal coordinate, 91, 93, 100, 101, 114
Normal mode frequencies, 100, 108
Normal mode vibrations, 104
Normal modes, 78, 80, 101
Normalization condition, 39, 43, 138
Normalization constant, 40, 53
Nuclear charge, 211
Nuclear quadrupole interaction, 177
Nuclear quadrupole moment, 177
Nuclear spin angular momentum, 136

O
O-branch, 190
Oblate symmetric top, 151
Oblate top, 156, 162
Odd function, 35, 72
Optical theorem, 229
Optical transition, 47
Orbital angular momentum, 223, 227
Orthogonal displacement vector, 102
Orthogonal function system, 40
Orthogonality, 87
Orthonormal function system, 40
Orthonormal relation, 48, 94
Orthonormal set, 51
Orthonormal vectors, 87

Orthonormality, 53
Outer form, 180
Outgoing spherical wave, 201
Overtone absorption, 49, 189
Oxyluciferin, 3
Ozone, 9

P
P-branch, 11, 189
p orbital, 140, 223
p wave, 223
Parity, 72
Partial wave, 230
Partial wave expansion, 224, 226, 228
Perturbation energy, 61
Perturbing term, 61
Phase shift, 218, 228, 230, 246
Photoabsorption, 11
Photoemission, 3
Photographic plate, 16
Physical quantity, 42, 45
π-conjugated chain, 5, 6
Planck constant, 5
Plane wave, 201
Point groups, 175
Polar angle, 122
Polar coordinate system, 122
Polyatomic molecules, 77
Position vector, 121
Potential energy, 22, 81
Principal axes of inertia, 149
Principal moments of inertia, 149
Probability current density, 197, 199, 202
Probability interpretation of wave functions, 198
Prolate symmetric top, 150, 162
Prolate top, 156

Q
Q-branch, 190
Quadratic force constant, 63
Quantization, 32, 93
Quantization axis, 169
Quantum mechanical tunneling, 73
Quantum mechanics, 26
Quantum number, 31, 95

R
R-branch, 11, 189
r_0 structure, 187, 250
r_α^0, 251
r_α^0 structure, 251, 252
r_α structure, 250
r_a structure, 238
r_e structure, 187
r_g structure, 239, 246, 250
r_s structure, 128, 254
r_z structure, 252, 257
Radial distribution curve, 17, 243
Radial distribution function, 243
Radial eigenfunction, 219
Radiation equilibrium, 10
Radiationless process, 3
Radio astronomy, 12
Radio telescope, 12
Radio waves, 12
Radius, 122
Raising operator, 58, 132
Reciprocal centimeter, 9
Recurrence formula, 30, 36, 53
Reduced mass, 23, 33, 121
Regular tetrahedral structure, 16
Relativistic corrections, 200, 203
Restoring force, 103
Rhodopsin, 3
Rigid rotor, 122, 124
Rodrigues formula, 140
Rotating sector, 16
Rotating sector method, 15
Rotational constant, 13, 124
Rotational effect, 239
Rotational energy, 120
Rotational isomers, 180, 255
Rotational levels, 120
Rotational quantum number, 11, 123
Rotational spectroscopy, 121
Rotational structure, 11, 69
Rotationally excited state, 14

S
S-branch, 190
s orbital, 140, 223
s wave, 223
Satellite, 11
Scalar product, 38, 43
Scattered electron beam, 207
Scattered spherical wave, 202
Scattering amplitude, 201, 211
Scattering angle, 218
Scattering intensity, 214
Scattering parameter, 16
Scattering problem, 199
Scattering state, 228
Scattering wave, 201
Schmidt orthogonalization, 154
Schrödinger equation, 27
Second-order cross terms, 101

Second-order perturbation, 62
Second overtone, 49
Selection rules, 48
Sensitizing dye, 2
Simple harmonic oscillation, 24
Simultaneous linear equation, 82, 98
Singlet state, 3
Skeletal structure, 10
Small-angle scattering, 244
sp^2 hybridized orbital, 4
Space-fixed coordinate system, 131, 141
Spectroscopic dissociation energy, 64
Spherical Bessel function, 222
Spherical harmonics, 136, 141, 162, 220
Spherical Neumann function, 222
Spherical symmetry, 207
Spherical top, 151
Spherically symmetric potentials, 212
Spring constant, 22
Stationary states, 74
Stratosphere, 11
Symmetric stretch, 108, 114
Symmetric stretch mode, 85
Symmetric top, 150, 156
Symmetric triatomic molecule, 79

T
Taurus, 12
Taurus Dark Cloud, 126
Taurus Molecular Cloud 1, 12
Taylor expansion, 252
Term value, 96
Theory of relativity, 203
Thermal equilibrium, 10
Thiacarbocyanine, 3
Third-order anharmonic constants, 114
Third-order anharmonic term, 62
Third-order terms, 97
Time-dependent Schrödinger equation, 74
TMC-1, 12
Total cross-section, 203, 229
Transition dipole moment, 47
Transition probability, 52
Translational motion, 86
Transposed matrix, 145
Triatomic molecule, 16
Trigonal pyramidal structure, 74
Troposphere, 11

U
Ultraviolet region, 14

V
Vertical displacement, 249
Vibration-rotation constant, 186, 253
Vibration-rotation interaction, 187
Vibration-rotation spectrum, 11
Vibrational effect, 186
Vibrational energy, 95
Vibrational ground level, 32
Vibrational ground state, 32, 186
Vibrational modes, 78
Vibrational quantum number, 41, 45, 69
Vibrational spectroscopy, 67
Vibrational transitions, 114
Vibrational wave functions, 117
Vibrationally excited level, 11, 32
Vibrationally excited state, 10, 14, 32, 188
Virial theorem, 54
Vitamin A, 4

W
Wang's matrix, 171
Wang's transformation, 171
Water, 9
Wave-like properties, 15
Wave number, 8, 67
Wave packet, 77
Wave vector, 200, 205

Z
Zenith angle, 122
Zero-point energy, 32
Zero-point vibration, 186
Zero-point vibrational level, 95
Zeros, 34

Formula Index

Br_2, 234
C_{60}, 151
CCl_4, 15
C_6H_5Cl, 152
$C_6H_5NH_2$, 152
C_6H_6, 150, 151
$CH_3CH_2CH_2Cl$, 255
CH_3CH_2Cl, 152
CH_3Cl, 141, 150
CH_3NHNH_2, 180
CH_4, 151
C_3O_2, 151
CO, 32, 78, 191
$^{12}C^{16}O$, 124
CO_2, 9, 11, 78, 79, 151, 188, 243, 246
CS_2, 79, 246
Cl_2, 234
$D^{35}Cl$, 33
H_2, 234
H_2O, 9, 11, 79, 80, 111, 141, 152
HC_3N, 12, 151
HC_5N, 12
HC_7N, 12
HCN, 151
HCl, 32, 40, 49, 78, 234
$H^{35}Cl$, 66
HO, 50
N_2, 48, 234
N_2O, 151
NF_3, 176, 177, 178
NH_3, 150, 151, 176
NO, 234
O_2, 48, 234, 239
O_3, 9, 11
OCS, 16, 126, 151, 178
PH_3, 176
SF_{16}, 151
SO_2, 16, 79, 80, 95, 105, 116, 152, 179, 183, 193

K. Yamanouchi, *Quantum Mechanics of Molecular Structures*,
DOI 10.1007/978-3-642-32381-2, © Springer-Verlag Berlin Heidelberg 2012